From the membrane to central metabolism: New insights into the diverse mechanisms controlling β-lactam resistance in MRSA

A thesis submitted to the National University of Ireland, Galway, for the Degree of Doctor of Philosophy by

Claire Fingleton, B.Sc

Microbiology, School of Natural Sciences,
National University of Ireland, Galway

April, 2021

Research supervisor

Prof. James P. O'Gara

Table of contents

Index of Figures

Index of Tables

Summary

Staphylococcus aureus is an important human pathogen, with the ability to colonise and cause disease, ranging in severity from superficial skin infections to life threatening invasive disease. The emergence of healthcare and community-acquired strains of methicillin resistant *Staphylococcus aureus* (MRSA), and their resistance to antibiotics makes it difficult to eradicate infections that would otherwise be treatable. This leads to poorer outcomes and increased morbidity and mortality for patients.

We have identified novel genetic factors which affect β-lactam resistance in community acquired-MRSA which will contribute to the understanding and development of therapeutic targets.

Disruption of the *cycA* gene, encoding an alanine permease, led to an increased susceptibility of MRSA to β-lactam antibiotics. In chemically defined media supplemented with glucose, the lack of CycA permease activity led to a reduction in alanine uptake by the cell, affecting peptidoglycan structure and cross-linking, rendering the *cycA* mutant susceptible to β-lactams. Exposure of the *cycA* mutant to the drug D-cycloserine, which inhibits alanine racemase and D-alanine ligase enzymes, exacerbated the impact of impaired alanine uptake and metabolism. This demonstrates the potential for D-cycloserine/oxacillin combinations as a new therapeutic option for the treatment of MRSA infections. The phenotypes of impaired alanine uptake and oxacillin susceptibility were not evident in a *cycA* mutant in CDM, indicating a role for another transporter in these growth conditions.

Mutation of the TCA cycle gene *sucC* in MRSA resulted in increased β-lactam susceptibility. Analysis of this mutant and the parent strain JE2 revealed that mutation of *sucC* was associated with altered concentrations of TCA cycle metabolites including an accumulation of succinyl-CoA, and perturbation of the succinylome. The *sucC* mutant showed differences in the succinylation pattern of the major autolysin Atl, and *sucC* had reduced autolytic activity. This work reveals

succinyl-CoA and protein succinylation as a potential therapeutic target, in the effort to sensitise MRSA to β-lactams. Future work will provide insight as to whether the autolysis and resistance phenotypes are interlinked, potentially identifying additional targets.

LspA is a signal peptidase of the lipoprotein processing pathway. We discovered that mutation of the *lspA* gene or inhibition of LspA activity by the drug globomycin led to increased resistance in MRSA. This effect does not appear to be linked to cell wall changes, and we hypothesize that accumulation of diacylglycerol or mislocalisation of lipoproteins at the cell membrane may be causing this phenotype. This work also demonstrates that the combination of an LspA inhibitor such as globomycin should not be used as treatment in combination with β-lactams, due to the risk that it would increase β-lactam resistance in an MRSA strain.

Declaration

This thesis consists of three manuscripts comprising chapters 2, 3 and 4. I am joint first author on Chapter 2, which has been submitted for publication. I am the first author on Chapter 3, which is in preparation. Chapter 4 is based on my contributions to the CycA project. I am the third author on the CycA paper published in the Journal of Infectious Diseases, and have carried out further work on this project as described in Chapter 4. My contribution to each chapter is also included in the Author Contributions section at the beginning of each chapter.

I declare that this thesis is my own and that my research described herein has not been previously submitted in part fulfilment of a degree to the National University of Ireland, Galway or to any other University. National University of Ireland, Galway library may lend or copy this thesis upon request.

_____

Claire Fingleton

Acknowledgements

I would like to thank everyone who has contributed to my PhD journey. First and foremost, I want to thank my supervisor Prof. James O'Gara. Your endless support, patience and positivity has carried me though this experience. At times when I couldn't see where it was going, your guidance and expertise was invaluable, and I could not have got to this point without you.

Thank you to Dr. Aoife Boyd, Dr. Conor O'Byrne and Dr. Ger Flemming for your help and advice each year at GRC meetings and throughout the PhD. To Prof. Paul Fey, Dr. Fareha Razvi and Prof. Vinai Thomas at the University of Nebraska Medical Centre, thank you for taking the time to discuss my work, and offering your advice and expertise to projects. A special thank you to Prof. Fey for welcoming me to Omaha for the Staphylococcal Genetics Workshop, I am sorry for falling asleep in that one lecture, it was the culmination of nights out with Staph Camp, nothing personal!

To Ann, Mike and Maurice, you welcomed me every time I knocked on your office doors for help. Ann, thank you for the plant cuttings, you'll be happy to hear the spider plant is potted and doing well! Mike, thank you for the pep talk and encouragement before the Hardiman interviews when I started. Maurice, thank you for all your help over the years. Whether it was placing orders, fixing our lab equipment, or lending us tools, you always went above and beyond to help in whatever way you could! Wishing you all the best in your retirement and I wish that we had been able to give you a proper party and send-off.

To everyone from the JOG lab, past and present, you have all made it a wonderful place to work. Laura, thank you for welcoming me into the lab when I started and helping me to settle in. You have been a great friend (except when you and Chris tried to lock me in the fridge), and I enjoyed all our office chats over the years. I know I made fun of your protocol book with its many coloured tabs, but in all seriousness, your knowledge, patience and experience was a huge support and I appreciate it. To Moya, Orla, Chloe and Merve, thank you for all the chats, laughs

and frustrations we have shared in the lab. Aaron, you are in good hands in the JOG lab and I hope you enjoy your PhD experience there! Merve, it's hard to believe that we only met in 2020 and I feel like you have been a friend for much longer. You have been such a big part of my life since you came to Galway, working together in the lab, or meeting in your estate for coffee during lockdown, or going for swims in Salthill. Thank you so much for all your support and encouragement in writing up. I really couldn't have got to this stage without you. Also a big thanks for the endless supply of Nespresso and oat milk in our office!

Merve and Siobhan, big thanks for all the Salthill swims that we have shared! Siobhan, when you first suggested it almost 3 years ago, I didn't think we'd get started much less keep it up. But meeting you both for sunrise, sunset or grey rainy swims was one of the things I looked forward to most over the years. Even though it was always cold and we complained at times, I wouldn't change any of it!

Siobhan, thank you for your friendship throughout the PhD. I remember you calling over to the lab with coffee and macaroons when I had some very long growth curves. Or the times I finished late in the lab and headed over to you with my pizza for a catch up. You've recently started your PhD journey and I hope that I can return the favour and be there for you along the way too. Roisin and Siobhan, thanks for our Mr Waffle catchups and dancing in the Quays over the past 4 years. Roisin, it was shortly before I started the PhD you had your first date with Stephen. It's hard to believe that so much time has passed, that I have got to this stage of the PhD, and you and Stephen will be getting married soon. I'm already looking forward to the wedding next year! Delphine, thank you for the coffees and chats, and the hiking adventures we've shared. I hope that we will get to do another Maamturks Challenges in the future and I promise I will train a bit harder to keep up with you next time!

To Annette, Muireann, Laura and Shagufa, thank you for all the laughs and tears we have shared over the past decade, especially in the canteen and library of GMIT. You have been there for me during the good and bad times and your friendship means so much to me. Thanks to my lecturers Mary McGrath and

Debbie Corcoran in GMIT who supported me in studying Medical Science and encouraged me to pursue my research interests.

To my buddy Chris, thank you for being by my side during our time in the lab and ever since then. From the coffee breaks and joe.ie quizzes in the office, to the hours chatting and joking in the lab, the early morning runs along Dangan and Salthill, and everything in between. I'm so glad that I got to share it with you. More recently thank you for making me all the dinners and endless cups of tea during write up, maybe I can take over for the next few months to balance things out! I love you lots and can't wait for our future adventures together.

To my parents Margaret and Dominic, and my sister Niamh, thanks for encouraging me throughout the PhD, even when it wasn't always clear what I was doing (sometimes I didn't know either!), and for the supply of food and dinners each time I was home. There's nothing I can say here that will fully capture what your love and support means to me. Most of all thanks for being there for me.

Chapter 1: Introduction

1.1 Clinical importance

Staphylococcus aureus is a coccoid Gram-positive of the Firmicute phylum. It is non-motile, non-sporulating and halotolerant. It can form part of normal human flora as a commensal, residing on the skin and mucus membranes without causing disease, and it is estimated that 60% of the population may be transiently colonised by *S. aureus* [1]. However it is also an opportunistic pathogen when conditions are favourable. Colonisation is reported to be a risk factor for infection [2, 3], but more commonly, infections are associated with breaches of the epithelial barrier for example via surgical site wounds, or indwelling medical devices such as catheters, valves and prosthetic joints [4]. *S. aureus* causes numerous diseases ranging in severity from skin and soft tissue infections such as impetigo, cellulitis and abscesses, to severe invasive conditions such as pneumonia, bacteraemia, endocarditis and osteomyelitis [4].

Following the introduction of penicillin to treat staphylococcal infections in the 1940s, penicillin resistant strains were quickly identified [5]. A similar pattern occurred again in the 1960s with the introduction of methicillin in 1961 and the subsequent detection of resistance [6], leading to the term methicillin resistant *S. aureus* (MRSA). The emergence of MRSA with resistance to β-lactam antibiotics, represents an additional complicating factor in the treatment of *S. aureus* infection. The glycopeptide antibiotic vancomycin became an important tool in treating such infections where β-lactams were no longer an option, however vancomycin-intermediate and resistant strains have also emerged [7].

1.2 Healthcare-associated MRSA (HA-MRSA) and community-associated MRSA (CA-MRSA)

Prior to the 1990's, MRSA infections were predominantly associated with hospital and residential care settings and were termed healthcare-associated MRSA (HA-MRSA) infections. These settings have a high proportion of medically vulnerable and immunocompromised individuals, providing *S. aureus* with a high-risk population in which to establish infection. This is exacerbated by the use of

antibiotics in such settings, which can promote further selection and transmission of antimicrobial resistance genes.

In the 1990s reports emerged of *S. aureus* infection in the wider community [8]. These infections were occurring in a range of individuals, many who did not have the recognized risk factors for MRSA infection and notably, had no prior exposure to healthcare settings [8]. The term community-associated MRSA (CA-MRSA) was used to differentiate these infections from their healthcare-associated counterparts. CA-MRSA is typically more virulent than HA-MRSA [9, 10]. It generally causes skin and soft tissue infections such as abscesses and cellulitis [1, 11], but also more severe instances of necrotizing pneumonia, fulminant necrotizing fasciitis, bacteraemia and endocarditis [12].

While both HA-MRSA and CA-MRSA strains possess the methicillin resistance gene, *mecA*, they can differ in their resistance profiles. CA-MRSA are typically more susceptible to antibiotic treatment [13]. This comes with a trade-off however; studies have shown that the reduced fitness cost associated with carrying fewer resistance genes facilitates their increased virulence [9, 10].

1.3 Peptidoglycan cell wall

The primary component of the staphylococcal cell wall is peptidoglycan. It plays a crucial role in maintaining cell shape and structural integrity. Peptidoglycan comprises the disaccharide N-acetylglucosamine (NAG)-N-acetylmuramic acid (NAM). NAM contains a pentapeptide stem which is crosslinked by a pentaglycine bridge. The synthesis of peptidoglycan occurs in the cytoplasm in a sequential manner by the enzymes MurABCDEF. Peptidoglycan precursor, UDP-NAM, is generated by MurA and MurB. MurA transfers enolpyruvate from phosphoenolpyruvate to UDP-NAG [14], which is then reduced by MurB in an NADPH-dependent reaction to form UDP-NAM [15]. MurC, MurD and MurE add amino acids L-alanine, D-iso-glutamine-and L-lysine respectively, while MurF adds D-ala-D-ala, in the form of a dipeptide [16, 17]. Additional enzymes, alanine racemase, Alr, and D-Ala-D-ala ligase, Dlr, are required to supply the D-alanine

dipeptide for peptidoglycan -pentapeptide synthesis [18]. The NAM-pentapeptide is then transferred from UDP to a membrane-embedded undecaprenyl-phosphate lipid carrier, Lipid I by MraY [19]. MurG adds NAG to Lipid I to form Lipid II, completing the basic peptidoglycan monomer [20]. FemA, FemB and FemX catalyse the addition of five glycine residues to the L-Lysine of the pentapeptide and crosslinking occurs between this lysine and the carboxyl group of D-Alanine at position 4 of an adjacent pentapeptide [21]. Once cytoplasmic activity is complete, flippase enzymes translocate this lipid II structure across the bacterial membrane to the periplasm and the newly synthesized peptidoglycan can be incorporated into the existing structure by transglycosylase and transpeptidase enzymes knowns as penicillin-binding proteins (PBPs).

S. aureus has four native membrane bound PBPs; PBP1, PBP2, PBP3, and PBP4, [22] catalysing transglycosylase (extension of the glycan chain) and transpeptidase (cross-linking) activity for peptidoglycan synthesis. PBP1 is an essential transpeptidase while also having a secondary role in cell division and separation [23]. PBP2 is the only PBP that can perform both transglycosylase and transpeptidase activity in *S. aureus*. In methicillin-susceptible *S. aureus* (MSSA) PBP2 is essential [24] but not in MRSA, as the alternative penicillin-binding protein PBP2a of MRSA can undertake transpeptidase activity in its place [25, 26]. However, when MRSA becomes exposed to β-lactams PBP2 becomes essential as cooperative functioning is needed between its transglycosylase domain and the transpeptidase domain of PBP2A for cell survival [25]. PBP3 is non-essential and its function is somewhat unknown; evidence suggests that it is associated with septum development and cell division but that alternative PBPs can take over its function [27]. PBP4 is also non-essential in *S. aureus* although it has been shown to be important for highly cross-linked peptidoglycan [28]. In addition to its transpeptidation domain, PBP4 has a carboxypeptidase domain, and is thought to play a role in *mecA*-independent (MSSA) β-lactam resistance as a penicillinase[28]. In CA-MRSA it is reported to play an important role in β-lactam resistance in addition to PBP2a [29].

1.4 Methicillin Resistant *Staphylococcus aureus* (MRSA)

S. aureus resistance to penicillin is mediated by *blaZ*, which encodes β-lactamase. This predominantly extracellular enzyme is produced upon exposure to β-lactam antibiotics and it hydrolyses the β-lactam ring, rendering the antibiotic inactive. *blaZ* is regulated by two adjacent genes, the anti-repressor *blaR1,* and the repressor *blaI* [30], encoding regulatory proteins BlaR1 and BlaI respectively. Following exposure to β-lactams, BlaR1 auto-cleaves and is thought to provide peptidase activity, leading to cleavage and inactivation of BlaI. This allows transcription of *blaZ* leading to β-lactamase production. Over 90% of staphylococcal isolates are reported to produce β-lactamase.

Methicillin resistance in *S. aureus* is conferred by the alternative penicillin-binding protein PBP2a, a78 kDa protein encoded by the *mecA* gene which is located on the a mobile genetic element, the staphylococcal cassette chromosome (SCC*mec*) [31, 32]. The mechanism of action of β-lactam antibiotics is to bind to, and inhibit PBPs, therefore preventing transpeptidase activity and the formation of new peptidoglycan. PBP2a confers β-lactam resistance as it has a lower affinity for β-lactams than the other PBPs [33], so it is not bound to and inhibited by β-lactam antibiotics. Thus, peptidoglycan synthesis can still take place in the presence of β-lactams. However as PBP2a has only transpeptidase activity, and not transglycosylase activity, it cannot entirely compensate for inactivation of native PBPs, and the transglycosylation activity of PBP2 is still needed for β-lactam resistance [26].

The *mecA* gene is regulated by two sets of regulatory systems, the MecI/MecR1 and the aforementioned BlaI/BlaR1 system [34]. *mecR1* and *mecI* are adjacent to *mecA* on the SCC*mec* element. MecI is a repressor of *mecA,* binding to its upstream promoter region [34]. MecR1 is a transmembrane signal transducer and when exposed to β-lactams, it becomes activated, cleaving the repressor MecI, and allowing *mecA* expression and synthesis of PBP2a [35, 36]. The MecI/MecR1 and BlaI/BlaR1 systems are capable of cross-talk due to sequence homology between

the *mecI-mecR1* and the *blaR1-blaI* regulatory genes, and there is evidence of MecI/BlaI heterodimers causing *mecA* repression [37]. The MecR1/MecI system is relatively slow at inducing *mecA* expression due to MecI binding tightly to the *mecA* promoter coupled with inefficient activation of MecR1 by β-lactam antibiotics [38]. Therefore, strains that possess *mecA* with an intact MecI/MecR1 system may appear phenotypically susceptible to methicillin despite their genetic make-up. However, selective pressure from antibiotics can lead to the acquisition of mutations in these regulatory genes, resulting in inactivation of the MecI repressor and enhancing PBP2a synthesis [39].

1.5 Heterogeneous and homogeneous resistance in MRSA

MRSA exhibit a heterogenous (HeR) pattern of resistance meaning that within a given population of MRSA, there exists subpopulations with varying resistance profiles. Upon exposure to β-lactams, the vast majority of cells (>99.9%) present with intermediate or low level resistance, while a small proportion (0.1-0.01%) are capable of undergoing a phenotypic switch to a homogenously resistant (HoR) phenotype upon exposure to high levels antibiotic (>100 µg/ml oxacillin) [40]. This HoR population is a uniform, highly resistant population that exhibits little variation in colony size on agar. The number and frequency at which these HoR subpopulations occur in MRSA is reproducible, strain specific and generally stable [41]. The emergence of a homogeneously resistant population upon exposure to high concentrations of antibiotic may help to explain treatment failure in a clinical setting where a strain initially appears phenotypically susceptible. The mechanisms underpinning the switch from heterogenous to homogenous resistance are not fully understood. While *mecA* is a primary genetic determinant for β-lactam resistance, variations in PBP2a levels do not correlate with resistance phenotypes [42] indicating that additional mutations are involved [40]. Several mutations, outside of the *mecA* regulon have been associated with the HoR phenotype and increased antibiotic resistance [42].

1.6 Accessory factors affecting methicillin resistance

1.6.1 Fem factors (factor essential for methicillin resistance)

While *mecA*-encoded PBP2a is the main determinant of methicillin resistance, numerous additional factors have been identified that also contribute to methicillin resistance, several of which are illustrated in Fig 1.1. The *fem* genes, *f*actors *e*ssential for *m*ethicillin resistance, [43] are a group of chromosomal genes outside the SCC*mec* locus. *femA* and *femB* are located in an operon together and play a role in the formation of the pentaglycine bridge which cross-links peptidoglycan [44]. *femA* is responsible for the addition of the 2nd and 3rd glycine residues to the pentaglycine bridge, and mutation of this gene was associated with impaired growth and dramatically reduced β-lactam MICs, rendering some strains clinically susceptible. Cell wall analysis revealed a reduction in the glycine content of the cell wall with a monoglycine bridge in place of the typical pentaglycine bridge and a reduction in peptidoglycan cross-linking [44]. *femB* is involved in the addition of the 3rd and 4th glycine residues to the pentaglycine bridge. Disruption of *femB* results in increased susceptibility to β-lactam antibiotics in a similar manner to that of a *femA* mutation, accompanied by reduced glycine content of the cell wall and reduced cross-linking [45]. Following the discovery of *femA* and *femB*, a 3rd factor was identified, *femX* or *fmhB*. It is responsible for the addition of the first glycine residue onto the stem peptide and is an essential gene in *S. aureus*. Inactivation of this *fem* results in the accumulation of un-crosslinked UDP-MurNAc pentapeptide precursors of peptidoglycan.

Beyond the pentaglycine crossbridge, *femC*, with similarity to *glnR* in *Bacillus subtilis* encodes a glutamate synthetase repressor. Inactivation of the *femC* gene exerts a polar effect on glutamine synthetase activity, causing shortage of glutamine and reduced amidation of the stem peptide, leading to decreased methicillin resistance. This phenotype could be restored by addition of exogenous glutamine in a defined media [46]. *femD* or *glmM* encodes a phosphoglucosamine mutase which catalyses the interconversion of glucosamine-6-phosphate to glucosamine-1-phosphate. Mutation of this gene results in inhibition of the first step of peptidoglycan precursor formation and consequent reduction in methicillin resistance. There is less available literature relating to *femE*, other than its function is unknown and inactivation slightly reduces methicillin resistance

[33]. The final *fem* gene, *femF* (*murE*), is responsible for incorporating lysine into the stem peptide. A *femF* mutant resulted in the accumulation of large amounts of UDP-linked muramyl dipeptide in the cytoplasmic wall precursor pool, and reduced pentapeptides, with dramatically increased susceptibility versus the parent strain [47].

1.6.2 *Fmt* genes

Outside of the *fem* family of genes, *fmtA*, *fmtB* and *fmtC* are also implicated in methicillin resistance. *fmtA* encodes a membrane bound, non-penicillin-binding protein, and inactivation of this gene led to reduction in cross-linking and amidation of peptidoglycan. This was accompanied by a decrease in methicillin resistance and a switch from a homogenous resistance phenotype to heterogenous resistance [48]. Since then, it has been demonstrated that expression of *fmtA* is controlled by the binding of global regulator SarA to its promoter region, following induction by cell wall targeting antibiotics [49]. *fmtB* (*mrp*) is a cell surface protein thought to play a role in cell wall biosynthesis. Inactivation of *fmtB* results in peptidoglycan with altered muropeptide composition and reduced β-lactam resistance. *fmtC* (*mprF*) appears to encode a membrane-associated protein, based on its hydrophobic N-terminus, and was implicated in both oxacillin and bacitracin resistance, and possibly in the lipid cycle of cell wall biosynthesis [50]. Further work showed that *fmtC/mprF* is involved in modification of phosphatidyl glycerol with L-lysine and the loss of same led to a negative charge of the membrane [51].

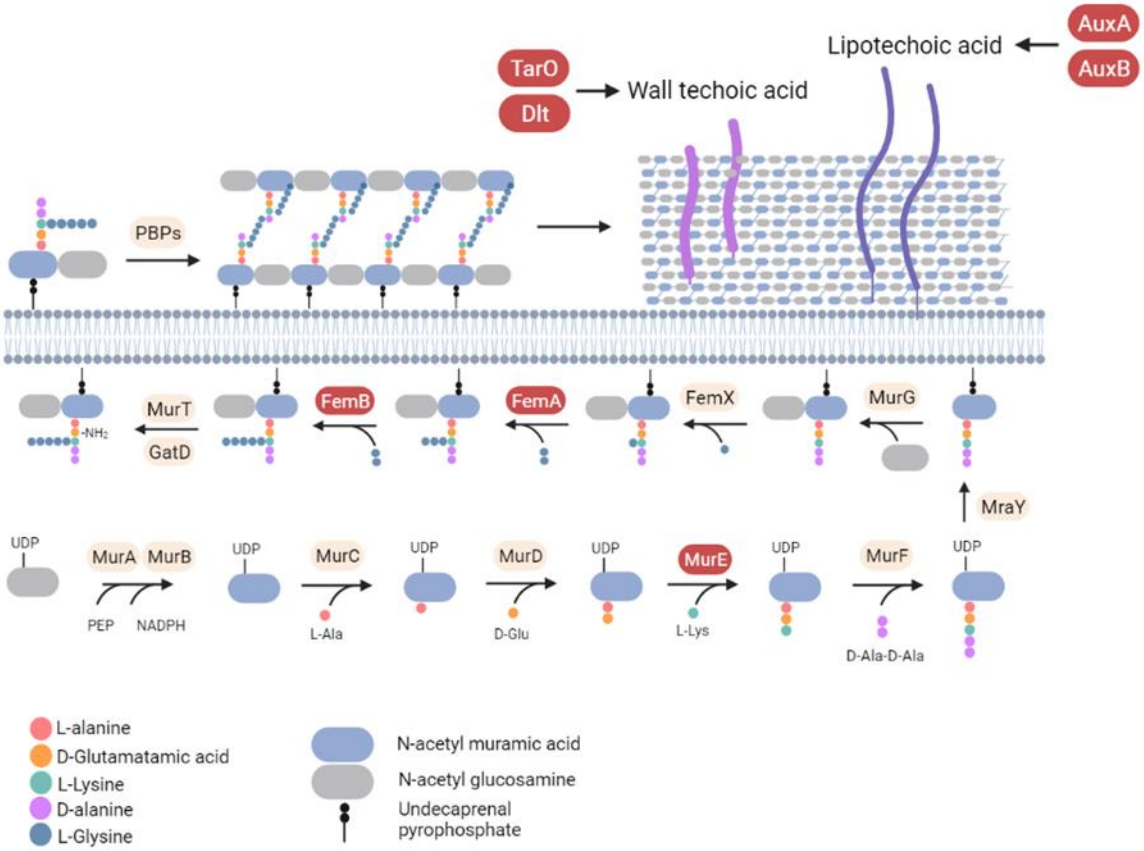

Figure 1.1. Accessory factors affecting β-lactam resistance in MRSA. (shown in red). *murE* is responsible for incorporating lysine into the stem peptide and mutation. *femA* is responsible for the addition of the 2nd and 3rd glycine residues to the pentaglycine bridge, while *femB* catalyses the addition of the 3rd and 4th glycine residues to the pentaglycine bridge. Mutation of these genes *murE*, *femA* or *femB* gene is associated with increased β-lactam susceptibility. AuxA and AuxB are transmembrane proteins, and mutation of their corresponding genes *auxA* and *auxB* leads to increased β-lactam susceptibility via impaired lipoteichoic acid stability. *TarO* and *dlt* affect β-lactam susceptibility via their effects on wall teichoic acids. *TarO* is a wall teichoic acid biosynthetic gene and mutation leads to increased methicillin susceptibility. Conversely, inactivation of the *dlt* operon, which plays a role in the transfer of D-alanine to teichoic acids, results in increased methicillin resistance.

1.6.3 Other genes affecting methicillin resistance

The llm gene, identified in 1994, encodes a 31-amino acid protein, believed to be membrane-associated due to its hydrophobic nature. Mutants were reported to have reduced methicillin resistance with concomitant increases in Triton X-100 induced autolysis. Since then, the *llm* gene has been identified as the wall teichoic

acid biosynthetic gene *tarO,* thus linking wall teichoic acid biosynthesis with β-lactam resistance [52, 53]. Teichoic acids are vital components of the staphylococcal cell wall. They consist of highly charged polymers of alternating phosphate and alditol groups, and are covalently linked to peptidoglycan. Inactivation of the *dlt* operon, involved in the transfer of D-alanine to teichoic acids, results in increased methicillin resistance [54]. Lipoteichoic acids, on the other hand, are bound to the cell membrane via glycolipids. Recently, *auxA* and *auxB* genes, encoding transmembrane proteins AuxA and AuxB respectively, have been implicated in β-lactam resistance. Mutation of these genes led to impaired lipoteichoic acid stability, which was accompanied by increased β-lactam susceptibility and decrease in autolytic activity [55].

Peptidoglycan hydrolases are a group of cell wall-associated enzymes, capable of cleaving bonds in peptidoglycan and/or its soluble fragments. The relationship between autolysis and β-lactam resistance appears to be complex with some disagreement in the literature. One report showed lower autolytic activity in homogenously resistant strains, versus heterogeneously resistant strains, although MIC measurements were not available [56]. However, another paper revealed faster rates of autolysis in homogenously resistant mutants compared to their heterogeneous counterparts [57]. This decreased autolysis of the heterogeneously resistant mutant strains was accompanied by reduced MICs. The major autolysin (Atl) in *S. aureus* is a bifunctional protein, which undergoes proteolytic cleavage to generate a two domain extracellular peptide with both amidase and glucosaminidase activity [58, 59]. Mutation of the *atl* gene leads to a modest reduction in oxacillin MIC [60]. In contrast, mutation of *lytH* resulted in expression of high-level homogenous resistance, where the parental strain had shown a heterogenous phenotype. The gene itself encodes a protein product that showed homology to the lytic enzyme LytC of *B. subtilis* [61].

The disruption of prenylation in MRSA has been linked to a range of phenotypes including decreased resistance to cell wall antibiotics, and increased resistance to aminoglycosides. This was demonstrated in a geranyltranstransferase (IspA)-

deficient strain and the altered resistance phenotype appears to arise due to differences in envelope composition of the *ispA* mutant [62].

Mutation of *hmrA* and *hmrB* genes led to an unusual resistance pattern whereby MRSA strain N315 was resistant to high concentrations of oxacillin (>64 - 512 µg/ml) yet susceptible to low concentrations (6 – 16 µg/ml), which is termed Eagle-type methicillin resistance [63, 64]. Overexpression of these genes led to increased methicillin resistance. HmrA is a putative aminohydrolase and HmrB is a homologue of an acyl-carrier protein in *Rhizobium leguminosarum.*

The lipoprotein PPIase PrsA was identified as playing a role in protein secretion in *B. subtilis* [65] and subsequently linked to glycopeptide and oxacillin resistance in *S. aureus* where disruption of the gene resulted in reduced resistance. A double mutant *htrA1/prsA* in the MRSA strain COL showed major increases in β-lactam susceptibility, due to the impact of these mutations on folding and maturation of PBP2a [65].

1.6.4 Signalling nucleotides

Cyclic-di-adenosine-monophosphate (c-di-AMP) is an important signalling nucleotide in Gram-positive organisms and plays a role in many crucial cell processes including osmotic and cell wall homeostasis. In *S. aureus*, c-di-AMP was identified in 2011 by Corrigan *et al.*, who characterised it and reported a role in methicillin resistance [66]. In this study, c-di-AMP was identified via the growth of lipoteichoic acid (LTA) mutants which were able to survive despite their LTA-deficiency. Typically, LTA mutants are severely impaired in their growth and morphology, requiring specific permissive conditions to overcome this [67]. Corrigan found that LTA mutants could also survive owing to mutations in the *gdpP* gene, which had phosphodiesterase activity and degraded c-di-AMP [66]. By mutating *gdpP*, degradation of c-di-AMP ceased, causing a dramatic increase in intracellular levels, in turn influencing cell size and envelope characteristics [66]. This included a significant increase in resistance to penicillin G and increased peptidoglycan cross-linking [66]. Building on this, it was reported that mutation in

dacA led to reduction in c-di-AMP levels, alongside increased growth rate and a reduction in oxacillin resistance, marked by a switch from homogenous to heterogenous phenotype [68, 69]. Investigations into the genetic mechanisms of antibiotic tolerance also found that mutations of *gdpP* resulted in increased β-lactam and glycopeptide tolerance [70].

1.6.5 Guanosine tetra/penta-phosphate

Guanosine tetra/penta-phosphate ((p)ppGpp) is another signalling molecule associated with increased homogeneous resistance phenotype. (p)ppGpp is an alarmone responsible for reducing unnecessary cell activities related to metabolism, protein synthesis and cell division, when the cell encounters metabolic stress. This signal for metabolic stress is predominantly amino acid starvation and when this occurs, RelA produces high levels of (p)ppGpp which has widespread effects on cell metabolism and gene transcription, termed the stringent response. The *relA* gene encodes a bifunctional RelA/SpoT homologue (RSH), and contains 4 domains including a hydrolysis domain that degrades (p)ppGpp and a synthetase domain that synthesises it. Mwagi *et al.* introduced *mecA* into several MSSA strains and found the majority of cells then expressed low level heterogenous methicillin resistance. A small proportion of cells expressing homogenous resistance were sequenced and found to contain a point mutation in *relA* after the synthetase domain, resulting in a premature stop codon and inactivation of the downstream hydrolysis domain. This mutation led to increased (p)ppGpp levels and therefore a constitutively active stringent response, as well as increased β-lactam resistance [71]. A relationship between the signalling molecules, (p)ppGpp and c-di-AMP, was discovered by transcriptional analysis of cells with high levels of c-di-AMP . (p)ppGpp was shown to competitively inhibit GdpP activity. Therefore, under stress conditions that trigger the stringent response and (p)ppGpp synthesis, GdpP activity is inhibited and leads to elevated c-di-AMP levels [71].

In addition to intrinsic factors, it must be acknowledged that the expression of

methicillin resistance is known to be strongly influenced by external factors such as temperature, osmolarity, the availability of divalent cations, calcium and magnesium, and the composition of the growth medium. This fact is routinely utilised in antimicrobial susceptibility tests, for example by supplementing growth medium with 2% NaCl or adding additional cations where required, and lowering the temperature to 35°C, to enable the phenotypic expression of antibiotic resistance.

1.6.6 Staphylococcal lipoproteins: function and biosynthesis

Bacterial lipoproteins were first discovered in *E. coli* in 1973 [72], and since then they have been linked to a wide variety of functions ranging from nutrient acquisition [73], signal transduction [74], respiration [75], protein folding [65], virulence [76], antibiotic resistance [77] and host invasion [78]. In Gram-positive bacteria lipoproteins are attached to the cytoplasmic membrane by their lipid anchor while the protein portion can extend into the cell wall and beyond [79, 80]. Using a combination of protein prediction models and experimental validation, the number of lipoproteins in *S. aureus* is estimated to be between 55 and 70 [81]. In MRSA strain USA300, 67 lipoproteins have been identified [79] and a large number were found to be involved in ion and nutrient transport. Several lipoproteins were ascribed miscellaneous functions including sex pheromone biosynthesis, respiration, chaperone-folding, and protein translocation. Fifteen were classified as tandem lipoproteins, of which 9 are “lipoprotein-like” lipoproteins, known to play a role in host cell invasion [78] while the function of several lipoproteins remains unknown.

Lipoproteins are translated in the form of precursor preprolipoproteins and contain a type type II signal peptide [82]. This signal peptide is recognised by translocation machinery in the cell, and preprolipoproteins are translocated to the cytoplasmic membrane, mainly by the general secretory (Sec) pathway [83]. The first enzyme in the processing pathway is diacyl glycerol transferase (Lgt) and it covalently attaches a diacylglycerol molecule that can anchor the lipoprotein in

the membrane [84]. Next, a type II signal peptidase called lipoprotein signal peptidase (LspA) cleaves the signal peptide [85]. Lgt and Lsp are conserved in all bacterial species. In Gram-negative bacteria, a third step is catalysed by the enzyme N-acyl transferase (Lnt). Although an Lnt enzyme or homolog has not been found in *S. aureus*, the identification of N-acylated lipoproteins indicates that N-acylation does occur in *S. aureus*. Recent work by Gardiner *et al.* (2020) has identified a 2-component regulatory system in *S. aureus*, LnsA and LnsB, which are reported to be necessary for acylation [86], although the mechanism remains to be discovered. Mutations in the *lgt* and *lspA* genes do not impact viability in Gram-positive bacteria [87], but are associated with growth, immunogenicity [88] and virulence [76] phenotypes.

1.6.7 TCA cycle

All of the macromolecules required for bacterial growth can be synthesised from 13 intermediates originating from central metabolism in the Embden-Meyerhof-Parnas (glycolytic) pathway, pentose phosphate pathway and the Tricarboxylic Acid (TCA) cycle. *S. aureus* possesses all three pathways although it lacks a glyoxylate shunt [89]. Carbohydrate catabolism occurs mainly via the glycolytic and pentose phosphate pathways, and TCA cycle gene activity is largely repressed by carbon catabolite repression when glucose is available [90]. Repression is not mediated by glucose directly but by early glycolysis intermediates glucose-6-phosphate and fructose-1,6-bisphosphate. During glycolysis, one molecule of glucose generates two molecules of pyruvate, while reducing two molecules of NAD^+ to NADH. The pyruvate generated by glycolysis is processed differently depending on environmental conditions, particularly oxygen availability. Under anaerobic conditions, pyruvate is reduced to lactic acid, with NADH serving as the electron donor, and the resulting reoxidation of NADH to NAD+ allows glycolysis to continue [90]. During aerobic conditions, pyruvate is oxidised to acetyl CoA and CO_2 by pyruvate dehydrogenase and acetyl-coA can be further oxidised to generate ATP and acetic acid.

Due to catabolite repression, these processes lead to accumulation of metabolites in the culture media in particular acetic acid and lactic acid. Exponential growth ceases as carbohydrates are depleted from the medium, and also due to the accumulation of lactic or acetic acid [89].

Post-exponential growth occurs as TCA cycle gene activity is de-repressed due to the depletion of glucose, and *S. aureus* reimports metabolites such as acetic acid and lactic acid which will serve as non-preferred carbon sources for TCA cycle activity. Acetyl-CoA is formed by the coupling of acetate to coenzyme A by acetyl-CoA synthetase in an ATP-dependant reaction and at this stage acetyl-CoA can enter the TCA cycle. Unlike many Gram-positive bacteria, *S. aureus* has a complete TCA cycle, although it lacks a glyoxylate shunt. This means that for every two carbons entering the TCA cycle, two carbons are lost as CO_2. For this reason, amino acids must be used as carbon donors to maintain the cycle. Overall, TCA cycle catabolism generates α-ketoglutarate, succinyl-CoA, oxaloacetate, ATP, and reducing potential in the form of NADH+ while consuming amino acids in the process [90].

1.7 Project Work

I was involved in the initial screen of the Nebraska Transposon Mutant Library, where I screened approximately 600 strains by cefoxitin disk diffusion testing. During this screen I noted several mutants which had altered oxacillin resistance versus the parent strain JE2. The *lspA* mutant NE1757, was one such strain, and I was responsible for characterising this mutant as described in chapter 3. Further work has been carried out by Dr Merve Zeden since the completion of my thesis.

Another mutant which I noted during the initial screen is the *cycA* permease mutant NE810. I worked on this strain in the early stages of the project performing transductions and synergism assays. A large body of work was then carried out by Dr Laura Gallagher and also our co-workers and collaborators, and the cycA manuscript was published. Following this publication, I worked on the next phase of the project which involved searching for a 2nd alanine permease. My contributions to the overall project *cycA* project are detailed in chapter 4.

The altered resistance phenotype of *sucC* mutant NE569 was noted by Dr Chris Campbell while screening the NTML. He carried out the initial work on the project while I was involved in the latter half. Dr Campbell performed a body of work including growth, susceptibility and complementation experiments, and the creation of double mutants and HORs. I confirmed the growth and MIC experiments, during which time I discovered and characterised the suppressor mutants. I prepared samples for our collaborators to use for proteomics and cell wall analysis, and based on the proteomics results I carried out the autolytic activity assays. Our detailed contributions are noted in Chapter 5 and in publication.

Chapter 2: Accumulation of succinyl-CoA perturbs the MRSA succinylome and is associated with increased susceptibility to β-lactam antibiotics

Chapter 2:

Accumulation of succinyl-CoA perturbs the MRSA succinylome and is associated with increased susceptibility to β-lactam antibiotics

Christopher Campbell[1‡], Claire Fingleton[1‡], Merve S. Zeden[1], Emilio Bueno[2], Laura A. Gallagher[1], Dhananjay Shinde[3], Jongsam Ahn[3], Heather M. Olson[4], Thomas L. Fillmore[4], Joshua N. Adkins[4], Fareha Razvi[3], Kenneth W. Bayles[3], Paul D. Fey[3], Vinai C. Thomas[3], Felipe Cava[2], Geremy C. Clair[4] and James P. O'Gara[1‡]

[1]Microbiology, School of Natural Sciences, National University of Ireland, Galway, Ireland.

[2]MIMS-Molecular Infection Medicine Sweden, Molecular Biology Department, Umeå University, Umeå, Sweden.

[3]Department of Pathology and Microbiology, University of Nebraska Medical Center, Omaha, Nebraska, USA.

[4]Biological Sciences Division, Pacific Northwest National Laboratory, Richland, Washington.

[‡]These authors contributed equally to this study

*Corresponding author; jamesp.ogara@nuigalway.ie

This chapter has been submitted for publication and my contributions to the final figures are as follows:

Figure 2.1C, 2.1D, 2.1E, 2.1F, 2.1G

Figure 2.2

Figure 2.3C, 2.3D

Figure 2.6B

Figure 2.7A

Table 2.1 (in conjunction with Dr. Chris Campbell)

2.1 Abstract

Penicillin binding protein 2a (PBP2a)-dependent resistance to β-lactam antibiotics in MRSA is regulated by the activity of the tricarboxylic acid (TCA) cycle via a poorly understood mechanism. We report that mutations in *sucC* and *sucD*, but not other TCA cycle enzymes, negatively impact β-lactam resistance without changing PBP2a expression. Increased intracellular levels of succinyl-CoA in the *sucC* mutant significantly perturbed lysine succinylation in the MRSA proteome. Suppressor mutations in *sucA* or *sucB*, responsible for succinyl-CoA biosynthesis, reversed *sucC* mutant phenotypes. The major autolysin (Atl) was the most succinylated protein in the proteome, and increased Atl succinylation in the *sucC* mutant was associated with loss of autolytic activity. Although PBP2a and PBP2 were also among the most succinylated proteins in the MRSA proteome, peptidoglycan architecture and cross linking were unchanged in the *sucC* mutant. These data reveal that perturbation of the MRSA succinylome impacts two interconnected cell wall phenotypes, leading to repression of autolytic activity and increased susceptibility to β-lactam antibiotics.

2.2 Importance

mecA-dependent methicillin resistance in MRSA is subject to regulation by numerous accessory factors involved in cell wall biosynthesis, nucleotide signalling and central metabolism. Here, we report that mutations in the TCA cycle gene, *sucC*, increased susceptibility to β-lactam antibiotics and was accompanied by significant accumulation of succinyl-CoA, which in turn perturbed lysine succinylation in the proteome. Although cell wall structure and cross-linking were unchanged, significantly increased succinylation of the major autolysin Atl, which was the most succinylated protein in the proteome, was accompanied by near complete repression of autolytic activity. These findings link central metabolism and levels of succinyl-CoA to the regulation of β-lactam antibiotic resistance in MRSA through succinylome-mediated control of two interlinked cell wall

phenotypes. Drug-mediated interference of the SucCD-controlled succinylome may help overcome β-lactam resistance.

2.3 Introduction

Staphylococcus aureus can establish infections in humans in a wide range of metabolic niches due to several signal transduction pathways, as well as virulence genes encoded in its genome. Significant advances have been made in the study of bacterial virulence factors and their functions in human disease. However, we have only just begun to understand the metabolic pathways required for bacterial proliferation in the host, and their contribution to antibiotic resistance.

The *blaZ*-encoded β-lactamase hydrolyses the β-lactam ring in penicillin, conferring penicillin resistance in *S. aureus* [31]. Methicillin resistance is mediated by the alternative penicillin-binding protein, PBP2a, encoded by *mecA* [91] located on a mobile genetic element, the Staphylococcal chromosome cassette (SCC*mec*) [32, 92]. PBP2a has low affinity for β-lactam antibiotics, and thus is able to crosslink peptidoglycan (PG) strands even in the presence of β-lactam antibiotics, and in this manner confers resistance [91]. Methicillin resistant *S. aureus* (MRSA) strains are resistant to methicillin as well as all the other β-lactam antibiotics [31, 91] consequently making infections with MRSA difficult to treat.

β-lactam resistance in *S. aureus* is typically expressed heterogeneously within a given population [71]. The majority of cells within a heterogeneous population exhibit susceptible or intermediate resistance to β-lactams. A sub-population of approximately 0.1% can survive antibiotic treatment and upon re-exposure to the antibiotic, a homogeneously resistant population emerges [71]. The mechanisms underpinning this switch from heterogeneous resistance (HeR) to homogenous resistance (HoR) are associated with accessory mutations outside *mecA* [93]. High level β-lactam resistance is accompanied by significant energy demands that impose a fitness cost on the cell [40, 42].

The activity of the tricarboxylic acid (TCA) cycle is an important source for the generation of NADH, and therefore membrane potential during aerobic respiration. Additionally, the TCA cycle generates metabolic intermediates that

are then used in various other pathways in the cell. The genes encoding enzymes for the TCA cycle are repressed when preferred nutrients, such as glucose remain available in the surrounding medium [94]. Once post-exponential growth is reached and glucose is depleted from the medium, TCA cycle gene expression is de-repressed in *S. aureus* [95-97]. The activity of the TCA cycle has previously been linked to β-lactam resistance in *S. epidermidis* where a dysfunctional TCA cycle is common among clinical isolates and is associated with alterations in the cell envelope and increased tolerance to β-lactams [98]. In *S. aureus*, TCA cycle activity regulates ATP levels, which controls tolerance to several antibiotics, including β-lactams [97]. Increased TCA cycle activity to fuel cell wall biosynthesis has also been shown to accompany mutations that enable the transition from the HeR to HoR phenotypes [99, 100]. Furthermore, disruption of the TCA cycle via mutations in *acn* and *citZ* has been reported to block the production of HoR mutants [99, 100].

Post-translational modification (PTM) of proteins is one of the most effective mechanisms in diversifying protein function and regulation [101]. PTMs can change the charge and structure of a protein, thus affecting activity as well as ability to interact with other proteins/binding partners [102, 103]. Lysine is a basic residue that is critical for protein structure and function [104]. The side chain of lysine in particular can be modified by a variety of PTMs including phosphorylation [105], succinylation [106-108], ubiquitination [109], methylation [110], acetylation [101, 111] and lipoylation [112]. Relatively little is known about PTMs in *S. aureus* metabolism and antibiotic resistance, and advances in our understanding of these systems will generate new insights into fundamental cellular processes and virulence mechanisms, and potentially identify new therapeutic targets.

In this study, we report that mutations in the succinyl-CoA synthetase genes, *sucC* and *sucD*, lead to increased susceptibility to β-lactam antibiotics in MRSA strain JE2. The impact of these mutations on growth was measured and compared to other TCA cycle mutants. The relative intracellular concentrations of metabolites from the pyruvate node of glycolysis and the TCA cycle were measured, and PG architecture and autolytic activity compared in the *sucC* mutant and wild-type JE2.

We describe the first profile of the lysine succinylome in MRSA and the impact of the *sucC* mutation on the global succinylome. Our data reveal that increased accumulation of succinyl-CoA from the TCA cycle increases susceptibility to β-lactam antibiotics and reduces autolytic activity via perturbation of global lysine succinylation in MRSA.

2.4 Results

2.4.1 TCA cycle genes *sucC* and *sucD* control resistance to β-lactam antibiotics in MRSA.

A screen of the Nebraska Transposon Mutant Library (NTML) [113] revealed that the TCA cycle mutants, NE569 (*sucC*::Tn) and NE1770 (*sucD*::Tn) were more susceptible to cefoxitin (Fig. 2.1A,B) and oxacillin (Fig. 2.1C; Table 2.1) compared to wild-type JE2. Other mutations in TCA cycle genes did not affect susceptibility to oxacillin (Table 2.1), specifically implicating *sucCD*-encoded succinyl-CoA synthetase in β-lactam resistance. The oxacillin MICs of the *sucC* and *sucD* mutants in Mueller-Hinton agar (MHA) were 2-4 μg/ml, compared to 32-64 μg/ml for JE2, as measured using E-test (Fig. 2.1C) and agar dilution assays (Table 2.1). Both mutants also exhibited reduced growth in Mueller-Hinton Broth (MHB) in the absence of antibiotic (Fig. 2.1D). Phage 80α-mediated backcross of the *sucC*::Tn allele into JE2, USA300 FPR3757 [92] and clinical MRSA strain DAR173 [114, 115], was accompanied by increased susceptibility to oxacillin (Fig. 2.1E, F, G; Table 2.1). In addition, both NE569 and NE1770 were successfully complemented by the *sucCD* genes carried on plasmid pLI50 (Table 2.1). The *sucC* and *sucD* genes are separated by only 21bp suggesting that they are organised in an operon (Fig. 2.1H) and that the transposon insertion in *sucC* is likely to have a polar effect on *sucD* expression. Consistent with this, NE569 was complemented by p*sucCD* but not by plasmids carrying *sucC* (p*sucC*) or *sucD* (p*sucD*) alone (Table 2.1, Fig. 2.1F). NE1770 was complemented by *psucCD*, and partially complemented by p*sucD*, but not by p*sucC* (Table 2.1, Fig. 2.1H).

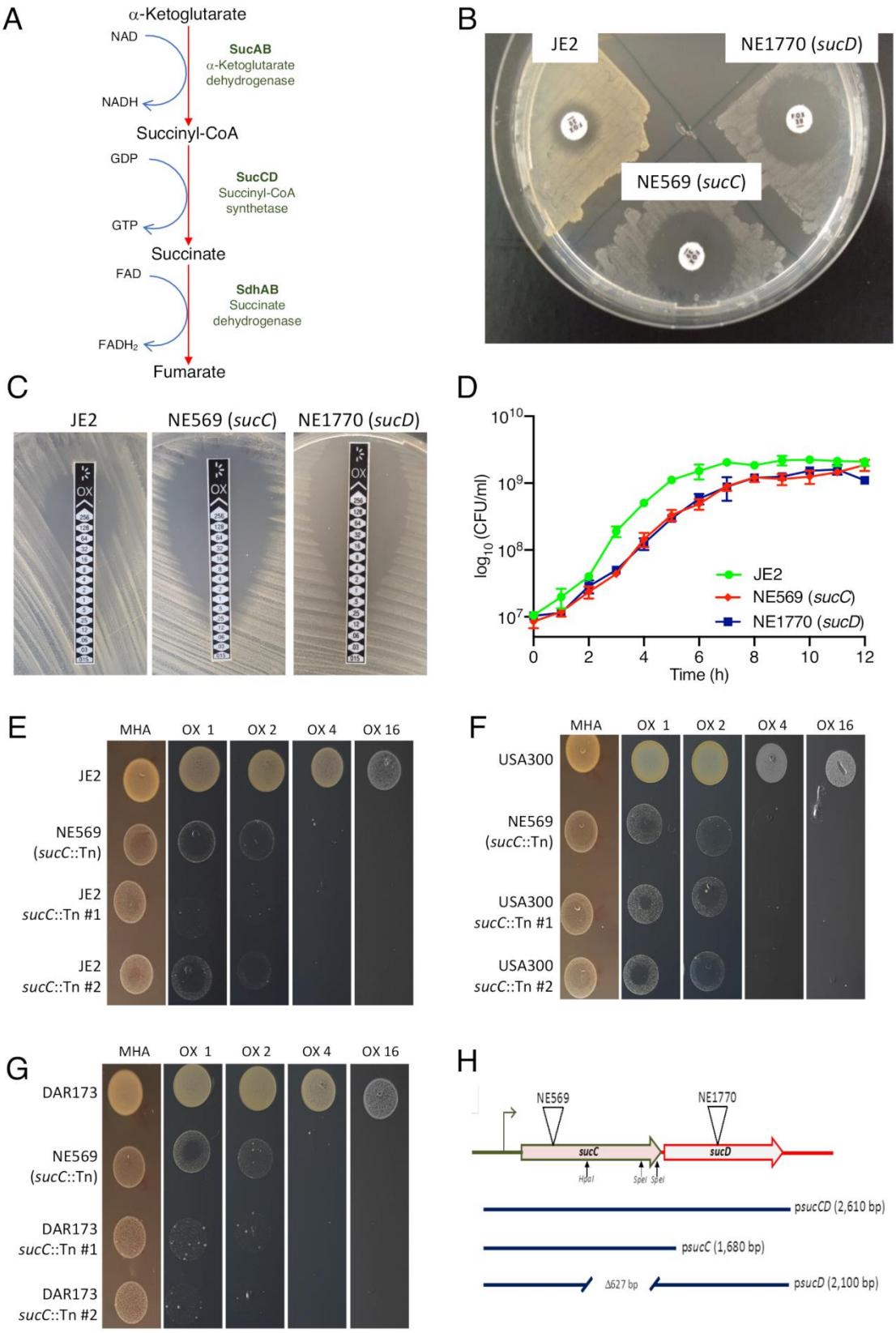

Fig 2.1. Mutation of *sucC* or *sucD* increases β-lactam susceptibility in MRSA and impairs growth in MHB.

A. *sucCD*-encoded succinyl-CoA synthetase catalyses the conversion of succinyl-CoA to succinate in the TCA cycle. SucAB-encoded α-ketoglutarate dehydrogenase

catalyses conversion of α-ketoglutarate to succinyl-CoA and SdhAB-encoded succinate dehydrogenase converts succinate to fumarate. B. Measurement of JE2, NE569 and NE1770 cefoxitin susceptibility by disk diffusion assay. C. E-test measurement of oxacillin minimum inhibitory concentrations for JE2, NE569 and NE1770. D. Growth of JE2, NE569 (*sucC*) and NE1770 (*sucD*) in MHB at 37°C. CFUs were enumerated at 1 hr intervals for 12 h. Data are the average of 3 independent experiments and error bars represent standard deviation. E. JE2, NE569 (*sucC*::Tn) and JE2 *sucC*::Tn transductants #1 and #2 spot-inoculated onto MHA and MHA oxacillin (OX) 1, 2, 4 and 16 μg/ml. F. DAR173, NE569 and DAR173 *sucC*::Tn transductants #1 and #2 spot-inoculated onto MHA and MHA OX 1, 2, 4 and 16 μg/ml. G. USA300, NE569 and USA300 *sucC*::Tn transductants #1 and #2 spot-inoculated onto MHA and MHA OX 1, 2, 4 and 16 μg/ml. These assays were repeated 3 times and a representative image is shown. H. Chromosomal organisation of the *sucCD* locus including location of transposon insertions in NE569 (*sucC*) and NE1770 (*sucD*). The parts of the *sucCD* operon carried on p*sucCD, psucC* and p*sucD* used in complementation experiments are indicated.

Table 2.1. Oxacillin minimum inhibitory concentrations of strains described in this study

Strain and relevant details	Oxacillin MIC (μg/ml)*
Wild type, *sucC* and *sucD* mutants	
JE2	32 - 64
NE569 (*sucC*::Tn)	2 - 4
NE1770 (*sucD*::Tn)	4
Complemented *sucC* and *sucD* mutants	
NE569 p*sucC*	0.5
NE569 p*sucD*	1
NE569 p*sucCD*	32
NE1770 p*sucC*	0.5
NE1770 p*sucD*	16
NE1770 p*sucCD*	32
Transduction of *sucC*::Tn into JE2, DAR173 and USA300	
JE2 *sucC*::Tn transductant #1	2 - 4
JE2 *sucC*::Tn transductant #2	2 - 4
DAR173	64
DAR173 *sucC*::Tn transductant #1	2 - 4
DAR173 *sucC*::Tn transductant #2	2 - 4
USA300	32 - 64
USA300 *sucC*::Tn transductant #1	4
USA300 *sucC*::Tn transductant #2	4
Other TCA cycle mutants	
NE547 (*sucA*)	32
NE1391 (*sucB*)	32
NE626 (*sdhA*)	32
NE808 (*sdhB*)	32

NE594 (*gltA*)	32
NE861 (*acn*)	32
NE491 (*icd*)	32
NE427 (*fumC*)	64
***sucC, sucA, sdhA* double mutants and *sucC* suppressor mutants**	
sucC::Tn-Kan^r	4
sucC/*sucA* double mutant	64
sucC/*sdhA* double mutant	8
sucC suppressor #1	64
sucC suppressor #2	64
sucC suppressor #3	64
***sucC* HoR and *sucC*/*relA* double mutants**	
sucC HoR1	>256
sucC HoR2	>256
NE1714 (*relA*)	>256
sucC/*relA* double mutant	>256

* Measured by agar dilution assays.

2.4.2 HoR mutants of NE569 (*sucC*) have mutations in *relA* and *relQ*.

Expression of the HoR phenotype is dependent on activation of the (p)ppGpp-mediated stringent response [9, 66, 68, 116]. The SucCD, succinyl CoA synthetase, produces GTP, which is a substrate for (p)ppGpp synthesis by the RelA/SpoT homolog (RSH), RelP and RelQ raising the possibility that the NE569 (*sucC*) or NE1770 (*sucD*) mutations may negatively affect (p)ppGpp production. To investigate the possible relationship between the impact of *sucCD* mutations and the stringent response, the ability of JE2, NE569 and NE1770 to produce HoR mutants on Brain Heart Infusion (BHI) agar supplemented with oxacillin 100 µg/ml was compared. Two stable NE569 HoR mutants, designated *sucC* HoR1 and *sucC*

HoR2 with oxacillin MICs >256 μg/ml (Fig. 2.S1A) were genome sequenced. *sucC* HoR1 had a single nucleotide deletion, frameshift mutation in *relA* (Table 2.2, Fig. 2.S1B), while *sucC* HoR2 had a non-synonymous point mutation, resulting in a $A_{178}V$ substitution in RelQ (Table 2.2, Fig. 2.S1C). The N-terminus of RelA contains (p)ppGpp hydrolase and synthase domains, while mutations in the C-terminal domain deregulate synthase activity [117-119]. The NTML *relA* mutant, NE1714, contains a transposon insertion in the C-terminal domain, and is associated with increased β-lactam resistance, presumably due to increased (p)ppGpp synthase activity (Table 2.1). To investigate the impact of the *relA*::Tn mutation on β-lactam susceptibility in NE569, a *relA*/*sucC* double mutant was constructed. First, the Erm^r marker in NE569 was swapped for a Kan^r marker, as described in the methods, to generate *sucC*::Tn-Kan^r. The *sucC*::Kan^r allele was then transduced into NE1714 using phage 80α. Similar to the *sucC* HoR mutants, the oxacillin MIC of the *relA*/*sucC* double mutant was also >256 μg/ml (Table 2.1). RelQ contains a (p)ppGpp synthase domain only, and has previously been implicated in adaptation to vancomycin and ampicillin-induced cell wall stress [120]. A *relQ* mutant is not available in the NTML indicating that this gene may be essential, and that the RelQ $A_{178}V$ substitution in *sucC* HoR2 may enhance ppGpp synthase activity to promote a HoR phenotype. Given that previous studies have demonstrated the role of ppGpp synthase mutations in the HoR phenotype [71, 120, 121], these data suggest that increased β-lactam susceptibility in the *sucCD* mutants is not related to impaired GTP/ppGpp production.

Table 2.2. Genomic changes in NE569 (*sucC*::Tn), *sucC* HoR1, *sucC* HoR2 and *sucC* suppressor mutants #1, #2 and #3.

Strain	Reference Position[1]	Type[2]	Ref.[3]	Allele[4]	Freq.[5]	Av. Quality[6]	Annotations	AA change[7]
NE569 (*sucC*::Tn)	1,247,099 -1,247,100	INS	TA	T-*Tn*-A	100	N/A	*Bursa aurealis* transposon	N/A
sucC HoR1	**994827**	**SNV**	**C**	**T**	**98.4**	**35.5**	**SAUSA300_RS04880, *relQ***	**$Ala_{178}Val$**
sucC HoR2	**1741861**	**DEL**	**A**	**-**	**97.2**	**37.2**	**SAUSA300_RS08665, *relA***	**$Tyr_{418}STOP$**
sucC supp. #1	1,247,099 -1,247,100	INS	TA	T-*Tn*-A	100	N/A	*Bursa aurealis* transposon	N/A
	528,497	SNV	C	A	100	36.8	SAUSA300_RS02515, *tatD* family deoxyribonuclease	$Cys_{242}STOP$
	1,439,926	**SNV**	**G**	**T**	**100**	**37.9**	**SAUSA300_RS07105, *sucA***	**Ser_9STOP**
sucC supp. #2	1,247,099 -1,247,100	INS	TA	T-*Tn*-A	100	N/A	*Bursa aurealis* transposon	N/A
	1,319,786	SNV	A	T	100	36.9	*hflX*	$Ile_{53}Phe$
	1,436,058	**SNV**	**A**	**G**	**100**	**33.1**	**SAUSA300_RS07100, *sucB***	**$Ile_{361}Thr$**
sucC supp. #3	1,247,099 -1,247,100	INS	TA	T-*Tn*-A	100	N/A	*Bursa aurealis* transposon	N/A
	1,436,186-1,436,231	**DEL**	**T-A**	**D46bp[8]**	**100**	**N/A**	**SAUSA300_RS07100, *sucB***	**N/A**

[1]Reference position: Position in the USA300 FPR3757 genome sequence (NC_007793.1).

[2]Type of mutation: SNV, single nucleotide variant; INS, insertion; DEL, nucleotide deletion.

[3]Ref: Nucleotide base in the USA300 FPR3757 reference genome.

[4]Allele: Nucleotide base at the same position in the sequenced strain.

[5]Freq.: % Frequency at which SNV/INS was found in the sequenced strain.

[6]Av. Quality: Average quality score. Higher scores indicate a smaller probability of error. A quality score of 30 represents an error rate of 1 in 1000, with a corresponding call accuracy of 99.9%

[7]AA change denotes the resulting amino acid change in the protein found in the sequenced strain as compared to the WT reference strain.

[8]Forty-six base pair deletion in *sucB* (AAATTAGCAATTTCTGCTTCGATTTCTGCAAAATTCTTTTTATC).

2.4.3 Mutations in *sucA* and *sucB* reverse NE569 (*sucC*) mutant phenotypes.

Faster-growing, more pigmented suppressor mutants were readily observed among colonies of NE569 grown on MHA (Fig. 2.2A). Three of these suppressor mutants were isolated and comparison of their genomic DNA sequences to NE569 identified mutations in either *sucA* or *sucB* (Table 2.2). The *sucA* gene, which encodes 2-oxoglutarate dehydrogenase E1 subunit, is found in a 2-gene operon with *sucB*, which encodes dihydrolipoyl succinyltransferase E2 subunit. Together SucAB catalyse the synthesis of succinyl-CoA, the substrate for SucCD complex (Fig. 2.1A). A single nucleotide variant (SNV) leading to Ser9STOP codon in SucA was present in *sucC* suppressor #1, *sucC* suppressor #2 had a SNV leading to a Ile361Thr substitution in SucB and *sucC* suppressor #3 had a 46bp deletion in *sucB*. The possible significance of SNVs in the *tatD* and *hflX* genes of *sucC* suppressors #1 and #2, respectively, is unknown. However, all 3 *sucC* suppressor mutants exhibited wild-type levels of oxacillin resistance (Table 2.1, Fig. 2.2B) implicating the *sucA* and *sucB* mutations in this phenotype.

The *sucC* suppressor #1 mutant, which was chosen for more detailed analysis, also exhibited wild-type growth in MHB (Fig. 2.2C). Similarly, in chemically defined media supplemented with glucose (CDMG), the NE569 growth defect was reversed by the *sucA* suppressor mutation (Fig. 2.2D). However, both NE569 and *sucC* suppressor #1 were unable to grow in chemically defined media lacking glucose (CDM) (Fig. 2.2E), which is consistent with previous results showing growth in CDM is dependent on an intact TCA cycle [94].

Extension of these experiments to NTML mutants revealed no change in oxacillin susceptibility in NE547 (*sucA*) and NE1391 (*sucB*) (Table 2.1). Using phage 80α to

disrupt *sucA* in the *sucC* mutant restored wild-type colony morphology, oxacillin resistance and growth (Fig. 2.3A, B, C). For control purposes, a *sucC*/*sdhA* double mutant was also constructed. The succinate dehydrogenase complex SdhAB catalyses the conversion of the SucCD product, succinate, to fumarate (Fig. 2.1A). Mutations in *sdhA* or *sdhB* did not impact susceptibility to oxacillin (Table 2.1) and the *sucC*/*sdhA* double mutant exhibited the same colony morphology, oxacillin resistance and growth characteristics as the *sucC* mutant (Fig. 2.3A, B, C). Taken together, these data demonstrate that mutations in *sucA or sucB* overcome the β-lactam susceptibility and growth defects of the *sucC* mutant.

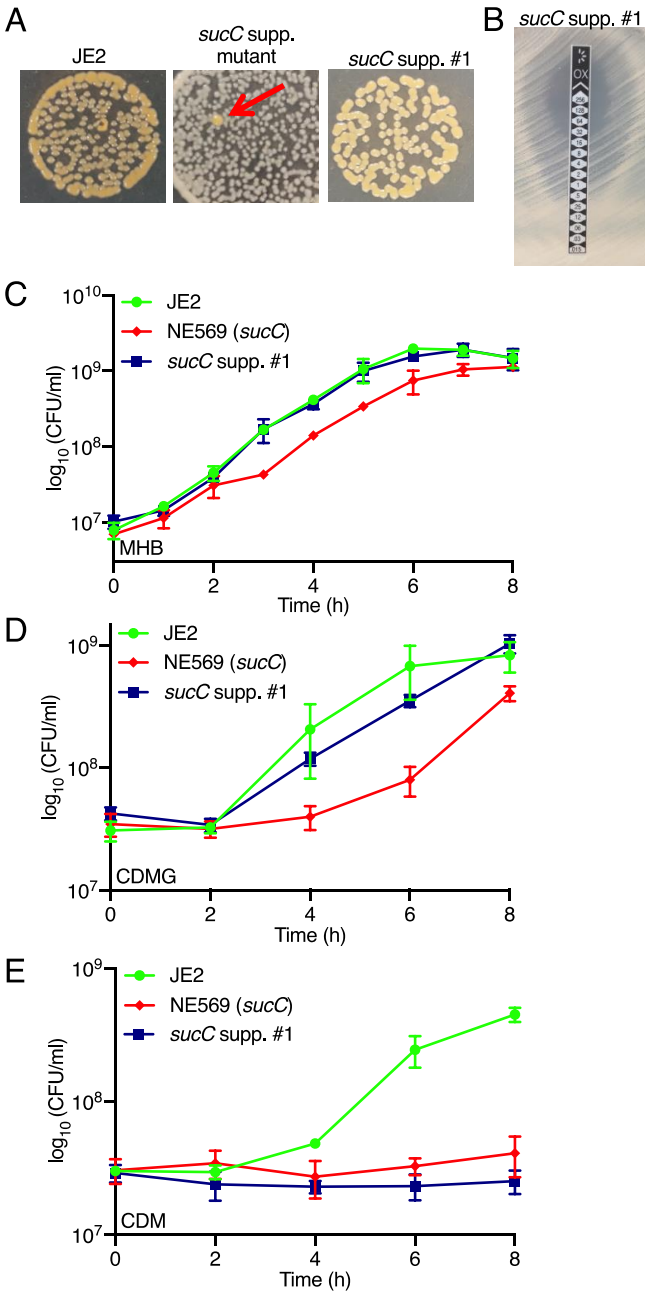

Fig. 2.2. *sucC* suppressor mutation is accompanied by restoration of wild-type colony morphology, oxacillin resistance and growth in MHB and CDMG, but not CDM.

A. JE2, NE569 (*sucC*), and isolated *sucC* suppressor #1 grown on MHA for 48 h at 37°C. Red arrow indicates faster growing, more pigmented suppressor mutant of NE569. B. M.I.C. Evaluator measurement of oxacillin MIC for *sucC* suppressor #1. Three independent measurements were performed and a representative image is shown. C, D and E. Growth of JE2, *sucC* (NE569) and *sucC* suppressor #1 in MHB (C), CDMG (D) or CDM (E). Growth was measured by enumerating the number of CFU/ml at 2 h intervals in flask cultures. The data presented are the average of at least 3 independent experiments and error bars represent standard deviation.

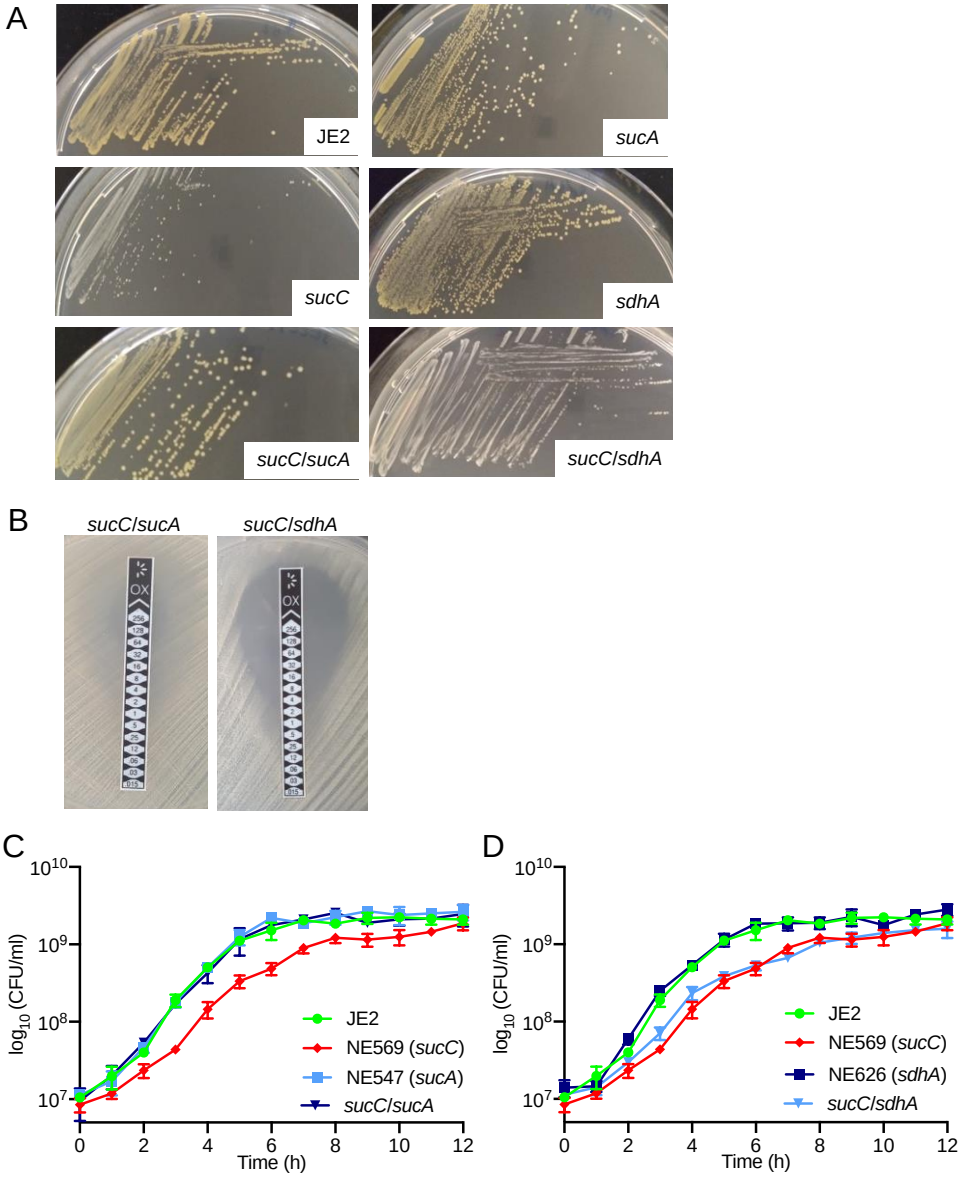

Fig. 2.3. Mutation of *sucA*, but not *sdhA*, in the *sucC* background restores wild-type colony morphology, β-lactam resistance and growth phenotypes.

A. Colony morphologies of JE2, NE569 (*sucC*), NE547 (*sucA*), NE626 (*sdhA*), *sucC*/*sucA* and *sucC*/*sdhA* grown for 24 h on MHA. B. M.I.C.Evaluator measurement of oxacillin MICs for the *sucA/sucC* and *sdhA/sucC* strains. Three independent measurements were performed for each strain and a representative image is shown. C. Growth of JE2, NE569 (*sucC*), NE547 (*sucA)* and *sucA*/*sucC.* D. Growth of JE2, NE569 (*sucC*), NE626 (*sdhA)* and *sdhA*/*sucC.* Growth experiments were performed in MHB at 37°C, and CFUs/ml enumerated at 1 h intervals for 12 h. All data presented are the average of 3 independent experiments and error bars represent standard deviation.

2.4.4 Succinyl-CoA is significantly increased in the *sucC* mutant.

LC-MS/MS was used to quantify the accumulation of intracellular metabolites from the TCA cycle and the pyruvate node of glycolysis in NE569 (*sucC*), NE569 p*sucCD* and *sucC* suppressor strain #1 collected from late exponential phase cultures grown aerobically in MHB. Consistent with the predicted impact of a *sucC* mutation, succinyl-CoA levels were significantly increased in NE569 (Fig. 2.4). Furthermore, accumulation of succinyl-CoA in the *sucC* mutant was accompanied by a concomitant decrease in the levels of succinate (Fig. 2.4). Succinyl-CoA was reduced to wild-type levels in *sucC* suppressor #1 and the complemented *sucC* mutant, implicating accumulation of this metabolite in *sucC*-dependent modulation of β-lactam resistance. Levels of α-ketoglutarate were also significantly increased in *sucC* suppressor #1 compared to JE2, NE569 and NE569 p*sucCD* (Fig. 2.4), supporting the conclusion that the SucA Ser_9STOP mutation in this strain has impaired α-ketoglutarate dehydrogenase activity. Mutation of *sucC* also impacted the glycolytic pathway as evidenced by significantly reduced phosphoenol pyruvate (PEP) and increased levels of pyruvate (Fig. 2.4). Levels of acetyl-CoA were also significantly reduced in the *sucC* mutant (Fig. 2.4), as were citrate and isocitrate, albeit not significantly, further demonstrating the impact of this mutation on TCA cycle homeostasis.

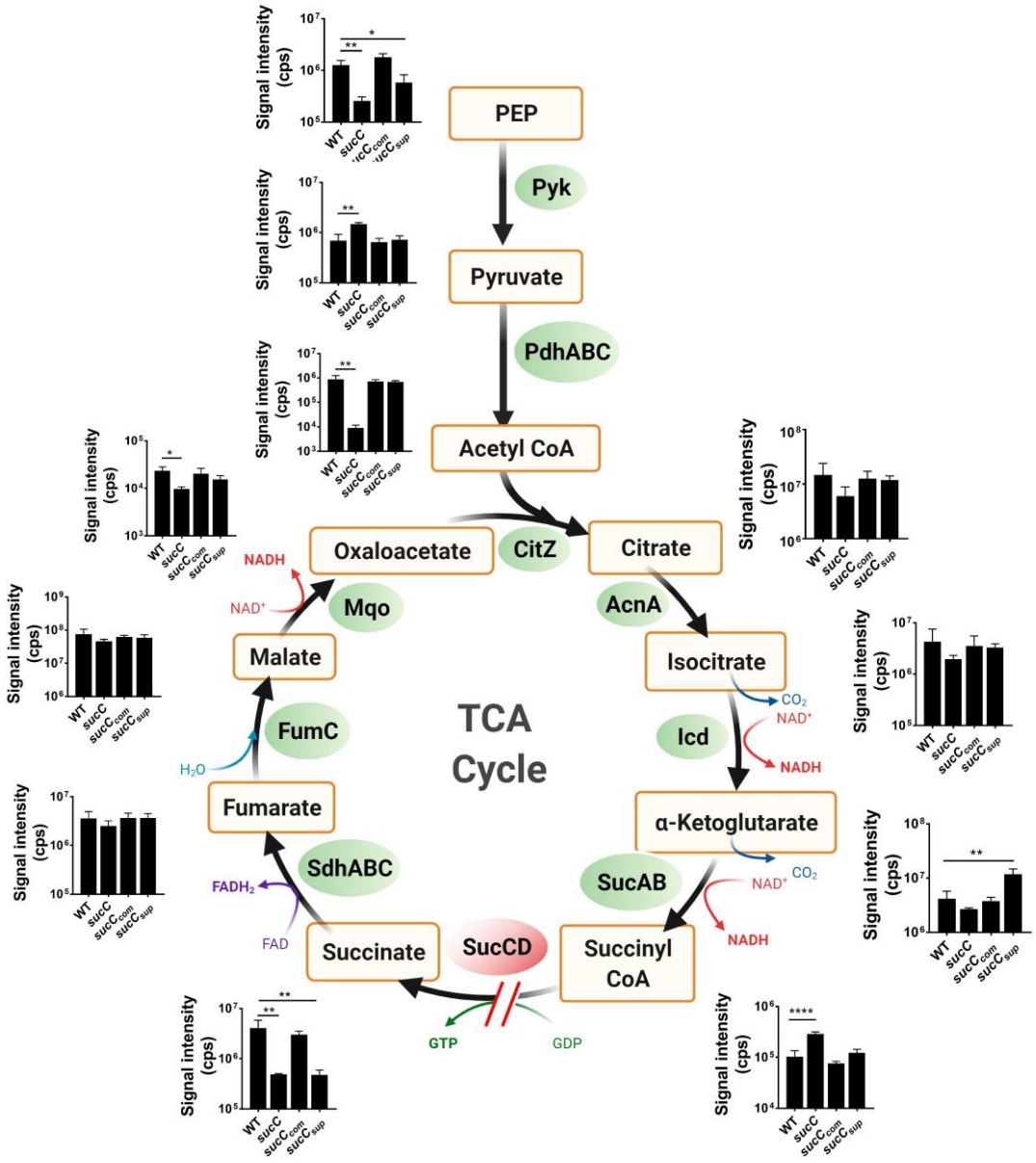

Fig. 2.4. Mutation of *sucC* alters the central metabolism in *S. aureus*. JE2, NE569 (*sucC*), *sucC*$_{comp}$ (NE569 p*sucCD*) and *sucC*$_{supp}$ (*sucC* suppressor #1, which has a SucA Ser$_9$STOP mutation) were grown aerobically in MHB.

Cells were harvested in the exponential phase (6 h), and intracellular metabolites associated with the pyruvate node and TCA cycle were analyzed using LC-MS/MS. The metabolites included in the analysis are indicated in the TCA cycle pathway, along with their associated enzymes. The slit arrow indicates a predicted break in the TCA cycle due to mutation of *sucC* in NE569. n=3; cps, count per second. The image was created using Biorender.com.

2.4.5 Mutation of *sucC* significantly impacts the global MRSA proteome.

Similar to acetyl-CoA, succinyl-CoA can react with the NH_3^+ group located on the lysine side-chain resulting in the succinylation of this residue in a pH and concentration-dependent manner [106, 123]. This PTM has been shown to occur extensively in prokaryotes [107, 108, 123-126] and a recent study demonstrated that a murine succinate dehydrogenase mutation altered succinyl-lysine distribution in chromatin [127]. Here, the accumulation of succinyl-CoA measured in the *sucC* mutant NE569 prompted us to investigate the global distribution of succinyl-lysines by analysing the bacterial proteome and succinylome using LC-MS/MS.

For these experiments, cells were collected from JE2 and NE569 cultures grown to exponential and stationary phase as described in the methods. The global proteome analysis, workflow summarised in Fig. 2.S2A, quantified approximately 90% (2,283) of the 2,607 predicted *S. aureus* proteins. After principal component analysis and batch correction, JE2 early exponential and exponential phase samples were found to be largely the same, but significantly different to JE2 stationary phase samples (Fig. 2.S2B). Compared to JE2, 381 proteins were significantly upregulated in NE569 during exponential growth (Fig. 2.S2C) and 330 proteins were upregulated in stationary phase (Fig. 2.S2D), including proteins involved in PG biosynthesis, cell wall organization and cell division. Significantly downregulated proteins in NE569 during exponential (307 proteins) and stationary phase (187 proteins) growth included virulence regulators (e.g., SaeS, SaeR, SarR, SarZ, AgrB), components of type-VII secretion systems, hemolysins, leukotoxins, and immune evasion/inactivation proteins (e.g., Spa, Sbi, SraP, PsmA1) (Fig. 2.S2C, D), suggesting that virulence of the *sucC* mutant may be attenuated.

2.4.6 Global patterns of protein succinylation were increased in the *sucC* mutant.

In total 9,545 peptides with succinylated lysine residues ($p<0.05$, A-Score>13)[128, 129] were identified. Peptides that could not be quantified in >75% of samples were disregarded, leaving 5,762 succinylated-lysine peptides derived from 1,000 unique proteins. The abundance of approximately 58% of the succinylated peptides (3,340) was significantly modulated (ANOVA adjusted $p<0.05$) (Fig. 2.5A). Hierarchical clustering revealed that while most of the changes in the succinylome were growth phase-dependent, succinylated peptides in Clusters 1 and 2 were more abundant in NE569 compared to JE2 in stationary phase and were associated with “penicillin binding”, “cytolysis”, “cell wall”, “amidase activity”, “transferase activity transferring acyl-groups”, “response to oxidative stress” and “metalloendopeptidase activity” (Fig. 2.5B).

The median number of succinylated peptides per protein was 3, and 670 proteins had <5 succinylated peptides. Intriguingly, the top 40 most succinylated proteins (Fig. 2.5C) had >20 succinyl peptides each, which represented >20% of all succinylated peptides. Consistent with a recent study in *S. epidermidis* [108], numerous proteins involved in glycolysis and the TCA cycle were highly succinylated. The major autolysin (Atl) was the most succinylated protein in JE2 and NE569, with the *mecA*-encoded penicillin binding protein 2a (PBP2a) and PBP2 also among the 40 most succinylated proteins (Fig. 2.5C). Atl had 102 succinylated peptides quantified, mapping to 82 succinyl-lysine sites, of which 12 showed significantly higher levels of succinylation in the *sucC* mutant in stationary phase (Student’s t-test $p<0.05$) (Fig. 2.5D).

Globally there were many differences between the succinylomes of JE2 and *sucC*, as shown in Tables 6.1 and Table 6.2. Table 6.1 lists the 296 proteins that have increased succinylation of 1 or more lysine residues in *sucC* versus JE2. Conversely Table 6.2 shows the 168 proteins that have increased succinylation of 1 or more lysine residues in JE2 compared to sucC. Given the large number of proteins that have differences in succinylation patterns between JE2 and sucC, the 21 peptides

shown in Table 6.3 provides a focused look at the 21 peptides that contain lysine residues with 2-fold or greater difference in succinylation between JE2 and sucC.

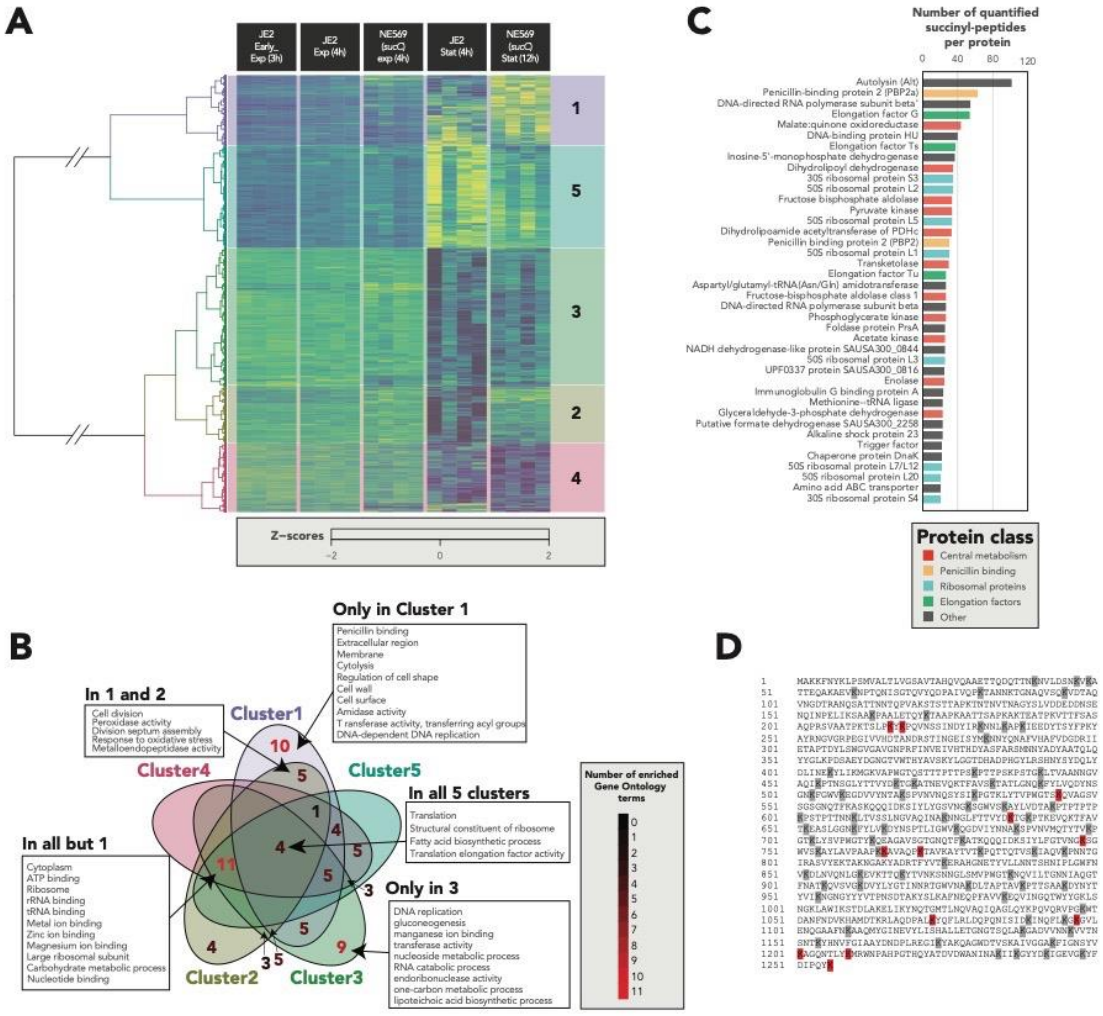

Fig. 2.5. Mutation of *sucC* perturbs lysine succinylation in the *S. aureus* proteome.

A. Heatmap depicting the quantifiable succinyl-lysine peptides significantly modulated (ANOVA adjusted p<0.05) derived from the proteomes of JE2 and NE569 (*sucC*) collected during early exponential, exponential and stationary phase growth. The hierarchical clustering was performed with the Ward method and Euclidean distances. B. Gene ontology enrichment analysis of succinylated peptides within and shared between heat map clusters. C. The 40 most succinylated proteins in *S. aureus* as indicated by the number of succinylated peptides per protein. D. Amino acid sequence of Atl highlighting all succinylated lysine residues in grey and lysine residues with significantly increased succinylation in NE569 (*sucC*) versus JE2 in red.

2.4.7 Mutation of *sucC* does not affect *mecA* transcription, PBP2a expression or peptidoglycan (PG) structure and cross-linking.

Lightcycler RT-qPCR analysis revealed that the relative expression of *mecA* was not significantly affected in NE569 compared to JE2 in BHI media or in BHI media supplemented with oxacillin 0.5 µg/ml (Fig. 2.6A). Western blotting also revealed similar PBP2a levels in JE2, NE569 and NE569 p*sucCD* grown in MHB with 2% NaCl at 35°C supplemented with 0.5 µg/ml oxacillin (Fig. 2.6B). The MSSA strain 8325-4 was included as a *mecA*-negative control.

Quantitative PG compositional analysis was performed using UPLC analysis of muramidase-digested muropeptide fragments extracted from exponential or stationary phase cultures of JE2, NE569 and *sucC* suppressor #1 grown in MHB or MHB supplemented with oxacillin 3 µg/ml or 32 µg/ml. The PG profiles of all 3 strains were similar under all growth conditions tested (Fig. 2.S3). Supplementation of MHB with oxacillin was associated with significant changes in muropeptide oligomerization and reduced cross-linking, but these effects were the same in all strains (Fig. 2.6C). Interestingly, although PBP2a is the second most succinylated protein in the *S. aureus* proteome (Fig. 2.5C) and contains 40 succinylated lysine residues, only the lysine residue K_{47}, which is not located near to the enzyme active site or dimerization domains, showed increased succinylation in the *sucC* mutant (MassIVE ID: MSV000086976 and MassIVE ID: MSV000086971), perhaps making it unlikely that this PTM influences the transpeptidase activity of this enzyme in NE569.

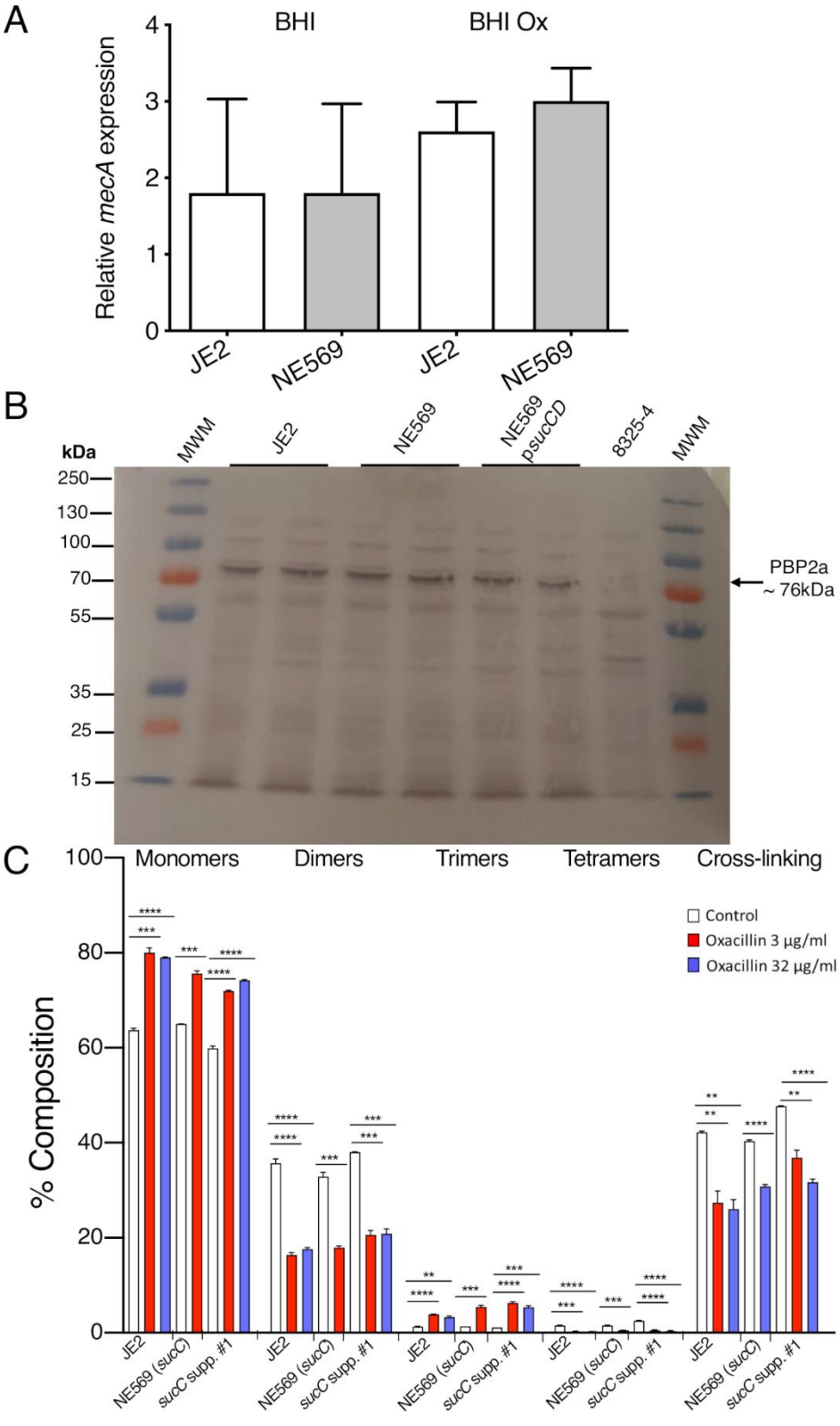
A
BHI
BHI Ox
Relative mecA expression
4
3
2
1
0
JE2
NE569
JE2
NE569
B
kDa
MWM
JE2
NE569
NE569 psucCD
8325-4
MWM
250
130
100
70
55
35
25
15
PBP2a
~ 76kDa
C
Monomers
Dimers
Trimers
Tetramers
Cross-linking
% Composition
100
80
60
40
20
0
Control
Oxacillin 3 µg/ml
Oxacillin 32 µg/ml
JE2
NE569 (sucC)
sucC supp. #1

Fig. 2.6. Mutation of *sucC* does not affect *mecA* transcription, PBP2a expression or peptidoglycan structure.

A. Comparison of *mecA* transcription relative to *gyrB* measured by LightCycler RT-qPCR in JE2 and NE569 (*sucC*) grown to exponential phase in BHI or BHI supplemented with 0.5 µg/ml oxacillin. Experiments were repeated at least 3 times and standard deviation shown. B. Western blot of PBP2a in JE2, NE569 (*sucC*), NE569 p*sucCD* and MSSA strain 8325-4 (negative control). Total protein was extracted from cells collected during the exponential phase of growth in MHB 2% NaCl supplemented with 0.5 µg/ml oxacillin, with the exception of 8325-4 which was grown without oxacillin. Eight µg of total protein was separated on a 7.5% Tris-Glycine gel, transferred to a PVDF membrane and probed with anti-PBP2a antibody (1:1000 dilution), followed by HRP-conjugated protein G (1:2000 dilution) and colorimetric detection with the Opti-4CN Substrate kit. Three independent experiments were performed and a representative blot is shown. C. Relative proportions of cell wall muropeptide fractions based on oligomerization and relative cross-linking efficiency in peptidoglycan extracted from JE2, NE569 (*sucC*) and *sucC* suppressor #1 grown to exponential phase in MHB or MHB supplemented with oxacillin 3 µg/ml or 32 µg/ml. PG analysis from NE569 (*sucC*) is shown only at oxacillin 3 µg/ml because 32 µg/ml exceeds its MIC. Each profile shown is a representative of 3 biological replicates. Significant differences were determined using Students t-test (**P < .01; ***P < .001; ****P<.0001).

2.4.8 Mutation of *sucC* does not impact susceptibility to the lipoteichoic acid synthase (LtaS) inhibitor Congo red or the alanylation inhibitor D-cycloserine (DCS).

Experiments comparing the susceptibility of JE2 and NE569 to Congo red revealed no differences (Fig. 2.S4). Similarly the DCS MIC for JE2 (32 μg/ml) was not significantly different to NE569, NE569 psucCD, or sucC suppressor #1, all of which had DCS MICs of 16-32 μg/ml. Congo red is a selective inhibitor of LtaS activity [130], while DCS blocks the D-alanine racemase and D-alanine ligase enzymes required for production of D-alanine [131, 132], an important precursor for PG, wall teichoic acid (WTA) and lipoteichoic acid (LTA) biosynthesis. Our data already showed that PG structure was unaffected by the sucC mutation (Fig. 2.6C) and these observations further suggest that altered expression or stability of WTA and LTA may not be involved in the reduced β-lactam susceptibility of NE569.

2.4.9 Autolytic activity is impaired in the *sucC* mutant.

The 12 lysine residues in Atl that exhibited increased levels of succinylation in the sucC mutant were evenly distributed throughout the protein, including within the amidase and glucosaminidase domains (Fig. 2.5D). To investigate if altered succinylation of Atl impacted its enzymatic activity, Triton X-100-induced autolysis was compared in JE2, NE569, NE569 p*sucCD*, *sucC* suppressor #1, *sucC*/*sucA* double mutant and the NE460 (*atl*) mutant. Autolytic activity was strikingly reduced in the *sucC* mutant compared to JE2, and this phenotype was complemented to wild-type levels in NE569 p*sucCD* and reversed in the *sucC*/*sucA* and the *sucA* Ser9STOP suppressor mutant strains (Fig. 2.7). Indeed, Triton-X-100-induced autolysis was similar in NE569 and NE460 (Fig. 2.7). These data suggest that the increased succinylation of the 12 lysine residues in Atl is associated with blocked autolytic activity by interfering with proteolytic cleavage of Atl or the activity of the amidase or glucosaminidase PG hydrolases. Although mutation of *atl* in several MRSA strains including the HoR strain COL was previously associated with reduced resistance to methicillin [60], the oxacillin MIC of *atl* mutant NE460 (32 μg/ml) was similar to the parent strain JE2. Mutation of Sle1, which like Atl is

required for daughter cell separation after cell division, has previously been reported to reduce autolytic activity [133] and increase MRSA susceptibility to oxacillin [134]. Succinyl-PTM of the Sle1 K200 residue was significantly increased in NE569 compared to JE2 (Student's t-test $p<0.05$) (Fig. 2.7B). Overall, our data reveal that accumulation of succinyl-CoA in the *sucC* mutant negatively impacts two interconnected cell wall-associated phenotypes; autolysis and susceptibility to β-lactam antibiotics.

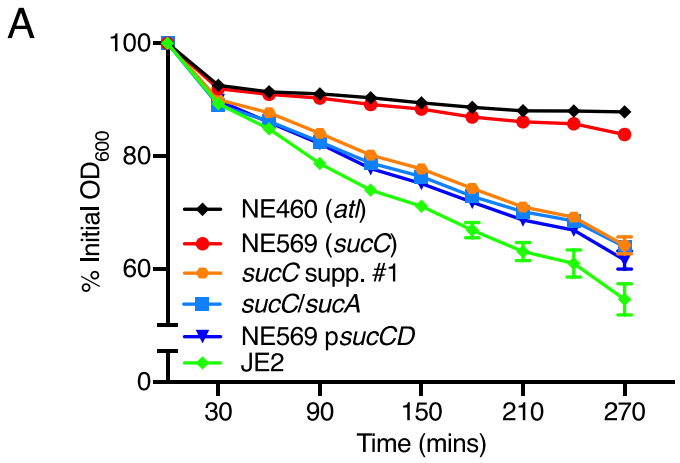

B

Sle1

```
1   MQKKVIAAIIGTSAISAVAATQANAATTHTVKPGESVWAISNKYGISIAK
51  LKSLNNLTSNLIFPNQVLKVSGSSNSTSNSSRPSTNSGGGSYYTVQAGDS
101 LSLIASKYGTTYQNIMRLNGLNNFFIYPGQKLKVSGTASSSNAASNSSRP
151 STNSGGGSYYTVQAGDSLSLIASKYGTTYQKIMSLNGLNNFFIYPGQKLK
201 VTGNASTNSGSATTTNRGYNTPVFSHQNLYTWGQCTYHVFNRRAEIGKGI
251 STYWWNANNWDNAAAADGYTIDNRPTVGSIAQTDVGYYGHVMFVERVNND
301 GSILVSEMNYSAAPGILTYRTVPAYQVNNYRYIH
```

Fig. 2.7. Increased succinylation of lysine residues in Atl and Sle1 is associated with reduced autolytic activity.

A. Triton X-100-induced autolysis of JE2, NE569 (*sucC*), *sucC* suppressor #1, *sucC*/*sucA* double mutant, NE569 p*sucCD* and NE460 (*atl*). The strains were grown to OD_{600} = 0.5 in MHB at 37°C, before being washed in cold PBS and resuspended in 0.1% Triton X-100 with OD_{600} adjusted to 1. The OD_{600} was monitored at 30-min intervals, and autolysis was expressed as a percentage of the initial OD_{600}. The experiments were repeated at least 3 times and error bars represent standard deviation. B. Amino acid sequence of Sle1 highlighting the K_{200} lysine residue (within a LysM domain (shaded grey) that is significantly more succinylated in NE569 (*sucC*) versus JE2 in red.

2.5 Discussion

The TCA cycle is centrally involved in the production of biosynthetic precursors, reducing potential and energy. In this study, we report that mutations in *sucC* and *sucD* genes encoding the α and β subunits of succinyl-CoA synthetase, which catalyses the conversion of succinyl-CoA to succinate, significantly increased susceptibility to β-lactams. The *sucC* and *sucD* mutants grew as smaller, less pigmented colonies on MHA and exhibited impaired growth in MHB. Genetically blocking the production of succinyl-CoA in the *sucC* mutant by mutating *sucA* or *sucB* reversed the growth and β-lactam susceptibility phenotypes. In contrast, mutation of *sdhA* in the *sucC* mutant had no phenotypic impact. Succinyl-CoA levels were significantly increased in the *sucC* mutant and were restored to wild-type levels by p*sucCD* complementation or mutation of *sucA*.

The accumulation of succinyl-CoA in the *sucC* mutant perturbed global protein succinylation, which is an important PTM previously described in several pathogens [106, 107, 126], including *S. epidermidis* [108]. Although several PBPs, including *mecA*-encoded PBP2a were among the proteins with the highest number of succinyl-lysines, PG architecture and cross-linking were unchanged in the *sucC* mutant, even under oxacillin stress when *mecA* expression is increased. The absence of structural changes in PG also indicates that the accumulation of succinyl-CoA does not impact β-lactam resistance via altered biosynthesis of lysine, which is an important component of the cell wall [16]. Succinyl-CoA is used in the biosynthesis of lysine from aspartate and in *Corynebacterium glutamicum*, disruption of the *sucCD* locus, and the resulting accumulation of succinyl-CoA was accompanied by overproduction of lysine [135]. It is difficult to envisage how increased lysine accumulation would reduce β-lactam resistance, and in any event the unchanged PG structure in the *sucC* mutant does not implicate lysine biosynthesis in this phenotype. Succinyl-CoA synthetase activity generates GTP, which is a substrate for RelA, RelP and RelQ enzymes that produce the stringent response alarmone (p)ppGpp. (p)ppGpp plays a central role in the control of MRSA β-lactam resistance [9, 66, 68, 116]. However, the ability of the *sucC* mutant to produce stable HoRs with mutations in *relA* or *relQ* suggests that intracellular GTP

is not limited in the *sucC* and *sucD* mutants or associated with reduced β-lactam resistance. Metabolomic analysis further revealed significantly reduced levels of acetyl-CoA in the *sucC* mutant raising the additional possibility that the acetylome may also have been perturbed. In this context, changes in PG acetylation have also been implicated in autolysis and antibiotic resistance [136] and future comparison of the acetylome and succinylome in *sucCD* mutants to identify proteins that are modified by both PTMs may provide further insights into how these mutations impact resistance.

The reduced pigmentation of the *sucCD* mutants may be a consequence of altered production of the *S. aureus* carotenoid staphyloxanthin, composed of a glucose residue esterified with a 30-carbon carboxylic acid chain and a 15-carbon fatty acid [137]. In *S. aureus* most fatty acids are odd numbered branched-chain fatty acids [138]. The β-oxidation of odd-numbered fatty acids generates acetyl-CoA and propionyl-CoA, of which the latter can be converted to succinyl-CoA. Interestingly, staphyloxanthin-derived lipids interact with flotillin to form functional membrane microdomains (FMMs) required for oligomerisation and activity of PBP2a [139]. In contrast to the reduced pigmentation, the proteomic analysis revealed increased levels of staphyloxanthin biosynthetic enzymes in the *sucC* mutant (MassIVE ID: MSV000086976 and MassIVE ID: MSV000086971), perhaps reflecting efforts by the *sucC* mutant to compensate for reduced pigmentation.

The discovery that Atl was the most succinylated protein in the MRSA proteome and that 12 of the 82 succinyl-lysines were significantly more succinylated in the *sucC* mutant suggested a potential connection to reduced β-lactam resistance. Fisher and Mobashery recently proposed a model in which the bactericidal activity of β-lactams is the result of deregulated Atl activity at the cell division septum [140]. Our data showing that autolytic activity was significantly reduced in the *sucC* mutant, and that the oxacillin MIC of the *atl* transposon mutant NE460 was unchanged are not consistent with this possibility. Furthermore, previous work in our laboratory linked increased autolytic activity with increased β-lactam resistance. Specifically *atl* transcription was activated in a HoR mutant of USA300 LAC (oxacillin MIC > 256 mg/ml), which exhibited significantly increased autolytic

activity, and growth of USA300 LAC in sub-MIC oxacillin was also associated with significantly increased autolysis [141]. Thus while it seems clear that autolysis and β-lactam susceptibility are interconnected, the precise mechanistic interactions between these two phenotypes needs to be elucidated further.

Processing of the Atl pro-protein, produces a signal peptide, a pro-peptide, a *N*-acetylmuramoyl-L-alanine amidase (AM) enzyme and a C-terminally located endo-β-*N*-acetylglucosaminidase enzyme (GL) [58]. The region between the AM and GL catalytic domains contains 3 repeat regions (R1–R3) with GW-dipeptide motifs required to target Atl pro-protein to the equatorial ring on the cell surface during cell division [142]. None of the 12 lysine residues exhibiting increased succinylation are in the AM catalytic domain, 5 are in the GL catalytic domain, 2 are in the pro-peptide region and the remaining 5 are in the R1 and R2 regions. The single lysine residue (K_{200}) of Sle1 that is more succinylated in the *sucC* mutant is located in a LysM cell wall hydrolase domain, and may be important for activity of the enzyme.

Susceptibility to the LtaS inhibitor Congo red was unchanged in the *sucC* mutant indicating that increased β-lactam susceptibility may not be associated with impaired expression or stability of WTA or LTA. Similarly, susceptibility to the alanylation inhibitor DCS was the same in the wild-type and *sucC* mutant. Given that D-alanine is an important component of PG, this observation is consistent with the absence of any changes in PG structure in the *sucC* mutant. Furthermore, because D-alanine is an important component of WTA and LTA, unchanged susceptibility to DCS does not point to roles for these cell envelope glycopolymers in *sucC*-dependent β-lactam susceptibility. Nevertheless, given that almost 58% of all quantifiable succinylated peptides were significantly changed in the *sucC* mutant, we propose a model in which perturbation of the succinylome likely modulates the activity of multiple enzymes, including Atl and Sle1, that collectively control growth and interconnected cell envelope characteristics such as autolysis and susceptibility to β-lactam antibiotics (Fig. 2.8). The FDA approved anti-cancer drug streptozotocin specifically targets succinyl-CoA synthetase in human cells to limit proliferation [143], and is used primarily to treat tumours that cannot be

surgically removed. The findings described in this study may open the door to the possibility of sensitizing MRSA to β-lactam antibiotics using compounds that specifically target succinyl-CoA synthetase or protein succinylation generally within the cell.

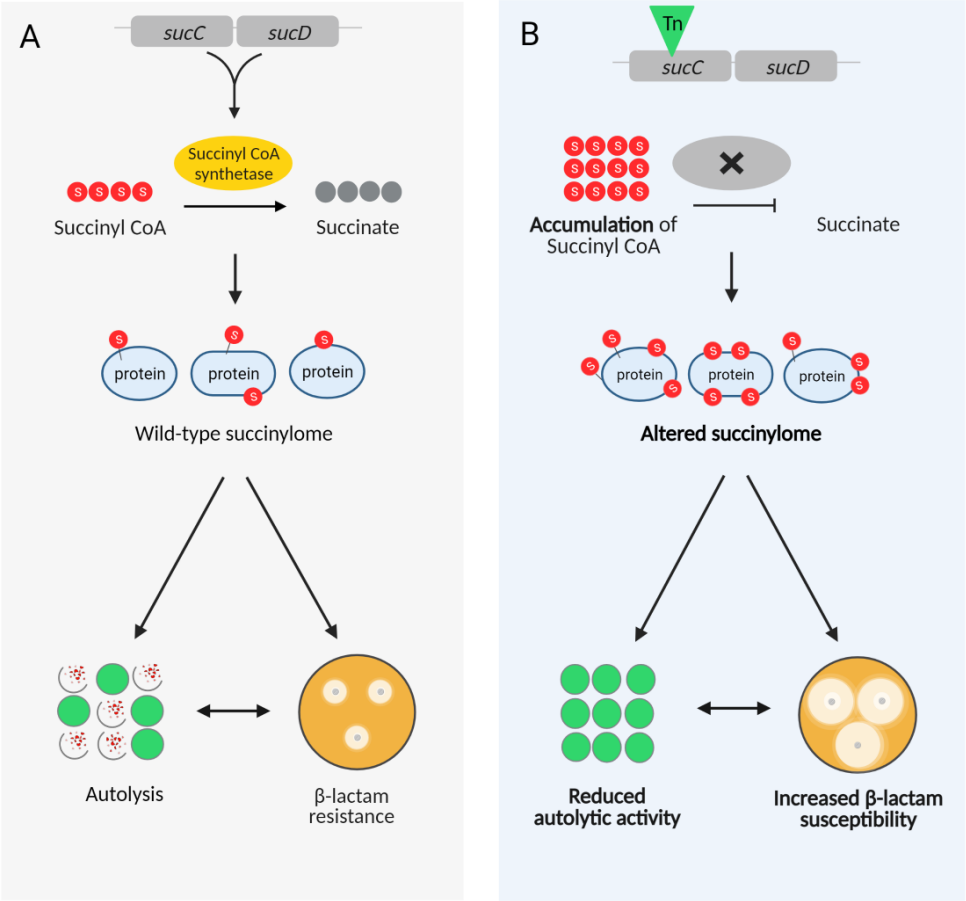

Fig. 2.8. Suggested model for succinylome-controlled regulation of two interconnected cell wall-associated phenotypes, namely autolysis and β-lactam susceptibility, in MRSA.

2.6 Materials and Methods

2.6.1 Bacterial strains and growth conditions.

Bacterial strains and plasmids used in this study are listed in Table 2.S1. *Escherichia coli* strains were cultured in Luria Bertani (LB) broth or agar (LBA). *S. aureus* strains were grown in Mueller-Hinton Broth (MHB), Mueller-Hinton Agar (MHA), Tryptic Soy Broth (TSB), Brain Heart Infusion (BHI), Tryptic Soy Agar (TSA), chemically defined medium (CDM) and CDM supplemented with glucose (CDMG), where indicated supplemented with erythromycin (Erm) 10 µg/ml, chloramphenicol (Cm) 10 µg/ml, ampicillin (Amp) 50 µg/ml or kanamycin (Km) 75 µg/ml. For growth experiments in MHB, 25 ml or 50 ml MHB in 250 ml flasks were used for a 10:1 or 5:1 flask to volume ratio, respectively. Overnight cultures in MHB were used to inoculate the media at a starting OD_{600} of 0.01 and flasks were incubated at 37°C shaking at 200 rpm. For CDM and CDMG growth experiments, overnight cultures were grown in TSB, washed once in 5 ml PBS, and used to inoculate 25 ml of CDMG or CDM in a 250 ml flask to a starting OD_{600} of 0.05. Flasks were incubated at 37°C shaking at 200 rpm. For all growth experiments, colony forming units (CFU) were enumerated in serially diluted 20 µl aliquots removed from flask cultures. At least 3 biological replicates were performed for each strain and average data presented. For experiments to compare growth in MH and MH supplemented with 5% glucose, cultures were grown at 37°C in 250 ml flasks with 50 ml media shaking at 200 rpm.

2.6.2 Cefoxitin disk diffusion assays and minimum inhibitory concentration (MIC) measurements.

Cefoxitin disk diffusion susceptibility testing was performed in accordance with Clinical Laboratory Standards Institute (CLSI) guidelines [144]. MIC measurements by broth microdilution or agar dilution were performed in accordance with CLSI methods for dilution susceptibility testing of staphylococci [145]. Disk diffusion and MIC results were interpreted using CLSI standard M100, and strains classified as susceptible or resistant [146]. For oxacillin MIC measurement, M.I.C.Evaluator

(Oxoid) strips were used in accordance with manufacturer guidelines. Strains were grown at 37°C on MHA for 24 h, 5 - 6 colonies were resuspended in 0.85% saline and adjusted to 0.5 McFarland standard. The supension was swabbed evenly 3 times across the surface of an MHA 2% NaCl plate (4 mm agar depth). An M.I.C.Evaluator strip was applied, before incubation for 24 h at 35°C. Three independent measurements were performed for each strain.

2.6.3 Genomic DNA (gDNA) extraction and whole genome sequencing (WGS).

gDNA extraction, sequencing by MicrobesNG (http://www.microbesng.uk) and analysis using CLC Genomics Workbench software were performed as described previously [147]. Sequence data for NE569 (sucC), sucC HoR1, sucC HoR2 and sucC suppressor mutants #1, #2 and #2 is available from the European Nucleotide Archive (project PRJEB43960, accession numbers ERS6142066-ERS6142071).

2.6.4 Genetic manipulation of *S. aureus*.

Phage 80α was used to transduce the transposon insertion from NE569 into JE2, DAR173 and USA300, to ensure background mutations were not responsible for the antibiotic resistance phenotype as described previously [147]. Transposon insertions were verified using PCR amplification of target loci.

A 1,680bp fragment encompassing the *sucC* gene and a 2,610bp fragment including both *sucC* and *sucD* were PCR amplified from JE2 genomic DNA using primers INF_sucC_F / INF_sucC_R and INF_sucCD_F / INF_sucCD_R, respectively (Table 2.S2) and cloned into the *E. coli-Staphylococcus* shuttle vector, pLI50, using the Clontech Infusion Cloning kit 2. The p*sucCD* plasmid was digested with *HpaI* and *SpeI*, treated with T4 DNA polymerase (Roche) and dNTPs to create a blunt-end fragment that was religated using T4 ligase (Roche). The resulting plasmid, designated p*sucD,* contained a 627bp deletion at the 5' end of the *sucC* gene with only the *sucD* gene remaining intact. Recombinant plasmids were first transformed into cold-competent *E. coli* HST08 (supplied with Clontech Infusion Cloning kit) before being transformed by electroporation into the restriction-deficient *S. aureus* strain RN4220 and finally into NE569 and NE1770.

Double mutants *sucC*/*sucA*, *sucC*/*sdhA* and *sucC/relA* were generated by first exchanging the *sucC*::Tn containing an erythromycin resistance (Erm^r) cassette in NE569, for a transposon containing a kanamycin resistance (Kan^r) cassette, generating strain *sucC*::Tn-Kan^r. This was performed by allelic exchange, using the plasmid pKAN and method described previously [148]. Genomic DNA extraction and PCR using primers suc_F and sucC_R was carried out to verify the allelic exchange process.

To construct the *sucC*/*relA* double mutant, the *sucC*::Tn-Kan^r was transduced into NE1714 and transductants were selected on TSA with 75 µg/ml kanamycin. To construct *sucC*/*sucA* and *sucC*/*sdhA* double mutants, the *sucA*::Tn allele from NE547 and the *sdhA*::Tn allele of NE626 were each transduced into *sucC*::Tn-Kan^r using phage 80α and transductants were selected on TSA with 10 µg/ml erythromycin. PCR was used to verify the transposon insertions in the double mutants using primers for *sucC*, *relA*, *sucA* and *sdhA* (Table 2.S2).

2.6.5 RNA purification and real time RT-PCR.

Cultures were grown in BHI media to mid-exponential phase. Harvested cells were pelleted and immediately stored at -20°C in RNAlater (Ambion) to ensure maintenance of RNA integrity. RNA was extracted as per manufacturers guidelines using RNA Mini-Extraction kit (Sigma). RNA integrity was examined visually by agarose gel electrophoresis and RNA concentration was determined using a Qubit Fluorometer 4 (Qiagen). Quantitative reverse transcription PCR (RT-qPCR) was used to measure mecA transcription on the Roche LightCycler 480 instrument using the LightCycler 480 Sybr Green Kit (Roche) with primers mecA1_Fwd and mecA1_Rev (Table 2.S2), as described previously [132]. The gyrB gene amplified with primers gyrB_Fwd and gyrB_Rev (Table 2.S2) served as an internal standard. Each RT-qPCR experiment was performed 3 times and average data presented including standard deviation.

2.6.6 PBP2a western blot analysis.

Overnight MHB cultures were used to inoculate 25 ml of MHB 2% NaCl, with or without 0.5 µg/ml oxacillin to a starting OD_{600} of 0.05, incubated at 35°C (200 rpm shaking) until an OD_{600} of 0.8 was reached before the cells were pelleted and resuspended in PBS to an OD_{600} of 10 and PBP2a Western blots performed as described previously [147]. Three independent experiments were performed, and a representative blot presented.

2.6.7 Isolation of *sucC* suppressor mutants.

While performing experiments comparing the growth of JE2 and the *sucC* mutant NE569, aliquots removed from 25 ml MHB cultures grown in 250 ml flasks were serially diluted and CFUs enumerated on MHA. Suppressor mutants of NE569 were readily identified on MHA due to their larger colony size and deeper pigmentation, which contrasted with the smaller, pale colony morphology of parental NE569. Three suppressor mutants (#1, #2 and #3) were chosen for further analysis. DNA extraction and PCR verification of the *Bursa aurealis* transposon using primers sucC_F and sucC_R (Table 2.S2) was performed to verify the presence of the *sucC* transposon insertion. Comparative genome sequence analysis was used to identify the suppressor mutations.

2.6.8 Oxacillin resistance population analysis.

Population analysis profiles (PAPs) was generated as described previously [149]. Overnight cultures were grown in BHI, adjusted to an OD_{600} of 1, 10-fold serially diluted from 10^{-1} to 10^{-7}, and a 20 µl aliquot of each dilution plated onto a series of BHI agar plates supplemented with oxacillin 0.25, 0.5, 1, 2, 4, 8, 16, 32, 64 and 128 µg/ml. CFUs were enumerated after overnight incubation at 37°C and the results were expressed as CFU/ml at each oxacillin concentration. Average data from 3 independent experiments are presented.

2.6.9 Isolation of homogeneously resistant (HoR) mutants.

Overnight cultures of NE569 were grown in BHI, adjusted to OD600 of 1, serially diluted and plated onto BHI agar supplemented with 100 µg/ml oxacillin and incubated at 37°C, to isolate HoR mutants. CFUs were enumerated on BHI agar to calculate the rate of HoR mutant production. HoR mutants were passaged for 14 days in antibiotic-free BHI broth to identify stable mutants that were then verified using PAPs and oxacillin MIC measurements. The experiments were performed twice and the results of 1 representative experiment presented.

2.6.10 LC-MS/MS metabolite analysis of NE569 (*sucC*), NE569 p*sucCD* and *sucC* suppressor #1.

For LC-MS/MS analysis, samples were prepared as previously described [150]. Briefly, strains were inoculated in MHB to an OD_{600} of 0.06 and grown aerobically (250 rpm, 37ºC) for 6 h. Culture volumes corresponding to OD_{600} of 10 were harvested and rapidly filtered through a membrane (0.45 µm, Millipore). The cells on the membrane were washed twice with 5 ml cold saline and immediately quenched in ice-cold 60% ethanol containing 2 µM Br-ATP as an internal control. The cells were mechanically disrupted using a bead homogenizer set to oscillate for 3 cycles (30 s) of 6800 rpm with a 10 s pause between each cycle. Cell debris was separated by centrifugation at 13,000 rpm. The supernatant containing intracellular metabolites were lyophilized, and stored at -80°C.

A triple-quadrupole-ion trap hybrid mass spectrometry (Sciex) connected with a Waters ultra-performance liquid chromatography I-class (UPLC) system was used for the metabolite analysis. The chromatographic separation was performed by ionic liquid chromatography using Column: XSELECT HSS XP (150 mm × 2.1 mm ID; 2.5 µm particle size) and a binary solvent system with a flow rate of 0.250 ml/min was used for chromatographic separation. Mobile phase A was composed of 10 mM tributylamine (TBA), 10 mM acetic acid, 5% methanol, and 2% 2-propanol; mobile phase B was 100% methanol. Column was maintained at 40°C and autosampler was maintained at 7 °C. The A/B solvent ratio was maintained at 90/10 for 1 min followed by a gradual increase of B to 65% for 10 min. B was

increased to 90% over next 1 min which was maintained for 4 min. The gradient was again reduced to 90/10 (A/B) within 0.5 min and was equilibrated for 5.5 min before the next run. A QTRAP® 6500+ mass spectrometry system (SCIEX) operated in negative ion mode was used for targeted quantitation in Multiple Reaction Monitoring (MRM) mode. MRM details for each analyte are listed in Table 2.S3. Electrospray ionization (ESI) parameters were optimized for 0.25 ml/min flow rate and are as follows: electrospray ion voltage of -4400 V, source temperature of 400°C, curtain gas of 40, and gas 1 and 2 of 40 and 45 psi, respectively. Analyzer parameters were optimized for each compound using manual tuning.

2.6.11 Proteomics sample preparation and analysis.

Cells were collected from 4 biological replicates of JE2 and NE569 (*sucC*) flask cultures grown to exponential and stationary phase in MHB. Due to different growth characteristics and CFUs/ml in wild-type and sucC mutant cultures (Fig. 2.S1), JE2 and NE569 cells were collected after 3 h and 4 h, respectively for exponential growth, and after 10 h and 12 h, respectively for stationary phase growth. As an added control 4 biological replicates of JE2 cells were also collected after 3 h (early exponential phase). Cell pellets were collected promptly from culture samples and snap frozen in liquid nitrogen.

The cell pellets from all 20 samples were lysed, denatured, and digested with trypsin before being labelled with tandem mass tags (TMT) using TMT11plex as described previously [151]. Because there were 20 samples and only 11 channels in the TMT11plex kit, an equal concentration of peptides from all the cell pellets was mixed to generate a reference sample used for normalization purposes. Two samples from each cell pellet were labelled with different isobaric labels and placed in each of the 2 TMT sets, the channel 131C was reserved for the reference sample. The peptide samples were cleaned-up by C18 solid phase extraction (SPE). An immunoaffinity purification was performed using the PTMScan Acetyl-Lysine Motif (Ac-K) Kit (Cell Signaling Technology, Danvers, MA) to bind acetyl peptides, thereby enriching succinyl-lysine peptides in the unbound fraction, which was cleaned-up using a C18 SPE and fractionated (into 12 fractions) using high pH

reverse phase chromatography as described previously [152]. Peptides were analyzed by reverse phase separation (C18) coupled with a QExactive HF-X mass spectrometer. The instrument .raw files generated were deposited and are available at MassIVE data repository, (MassIVE ID: MSV000086976 and MassIVE ID: MSV000086971). Raw MS data were searched with MS-GF+ [153] against Uniprot/SwissProt *S. aureus* database (UP000001939), bovine trypsin and human keratin sequences. Methionine oxidation and succinylation were set as dynamic modifications, cysteine alkylation and TMT labelling of N-termini and lysines were set as static modifications. The identified spectra were filtered based on their MS-GF+ scores, resulting in false discovery rate (FDR) <1%. For quantitative analysis, the TMT reporter ion intensities were extracted with MASIC [154]. Intensities were normalized to reference channel intensity. Analytes were considered for quantification when reporters were observed for at least ¾ of the samples per given condition. The subsequent data was log2-transformed, median-centred and batch-corrected [128]. ANOVA and Student's t-tests were used to determine significance. The DAVID modified Fisher's exact test (EASE score, [155] was used to measure significant enrichment of Gene Ontology (GO) terms in proteins whose abundance was altered by the *sucC* mutation.

2.6.12 Peptidoglycan (PG) analysis.

Wild-type JE2, NE569 and *sucC* suppressor #1 were grown in MHB and MHB supplemented with oxacillin 3 µg/ml or 32 µg/ml. For each strain and growth condition tested, independent quadruplicate 50 ml cultures were grown in flasks at 37°C with 200 rpm shaking, to an OD_{600} of 0.5 and cell pellets were collected promptly and snap frozen in liquid nitrogen. PG was extracted from the samples as described previously [132, 156].This analysis of wild-type JE2 PG was also used as a part of a separate study [147], and is reported again in this paper for comparison with NE569 and *sucC* suppressor #1. Mass spectrometry (MS) was performed on a Waters XevoG2-XS QTof mass spectrometer. Structural characterization of muropeptides was determined based on their MS data and MS/MS fragmentation pattern, matched with PG composition and structure reported previously [157-160].

2.6.13 Autolytic activity assays.

Two hundred µl inoculums from overnight cultures were inoculated into 20 ml TSB, grown at 37°C (200 rpm) to OD600 of 0.5, washed with 20 ml cold PBS, resuspended in 5 ml cold PBS and then adjusted to OD600 of 1. One ml of the cell suspension was transferred to a cuvette and Triton X-100 was added at a final concentration of 0.1% v/v. The initial OD600 was recorded before incubation at 37°C with shaking (200 rpm). Thereafter the OD600 was recorded every 30 min for 4 h, and autolytic activity expressed as a percentage of the initial OD600. NE460 (*atl*::Tn) was used as a control and at least 3 biological replicates performed for each strain.

2.7 Supplemental Figures and Tables

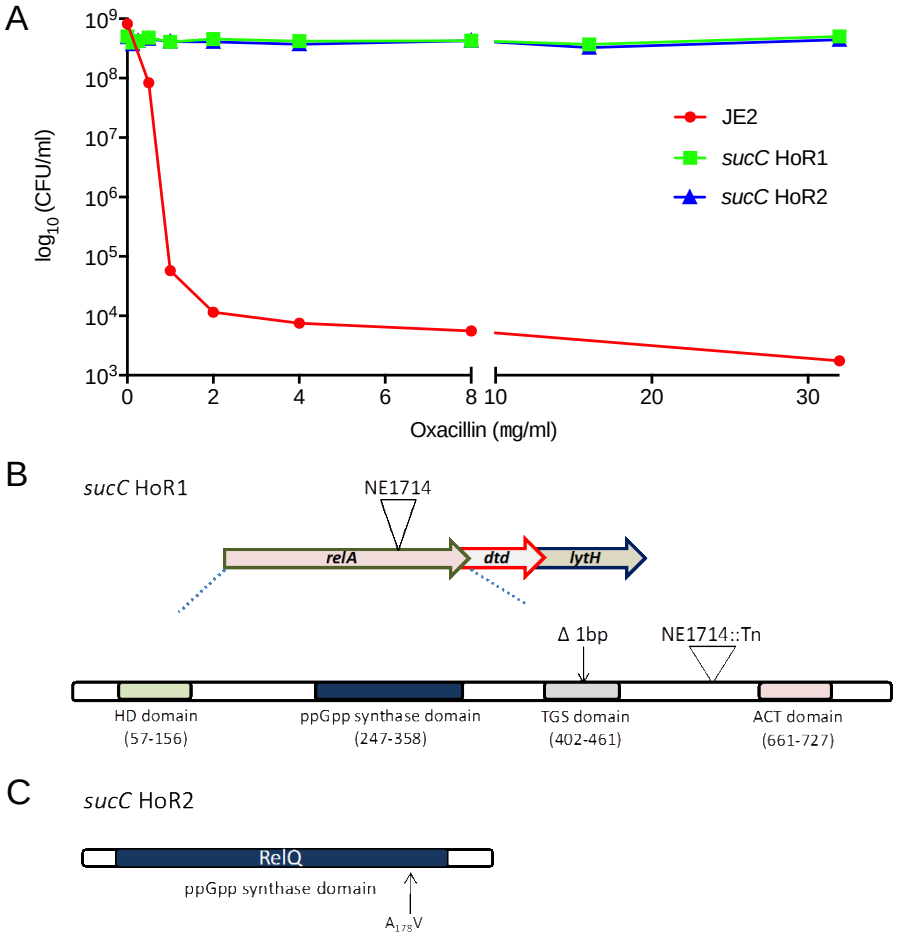

Fig.2. S1. NE569 (*sucC*) HoR mutants contain RSH (*relA*) and *relQ* mutations.

A. Population analysis profiling of JE2, *sucC* HoR1 and *sucC* HoR2 grown in BHI broth to exponential phase, adjusted to OD_{600} of 1 and serially diluted before plating onto BHI agar supplemented with increasing concentrations of oxacillin (0-100 µg/ml) for enumeration of CFUs. This assay was repeated three times and data from a representative experiment is shown. B. *relA-dtd-lytH* operon in *S. aureus* and RSH (RelA) domain architecture including the location of the 1bp deletion in *sucC* HoR1 and the Tn insertion in NE1714. C. Location of A178V mutation in ppGpp synthase domain of RelQ in strain *sucC* HoR2.

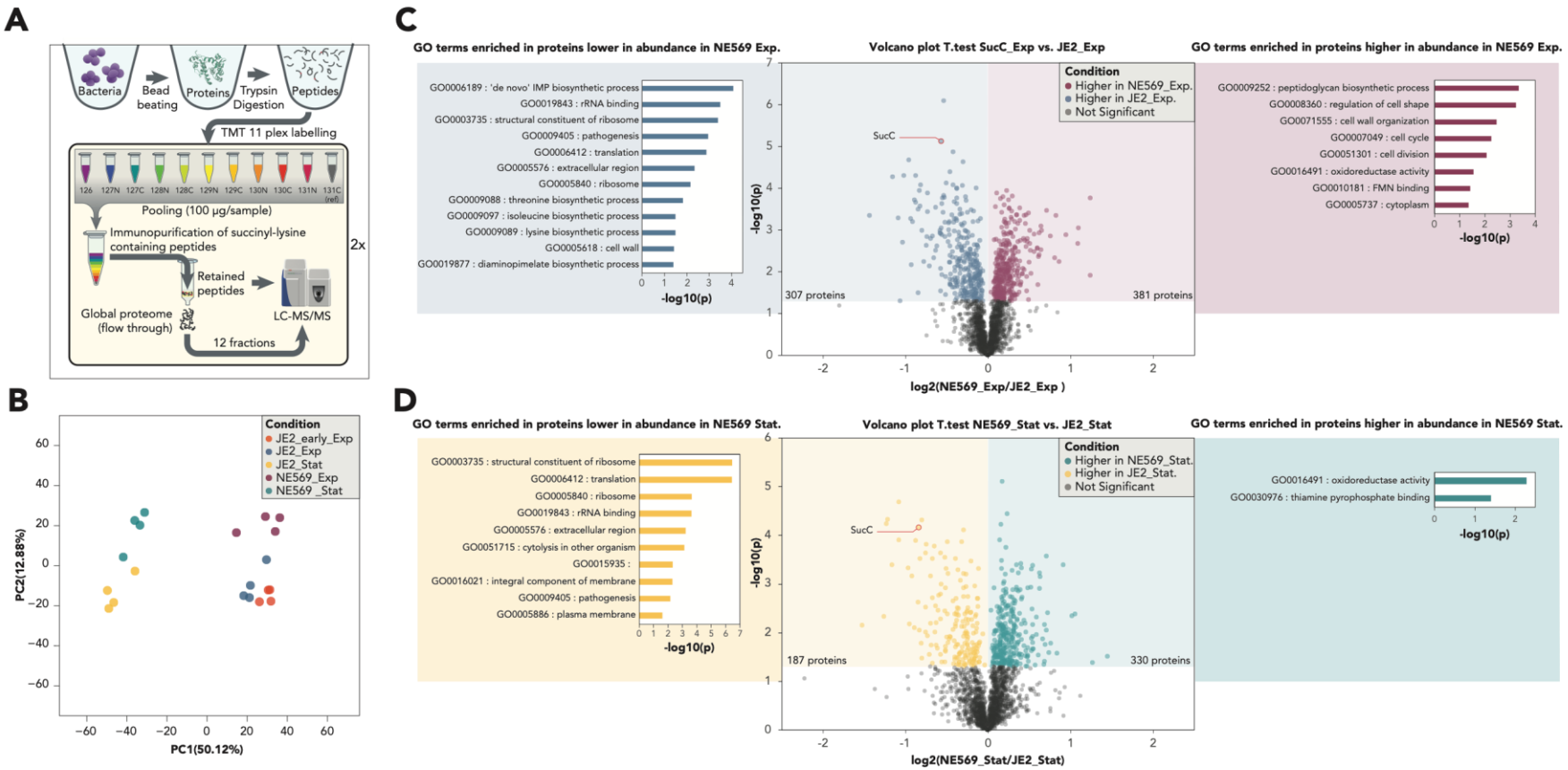
A
Bacteria
Bead beating
Proteins
Trypsin Digestion
Peptides
TMT 11 plex labelling
126 127N 127C 128N 128C 129N 129C 130N 130C 131N 131C (ref)
Pooling (100 µg/sample)
Immunopurification of succinyl-lysine containing peptides
2x
Retained peptides
Global proteome (flow through)
LC-MS/MS
12 fractions
B
Condition
JE2_early_Exp
JE2_Exp
JE2_Stat
NE569_Exp
NE569 _Stat
PC2(12.88%)
PC1(50.12%)
C
GO terms enriched in proteins lower in abundance in NE569 Exp.
GO0006189 : 'de novo' IMP biosynthetic process
GO0019843 : rRNA binding
GO0003735 : structural constituent of ribosome
GO0009405 : pathogenesis
GO0006412 : translation
GO0005576 : extracellular region
GO0005840 : ribosome
GO0009088 : threonine biosynthetic process
GO0009097 : isoleucine biosynthetic process
GO0009089 : lysine biosynthetic process
GO0005618 : cell wall
GO0019877 : diaminopimelate biosynthetic process
-log10(p)
Volcano plot T.test SucC_Exp vs. JE2_Exp
Condition
Higher in NE569_Exp.
Higher in JE2_Exp.
Not Significant
SucC
307 proteins
381 proteins
-log10(p)
log2(NE569_Exp/JE2_Exp)
GO terms enriched in proteins higher in abundance in NE569 Exp.
GO0009252 : peptidoglycan biosynthetic process
GO0008360 : regulation of cell shape
GO0071555 : cell wall organization
GO0007049 : cell cycle
GO0051301 : cell division
GO0016491 : oxidoreductase activity
GO0010181 : FMN binding
GO0005737 : cytoplasm
-log10(p)
D
GO terms enriched in proteins lower in abundance in NE569 Stat.
GO0003735 : structural constituent of ribosome
GO0006412 : translation
GO0005840 : ribosome
GO0019843 : rRNA binding
GO0005576 : extracellular region
GO0051715 : cytolysis in other organism
GO0015935 :
GO0016021 : integral component of membrane
GO0009405 : pathogenesis
GO0005886 : plasma membrane
-log10(p)
Volcano plot T.test NE569_Stat vs. JE2_Stat
Condition
Higher in NE569_Stat.
Higher in JE2_Stat.
Not Significant
SucC
187 proteins
330 proteins
-log10(p)
log2(NE569_Stat/JE2_Stat)
GO terms enriched in proteins higher in abundance in NE569 Stat.
GO0016491 : oxidoreductase activity
GO0030976 : thiamine pyrophosphate binding
-log10(p)

Fig. 2.S2. Mutation of *sucC* impacts the MRSA global proteome.

A. Workflow for MRSA proteome and succinylome analysis by LC-MS/MS. B. Principal component analysis grouping protein samples by strain and growth phase. C. Comparison of the relative abundance of proteins from JE2 and NE569 (*sucC*) exponential phase cultures. The volcano plot depicts the fold-change and the -log10(p) of the Student's t-test. The bar plots show the GO terms significantly enriched (EASE modified Fisher's exact $p<0.05$) either for the protein significantly less abundant in NE569 (left) or more abundant in NE569 (right). D. Comparison of the relative abundance of proteins from JE2 and NE569 (*sucC*) stationary phase cultures. The volcano plot depicts the fold-change and the -log10(p) of the Student's t-test. The bar plots show the GO terms significantly enriched (EASE modified Fisher's exact $p<0.05$) either for the protein significantly less abundant in NE569 (left) or more abundant in NE569 (right).

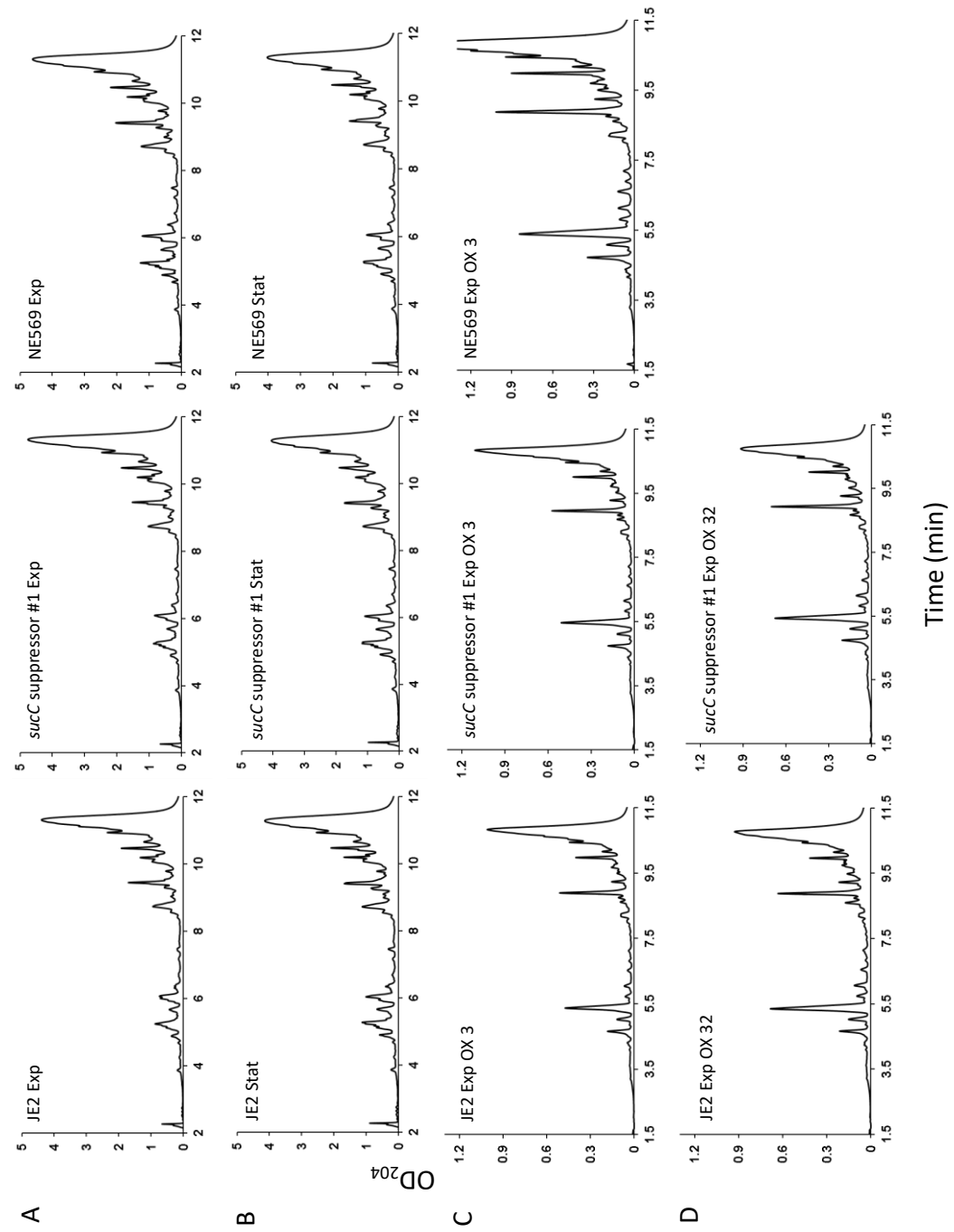

Fig. 2.S3. Mutation of sucC does not affect PG structure and cross-linking.

Representative UV chromatograms of PG extracted from JE2, *sucC* suppressor strain #1 and NE569 (*sucC::*Tn) grown in MHB with oxacillin as indicated. A. Exponential phase. B. Stationary (Stat) phase. C. Exponential phase (Exp) with oxacillin (OX) 3 µg/ml. D. Stationary phase with oxacillin (Ox) 32 µg/ml. PG analysis from NE569 (*sucC*) is shown only at 3 µg/ml oxacillin because 32 µg/ml exceeds its MIC. Three biological replicates were analysis and representative chromatograms are shown.

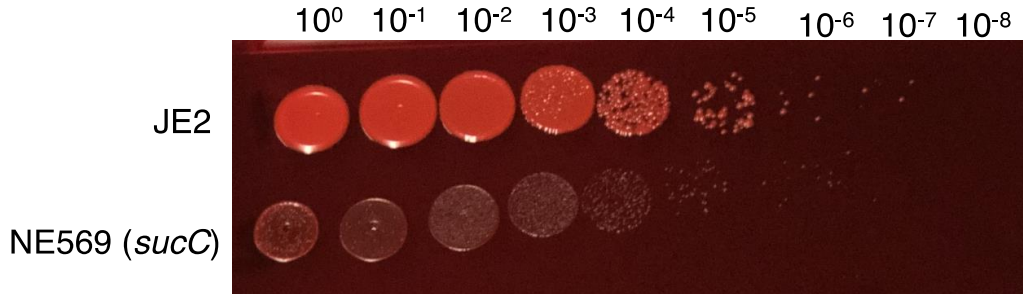

Fig. 2.S4. Mutation of *sucC* does not affect susceptibility to Congo Red.

Serial dilution of JE2 and NE569 (*sucC*) on MHA supplemented with 0.125% Congo red incubated for 24 h at 37°C. Three biological replicates were analysed and a representative plate is shown.

Table 2.S1. Bacterial strains and plasmids used in this study.

Strain/Plasmid	Relevant details	Source/reference
***Escherichia coli* strain**		
HST08	TaKaRa *E. coli* HST08 Premium Electro-Cells	TaKaRa
***Staphylococcus aureus* strains**		
USA300 FPR3757	Community associated MRSA isolate of USA300 lineage. SCCmec type IV. Clonal complex 8.	(4)
JE2	Plasmid-cured derivative of USA300 LAC	(28)
NE569	JE2 *sucC*::Tn. Erm^r	(28)
sucC::Tn-Kan^r	JE2 *sucC*::Tn. Kan^r	This study
sucC HoR1	HoR mutant of NE569. RelQ $Ala_{178}Val$ mutation.	This study
sucC HoR2	HoR mutant of NE569. RelA Tyr_{418}STOP mutation.	This study
sucC suppressor #1	NE569 suppressor mutant. *sucA* SER_9STOP mutation.	This study
sucC suppressor #2	NE569 suppressor mutant. *sucB* $Ile_{361}Thr$ mutation.	This study
sucC suppressor #3	NE569 suppressor mutant. *sucB* 46bp deletion.	This study
NE1770	JE2 *sucD*::Tn. Erm^r	(28)
NE1724	JE2 *pdhA*::Tn. Erm^r	(28)

NE1758	JE2 *pdhB*::Tn. Erm^r	(28)
NE594	JE2 *gltA*::Tn. Erm^r	(28)
NE861	JE2 *acn*::Tn. Erm^r	(28)
NE491	JE2 *icd*::Tn. Erm^r	(28)
NE547	JE2 *sucA*::Tn. Erm^r	(28)
NE1391	JE2 *sucB*::Tn. Erm^r	(28)
NE626	JE2 *sdhA*::Tn. Erm^r	(28)
NE808	JE2 *sdhB*::Tn. Erm^r	(28)
NE427	JE2 *fumC*::Tn. Erm^r	(28)
NE1003	JE2 *mqo* E1::Tn. Erm^r	(28)
NE1381	JE2 *mqo* E2::Tn. Erm^r	(28)
NE460	JE2 *atl*::Tn. Erm^r	(28)
NE1714	JE2 *relA*::Tn. Erm^r	(28)
sucC/*sucA*	*sucC*/*sucA* double mutant. Constructed by transduction of *sucA*::Tn allele from NE547 into *sucC*::Tn-Kan^r. Erm^r, Kan^r	This study
sucC/*sdhA*	*sucC*/*sdhA* double mutant. Constructed by transduction of *sdhA*::Tn allele from NE626 into *sucC*::Tn-Kan^r. Erm^r, Kan^r	This study
sucA/*relA*	*sucC*/*relA* double mutant. Constructed by transduction of *relA*::Tn allele from NE1714 into *sucC*::Tn-Kan^r. Erm^r, Kan^r	This study
RN4220	Restriction-deficient *S. aureus*.	(81)
DAR173	MRSA; SCC*mec* type IV; Clonal complex 5.	(29, 30)
ATCC 29213	MSSA strain for MIC susceptibility testing.	ATCC
ATCC 25923	MSSA strain for disk diffusion susceptibility testing.	ATCC
Plasmids		
pLI50	*E. coli-Staphylococcus* shuttle vector. Amp^r (*E. coli*), Cm^r (*Staphylococcus*).	(82)
pKAN	Plasmid to replace *bursa aurealis* Erm^r marker with Kan^r marker. Kan^r, Cam^r	(68)
p*sucC*	pLI50 carrying the *sucC* gene from JE2. Cm^r	This study

p*sucCD*	pLI50 carrying the *sucCD* genes from JE2. Cm^r	This study
p*sucD*	pLI50 carrying the *sucD* gene from JE2. Derivative of p*sucCD* with a 627 bp deletion at the 5′ end of *sucC*. Cm^r	This study

Table 2.S2. Oligonucleotide primers used in this study.

Target gene	Primer name	Primer sequence (5′-3′)
sucC	sucC_F	TACTCAAATCGCCATGCAGC
	sucC_R	AATGACTGAAACCGTTGCCC
sucCD	sucCD_R	CGCACGACAAATAGCCCATT
mecA	mecA_F	CATATCGTGAGCAATGAACTGA
	mecA_R	CATCGTTACGGATTGCTTCA
relA	relA_F	TGGCTTTGCACCTGTTAGAA
	relA_R	TTTTGCCGTCCTGACTTTCA
sucA	sucA_F	GGCGGTAATGGACTCGGATT
	sucA_R	TCTACGCTATCCCCTACGTT
sdhA	sdhA_F	TGGGGTGGACTTCAATCTCC
	sdhA_R	TGTGTTTCATGTTGTGGAGTGT
Infusion primers		
sucC	INF_sucC_F	TCGTCTTCAAGAATTGACGCTTGATAATGCACTG
	INF_sucC_R	TACCGAGCTCGAATTCCTTTACCAGGCGTCACA
sucCD	INF_sucCD_F	TCGTCTTCAAGAATTTACTCAAATCGCCATGCAGC
	INF_sucCD_R	TACCGAGCTCGAATTCGCACGACAAATAGCCCATT
RT-PCR primers		
mecA	mecA1_Fwd	TGCTCAATATAAAATTAAAACAAACTACGGTAAC
	mecA1_Rev	GAATAATGACGCTATGATCCCAA

gyrB	gyrB_Fwd	CCAGGTAAATTAGCCGATTGC
	gyrB_Rev	AAATCGCCTGCGTTCTAGAG

Table 2.S3. Table of MRM transitions for all metabolites measure

Component Name	MRM Transitions	Collision energy (V)
Oxaloacetate	131.0 / 87.0	-9.6
Fumarate	115.0 / 71.0	-13
Acetyl-CoA	808.0 / 79.0	-150
Succinyl-CoA	866.0 / 765.4	-26
Malate	133.0 / 115.0	-14.7
Pyruvate	87.0 / 32.0	-14
Citrate	190.9 / 111.1	-16.1
Isocitrate	190.9 / 173.0	-13
Succinate	117.0 / 99.0	-14
Phosphoenolpyruvate	167.0 / 79.0	-14.6
α-Ketoglutarate	145.0 / 101.0	-15
Br-ATP	585.8 / 79.0	-120

2.8 Data availability

Proteomic .raw files generated during this study are available at MassIVE data repository (MassIVE ID: MSV000086976 and MassIVE ID: MSV000086971). The Uniprot/SwissProt *S. aureus* database (UP000001939) was used as a reference for the proteomic analysis.

Whole genome sequence data is available from the European Nucleotide Archive (project PRJEB43960, accession numbers ERS6142066-ERS6142071). The SAUSA300_FRP3757 (TaxID:451515) reference genome sequence is available from NCBI.

2.9 Author contributions:

Claire Fingleton: Conceptualization, Formal analysis, Investigation, Methodology, Writing - original draft, Writing - review & editing

Chris Campbell: Conceptualization, Formal analysis, Investigation, Methodology, Writing - original draft, Writing - review & editing

Merve S. Zeden: Data curation, Formal analysis, Investigation, Methodology, Writing - original draft, Writing - review & editing

Emilio Bueno: Formal analysis, Investigation, Methodology, Writing - review & editing

Laura A. Gallagher: Formal analysis, Investigation, Methodology

Dhananjay Shinde: Investigation, Methodology

Jongsam Ahm: Investigation, Methodology

Heather M. Olson: Investigation, Methodology

Thomas L. Fillmore: Investigation, Methodology

Joshua N. Adkins: Funding acquisition, Supervision, Formal analysis, Writing - review & editing

Fareha Razvi: Formal analysis, Writing - review & editing

Kenneth W. Bayles: Funding acquisition, Supervision, Writing - review & editing

Paul D. Fey: Funding acquisition, Supervision, Writing - review & editing

Vinai C. Thomas: Formal analysis, Funding acquisition, Supervision, Investigation, Methodology, Writing - review & editing

Felipe Cava: Funding acquisition, Formal analysis, Supervision, Writing - review & editing

Geremy C. Clair: Conceptualization, Formal analysis, Investigation, Methodology, Supervision, Writing - review & editing

James P. O'Gara: Conceptualization, Formal analysis, Funding acquisition, Project administration, Supervision, Writing - original draft, Writing - review & editing

2.10 Acknowledgements

C.C., C.F., M.S.Z. L.A.G. and J.P.O'G. were supported by grants from the Health Research Board (HRA-POR-2015-1158 and ILP-POR-2019-102) (www.hrb.ie), the Irish Research Council (GOIPG/2014/763 and GOIPG/2016/36) (www.research.ie) and Science Foundation Ireland (19/FFP/6441) (www.sfi.ie). E.B. and F.C. were supported by a grant from Svenska Forskningsrådet Formas. G.C., H.B., T.F. and J.A. were supported by the IARPA FunGCAT program, NIGMS grant GM103493 and Department of Energy contract DE-AC05-76RLO 1830. K.W.B., P.D.F., V.C.T., D.S., J.A. and F.R. were supported by National Institute of Allergy and Infectious Diseases (NIAID) grant P01-AI83211. K.W.B. and J.A. were supported by NIAID grant R01-AI125589. D.S. and V.C.T were supported by grant NIAID R01AI125588.

The funders had no role in study design, data collection and interpretation, or the decision to submit the work for publication.

Chapter 3: Mutation of lipoprotein processing pathway gene *lspA* or inhibition of LspA activity by globomycin increases MRSA resistance to β-lactam antibiotics

Chapter 3:

Mutation of lipoprotein processing pathway gene *lspA* or inhibition of LspA activity by globomycin increases MRSA resistance to β-lactam antibiotics

Claire Fingleton[1], Merve S. Zeden[1], Emilio Bueno[2], Felipe Cava[2] and James P. O'Gara[1]*

[1]Microbiology, School of Natural Sciences, National University of Ireland, Galway, Ireland.

[2]Department of Molecular Biology, Umeå University, MIMS - Laboratory for Molecular Infection Medicine Sweden, Umeå, Sweden.

*For correspondence: jamesp.ogara@nuigalway.ie

Running title: Lipoprotein processing and β-lactam susceptibility in MRSA

This chapter has been submitted for publication and my contributions to the final figures are as follows: Figures 1, 2, 3A, 4, 5, 7, 8, S1, S2, S3, S5, S6, S7

Additional contributions:
Figure 3B, S4: Dr Emilio Bueno and Dr Felipe Cava, Umeå University, Sweden.
Figure 6: Dr Merve Suzan Zeden, National University of Ireland, Galway

3.1 Abstract

The *Staphylococcus aureus* cell envelope comprises of numerous components, including peptidoglycan (PG), wall teichoic acids (WTA), lipoteichoic acids (LTA), targeted by antimicrobial drugs. MRSA resistance to methicillin is mediated by the *mecA*-encoded β-lactam-resistant transpeptidase, penicillin-binding protein 2a (PBP2a). However, PBP2a-dependent β-lactam resistance is also modulated by the activity of pathways involved in the regulation and/or biosynthesis of PG, WTA or LTA. Here, we report that mutation of the lipoprotein signal peptidase II gene, *lspA*, from the lipoprotein processing pathway, significantly increased β-lactam resistance in MRSA. Mutation of *lgt*, which encodes diacylglycerol transferase (Lgt) responsible for synthesis of the LspA substrate did not impact β-lactam susceptibility. Consistent with previous reports, *lgt* and *lspA* mutations impaired growth in chemically defined, but not complex media. MRSA exposure to the LspA inhibitor globomycin also increased β-lactam resistance. Mutation of *lgt* in a *lspA* background reduced β-lactam resistance to wild type levels. The *lspA* mutation had no effect on PBP2a expression, PG composition or autolytic activity indicating a potential role in the WTA or LTA synthetic pathways. However, mutation of *lgt,* or multicopy *lspA* expression, but not mutation of *lspA* alone*,* significantly increased susceptibility to the lipoteichoic acid synthase inhibitor Congo red revealing complex interplay between lipoprotein processing mutations and the expression/stability of cell surface glycopolymers. These findings indicate that *lspA* mutation increases MRSA resistance to β-lactam antibiotics through impacts on cell envelope components other than PG.

3.2 Introduction

The cell envelope of *Staphylococcus aureus* comprises a cytoplasmic membrane surrounded by a thick peptidoglycan layer, cell wall-anchored proteins, lipoteichoic acids (LTA), wall teichoic acids (WTA) and cell surface proteins. Accurate biosynthesis, assembly and stability of these cell envelope components is essential for the growth and pathogenicity of *S. aureus*, and is the target of numerous antimicrobial agents [161]. The peptidoglycan layer determines cell shape and protects the cell from osmotic lysis. In addition, cell surface proteins have important roles in adhesion, biofilm formation, and immune evasion, and teichoic acids are involved in protecting the cell from the activity of cationic antimicrobial peptides.

Methicillin resistance in MRSA is mediated by the *mecA*-encoded, low-affinity penicillin-binding protein 2a (PBP2a) carried on the mobile staphylococcal cassette chromosome *mec* (SCC*mec*). Carriage of the SCC*mec* element by *S. aureus* is associated with expression of heterogenous, low level resistance (HeR) to β-lactam antibiotics [32, 91, 92]. Growth of HeR MRSA strains on elevated β-lactam concentrations can select for homogeneously resistant (HoR) MRSA mutants. Many accessory mutations associated with the HoR phenotype occur in chromosomal loci outside SCC*mec* and are frequently associated with activation of the stringent response, cyclic-di-adenosine monophosphate (c-di-AMP) signalling pathway [9, 66, 68, 93], the activity of RNA polymerase [162] and the ClpXP chaperone-protease complex [163, 164].

Bacterial lipoproteins are a class of lipid-modified membrane proteins, involved in a range of diverse functions such as; nutrient acquisition [73], signal transduction [74], respiration [75], protein folding [65], virulence [76], antibiotic resistance [77] and host invasion [78]. Mature lipoproteins are composed of lipid moieties, specifically acyl groups, linked to the N-terminus of a protein. The hydrophobic nature of the acyl groups serves as a membrane anchor for the lipoprotein [80]. In Gram-negative bacteria, lipoproteins reside in both the cytoplasmic and outer

membranes, while in Gram-positive bacteria they are anchored in the outer leaflet of the cytoplasmic membrane and the protein portion may extend into the cell wall and beyond [79].

Lipoprotein genes are estimated to comprise 1-3% of all genes in bacterial genomes [79]. While many lipoproteins have been identified and experimentally validated, others remain only putatively identified using predictive software, thus their functions are unknown [165]. A recent bioinformatic evaluation of Staphylococcal lipoproteins in the MRSA strain USA300 identified 67 lipoproteins, comprising 2.57% of all genes [79]. When grouped by function, 25 of the 67 lipoproteins were implicated in ion, notably iron, and nutrient transport, 8 were ascribed miscellaneous functions including sex pheromone biosynthesis, respiration, chaperone-folding, and protein translocation and 15 were classified as tandem lipoproteins, of which 9 are “lipoprotein-like” lipoproteins, known to play a role in host cell invasion [78]. The remaining 19 lipoproteins were not assigned any known function.

Lipoproteins are synthesised in a precursor form called preprolipoproteins. The N-terminal domain includes a type II signal peptide, approximately 20 amino acids in length [82], which enables translocation of preprolipoproteins to the cytoplasmic membrane, predominantly via the general secretory (Sec) pathway [83]. The signal peptide has 3 distinct domains; a positively charged N domain, a hydrophobic H domain and a C-terminal lipobox. The lipobox is comprised of a conserved 3-amino acid sequence $[LVI]_{-3}$ $[ASTVI]_{-2}$ $[GAS]_{-1}$ in front of an invariant cysteine residue $[C]_{+1}$ [166, 167]. This lipobox serves as a recognition site for enzymes of the lipoprotein processing pathway, enabling lipid modification of the cysteine residue, and cleavage of the signal peptide between the amino acid at position -1 and the +1 cysteine [166].

The first enzyme in the lipoprotein processing pathway is diacylglycerol transferase (Lgt) which covalently attaches a diacylglycerol residue from phosphatidyl glycerol onto the sulfhydryl group of the invariant cysteine, resulting in a prolipoprotein [84]. This diacylglycerol serves as a membrane anchor. Next,

the type II lipoprotein signal peptidase (Lsp) cleaves the signal peptide between the amino acid at position -1 and +1, leaving the invariant cysteine residue as the new terminal amino acid [85]. Lgt and Lsp are conserved in all bacterial species. In Gram-negative bacteria, a third step is catalysed by the enzyme N-acyl transferase (Lnt), which transfers an N-acyl group onto the invariant cysteine residue at the N-terminal of the protein [168]. Lnt homologs have been identified in high-GC Gram-positive bacteria [169] but not in low-GC Firmicutes. Despite the lack of an apparent Lnt homolog, N-acylated lipoproteins have been identified in *S. aureus* [170] and recent work has identified two novel non-contiguous genes *lnsA* and *lnsB* which catalyse the N-terminal acylation of lipoproteins in *S. aureus* [86]. The membrane metalloprotease Eep and the EcsAB transporters were shown to be involved in the processing and export of linear peptides, including the signal peptide cleaved by LspA in the lipoprotein processing pathway [171-173]. Lgt and Lsp are essential for the viability of Gram-negative bacteria [174]. In contrast, *lgt* and *lspA* mutations do not impact viability in Gram-positive bacteria [87], but are associated with changes in growth, immunogenicity [88] and virulence [76].

In this study, we characterised the impact of *lspA* and *lgt* mutations, alone and in combination, on susceptibility to β-lactams, D-cycloserine and Congo red, as well as growth, PBP2a expression, peptidoglycan structure, and autolytic activity in MRSA. The impact of globomycin, which is known to inhibit LspA activity, on β-lactam susceptibility was also characterised. Our data suggest that accumulation of the LspA substrate, diacylglyceryl-prolipoprotein, modulates resistance to β-lactam antibiotics in MRSA.

3.3 Results

3.3.1 Mutation of *lspA* in MRSA increases resistance to β-lactam antibiotics.

The Nebraska Transposon Mutant Library (NTML) [113] was screened to identify mutants exhibiting altered susceptibility to cefoxitin, which is recommended as a surrogate for measuring *mecA*-mediated oxacillin resistance in clinical laboratories, in accordance with Clinical and Laboratory Standards Institute (CLSI) guidelines for disk diffusion susceptibility assays. Mutants identified by this screen included NE869 (*yjbH)* [175], NE1909 (*sagA*) [176] and NE810 (*cycA*)[132], all of which have previously been implicated in β-lactam resistance. A novel mutant identified in this screen was NE1757 (*lspA*::Tn), which exhibited increased resistance to cefoxitin (Fig 3.1A, B). PCR was used to confirm the presence of *lspA*::Tn allele in NE1757 (data not shown). Using E-test strips, as described in the methods, oxacillin MIC of the *lspA* transposon mutant NE1757 was found to be 128 - 256 μg/ml, compared to 32 - 64 μg/ml for wild-type JE2 (Fig. 3.1C). Two independent JE2 transductants carrying the *lspA*::Tn allele from NE1757 also exhibited increased resistance to oxacillin (Fig. 3.1C). The *lspA* gene appears to be in a 2-gene operon with the pseudouridylate synthase gene, *rluD* (Fig. 3.1D). The oxacillin MIC of the NTML *rluD*::Tn mutant NE793 was that same as JE2 (32 μg/ml) indicating that the increased β-lactam resistance of NE1757 was not due to downstream polar effects of the transposon insertion in *lspA*.

The increased oxacillin resistance phenotype of NE1757 was complemented by the introduction of a plasmid (pLI50)-borne copy of the wild type *lspA* gene (p*lspA*) into the mutant. Growth of JE2, NE1757, NE1757 pLI50 and NE1757 p*lspA* on MHA 2% NaCl supplemented with oxacillin 32 μg/ml visually demonstrated that carriage of the complementation plasmid p*lspA* reversed the increased oxacillin resistance phenotype of NE1757 (Fig. 3.S1). Measurement of oxacillin MICs by agar dilution showed that NE1757 and NE1757 pLI50 had MICs of 256 μg/ml, while JE2 and NE1757 p*lspA* had MICs of 64 μg/ml (Table 3.1).

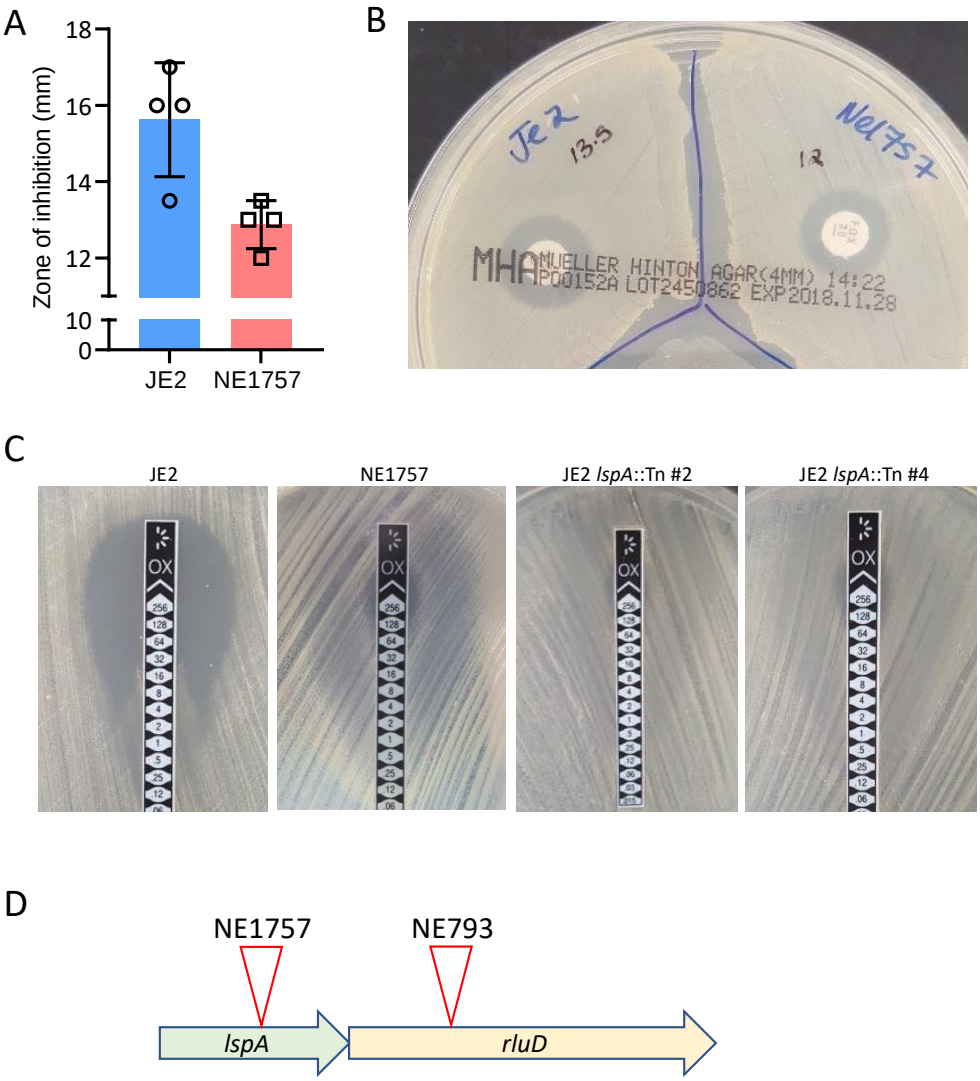

Fig. 3.1. Mutation of *lspA* increases resistance to cefoxitin and oxacillin.

(A) Average diameters of the cefoxitin disk zones of inhibition for JE2 and NE1757 (*lspA*::Tn) from 4 independent experiments, plotted using Prism software (GraphPad). (B) Representative image of JE2 (left) and NE1757 (right) grown on MH agar with a cefoxitin 30 µg disk. (C) M.I.C.Evaluator measurement of oxacillin minimum inhibitory concentrations (MICs) in JE2, NE1757 (*lspA*::Tn), and two independent JE2 transductants (#2 and #4) carrying the *lspA*::Tn allele grown on MHB 2% NaCl agar. This assay was repeated 3 independent times for each strain and a representative image is shown. (D) Organisation of the *lspA*/*rluD* operon including the approximate locations of the transposon insertions in NE1757 and NE793.

Table 3.1. Antibacterial activity of oxacillin, cefotaxime, nafcillin, vancomycin and d-cycloserine (MIC measurements; µg/ml1) against ATCC 29213 (control), JE2, NE1757 (*lspA*::Tn), NE1757 p*lspA*, NE1757 pLI50, NE1757 MM (markerless *lspA* mutant), NE1757 MM p*lspA*, JE2 *lspA*::Tn #2 (transductant), NE1905 (*lgt*::Tn), NE1757/NE1905 double mutant *lspA/lgt* and NE107 (*ecsB*).

Strain	Oxacillin	Cefotaxime	Nafcillin	Vancomycin	D-Cycloserine
ATCC 29213	≥1	2	0.5	1	32
JE2	32 - 64	64	32	1	32
NE1757 (*lspA*)	128 - 256	256	64	1	16 - 32
NE1757 p*lspA*	64	64	32	1	16 - 32
NE1757 pLI50	256	256	-	1	16 - 32
lspA MM	128 - 256	256	64	-	-
lspA MM p*lspA*	64	64	32	-	-
JE2 *lspA*::Tn #2	128 - 256	256	-	1	16 - 32
NE1905 (*lgt*)	64	64	32	1	16 - 32
lspA MM/NE1905 (*lspA*/*lgt*)	64	128	32	1	16
NE107 (*ecsB*)	64	64	32	1	16 - 32

[1] MIC measurements (µg/ml) were performed by MH agar dilution in accordance with CLSI standards.

Comparison of JE2 and NE1757 growth in MHB, MHB 2% NaCl, TSB and TSB 0.5 µg/ml oxacillin revealed no significant differences (Fig. 3.S2). Similarly, population analysis profiling revealed that the heterogeneous pattern of oxacillin resistance expressed by JE2 was unchanged in NE1757 (Fig. 3.S3). These observations indicate that the increased β-lactam resistance phenotype of NE1757 was not attributable to any growth advantage or change in the heterogeneous/homogeneous oxacillin resistance profile.

Comparative WGS analysis confirmed that the only change in the NE1757 genome was the insertion of the *Bursa aurealis* transposon in the *lspA* gene at position 1192002 (Table 3.S1) and there were no SNPs present. The NE1757 genome was also checked manually for zero coverage regions to confirm the absence of any large deletions and insertions. Taken together these data indicate that mutation of *lspA*, which encodes lipoprotein signal peptidase II involved in the lipoprotein processing pathway (Fig. 3.2), increases resistance to oxacillin and cefoxitin in JE2.

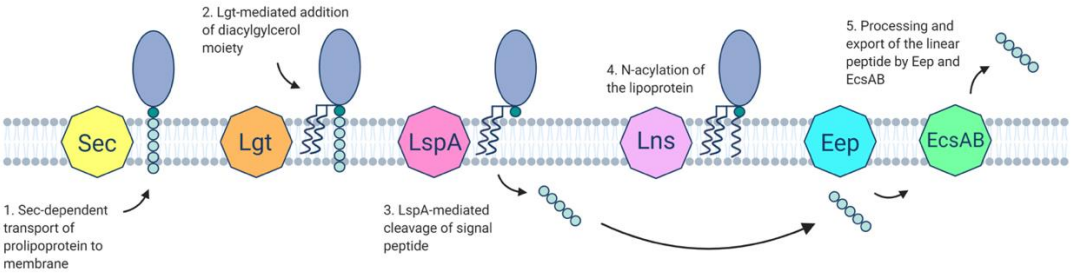

Fig. 3.2. Role of LspA in the proposed model of lipoprotein processing in Gram-positive bacteria.

Lipoproteins are synthesized in the cytoplasm as precursors. 1. Prolipoprotein is translocated usually via the Sec machinery through recognition of its signal peptide (SP). This sequence also contains the lipobox specific for bacterial lipoproteins. 2. Diacylglyceryl transferase (Lgt) catalyzes the transfer of a diacylglyceryl group from phosphatidylglycerol onto the prolipoprotein resulting in diacylglyceryl-prolipoprotein. 3. Lipoprotein signal peptidase II (LspA) recognizes the diacylglyceryl-modified signal peptide and cleaves between the amino acid at position-1 and the lipid-modified cysteine residue at +1. 4. The lipoprotein N-acylation transferase system (Lns) converts diacyl lipoproteins to triacylated lipoprotein (29). 5. Eep and EcsAB play roles in the processing and secretion of linear peptides (32).

3.3.2 Mutation of *lspA* does not affect PBP2a expression or peptidoglycan structure and cross-linking.

Western blotting was used to compare PBP2a levels in JE2, NE1757 and NE1757 p*lspA.* The MSSA strain 8325-4 was included as a *mecA*-negative control. Growth of JE2 and NE1757 in MHB without 2% NaCl at 37°C (data not shown) or MHB with 2% NaCl at 35°C supplemented with 0.5 µg/ml oxacillin (Fig. 3.3A) revealed similar levels of PBP2a expression in all strains. Eight mg total protein was used in the Western blot experiments and Coomassie staining of the Tris-Glycine gel after transfer for PVDF membrane was used to confirm equal loading (Fig. 3.3B).

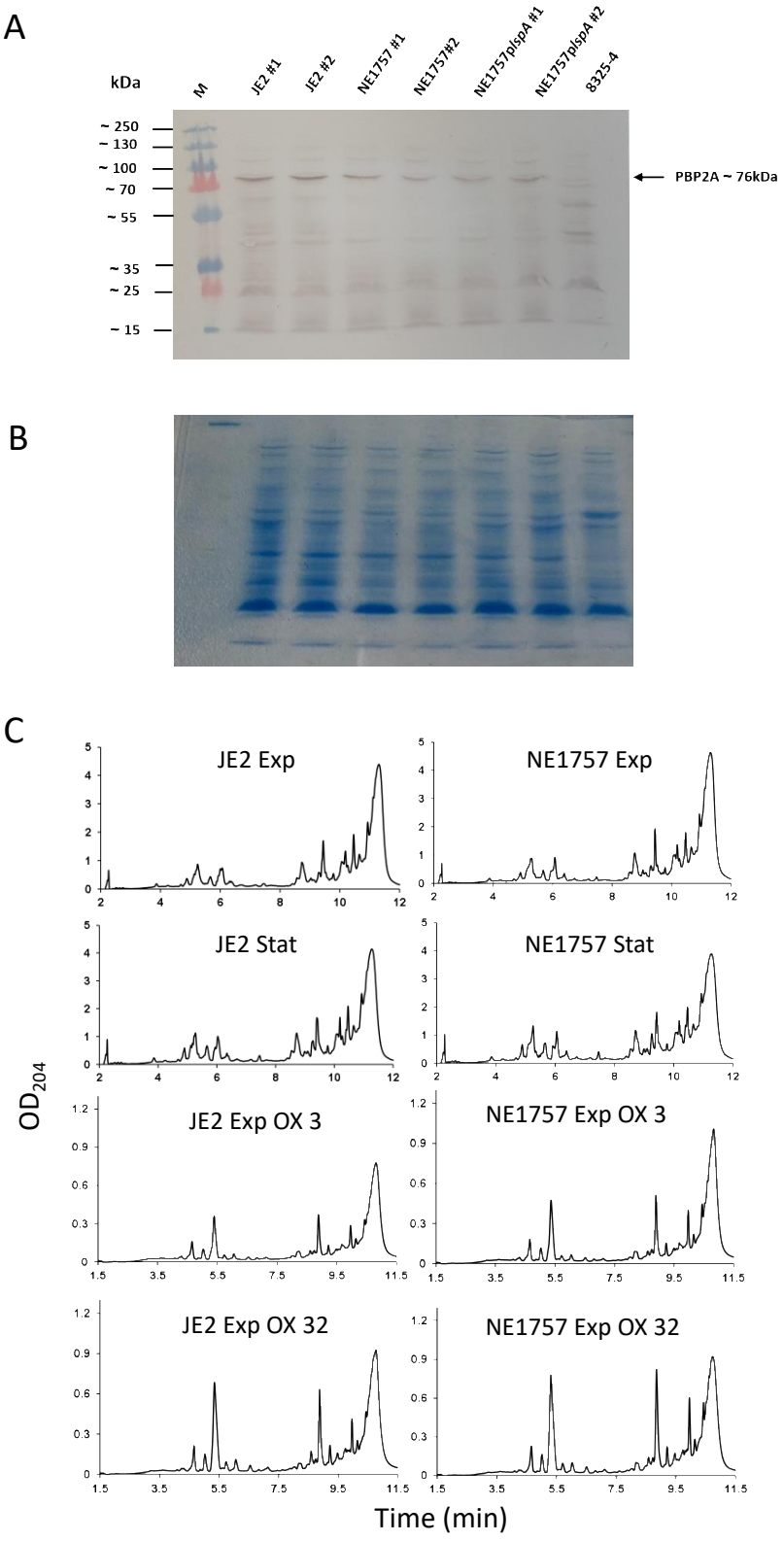
A
kDa
M
JE2 #1
JE2 #2
NE1757 #1
NE1757#2
NE1757plspA #1
NE1757plspA #2
8325-4
~ 250
~ 130
~ 100
~ 70
~ 55
~ 35
~ 25
~ 15
PBP2A ~ 76kDa
B
C
JE2 Exp
NE1757 Exp
JE2 Stat
NE1757 Stat
JE2 Exp OX 3
NE1757 Exp OX 3
JE2 Exp OX 32
NE1757 Exp OX 32
OD204
Time (min)

Fig. 3.3. Mutation of *lspA* does not affect PBP2a expression levels or peptidoglycan structure and cross-linking.

(A) Western blot of PBP2a protein in JE2, NE1757 (*lspA*), NE1757 p*lspA* and MSSA strain 8325-4 (negative control). Cells were grown to exponential stage in MHB 2% NaCl supplemented with 0.5 μg/ml oxacillin, with the exception of 8325-4 which was grown in MHB 2% NaCl. For each sample, 8 μg total protein was run on a 7.5% Tris-Glycine gel, transferred to a PVDF membrane and probed with anti-PBP2a (1:1000), followed by HRP-conjugated protein G (1:2000) and colorimetric detection with Opti-4CN Substrate kit. Three independent experiments were performed, and a representative image is shown. (B) Coomassie staining of the Tris-Glycine gel after transfer of protein to the PVDF membrane used in the PBP2a Western blot (C) Representative UV chromatograms of peptidoglycan extracted from JE2 and NE1757 collected from cultures grown to exponential or stationary phase in MHB or MHB supplemented with oxacillin 3 μg/ml or 32 μg/ml. Each profile shown is a representative of 3 biological replicates.

Quantitative peptidoglycan compositional analysis was performed using Ultra Performance Liquid Chromatography (UPLC) analysis of muramidase-digested muropeptide fragments extracted from exponential or stationary phase cultures of JE2 and NE1757 grown in MHB or MHB supplemented with oxacillin 3 μg/ml or 32 μg/ml. The PG profile of JE2 and the *lspA* transposon mutant NE1757 were similar under all growth conditions tested (Fig. 3.3C). Thus, supplementation of MHB with oxacillin was associated with significant changes in muropeptide oligomerization and reduced cross-linking, but these effects were the same in both JE2 and NE1757 (Fig. 3.S4). The total PG concentrations extracted from JE2 and NE1757 cell pellets were also the same (data not shown). Comparison of Triton X-100-induced autolysis in JE2 and NE1757 also revealed identical autolytic profiles (Fig. 3.S5).

Finally, the NaCl tolerance phenotypes of JE2 and NE1757 were also similar (Fig. 3.S6), indicating that c-di-AMP signalling, which has previously been implicated in the control of β-lactam resistance, autolytic activity and NaCl tolerance [66, 68] was unaffected by the *lspA* transposon mutation. These data indicate that increased β-lactam resistance in the *lspA* transposon mutant was not associated

with significant changes in PG abundance, structure, cross-linking, c-di-AMP signalling or autolytic activity.

3.3.3 Exposure to the LspA inhibitor globomycin also increases β-lactam resistance.

Globomycin is a natural peptide antibiotic, first discovered in 1978, produced by 4 different strains of *Actinomycetes* [177, 178]. It is an inhibitor of LspA and works by sterically blocking the active site of the enzyme [179]. Globomycin has moderate to strong antibacterial activity against many Gram-negative species and has been proposed to cause disruption of cell surface integrity [180]. However, despite its ability to inhibit LspA, globomycin does not have significant antimicrobial activity against Gram-positive bacteria including *S. aureus*, with MICs >100 μg/ml [177, 178, 181].

Because the *lspA*::Tn allele was associated with increased resistance to β-lactams, we hypothesized that chemical inhibition of LspA by globomycin may also be associated with increased β-lactam resistance. To test this hypothesis, the susceptibility of JE2 and NE1757 to oxacillin was determined in the presence or absence of globomycin. A series of JE2 and NE1757 cultures grown in MHB 2% NaCl were used to determine that oxacillin 40 μg/ml inhibited growth of JE2 but not NE1757 (Fig. 3.4A) as predicted. Next, JE2 MHB 2% NaCl 40 μg/ml oxacillin cultures were further supplemented with 10, 20, 30, 40 or 50 μg/ml globomycin (Fig. 3.4B). Oxacillin-induced inhibition of JE2 growth was rescued by globomycin, optimally at 10, 20 and 30 μg/ml (Fig. 3.4B). Growth of JE2 in 40 μg/ml oxacillin and 50 μg/ml globomycin was substantially impacted compared to lower globomycin concentration (Fig. 3.4B) indicating that the ability of globomycin to increase oxacillin resistance is dose-dependant.

These experiments were extended to USA300_FPR3757, from which JE2 is derived and ATCC43300, a *Staphylococcus* Cassette Chromosome *mec* (SCC*mec*) type II MRSA clinical isolate. Oxacillin concentrations of 50 μg/ml and 30 μg/ml inhibited growth of USA300 and ATCC4330, respectively (Fig. 3.5). Globomycin concentrations (determined empirically for each strain) of 20 μg/ml for USA300

(Fig. 3.4C) and 30 μg/ml for ATCC43300 (Fig. 3.4D) rescued growth in the presence of oxacillin. These data demonstrate that the increased oxacillin resistance phenotype observed in the *lspA* mutant NE1757, can be replicated by globomycin-induced inhibition of LspA activity in wild type JE2 and other MRSA strains USA300 and ATCC43300.

In contrast to the observation that globomycin increased β-lactam resistance in wild type JE2, USA300 and ATCC43300, the growth of NE1757 in a range of globomycin concentrations from 10 – 50 μg/ml had a dose-dependent and negative effect on growth in the presence of oxacillin 40 μg/ml (Fig. 3.S7). Taken together, these data suggest that globomycin, through inhibition of LspA, overcomes the activity of oxacillin in MRSA. However, in the *lspA* transposon mutant, the combination of globomycin and oxacillin interferes with growth of JE2, particularly at higher concentrations of globomycin, perhaps due to off-target effects.

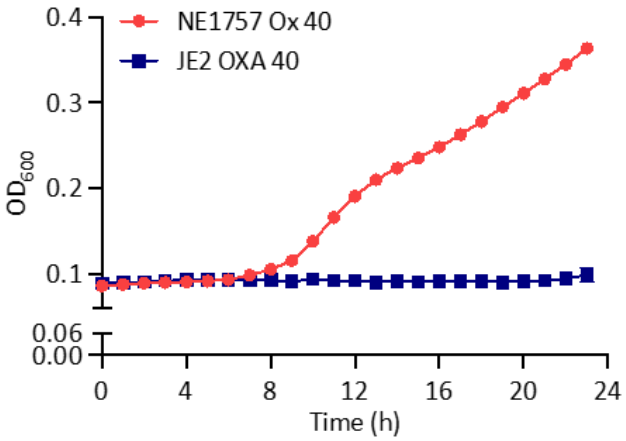
NE1757 Ox 40
JE2 OXA 40
OD600
0.4
0.3
0.2
0.1
0.06
0.00
0
4
8
12
16
20
24
Time (h)

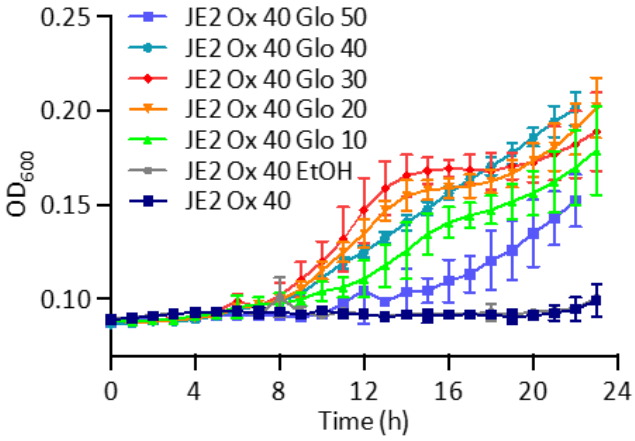
JE2 Ox 40 Glo 50
JE2 Ox 40 Glo 40
JE2 Ox 40 Glo 30
JE2 Ox 40 Glo 20
JE2 Ox 40 Glo 10
JE2 Ox 40 EtOH
JE2 Ox 40
OD600
0.25
0.20
0.15
0.10
0
4
8
12
16
20
24
Time (h)

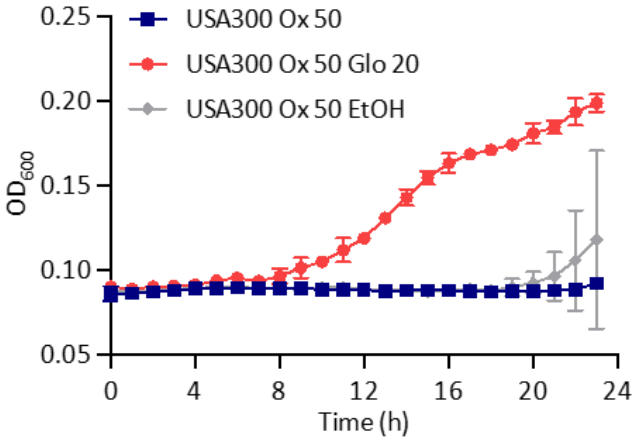
USA300 Ox 50
USA300 Ox 50 Glo 20
USA300 Ox 50 EtOH
OD600
0.25
0.20
0.15
0.10
0.05
0
4
8
12
16
20
24
Time (h)

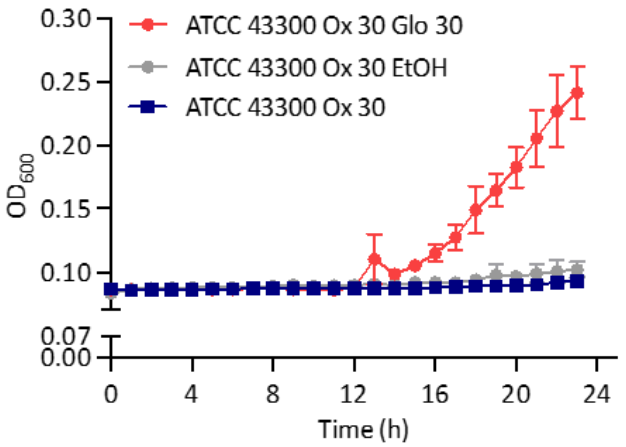
ATCC 43300 Ox 30 Glo 30
ATCC 43300 Ox 30 EtOH
ATCC 43300 Ox 30
OD600
0.30
0.25
0.20
0.15
0.10
0.07
0.00
0
4
8
12
16
20
24
Time (h)

Fig. 3.4. Mutation of *lspA* or exposure to globomycin increases oxacillin resistance.

(A) JE2 and NE1757 (*lspA*) grown in MHB 2% NaCl supplemented with oxacillin 40 µg/ml. (B) JE2 grown in MHB 2% NaCl supplemented with oxacillin 40 µg/ml and globomycin concentrations ranging from 10-50 µg/ml or MHB 2% NaCl supplemented with oxacillin 40 µg/ml and 0.6% ethanol (control solvent for globomycin). (C) USA300 grown in MHB 2% NaCl supplemented with oxacillin 50 µg/ml, MHB 2% NaCl supplemented with oxacillin 50 µg/ml and globomycin 20 µg/ml or MHB 2% NaCl supplemented with oxacillin 50 µg/ml and 0.6% ethanol (control solvent for globomycin). (D) ATCC 43300 grown in MHB 2% NaCl supplemented with oxacillin 30 µg/ml, MHB 2% NaCl supplemented with oxacillin 30 µg/ml and globomycin 30 µg/ml or MHB 2% NaCl supplemented with oxacillin 50 µg/ml and 0.6% ethanol (control solvent for globomycin). The oxacillin and globomycin concentrations used in these experiments were determined empirically for each strain. Cultures were grown in a Tecan Sunrise incubated microplate reader for 24 h at 35^{o}C. OD_{600} was recorded at 1 hour intervals and growth curves were plotted in Prism software (GraphPad). The data presented are the average of 3 independent biological replicates, and error bars represent standard deviations.

To determine if globomycin could also increase resistance to other classes of β-lactam antibiotics, its effect on cefotaxime resistance in JE2, USA300 and ATCC43300 was evaluated. Cefotaxime was chosen because it is a 3rd generation cephalosporin with broad spectrum activity against Gram-positive and Gram-negative bacteria commonly used in the clinic, whereas oxacillin is a narrow-spectrum penicillin antibiotic. Cefotaxime 40 µg/ml inhibited growth of JE2 and USA300 (Fig. 3.5A and B), while 30 µg/ml inhibited growth of ATCC43300 (Fig. 3.5C). Globomycin (30 µg/ml) rescued growth of all three strains in cefotaxime (Fig. 3.5A, B and C) suggesting that globomycin-mediated inhibition of LspA may overcome the activity of many or all β-lactam antibiotics. These data also validate the conclusion that the mutation of *lspA* can in itself increase β-lactam resistance in MRSA.

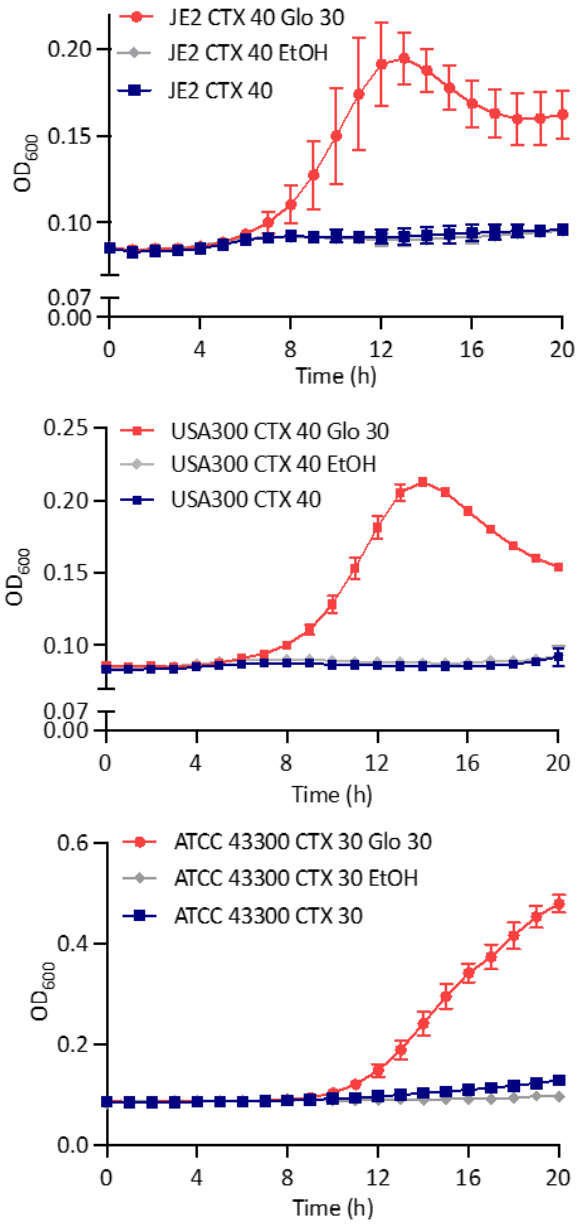

Fig. 3.5. Globomycin increases cefotaxime resistance in JE2, USA300 and ATCC43300.

(A) JE2 was grown in MHB 2% NaCl supplemented with cefotaxime (CTX) 40 µg/ml, MHB 2% NaCl supplemented with CTX 40 µg/ml and globomycin (Glo) 30 µg/ml or MHB 2% NaCl supplemented with CTX 40 µg/ml and 0.6% ethanol (control solvent for Glo). (B) USA300 was grown in MHB 2% NaCl supplemented with CTX 40 µg/ml, MHB 2% NaCl supplemented with CTX 40 µg/ml and Glo 30 µg/ml or MHB 2% NaCl supplemented with CTX 40 µg/ml and 0.6% ethanol (control solvent for Glo). (C) ATCC 43300 was grown in MHB 2% NaCl supplemented with CTX 30 µg/ml, MHB 2% NaCl supplemented with CTX 30 µg/ml and Glo 30 µg/ml or MHB 2% NaCl supplemented with CTX 30 µg/ml and 0.6% ethanol (control solvent for Glo). The CTX and Glo concentrations used in these experiments were determined

empirically for each strain. The cultures were grown in a Tecan Sunrise incubated microplate reader for 20 h at 35^{o}C OD_{600} was recorded at 1-hour intervals and growth curves were plotted in Prism software (GraphPad). The data presented are the average of 3 independent biological replicates, and error bars represent standard deviations.

3.3.4 Mutation of *lgt* in the *lspA* background restores wild type levels of β-lactam resistance.

LspA catalyses the second major step in the lipoprotein processing pathway (Fig. 3.2). To probe the contribution of lipoprotein processing to LspA-controlled oxacillin resistance, we compared the impact of *lgt*, *lspA* and *lgt*/*lspA* mutations on growth and resistance to oxacillin, as well as cefotaxime, nafcillin and vancomycin. Lgt catalyses the addition of a diacylglycerol moiety onto preprolipoproteins, from which the signal peptide is then cleaved by LspA (Fig. 3.2). To construct a *lspA*/*lgt* double mutant the erythromycin resistance marker of the *lspA*::Tn allele in NE1757 was first exchanged for a markerless transposon to generate a strain designated *lspA* MM into which the erythromycin-marked *lgt*::Tn allele from NE1905 was transduced.

Comparison of growth of JE2, NE1757, *lspA* MM, NE1905 and the *lspA*/*lgt* double mutant *lspA* MM /NE1905 revealed no significant differences MHB, MHB with 2% NaCl or TSB (Fig. 3.6A, B, C). However, consistent with previous analysis of a *lgt* mutant [88], the *lspA*, *lgt* and in particular the *lspA*/*lgt* mutants exhibited impaired growth in CDM (Fig. 3.6D), suggesting that aberrant lipoprotein processing may affect nutrient acquisition under substrate-limiting conditions.

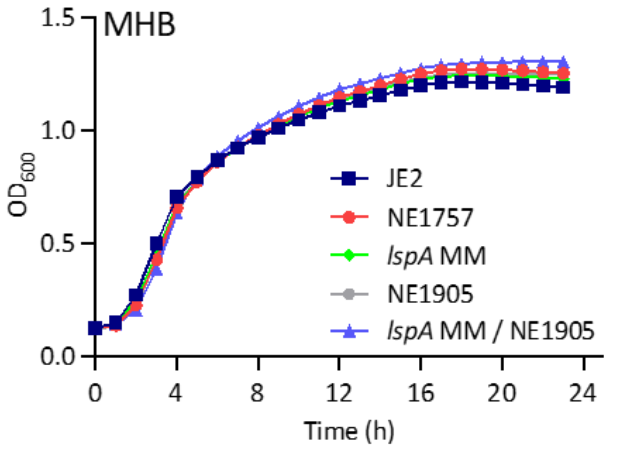
MHB
1.5
1.0
0.5
0.0
OD600
0
4
8
12
16
20
24
Time (h)
JE2
NE1757
lspA MM
NE1905
lspA MM / NE1905

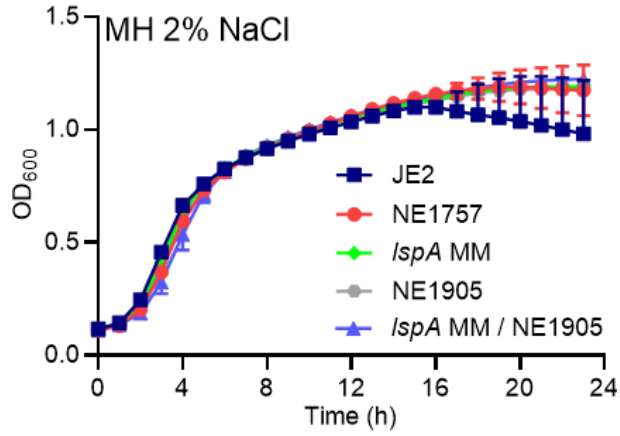
MH 2% NaCl
1.5
1.0
0.5
0.0
OD600
0
4
8
12
16
20
24
Time (h)
JE2
NE1757
lspA MM
NE1905
lspA MM / NE1905

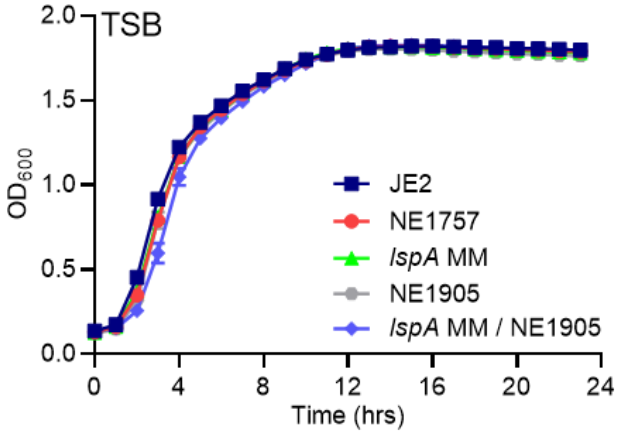
TSB
2.0
1.5
1.0
0.5
0.0
OD600
0
4
8
12
16
20
24
Time (hrs)
JE2
NE1757
lspA MM
NE1905
lspA MM / NE1905

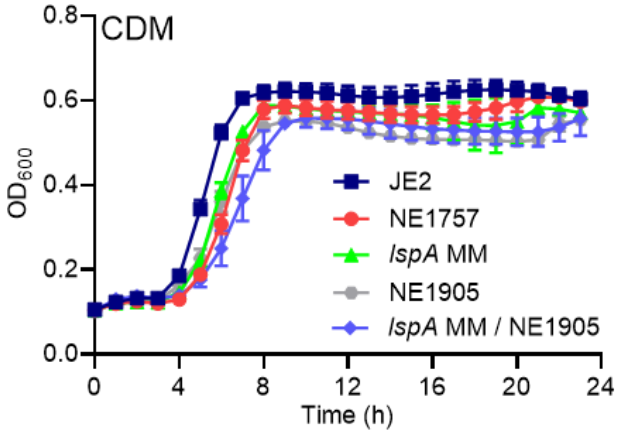
CDM
0.8
0.6
0.4
0.2
0.0
OD600
0
4
8
12
16
20
24
Time (h)
JE2
NE1757
lspA MM
NE1905
lspA MM / NE1905

Fig. 3.6. Mutation of *lspA* or *lgt* impacts growth in nutrient limited media but not in complex media.

Growth of JE2 wild type, NE1757 (*lspA*::Tn), *lspA* MM (markerless *lspA*::Tn), NE1905 (*lgt*::Tn) and *lspA* MM/NE1905 (*lspA*::Tn MM / *lgt*::Tn) in Muller Hinton broth (A), Muller Hinton broth with 2% NaCl (B), TSB (C), and chemically-defined medium (D). Growth experiments were performed in 96-well hydrophobic plates in a Tecan Sunrise incubated microplate reader for 24 h at 37^{o}C. OD_{600} was recorded at 1-hour intervals and growth curves were plotted in Prism software (GraphPad). The data presented are the average of 3 independent biological replicates, and error bars represent standard deviations.

The *lgt* mutant NE1905 exhibited no changes in susceptibility to oxacillin, cefotaxime, nafcillin or vancomycin (Table 3.1). As observed for oxacillin, the *lspA* mutant NE1757 was more resistant to cefotaxime and nafcillin and these phenotypes were complemented by the p*lspA* plasmid (Table 3.1). Neither the *lspA* nor *lgt* mutations increased resistance to vancomycin (Table 3.1). Oxacillin and nafcillin MICs were reduced to wild type levels in the *lspA*/*lgt* double mutant, and the cefotaxime MIC was significantly reduced (Table 3.1).

Taken together, these data indicate that while mutation of *lspA* or *lgt* or both impact growth in CDM, only mutation of *lspA* alone is associated with increased β-lactam resistance. The *lgt* mutation and possible accumulation of unprocessed prolipoproteins (Fig. 3.7B, D) does not increase β-lactam resistance, whereas the possible accumulation of diacylglyceryl-lipoprotein in a *lspA* mutant (Fig. 3.7C) is associated with this phenotype. The oxacillin, cefotaxime and nafcillin MICs of the *ecsB* mutant from the NTML were the same as wild type (Table 3.1) indicating that downstream processing of the LspA-cleaved signal peptide is not associated with altered β-lactam resistance. The lack of change in the *ecsB* resistance phenotype would support the conclusion that it is the accumulation of diacylglycerol-lipoprotein impacting resistance and not perturbations in the lipoprotein processing pathway itself.

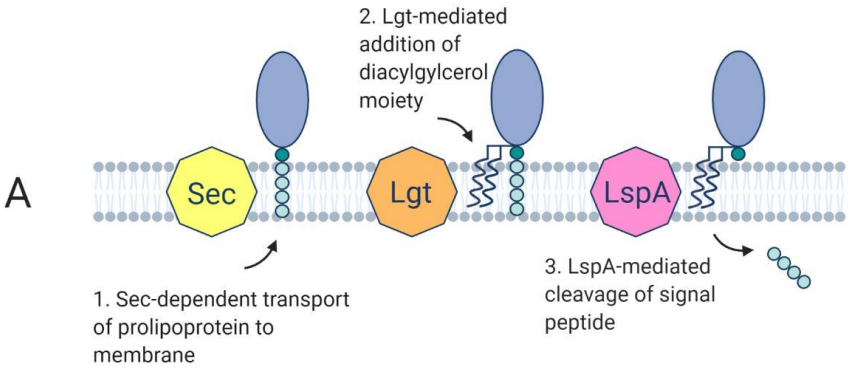
A
2. Lgt-mediated addition of diacylgylcerol moiety
Sec
Lgt
LspA
1. Sec-dependent transport of prolipoprotein to membrane
3. LspA-mediated cleavage of signal peptide

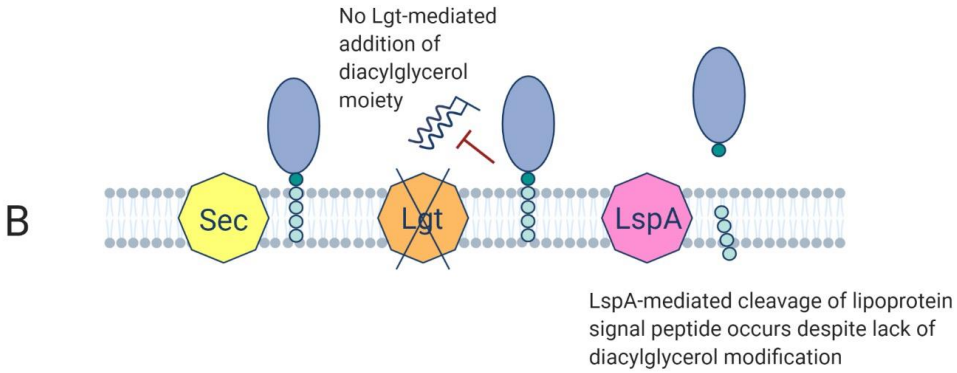
B
No Lgt-mediated addition of diacylglycerol moiety
Sec
Lgt
LspA
LspA-mediated cleavage of lipoprotein signal peptide occurs despite lack of diacylglycerol modification

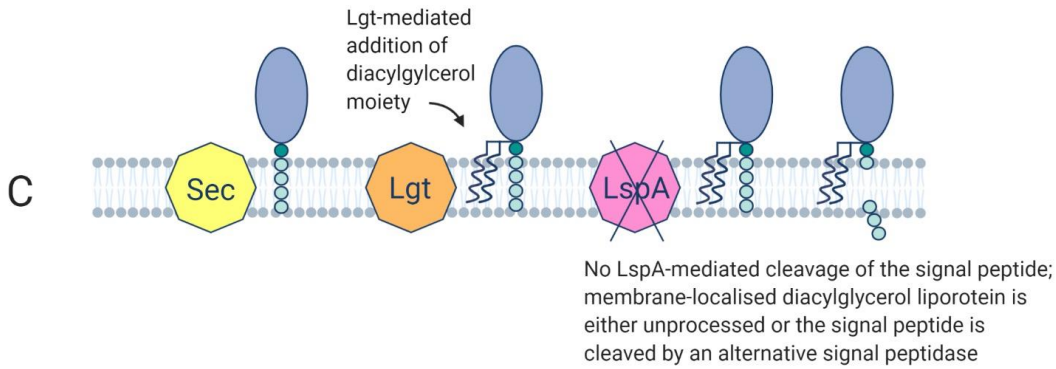
C
Lgt-mediated addition of diacylgylcerol moiety
Sec
Lgt
LspA
No LspA-mediated cleavage of the signal peptide; membrane-localised diacylglycerol liporotein is either unprocessed or the signal peptide is cleaved by an alternative signal peptidase

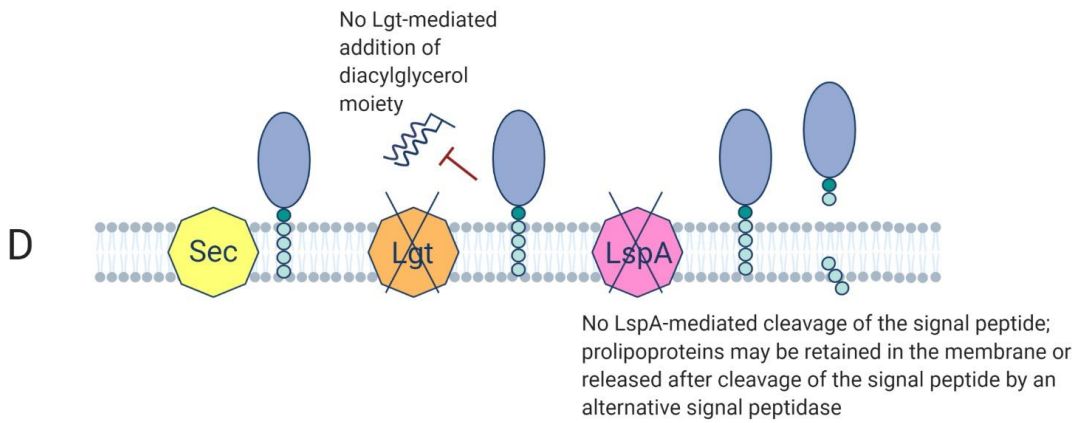
D
No Lgt-mediated addition of diacylglycerol moiety
Sec
Lgt
LspA
No LspA-mediated cleavage of the signal peptide; prolipoproteins may be retained in the membrane or released after cleavage of the signal peptide by an alternative signal peptidase

Fig. 3.7. Suggested model depicting the possible impacts of *lgt*, *lspA* and *lgt/lspA* mutations on lipoprotein processing in *S. aureus*.

(A) Overview of lipoprotein processing in Gram-positive bacteria. (B) The *lgt* mutant lacks diacylglyceryl transferase activity suggesting that diacylglycerol may not be added to the prolipoprotein. In this scenario, the prolipoprotein might still be released from the membrane due to LspA-mediated cleavage of the signal peptide. (C) In the *lspA* mutant, LspA-mediated cleavage of the signal peptide is proposed to be lost, but an alternative signal peptidase may undertake this activity. (D) We propose that prolipoproteins are not processed in mutants lacking Lgt and LspA activity, and may be retained in the membrane or released after cleavage of the signal peptide by an alternative signal peptidase.

3.3.5 Mutation of *lgt* increases susceptibility to the lipoteichoic acid synthase inhibitor Congo red.

Congo red was recently identified as a selective inhibitor of lipoteichoic acid synthase (LtaS) activity [130]. To investigate the possible involvement of LTA expression or stability in the increased resistance of the *lspA* mutant to β-lactams serial dilutions of overnight *lspA*, *lgt* and *lspA*/*lgt* mutant cultures were spotted onto TSA 0.125% Congo Red. Our data showed that mutation of *lgt* dramatically increased susceptibility to the selective LtaS inhibitor Congo red (Fig. 3.8) suggesting that impaired lipoprotein processing affects the expression or stability of LTA. However, while the *lgt*/*lspA* double mutant was even more susceptible to Congo red than the single *lgt* mutant, the single *lspA* mutations in NE1757 and NE1757 MM did not significantly alter Congo red susceptibility and complementation of NE1757 was also associated with increased susceptibility (Fig. 3.8). These data show that mutation of *lgt* or multicopy expression of *lspA* both increase susceptibility to this LTA inhibitor indicating that the lipoprotein processing pathway impacts LTA synthesis/stability in a complex manner. The mutations in the *lgt* and *lspA* genes alone, and in particular when combined, significantly increased resistance to the alanylation pathway inhibitor D-cycloserine (DCS) (Table 3.1). However, lack of correlation between the effects of *lgt* and *lspA* mutations on susceptibility to Congo red, DCS and β-lactams indicates that further analysis is needed to better understand the interactions between

lipoprotein processing pathway intermediates and the expression/stability of LTA and WTA.

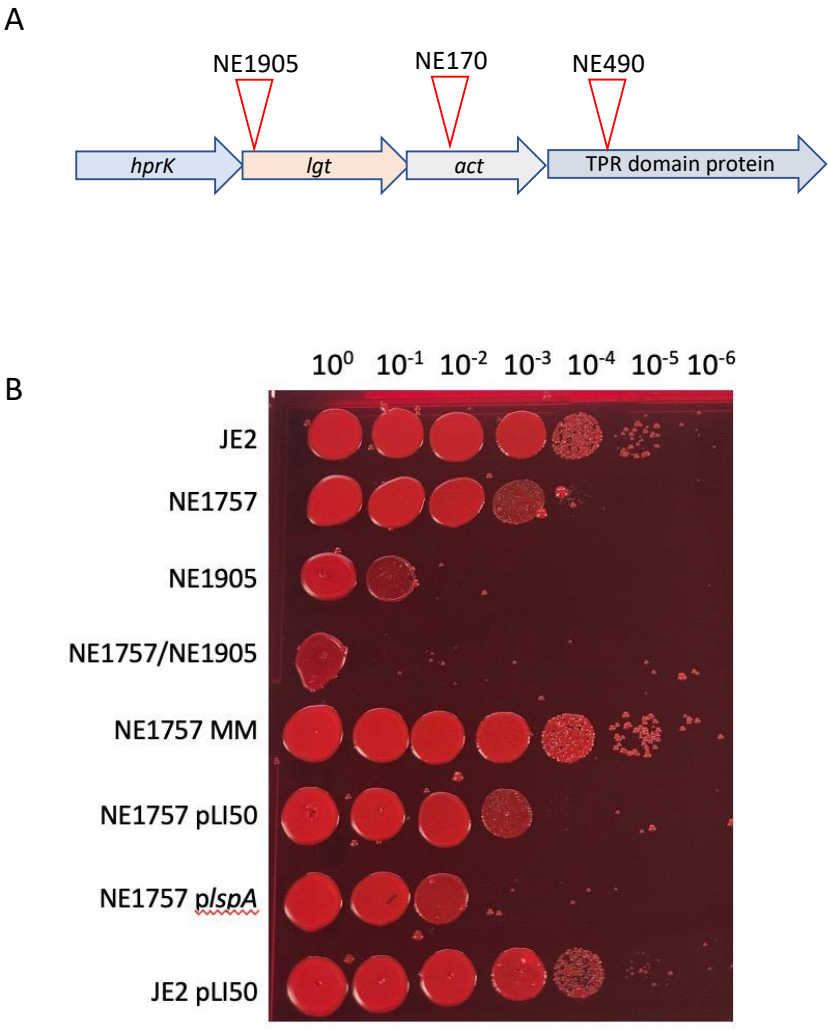

Fig. 3.8. Mutation of *lgt* increases susceptibility to Congo red.

(A) Organisation of the *lgt* operon including approximate locations of transposon insertions in NE1905 (*lgt*), NE170 (putative acetyltransferase) and NE490 (TPR domain-containing protein). (B) Overnight cultures of JE2, NE1757 (*lspA*::Tn), NE1905 (*lgt*), *lspA* MM/NE1905 (*lspA* MM/*lgt*::Tn), *lspA* MM (markerless *lspA* mutation), NE1757 pLI50, NE1757 p*lspA* and JE2 pLI50 were grown in TSB (without antibiotic selection), normalised to an OD600 of 1 in PBS, serially diluted and spotted onto TSA plates supplemented with 0.125% Congo red, and the plates were incubated for 24 h at 37°C. A representative image is shown.

3.4 Discussion

Advances in our understanding of the accessory factors that control levels of *mecA*/PBP2a-dependent resistance to methicillin has the potential to reveal new therapeutic targets and drugs that may facilitate the reintroduction of other β-lactam antibiotics for the treatment of MRSA infections. In this study, we demonstrated that mutation of the lipoprotein processing pathway gene *lspA*, or inhibition of LspA with globomycin increased resistance to β-lactam antibiotics. Although numerous mutations impacting the stringent response (ppGpp) and c-di-AMP signalling are associated with the transition from a heterogeneous to homogeneous pattern of resistance and elevated PBP2a expression [9, 93], our data show that the *lspA* mutation was not associated with a HoR phenotype, increased PBP2a expression, or altered NaCl tolerance (which is controlled by c-di-AMP) [66, 68]. However, changes in β-lactam resistance independent of altered PBP2a expression are well known [40, 55, 182], and several auxiliary factors known to influence β-lactam resistance in MRSA have been described [29, 53, 55, 183-185]. In addition to unchanged PBP2a protein levels, no evidence of peptidoglycan remodelling was observed in NE1757 after growth in the presence or absence of oxacillin, potentially implicating wall teichoic acid (WTA) or lipoteichoic acid (LTA) synthesis or stability in the *lspA* mutant phenotype. Inhibition of WTA synthesis was previously shown to decrease β-lactam resistance in a PBP2a-independent manner [53]. Reduced LTA stability, as evidenced by increased susceptibility to the selective lipoteichoic acid synthase inhibitor Congo red, was recently correlated with a PBP2a-independent reduction in β-lactam resistance in auxiliary factor *auxA* and *auxB* mutants [55]. Interestingly AuxA is structurally similar to SecDF [55] and may interact with the Sec pathway and lipoprotein processing (Fig. 3.7). The *lgt* mutant was significantly more susceptible to Congo red than the *lspA* mutant and multicopy expression of *lspA* also increased Congo red susceptibility suggesting that although the lipoprotein processing pathway modulates LTA synthesis/stability, the relationship between these two pathways appears to be complex.

Consistent with previous studies of lipoprotein pathway processing mutants in *S. aureus* [88], *Listeria monocytogenes* [189] and *Streptococcus agalactiae* [190], our analysis also showed that the *lgt, lspA* and *lgt*/*lspA* double mutants all exhibited impaired growth in CDM but not in TSB or MHB indicating that the impact of lipoprotein processing pathway mutations on nutrient acquisition and growth under nutrient limiting conditions can be compensated in rich media.

Mutation of the *lgt* gene from the lipoprotein processing pathway (Figs. 3.2, 3.7) did not affect β-lactam resistance and introduction of the *lgt* mutation into a *lspA* mutant reduced wild type levels of resistance. These data suggest that accumulation of diacylglycerol lipoprotein may be associated with elevated β-lactam resistance. Consistent with this possibility, lipoproteins were retained in the membrane of a *S. agalactiae lspA* mutant, but were released into the supernatant in large concentrations by *lgt* and *lgt/lspA* mutants [190]. Lipoproteins synthesised by the *S. agalactiae lspA* mutant retained their signal peptide, which was absent in a *lgt* mutant with LspA activity. Importantly, signal peptide processing also occurred in the *lgt/lspA* double mutant, albeit with cleavage occurring between different amino acids, implicating the involvement of an alternative signal peptidase. Our analysis revealed no change in oxacillin susceptibility in the MRSA *lgt*/*lspA* double mutant, indicating that even if an alternative peptidase can cleave the signal peptide, this may not impact β-lactam resistance. Furthermore, mutation of *ecsB*, which has recently been implicated in export of linear peptides from the lipoprotein processing pathway in *S. aureus* [173], did not change the oxacillin MIC in JE2 (Table 3.1) also indicating that downstream processing of signal peptides cleaved from lipoproteins by LspA is not associated with altered β-lactam resistance. In *L. monocytogene*s, deletion of *lgt* also led to significant release of lipoproteins into the supernatant. However, treatment of the *L. monocytogenes lgt* mutant with globomycin (inhibiting LspA activity) resulted in enhanced lipoprotein retention in the membrane [189], suggesting that the impact of globomycin and *lspA* mutation on lipoprotein processing is not necessarily the same. In a *S. aureus lgt* mutant, the Götz group

reported that the majority of lipoprotein (lacking signal peptide) was released into the supernatant [88].

Taken together, the data suggest that accumulation of membrane-anchored diacylglycerol lipoprotein with uncleaved signal peptide, or lipoprotein that is mislocalised or released due to aberrant signal peptide processing by an alternative peptidase, is accompanied by increased β-lactam resistance in MRSA.

3.5 Experimental procedures

3.5.1 Bacterial strains and culture conditions.

Bacterial strains and plasmids used in this study are listed in Table 3.S2. Escherichia coli strains were grown in Luria-Bertani (LB) broth or agar (LBA). *S. aureus* strains were grown in Tryptic Soy Broth (TSB), Tryptic Soy Agar (TSA) or chemically defined medium (CDM) [94]. Muller Hinton Broth (MHB) or Muller Hinton Agar (MHA) (Oxoid) supplemented with 2% NaCl where indicated, were used for antimicrobial susceptibility testing (AST). Antibiotic concentrations used were 10 µg/ml erythromycin, 10 µg/ml chloramphenicol, 75 µg/ml kanamycin, 100 µg/ml ampicillin.

Two hundred and fifty ml flasks were filled with 25 ml growth media, and overnight cultures were used to inoculate the media at a starting OD600 of 0.05. Overnight cultures were grown in TSB, and washed once in 5 ml PBS before being used to inoculate CDMG and CDM cultures.

Flasks were incubated at 37°C shaking at 200 rpm. OD600 readings were measured at 1 - 2 h intervals. Colony forming units (CFU) were enumerated in serially diluted 20 µl aliquots removed from flask cultures. Three independent biological replicates were performed for each strain and the resulting data plotted using GraphPad Prism software.

Data from growth experiments in a Tecan Sunrise microplate instrument were recorded by Magellan software. Overnight cultures were adjusted to an OD_{600} of 1 in fresh media and 10 µl inoculated into 200 µl media per well before being incubated at 37°C for 24 h with shaking. OD_{600} was recorded every 15 min. For CDM, overnight TSB cultures were first washed in 5 ml PBS and adjusted to OD_{600} of 1 in PBS.

3.5.2 Genetic manipulation of *S. aureus*.

Phage 80α transduction was used to verify the association between antibiotic resistance phenotypes and transposon insertion-marked mutations from the NTML as described previously [132]. Transductants were verified by PCR amplification of the target locus using primers listed in Table 3.S3. The plasmid pTnT, which contains a truncated, markerless transposon was used to construct a markerless *lspA* mutant designated *lspA* MM, as described previously [148]. A double *lspA*/*lgt* double mutant was subsequently constructed using phage 80α to transduce the *lgt*::Tn allele from NE1905 into *lspA* MM. A 1324 bp fragment encompassing the *lspA* gene was PCR amplified from JE2 genomic DNA using primers NE1757_INF#3_Fwd and NE1757_INF#3_Rev (Table 3.2), purified with GenElute™ PCR Clean-Up Kit and cloned into the *E. coli* - *Staphylococcus* shuttle vector pLI50 digested with *Eco*RI (New England Biolabs) using In-Fusion HD Cloning Kit (Clontech) to generate p*lspA.* Using electroporation*,* p*lspA* was transformed sequentially into Stellar (*E. coli* HST08) (Clontech), *S. aureus* RN4220 and finally NE1757.

3.5.3 Disk diffusion susceptibility assays.

Cefoxitin disk diffusion susceptibility assays were performed in accordance with CLSI guidelines [144]. Briefly, isolates were grown at 37°C on MHA for 24 h and 5 - 6 colonies were resuspended in 0.85% saline to OD_{600} of 0.08 - 0.1 (0.5 McFarland; 1×10^8 CFU/ml) and swabbed onto MHA plates with a uniform agar depth of 4 mm. A 30 µg cefoxitin disk (Oxoid) was applied, the plate incubated at 35°C for 16 - 18 h and the zone of inhibition diameter measured. Strains were classified as sensitive, intermediate, or resistant, according to CLSI criteria [146].

3.5.4 Minimum inhibitory concentration (MIC) measurements.

For oxacillin M.I.C.Evaluators (Oxoid) several colonies from 24 h MHA plates were resuspended in 0.85% saline to OD_{600} of 0.08 - 0.1, (0.5 McFarland standard) and

evenly swabbed onto MHA 2% NaCl (4 mm agar depth). An M.I.C.Evaluator strip was applied and the plate incubated at 35°C for 24 h. Three biological repeats were performed for each strain.

MIC measurements by broth microdilution or agar dilution were performed in accordance with CLSI methods for dilution susceptibility testing of staphylococci [145]. For broth microdilution MIC measurements using 96-well plates, each plate row was used to prepare two-fold dilutions of antibiotic in MHB, typically ranging from 256 - 0.5 µg/ml across 10 wells. For oxacillin and nafcillin MIC measurements, MHB 2% NaCl was used. Several colonies from 24 h MHA plates were resuspended in 0.85% saline to OD_{600} of 0.08 - 0.1 (0.5 McFarland standard), diluted 1:20 in 0.85% saline and 10 µl of this cell suspension used to inoculate each well (approximately 5×10^4 CFU/well) in a final volume of 100 ml. The plates were incubated at 35°C for 16 - 20 h, or 24 h incubation for oxacillin and nafcillin. The MIC was the lowest concentration of antimicrobial agent that completely inhibited growth.

Freshly prepared MHA plates (with 2% NaCl when using oxacillin and nafcillin) were supplemented with antimicrobial agents at 0.5, 1, 2, 4, 8, 16, 32, 64, 128 and 256 µg/ml to perform agar dilution MIC measurements. For the inoculum, several colonies from a 24-hour MHA plate were resuspended in 0.85% saline to give 0.5 McFarland or OD_{600} of 0.08 - 0.1 (1 - 2 x 10^8 CFU/ml). This was further diluted 1:20 in 0.85% saline and 4 µl was spot-inoculated onto each plate, yielding a final inoculum of 10^4 CFU per spot of 5-8 mm diameter). The MIC was the lowest concentration of antimicrobial agent that completely inhibited growth after 16-18 h (24 h for oxacillin and nafcillin) at 35°C, disregarding a single colony or a faint haze associated with the inoculum. MIC results were interpreted using CLSI standard M100, and strains classified as susceptible or resistant [146].

Congo red susceptibility assays were performed as described previously [191]. Briefly, overnight cultures grown in TSB were adjusted to an OD_{600} of 1 in PBS, serially diluted and spotted onto TSA plates supplemented with 1% aqueous Congo red solution (VWR) to a final concentration of 0.125%. Plates were

incubated for 24 h at 37°C. These assays were performed with at least 3 biological repeats and a representative image is shown for TSA 0.125% Congo red.

3.5.5 Autolytic activity assays.

Overnight cultures (20 ml) were inoculated into 20 ml TSB, grown at 37°C (200 rpm) to OD_{600} of 0.5, washed with 20 ml cold PBS, resuspended in 1 ml cold PBS and finally adjusted to OD_{600} of 1. Triton X-100 was added at a final concentration of 0.1% v/v and the cell suspension incubated at 37°C with shaking (200 rpm). OD_{600} was recorded every 30 min for 4 h. Autolytic activity was expressed as a percentage of the initial OD_{600}. NE406 (*atl*::Tn) was used as a control and at least 3 biological replicates performed for each strain.

3.5.6 Globomycin and β-lactam antibiotic synergy/antagonism assays.

One hundred µl of MHB cefotaxime or MHB 2% NaCl oxacillin was added to the individual wells of 96-well plates. The oxacillin or cefotaxime concentration chosen for each strain was based on approximate MICs i.e., the lowest antibiotic concentration that inhibited growth. Overnight MHB cultures were resuspended in PBS at OD_{600} of 0.1 (0.5 McFarland standard) and then further diluted 1:20 before 10 µl (approximately 5×10^5 CFU/ml) was added to each well and the plates were incubated at 35°C with shaking on a Tecan Sunrise microplate instrument for 20 h (cefotaxime) or 24 h (oxacillin). Globomycin ranging from 10 - 100 µg/ml was added to the cefotaxime or oxacillin cultures to measure potential synergism or antagonism. Three independent biological replicates were performed for each strain and antibiotic combination.

3.5.7 PBP2a western blot analysis.

Overnight MHB cultures were used to inoculate 25 ml of MHB 2% NaCl, with or without 0.5 µg/ml oxacillin to a starting OD_{600} of 0.05, incubated at 35°C (200 rpm

shaking) until an OD_{600} of 0.8 was reached before the cells were pelleted and resuspended in PBS to an OD_{600} of 10. Six µl of lysostaphin (10 µg/ml) and 1 µl of DNase (10 µg/ml) was added to 500 µl of this concentrated cell suspension before being incubated at 37°C for 40 min. Next, 50 µl of 10% SDS was added and the incubation continued for a further 20 min. The lysed cells were then pelleted in a microcentrifuge for 15 min, following which the protein-containing supernatant was collected and total protein concentration determined using the Pierce® BCA Protein Assay Kit. Samples containing 8 µg total protein were mixed 1:1 with protein loading buffer (2x) (National Diagnostics) and incubated at 95°C for 5 min and loaded onto a 7.5% Tris-Glycine gel and separated at 120 V for 60 mins. Electrophoretic transfer to a PVDF membrane was carried out at 30 V for 30 min on the Trans-Blot Turbo Transfer System (Biorad). The PVDF membrane was blocked overnight in 5% skim milk powder in PBS at 4°C. The following day, the membrane was washed in fresh PBS. Anti-PBP2a (Abnova) was diluted 1:1000 in PBS-Tween 20 (0.1%) and incubated with the membrane for 1 h at room temperature. The membrane was washed in PBS to remove unbound antibody. The secondary antibody, HRP-rec-Protein G (Invitrogen) was diluted 1:2000 in PBS-Tween 20 (0.1%) and incubated with the membrane at room temperature for 1 h. Visualisation of the membrane was performed with the Opti-4CN Substrate kit (Biorad). Three independent experiments were performed and representative images of the developed PVDF membrane were recorded.

3.5.8 Population level antibiotic resistance profile analysis.

Characterisation of the population resistance profile was performed as described previously [149]. Overnight cultures were grown in TSB, adjusted to an OD_{600} of 1, 10-fold serially diluted from 10^{-1} to 10^{-7}, and a 20 µl aliquot of each dilution plated onto a series of TSA agar plates supplemented with oxacillin 0.25, 0.5, 1, 2, 4, 8, 16, 32, 64 and 128 µg/ml. CFUs were enumerated after overnight incubation at 37°C and the results were expressed as CFU/ml at each oxacillin concentration. Three independent experiments were performed for each strain.

3.5.9 Antibiotic tolerance assay.

Tolerance assays were performed as described previously [70]. Briefly overnight TSB cultures were sub-cultured into 25 ml of fresh TSB in 250 ml flasks at a starting OD_{600} of 0.05 and grown to an OD_{600} of 0.5 at 37°C with 200 rpm shaking. At this time (T0) an aliquot was removed for CFU enumeration and 12.5 µg/ml oxacillin promptly added before the cultures were re-incubated. Antibiotic tolerance was expressed as the % CFU/ml after 2, 4, 6, 8 and 24 h growth in the antibiotic compared to the CFU/ml at T0. The results represent 3 biological replicates of each strain.

3.5.10 Salt tolerance assay.

Overnight TSB cultures were adjusted to an OD_{600} of 1 in fresh TSB and serially diluted from 10^{-1} to 10^{-7}. Four µl of each dilution was spot-inoculated onto TSA 2.2M NaCl plates and incubated at 37°C overnight.

3.5.11 Genomic DNA extraction and Whole Genome Sequencing (WGS).

Genomic DNA (gDNA) extractions were performed using the Wizard® Genomic DNA Purification Kit (Promega) following pre-treatment of *S. aureus* cells with 10 µg/ml lysostaphin (Ambi Products LLC) at 37°C for 30 min. WGS was performed by MicrobesNG (http://www.microbesng.uk) using an Illumina sequencing platform with 2x250 bp paired-end reads. CLC Genomics Workbench software (Qiagen) was used for genome sequencing analysis of strains. As a reference genome, a contig was produced for wild type JE2 by mapping Illumina reads onto the closely related USA300 FPR3757 genome sequence (RefSeq accession number NC_07793.1). The Illumina short read sequences from NE1757 were then mapped onto the assembled JE2 sequence and the presence of the transposon insertion confirmed. Single Nucleotide Polymorphisms (SNPs), deletions or insertions were mapped in the NE1757 genome and the presence of large deletions ruled out by manually searching for zero coverage regions using the CLC Genomics Workbench software.

3.5.12 Peptidoglycan analysis.

For each strain and growth condition tested, independent quadruplicate 50 ml cultures were grown to an OD_{600} of 0.5, harvested and resuspended in 5 ml PBS before peptidoglycan was extracted as described previously [132, 156]. Mass spectrometry was performed on a Waters XevoG2-XS QTof mass spectrometer. Structural characterization of muropeptides was determined based on their MS data and MS/MS fragmentation pattern, matched with PG composition and structure reported previously [157-160].

3.6 Supplementary Figures and Tables

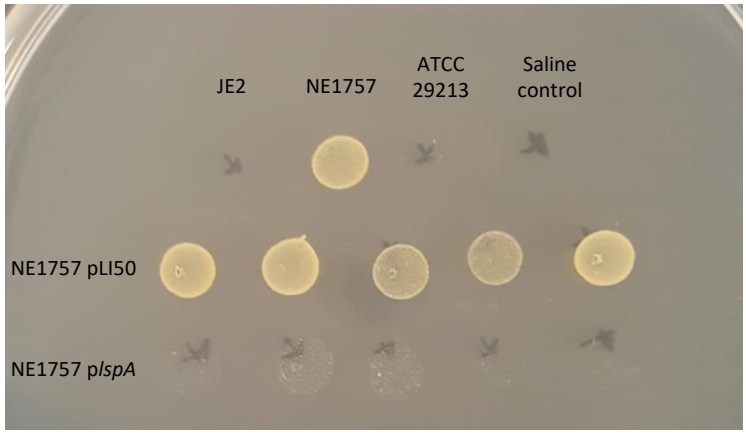

Supplementary Fig. 3.S1. Complementation of the NE1757 mutant with the *lspA* gene is accompanied by a wild-type oxacillin resistance phenotype.

JE2, NE1757 (*lspA*::Tn), NE1757 pLI50 and NE1757 p*lspA* were grown on MHA 2% NaCl supplemented with oxacillin 32 µg/ml. The plate shows 5 biological replicates each for NE1757 pLI50 and NE1757 p*lspA.* ATCC 29213 was included as an oxacillin susceptible control.

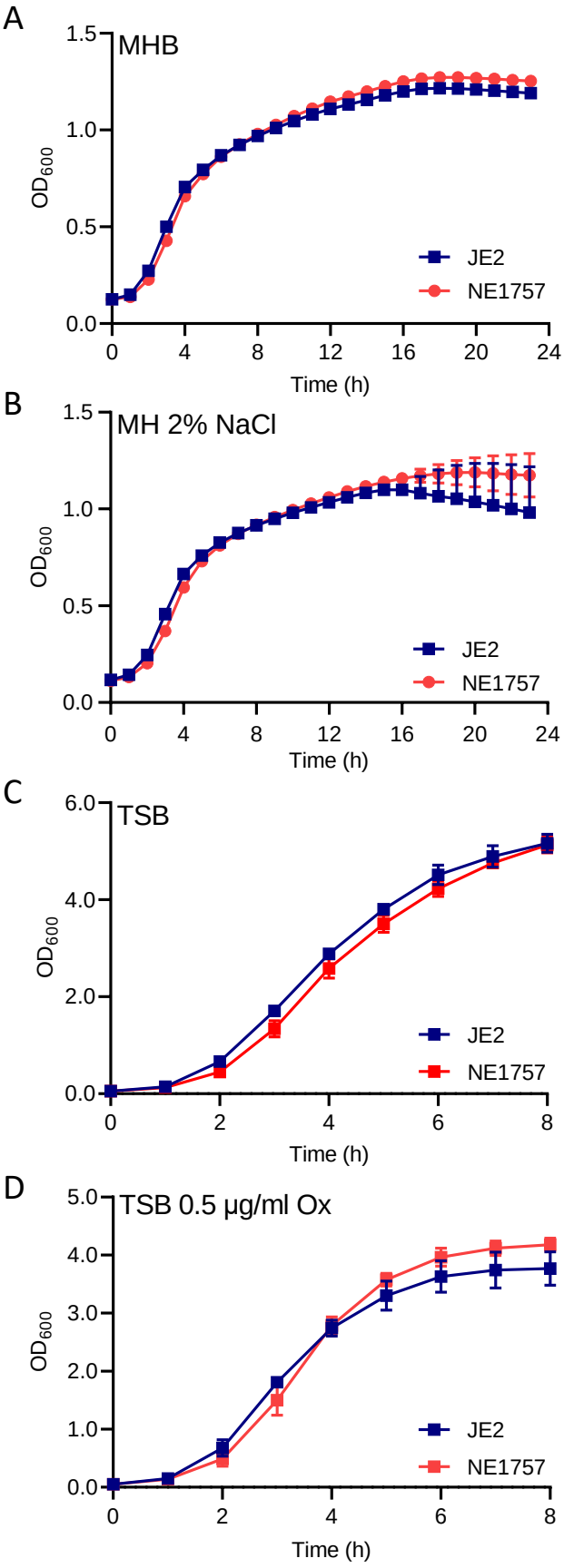
A
MHB
OD600
Time (h)
JE2
NE1757
B
MH 2% NaCl
OD600
Time (h)
JE2
NE1757
C
TSB
OD600
Time (h)
JE2
NE1757
D
TSB 0.5 µg/ml Ox
OD600
Time (h)
JE2
NE1757

Supplementary Fig. 3.S2. Mutation of *lspA* does not impact growth in MHB or TSB media.

Growth of JE2 and NE1757 cultures in (A) MHB, (B) MHB 2% NaCl, (C) TSB and (D) TSB 0.5 µg/ml oxacillin. MHB cultures were grown in 96-well plates in a Tecan Sunrise incubated microplate reader for 24 h at 37˚C. The OD_{600} was recorded at 15 min intervals and growth curves were plotted in Prism software (GraphPad). TSB cultures were grown in flasks and the OD_{600} monitored every 2 h. All data presented are the average of 3 independent biological replicates, and error bars represent standard deviations.

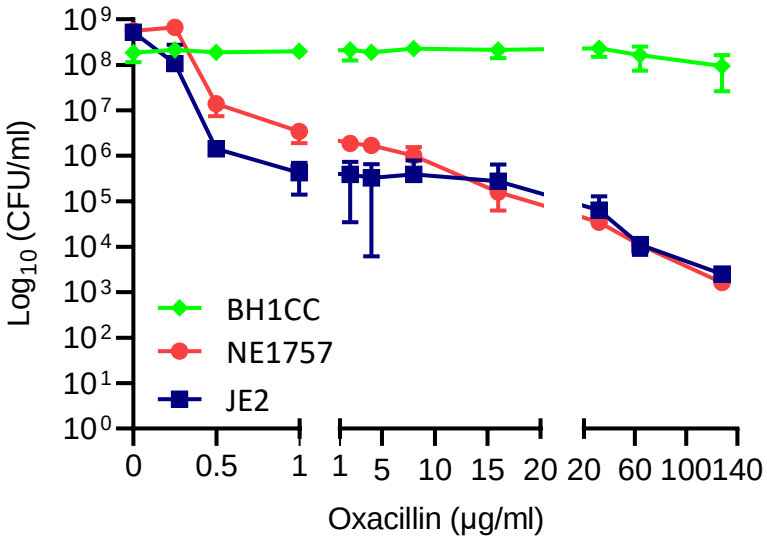

Supplementary Fig. 3.S3. NE1757 (*lspA*) exhibits heterogenous resistance to oxacillin.

Overnight cultures of JE2, NE1757 and BH1CC were grown in TSB, adjusted to OD_{600} of 1, serially diluted and plated onto TSA and TSA supplemented with 0.25, 0.5, 1, 2, 4, 8, 16, 32, 64 and 128 µg/ml oxacillin. CFUs were enumerated after overnight incubation at 37°C. The data are expressed as CFU/ml at each oxacillin concentration, plotted using Prism software (GraphPad). Three independent population analysis profile experiments were performed, and error bars represent standard deviations. BH1CC, which exhibits homogenous oxacillin resistance, was included as a control.

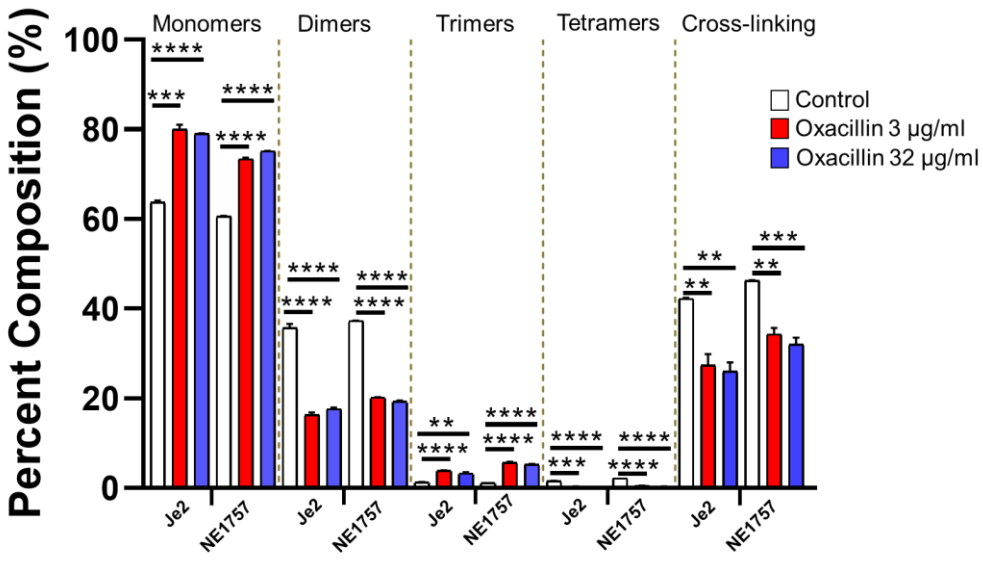

Supplementary Fig. 3.S4. Relative proportions of cell wall muropeptide fractions based on oligomerization and relative cross-linking efficiency of cell wall muropeptide fractions in peptidoglycan extracted from JE2 and NE1757.

Cells were collected from cultures grown to exponential phase in MHB or MHB supplemented with oxacillin 3 µg/ml or 32 µg/ml. Each profile shown is a representative of 3 biological replicates. Significant differences determined using Students t-test (**P < .01; ***P < .001; ****P<.0001).

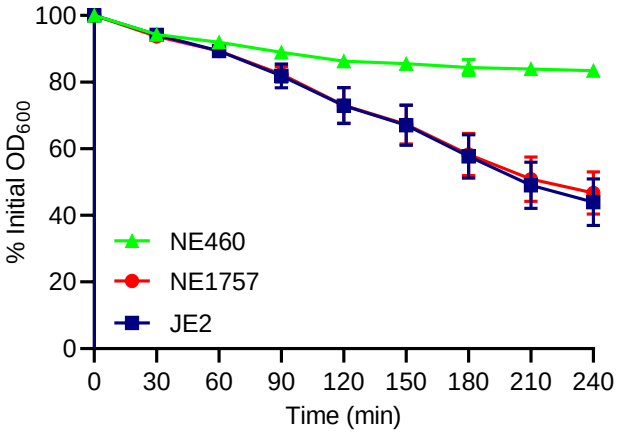

Supplementary Fig. 3.S5. Autolytic activity is unaffected by the *lspA* mutation. Triton X-100-induced autolysis of JE2, NE1757 (*lspA*::Tn) and NE406 (*atl*::Tn, negative control).

The strains were grown to OD_{600} = 0.5 in MHB medium at 37°C, before being washed in cold PBS and resuspended in 0.1% Triton X-100. The OD_{600} was monitored, and autolysis was expressed as a percentage of the initial OD_{600}. The experiments were repeated 3 independent times, plotted using Prism software (GraphPad) and standard deviations are shown.

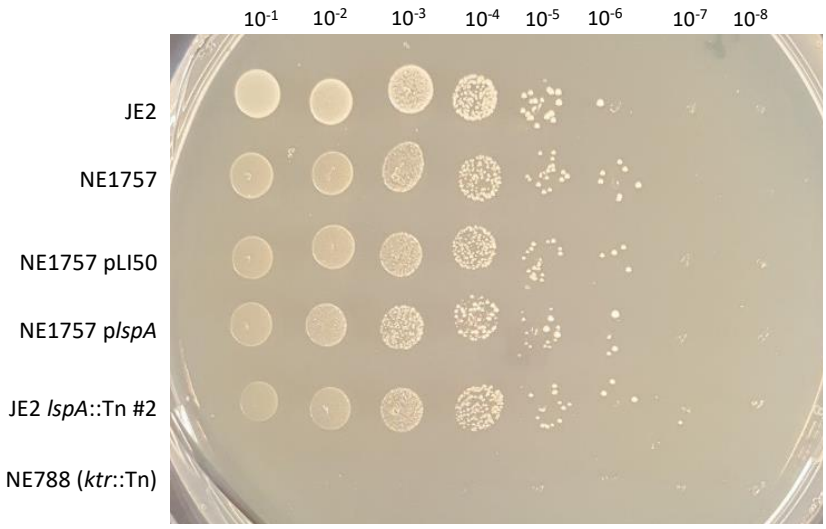

Figure 3.S6. Mutation of *lspA* has no significant impact on salt tolerance in JE2.

Overnight cultures of JE2, NE1757, NE1757 pLI50, NE1757 p*lspA*, JE2 *lspA*::Tn #2 transductant and NE788 (JE2 *ktr*::Tn, NaCl-sensitive control) were grown in TSB and cell density was standardised to OD_{600} of 1. Four ml aliquots from 10-fold serial dilutions were spotted onto TSA supplemented with 2.2 M NaCl and the plates incubated overnight at 37°C. Three independent experiments were carried out and a representative plate is shown.

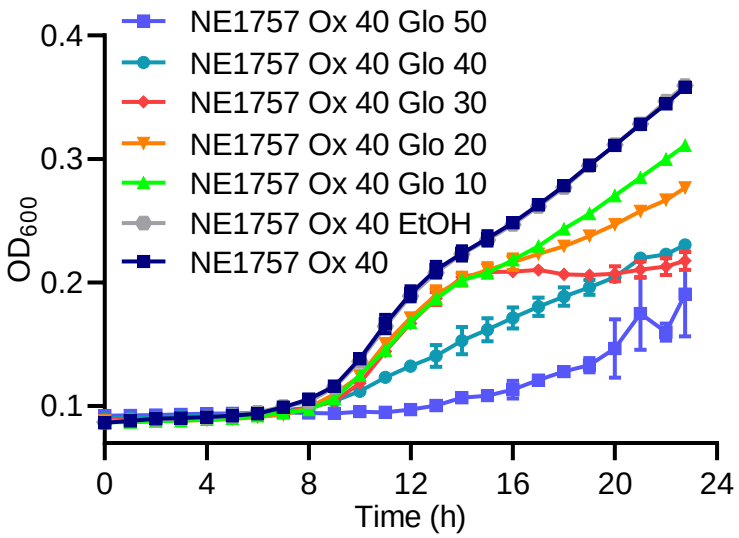

Supplementary Fig. 3.S7. Globomycin does not increase oxacillin resistance in the *lspA* mutant NE1757.

NE1757 was grown in MHB 2% NaCl supplemented with a sub-inhibitory concentration of oxacillin (40 µg/ml) and a range (10 – 50 µg/ml) of globomycin concentrations. The solvent for globomycin, 0.6% ethanol, was included as a control. The cultures were grown in a Tecan Sunrise incubated microplate reader for 24 h at 35°C. OD_{600} was recorded at 15 min intervals and growth curves were plotted in Prism software (GraphPad). The data presented are the average of 3 independent biological replicates, and error bars represent standard deviations.

Supplementary Table 3.S1. Genome sequence changes in NE1757 (*lspA*::Tn)

Reference Position[1]	Type[2]	Ref.[3]	Allele[4]	Freq.[5]	Annotation
1192002 - 1192003	INS	TA	T-Tn-A	100	*Bursa aurealis* transposon

[1]Reference position: Position in the USA300 FPR3757 genome sequence (NC_007793.1).

[2]Type of mutation: INS, insertion.

[3]Ref: Nucleotide base in the USA300 FPR3757 reference genome.

[4]Allele: Nucleotide base at the same position in NE1757.

[5]Freq.: % Frequency at which INS was found in NE1757 compared to JE2.

Table 3.S2. Bacterial strains and plasmids used in this study

Strain/plasmid	Description and resistance	Source/reference
***Escherichia coli* strains**		
HST08	TaKaRa *E. coli* HST08 Premium Electro-Cells	TaKaRa
HST08 pLI50	*E. coli* HST08 pLI50; Amp^R	This study
HST08 p*lspA*	*E. coli* HST08 p*lspA*; Amp^R	This study
***Staphylococcus aureus* strains**		
JE2	JE2 (plasmid-cured derivative of strain LAC)	[113]
8325-4	NCTC 8325 derivative cured of prophages, methicillin susceptible, CC8.	[192]
RN4220	RN4220 (Restriction-deficient derivative of 8325-4)	[193]
BHICC	MRSA clinical isolate; SCC*mec* type II; CC8	[132]
ATCC 29213	Quality control strain for susceptibility testing; oxacillin sensitive	*S. aureus* ATCC 29213
ATCC 43300	Quality control strain for susceptibility testing; oxacillin resistant, SCC*mec* Type II	*S. aureus* ATCC 43300
USA300	USA300_FPR3757	[92]
NE1757 (*lspA*)	JE2 *lspA*::Tn; Erm^R	[113]
NE1905 (*lgt*)	JE2 *lgt*::Tn; Erm^R	[113]
NE1757 MM	JE2 *lspA*:Tn (truncated, markerless Tn); Erm^S	This study
NE1757/NE1905	JE2 *lspA* MM *lgt*::Tn; Erm^R	This study
RN4220 pTnT	RN4220 pTnT	[113]
RN4220 pLI50	RN4220 pLI50; Cam^R	This study
RN4220 p*lspA*	RN4220 p*lspA*	This study
NE1757 p*lspA*	JE2 *lspA*::Tn p*lspA*; Erm^R Cam^R	This study
NE1757 pLI50	JE2 *lspA*::Tn pLI50; Erm^R Cam^R	This study
JE2 pLI50	JE2 pLI50; Cam^R	This study
lspA MM pLI50	JE2 *lspA* MM pLI50; Cam^R	This study

lspA MM p*lspA*	JE2 *lspA* MM p*lspA*; Cam^R	This study
JE2 *lspA*::Tn #2	JE2 *lspA*::Tn; Erm^R	This study
JE2 *lspA*::Tn #4	JE2 *lspA*::Tn; Erm^R	This study
NE788	JE2 *trkA*::Tn; Erm^R	[113]
NE460	JE2 *atl*::Tn; Erm^R	[113]
NE107	JE2 *ecsB*::Tn; Erm^r	[113]
Plasmids		
pTnT	Plasmid to replace Erm^R marker from transposon mutants with a markerless mutation. Cam^R	[148]
pLI50	*S. aureus-E. coli* shuttle vector	[194]
p*lspA*	pLI50 carrying the *lspA* gene from JE2	This study

Table 3.S3. Oligonucleotides used in this study

Target	**Name**	**Primer Sequence (5' – 3')**
lspA (infusion primers)	NE1757_INF#3_Fwd	TCGTCTTCAAGAATTTTATGAAGGAG GCTGGGACA
	NE1757_INF#3_Rev	TACCGAGCTCGAATTCAGGCAGCAAC TTATCTACACG
Tn-check primers	**Name**	**Primer Sequence (5' – 3')**
lspA	NE1757_fwd	GTTCCAGCCTGCTTTCCTAATT
	NE1757_rev	ACACGCATACCTGTTTGTTCT
lgt	NE1905_fwd	GCATTAACACGGCCGAAGAA
	NE1905_rev	CAACCGTACCAGCTGCAAC

3.7 Acknowledgements

This study was funded by grants from the Health Research Board (HRA-POR-2015-1158 and ILP-POR-2019-102) (www.hrb.ie), the Irish Research Council (GOIPG/2016/36) (www.research.ie), Science Foundation Ireland (19/FFP/6441) (www.sfi.ie) to J.P.O'G, and Svenska Forskningsrådet Formas to F.C. We are grateful to Christopher Campbell and Laura Gallagher for assistance and advice throughout this study. The illustrations in Figures 2 and 8 were created with Biorender.com.

Chapter 4: Roles of *cycA* and *ecsB* in the susceptibility of MRSA to β-lactam antibiotics

Chapter 4:

Roles of *cycA* and *ecsB* in the susceptibility of MRSA to β-lactam antibiotics

The work described in this chapter is part of a wider collaborative effort, part of which has been published:

Gallagher LA, Shears RK, **Fingleton C**, Alvarez L, Waters EM, Clarke J, Bricio-Moreno L, Campbell C, Yadav AK, Razvi F, O'Neill E, O'Neill AJ, Cava F, Fey PD, Kadioglu A, O'Gara JP. 2020. Impaired Alanine Transport or Exposure to D-Cycloserine Increases the Susceptibility of MRSA to beta-lactam Antibiotics. J Infect Dis **221:**1000-1016.

My specific contributions are as follows:

Identification of *cycA* mutant during the oxacillin screen of the NTML and transduction of *cycA*::Tn into JE2

Figure 4.1B (MIC measurements), Figure 4.1D (Susceptibility to DCS)

Figure 4.2 (In conjunction with Laura Gallagher)

Figures 4.7, 4.8, 4.9, 4.10

Addition work:

The amino acid analysis in Figures 4.3, 4.4 and 4.6 was performed by the Protein Structure Core Facility, University of Nebraska Medical Center.

The data in Figure 4.5 was generated by Dr Rebecca Shears in the laboratory of Prof Aras Kadioglu in the University of Liverpool.

The data in Figures 4.11 and 4.12 was generated by Dr Fareha Ravzi in the laboratory of Prof Paul Fey at the University of Nebraska Medical Centre, Omaha.

4.1 Abstract

Prolonging the clinical effectiveness of β-lactams, which remain first-line antibiotics for many infections, is an important part of efforts to address antimicrobial resistance. We report here that inactivation of the predicted D-cycloserine (DCS) transporter gene *cycA* re-sensitized MRSA to β-lactam antibiotics. The *cycA* mutation also resulted in hyper-susceptibility to DCS, an alanine analogue antibiotic that inhibits alanine racemase and D-alanine ligase required for D-alanine incorporation into cell wall peptidoglycan (PG). Alanine transport was impaired in the *cycA* mutant and this correlated with increased susceptibility to oxacillin and DCS. DCS re-sensitised MRSA to β-lactams *in vitro* and significantly enhanced MRSA eradication by oxacillin in a mouse bacteraemia model. However, the *cycA* mutant did not exhibit increased susceptibility to β-lactams *in vivo* and further *in vitro* experiments revealed that this mutant exhibited wild type levels of oxacillin resistance during growth in chemically defined media lacking glucose (CDM), when amino acids are known to be used as carbon sources. This data suggested that an alternative alanine permease(s) is active during growth in CDM. A screen of putative membrane transporter mutants revealed that mutation of both *cycA* and *ecsB* increased β-lactam susceptibility in CDM, but was not accompanied by reduced alanine consumption from the media, suggesting that the pleiotropic effects of the *ecsB* mutation do not include impaired alanine transport. Work is ongoing in our laboratory to identify alanine transporters active in CDM. These findings reveal alanine transport as a new therapeutic target to enhance the susceptibility of MRSA to β-lactam antibiotics.

4.2 Introduction

Whilst many bacteria can exhibit resistance to select antimicrobials, isolates of the human pathogen *Staphylococcus aureus* can express resistance to all licensed anti-staphylococcal drugs. This results in significant morbidity and mortality, with up to 20% of patients with systemic methicillin resistant *S. aureus* (MRSA) infections dying, despite receiving treatment with anti-staphylococcal drugs [195]. As part of our efforts to identify improved therapeutic approaches for MRSA infections, we recently described the novel use of β-lactam antibiotics to attenuate the virulence of MRSA-induced invasive pneumonia and sepsis [122]. We demonstrated that oxacillin-induced repression of the Agr quorum-sensing system and altered cell wall architecture resulted in downregulated toxin production and increased MRSA killing by phagocytic cells, respectively [122]. Supporting this *in vitro* data, a randomised controlled trial involving 60 patients showed that the β-lactam antibiotic flucloxacillin in combination with vancomycin shortened the duration of MRSA bacteraemia from 3 days to 1.9 days [196, 197].

Because expression of methicillin resistance in *S. aureus* impacts fitness and virulence and is a regulated phenotype, further therapeutic interventions may also be possible. The complexity of the methicillin resistance phenotype is evident among clinical isolates of MRSA, which express either low-level, heterogeneous (HeR) or homogeneous, high-level methicillin resistance (HoR) [198-200]. Exposure of HeR isolates to β-lactam antibiotics induces expression of *mecA,* which encodes the alternative penicillin binding protein 2a (PBP2a) and can select for mutations in accessory genes resulting in a HoR phenotype, including mutations that affect the stringent response and c-di-AMP signalling [68, 70, 71, 119, 120]. Because accessory genes can influence the expression of methicillin resistance in MRSA, targeting the pathways associated with such genes may identify new ways to increase the susceptibility of MRSA to β-lactams. To pursue this, we performed a forward genetic screen to identify loci that impact the expression of resistance to β-lactam antibiotics in MRSA. Using the Nebraska Transposon Mutant Library (NTML), which comprises 1,952 sequence-defined

transposon insertion mutants [113], inactivation of a putative amino acid permease gene, *cycA*, was found to reduce resistance to cefoxitin, the β-lactam drug recommended by the Clinical and Laboratory Standards Institute for measuring *mecA*-mediated methicillin resistance in MRSA isolates. Amino acid transport and susceptibility to oxacillin and DCS were compared in the wild-type and *cycA* mutant grown in chemically defined media (CDM), CDM supplemented with glucose (CDMG) and other complex media. The activity of DCS and β-lactams, alone and in combination, against MRSA was measured *in vitro* and in a mouse model of bacteraemia. The role of the *ecsB* gene in β-lactam resistance and alanine transport in CDM is described. Our experiments suggest that therapeutic strategies targeting alanine transport, which was required for resistance to β-lactams and DCS.

4.3 Results

4.3.1 Mutation of *cycA* increases the susceptibility of MRSA to β-lactam antibiotics and D-cycloserine.

To identify new ways of controlling expression of methicillin resistance, we sought to identify novel mutations involved in this phenotype. An unbiased screen of the NTML to identify mutants with increased susceptibility to cefoxitin identified NE810 (SAUSA300_1642) (Fig. 4.1A), which also exhibited a >128-fold increase in susceptibility to oxacillin (Fig. 4.1B). NE810 was previously identified among several NTML mutants reported to be more susceptible to amoxicillin [201], but was not investigated further. Expression of *mecA* was not affected in NE810 (Fig. 4.1C) and genome sequence analysis revealed an intact SCC*mec* element and the absence of any other mutations. NE810 was successfully complemented (Fig. 4.1B), and transduction of the SAUSA300_1642 allele into JE2 was also accompanied by increased cefoxitin and oxacillin susceptibility (Table 4.1).

Table 4.1. Antibacterial activity (minimum inhibitory concentrations, MIC) and drug synergy (fractional inhibitory concentration indices, ΣFIC) of D-cycloserine (DCS) and several β-lactam antibiotics with different PBP specificity, namely oxacillin (OX; PBP1, 2, 3), nafcillin (NAF; PBP1), cefoxitin (FOX; PBP4), imipenem (IMP; PBP1) and clindamycin (CLI) alone and in β-lactam combinations.

Antibiotic → / ↓ Strain	OX*	NAF*	DCS*	FOX*	DCS/FOX** (ΣFIC)***	IPM*	DCS/IPM** (ΣFIC)***	CLI*	DCS/CLI** (ΣFIC)***
JE2	64	32	32	64	8/8 (0.37)	1	ND	0.25	ND
NE810 (*cycA*)	0.25	0.5	2	8	ND	0.125	ND	ND	ND
USA300	64	32	32	64	8/8 (0.37)	1	ND	2048	32/2048 (2)
USA300 *cycA*	0.25	1	2	8	ND	0.125	ND	ND	ND
COL	512	256	64	512	8/128 (0.37)	256	8/64 (0.37)	0.5	ND

* MIC values for each antibiotic when measured individually; µg/ml

** MIC values for each antibiotic when measured in combination, also known as the fractional inhibitory concentration (FIC); µg/ml

*** FIC indices (ΣFIC) for the antibiotic combination. ΣFIC = FIC A + FIC B, where FIC A is the MIC of DCS in combination with the β-lactam/MIC of DCS alone, and FIC B is the MIC of the β-lactam in combination with DCS/MIC of the beta-lactam alone. The combination is considered synergistic when the ΣFIC is ≤0.5, indifferent when the ΣFIC is >0.5 to <2.

‡ND. Not determined if strain is susceptible (or hyper-resistant) to β-lactam antibiotic or for *cycA* mutants with reduced DCS & β-lactam MIC

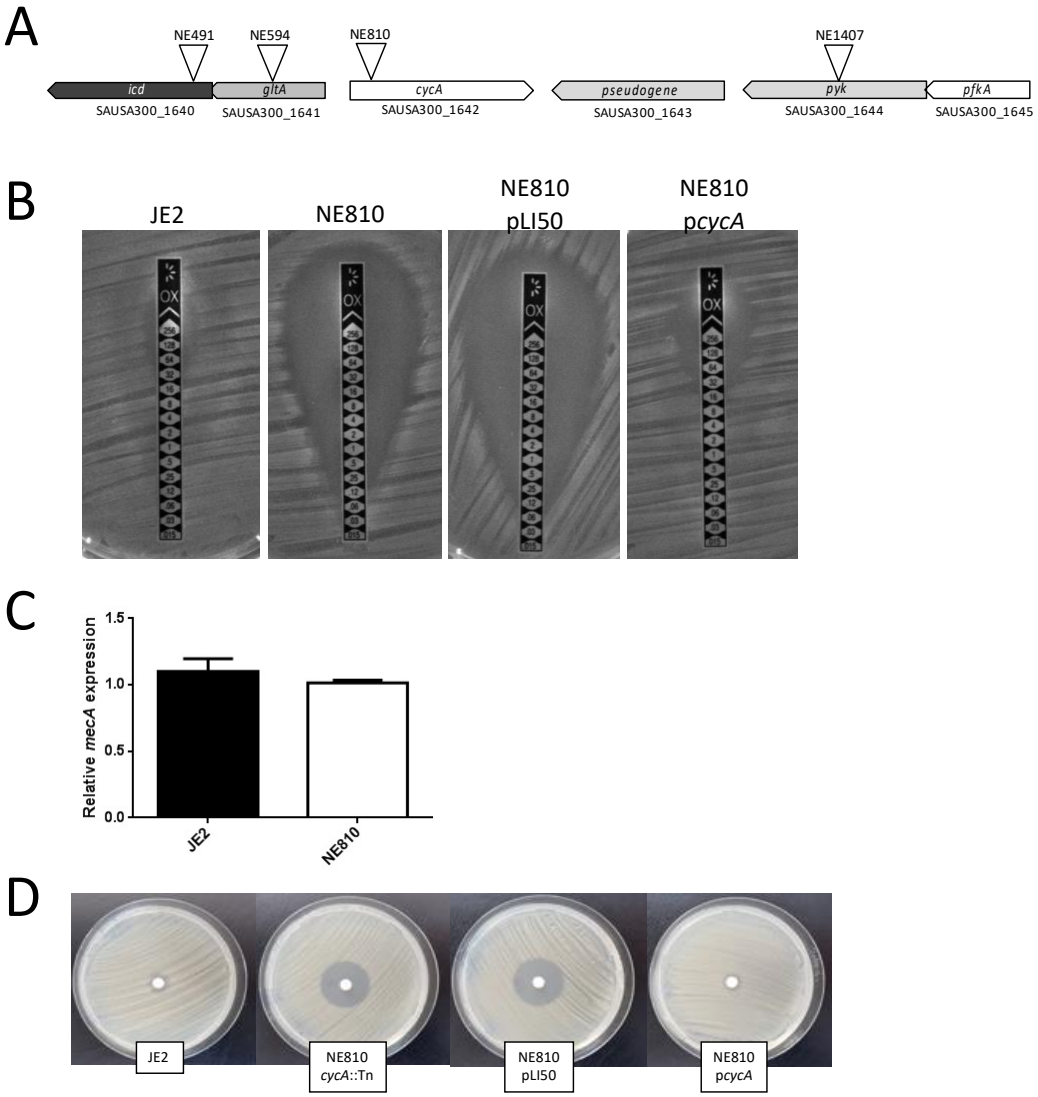

Fig. 4.1. Mutation of *cycA* increases the susceptibility of MRSA to β-lactam antibiotics and D-cycloserine.

A. Chromosomal location of *cycA* and neighbouring genes *icd* (isocitrate dehydrogenase), *gltA* (citrate synthase), *pyk* (pyruvate kinase) and *pfkA* (6-phospho-fructokinase). The locations of transposon insertions in NE810, NE491, NE594 and NE1497 mutants from the Nebraska library are indicated. B. E-test measurement of oxacillin minimum inhibitory concentrations (MICs) in JE2 (wild type), NE810 (*cycA*::Tn), NE810 carrying pLI50 (control) and p*cycA*. C. Comparison of relative *mecA* gene expression by LightCycler RT-PCR in JE2 and NE810 grown to OD_{600}=3 in BHI media. The data are the average of three independent experiments and standard deviations are shown. D. Comparison of zones of inhibition around D-cycloserine 30 µg disks on lawns of JE2, NE810 (*cycA*::Tn), NE810 pLI50 (control) and NE810 p*cycA* grown on Mueller Hinton (MH) agar.

SAUSA300_1642 is annotated as a serine/alanine/glycine transporter with homology to CycA in *Mycobacterium tuberculosis* [202, 203] required for DCS resistance in *Mycobacteria* [202, 203]. In contrast to the observations in *Mycobacteria*, our data showed that NE810 and several unrelated MRSA strains carrying the *cycA* mutation were significantly more susceptible to DCS than the wild type JE2 (Fig. 4.1D, Table 4.1). The *cycA* mutation also reduced the DCS MIC of the MSSA strains 8325-4 and ATCC29213 from 32 to 4 µg/ml. DCS inhibits alanine racemase (Alr) that converts L-alanine to D-alanine and the Ddl, D-alanyl:D-alanine ligase [131]. A mutant in the putative *ddl* SAUSA300_2039 gene is not available in the NTML library, suggesting that it may be essential. However, the *alr* mutant NE1713 was significantly more susceptible to cefoxitin (Fig. 4.2A; MIC=16 µg/ml) and DCS (Fig. 4.2B; MIC <0.25 µg/ml), consistent with an important role for D-alanine in resistance to both antibiotics.

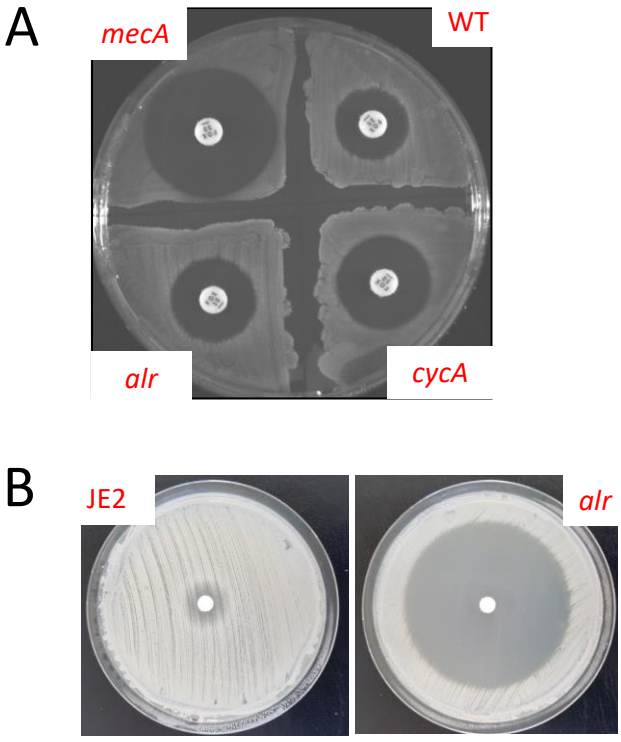

Fig. 4.2. Susceptibility of JE2, NE810, NE1868 and NE1713 to cefoxitin and D-cycloserine

A. Susceptibility of JE2 (wild type), NE1868 (*mecA*::Tn), NE810 (*cycA*::Tn), and NE1713 (*alr*::Tn) grown on MH agar to cefoxitin (FOX, 30 mg disks). B. Susceptibility

of JE2 (wild type) and NE1713 (*alr*::Tn) grown on MH agar to D-cycloserine (DCS, 30 mg disks).

4.3.2 CycA is required for alanine transport and D-ala-D-ala incorporation into the peptidoglycan stem peptide.

To investigate the role of CycA as a potential permease, JE2 and NE810 were grown for 8 h in chemically defined media containing 14mM glucose (CDMG) and amino acid consumption in spent media was measured. Although no growth rate or yield difference was noted between JE2 and NE810 in CDMG (Fig. 4.3A), alanine uptake by NE810 was significantly impaired compared to JE2 (Fig. 4.3B). Utilisation of other amino acids by NE810 and JE2, including serine and glycine, were similar (Fig. 4.4). Impaired alanine transport in the *cycA* mutant grown in CDMG correlated with increased susceptibility to oxacillin (1 µg/ml) (Fig. 4.3C) and DCS (1 µg/ml) (Fig. 4.3D). These data demonstrate for the first time that CycA in *S. aureus* is required for alanine transport.

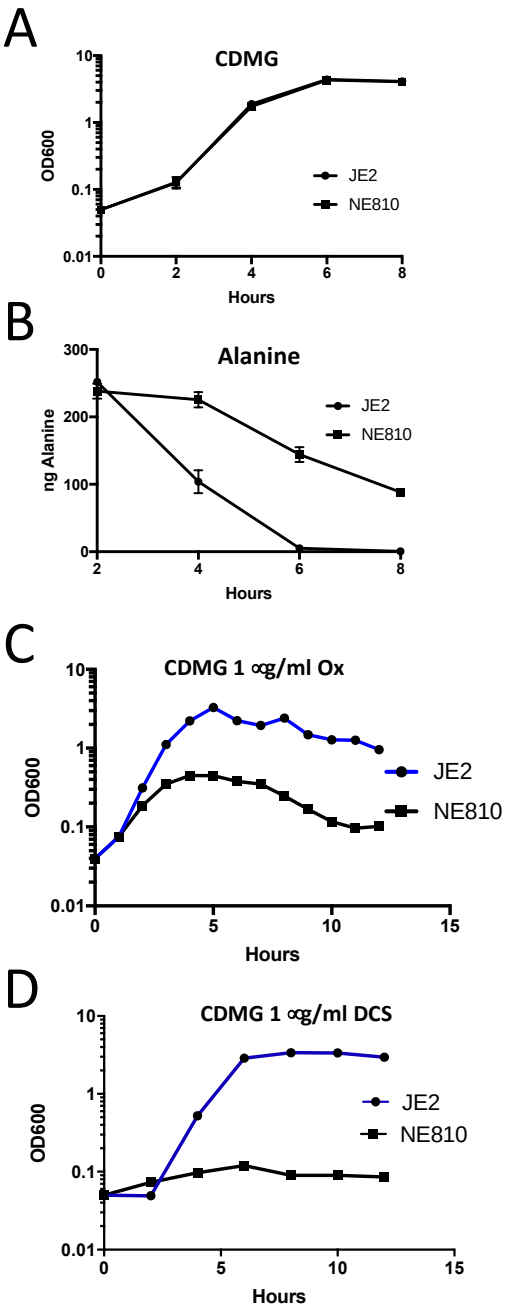

Fig. 4.3. Mutation of *cycA* impairs alanine uptake.

A. Growth of JE2 and NE810 in chemically defined media supplemented with glucose (CDMG). Cell density was measured at OD_{600}. B. Alanine consumption by JE2 and NE810 grown aerobically in CDMG. Residual amino acid was measured in spent media after 2, 4, 6 and 8 h growth. C and D. Growth of JE2 and NE810 cultures for 12 h in CDMG supplemented with 1 mg/ml oxacillin (C) or 1 mg/ml D-cycloserine (D). Cell density was measured at OD_{600}.

4.3.3 Mutation of *cycA* or exposure to D-cycloserine increases the susceptibility of MRSA to β-lactam antibiotics.

Previously reported synergy between DCS and β-lactam antibiotics [131, 204] suggests that impaired alanine uptake in the *cycA* mutant may have the same impact on cell wall biosynthesis as DCS-mediated inhibition of Alr and Ddl. To further investigate this, we compared the activity of DCS and β-lactam antibiotics, alone and in combination, against JE2 and NE810. Checkerboard microdilution assay fractional inhibitory concentration indices (ΣFICs ≤0.5) revealed synergy between DCS and several licensed β-lactam antibiotics with different PBP selectivity against JE2 and USA300 FPR3757 (Table 4.1). Oxacillin and nafcillin were not included in checkerboard assays because measurement of their MICs involves supplementing the media with 2% NaCl, which distorts the MIC of DCS (data not shown).

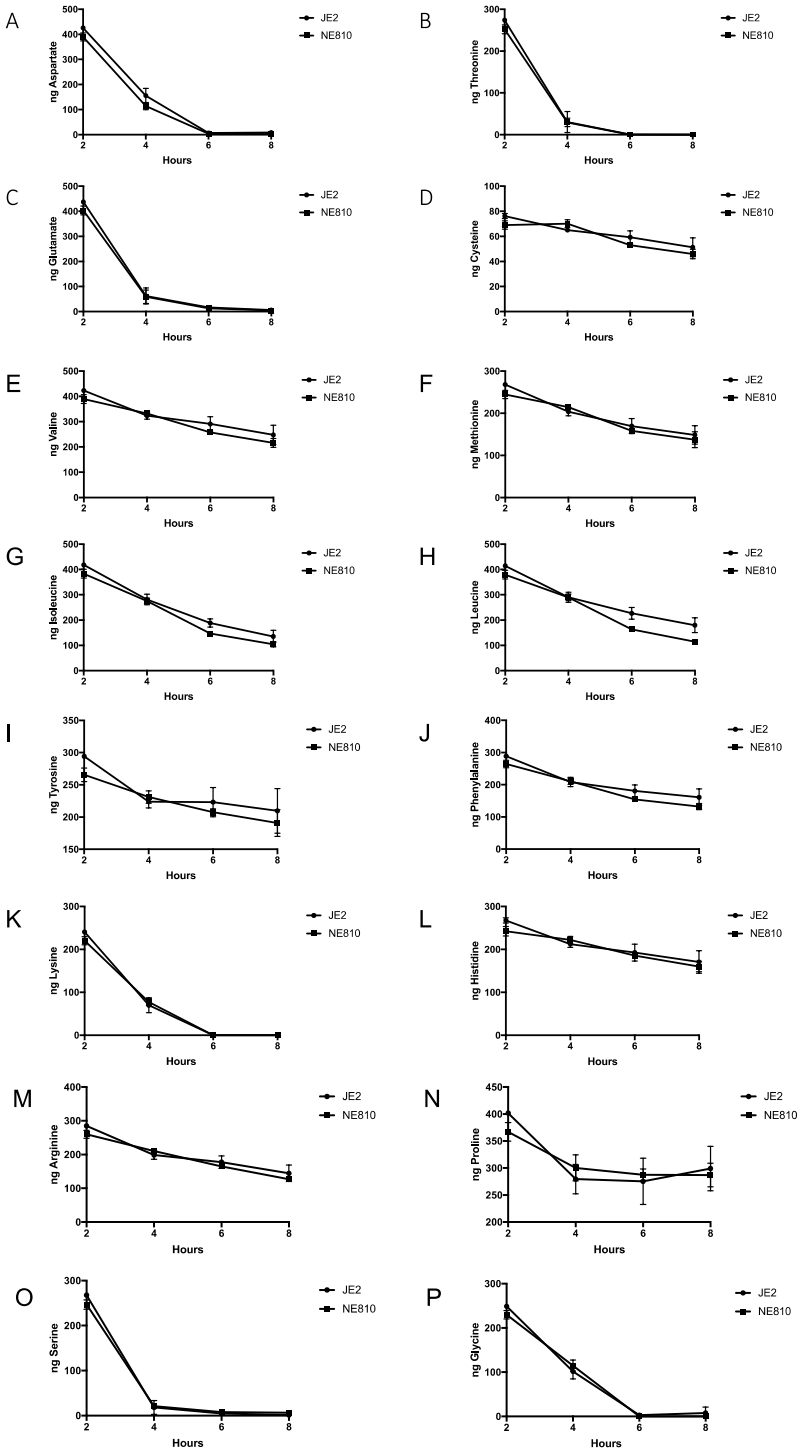

Fig. 4.4. Amino acid consumption by JE2 and NE810 grown aerobically in chemically defined media containing 14 mM of glucose (CDMG).

Residual amino acids were measured in spent media after 0, 4, 6 and 8 h growth.

4.3.4 Combination therapy with DCS and oxacillin significantly reduces the bacterial burden in the kidneys and spleen of mice infected with MRSA.

These experiments were carried out by Dr Rebecca Shears in the laboratory of Prof Aras Kadioglu at the University of Liverpool. This data is included in this thesis as background and context for the experiments I performed subsequently.

The virulence of the NE810 mutant and the therapeutic potential of oxacillin in combination with DCS in the treatment of MRSA infections were assessed in mice. Treatment with oxacillin or DCS alone significantly reduced the number of CFUs recovered from the kidneys of mice infected with JE2 (Fig. 4.5). Furthermore, the oxacillin/DCS combination was significantly more effective than either antibiotic alone and the combination was equally effective in reducing the bacterial burden in the kidneys of animals infected with JE2 or NE810 when compared to no treatment ($p \leq 0.0001$) (Fig. 4.5) demonstrating the capacity of DCS to significantly potentiate the activity of β-lactam antibiotics against MRSA under *in vivo* conditions. Unexpectedly, oxacillin- or DCS-mediated eradication of NE810 infections in the kidneys was similar to JE2 (Fig. 4.5).

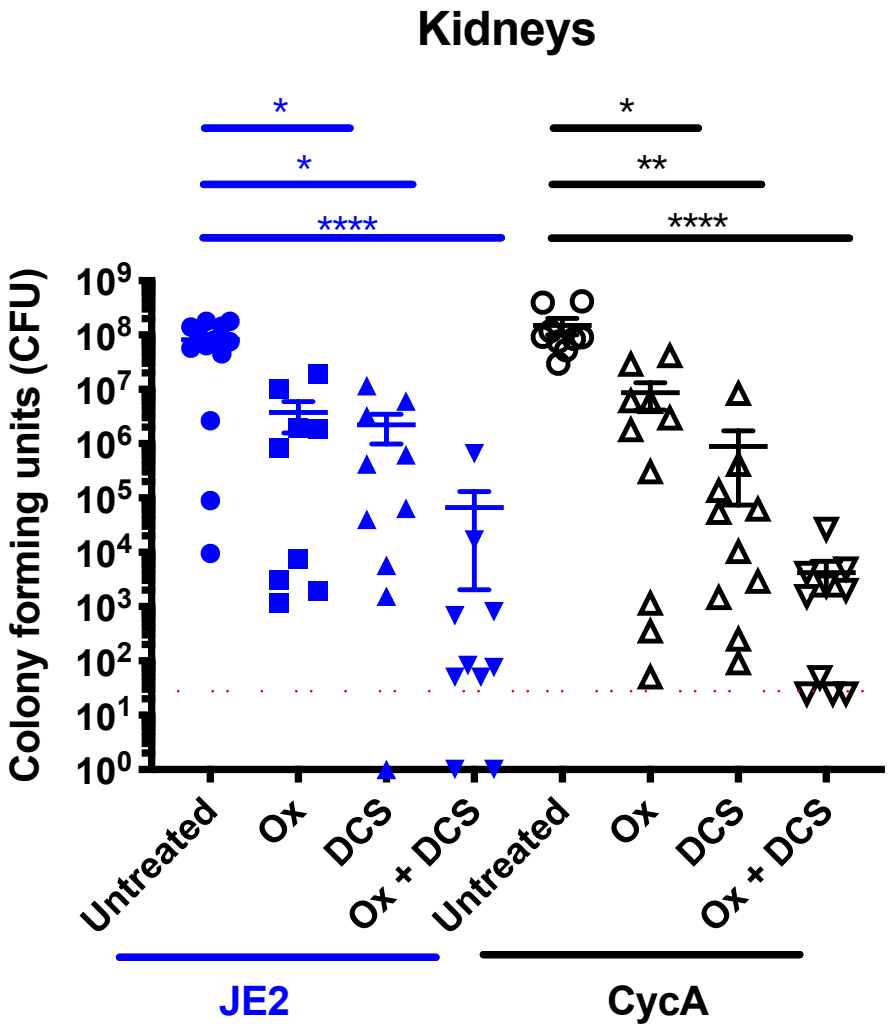

Fig. 4.5. Combination therapy with D-cycloserine and oxacillin significantly reduces the bacterial burden in the kidneys of mice infected with MRSA.

The number of colony-forming units (CFU) recovered from the kidneys of mice infected by tail vein injection with 5×10^6 JE2 or NE810 (*cycA*) and left untreated or treated with 75 mg of oxacillin (Ox)/kg, 30mg of DCS/kg or a combination of both Ox and DCS delivered subcutaneously every 12 hours for 5 days. The first antibiotic dose was given 16 hours after infection. Significant differences determined using one-way ANOVA with Kruskal-Wallis test followed by Dunn's multiple comparisons test are denoted using asterisks (*p≤0.05, **p≤0.01, ****p≤0.0001). The limit of detection (50 colonies) is indicated with a hashed red line.

This data was generated by Dr Rebecca Shears in the laboratory of Prof Aras Kadioglu in the University of Liverpool.

4.3.5 Alanine transport and resistance to oxacillin and DCS in chemically defined medium are not dependent on *cycA*.

The failure of oxacillin or DCS treatment to enhance the eradication of NE810 infections in the mouse bacteraemia model prompted us to further characterise the growth conditions used for the *in vitro* antibiotic susceptibility assays. Specifically, the role of glucose in CycA-dependant alanine transport, which has previously been reported to increase the growth requirement for amino acids [94], and which we reasoned may be important for CycA-dependent alanine transport. Growth of JE2 and NE810 was similar in CDM lacking glucose (Fig. 4.6A) and uptake of alanine (Fig. 4.6B) was unchanged in NE810 compared to JE2. Furthermore, NE810 and JE2 grew equally well in CDM supplemented with oxacillin and DCS (Fig. 4.6C and D). These data explain in part why the *cycA* mutant does not exhibit increased β-lactam and DCS susceptibility in the mouse bacteraemia model and further reveal the strong correlation between alanine transport and susceptibility to oxacillin and DCS. Moreover, these data suggest that another alanine transporter(s) is active during growth in CDM.

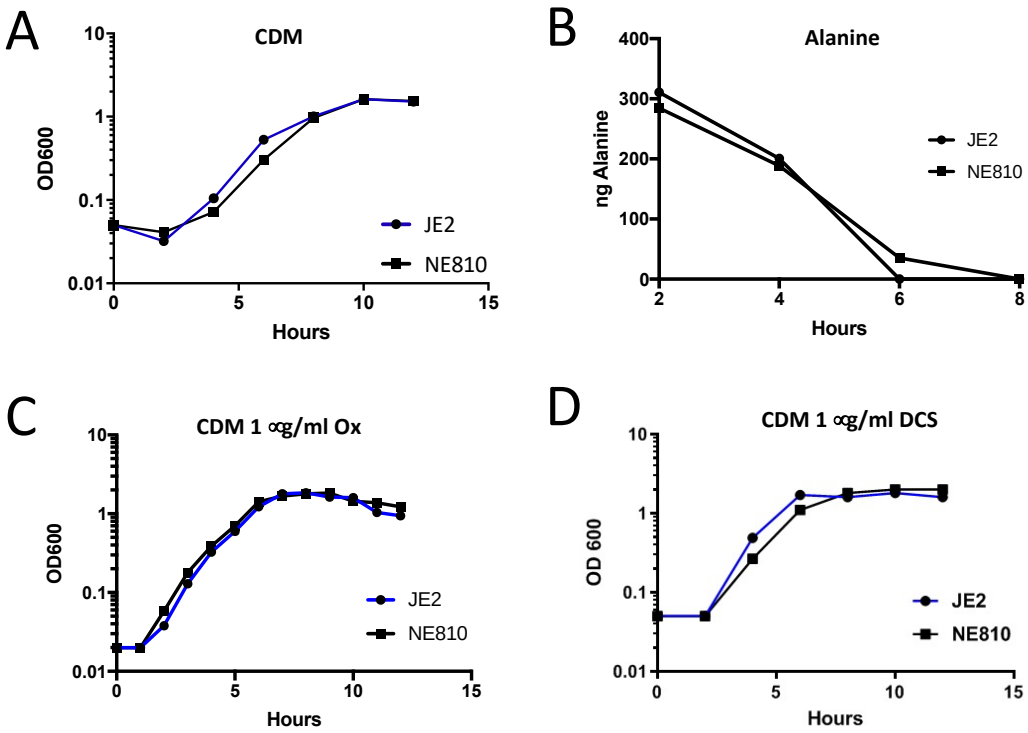

Fig. 4.6. Alanine transport and resistance to oxacillin and D-cycloserine in chemically defined medium are *cycA*-independent.

A. Growth of JE2 and NE810 in chemically defined medium lacking glucose (CDM). Cell density was measured at A_{600}. B. Alanine consumption by JE2 and NE810 grown aerobically in CDM. Residual amino acid was measured in spent media after 2, 4, 6 and 8 h growth. C and D. Growth (cell density at OD_{600}) of JE2 and NE810 cultures for 12 h in CDM supplemented with 1 mg/ml oxacillin (C) or 1 mg/ml DCS (D).

4.3.6 Mutation of *escB* and *cycA* increases susceptibility to oxacillin in chemically defined media (CDM).

To identify the alanine transporter(s) active in CDM, we focused on several genes predicted to encode membrane transporters that our research group previously showed were up-regulated during growth in sub-inhibitory concentrations of oxacillin [122]. We hypothesised that the regulation of these genes by oxacillin may suggest that they transport amino acids to counteract β-lactam-induced cell wall stress. These genes/mutants, listed in Table 4.2 include SAUSA300_0851, *mnhE* (NE1292), putative monovalent cation/H^+ antiporter (NE18); SAUSA300_1785, *ecsB*, putative ABC transporter (NE107); SAUSA300_2391, *opuCc*, glycine betaine ABC transporter (NE961); SAUSA300_2357-2359 operon, and a putative amino acid ABC transporter (NE1592). Two carbohydrate permeases upregulated by oxacillin (*fruA* and *gntP*) were also examined. The mutants were first grown in CDM supplemented with a sub-inhibitory concentration of oxacillin (1 μg/ml), as impaired alanine consumption may correlate with increased susceptibility to oxacillin, as observed with the *cycA* mutant in CDMG. None of the NTML mutant strains listed in Table 4.2 exhibited impaired growth compared to wild-type JE2 in CDM Ox (Fig. 4.7) suggesting that multiple permeases (including CycA) may transport alanine during growth in CDM and may be able to functionally substitute for each other.

Table 4.2. Genes encoding putative membrane transporters previously reported to be up-regulated during growth in sub-inhibitory oxacillin [122].

NTML	Locus tag	Gene	Details
NE18	SAUSA300_RS10115	*tagG*	Transport permease protein
NE107	SAUSA300_RS09775	*ecsB*	Putative ABC transporter protein EcsB
NE228	SAUSA300_RS13015	*tcyC*	Amino acid ABC transporter ATP-binding protein
NE271	SAUSA300_RS13230	*opuCd*	Glycine betaine/carnitine/choline transport system permease
NE661	SAUSA300_RS03305	*mnhG*	Putative monovalent cation/H+ antiporter subunit G
NE768	SAUSA300_RS03675	*fruA*	Fructose specific permease
NE782	SAUSA300_RS13240	*opuCb*	Glycine betaine/carnitine/choline ABC transporter
NE961	SAUSA300_RS13235	*opuCc*	Glycine betaine/carnitine/choline ABC transporter
NE1292	SAUSA300_RS03295	*mnhE2*	Putative Na+/H+ antiporter, MnhE component
NE1592	SAUSA300_RS13025	*tcyA*	Amino acid ABC transporter amino acid-binding protein
NE1882	SAUSA300_RS13245	*opuCa*	Glycine betaine/carnitine/choline ABC transporter ATP-binding protein

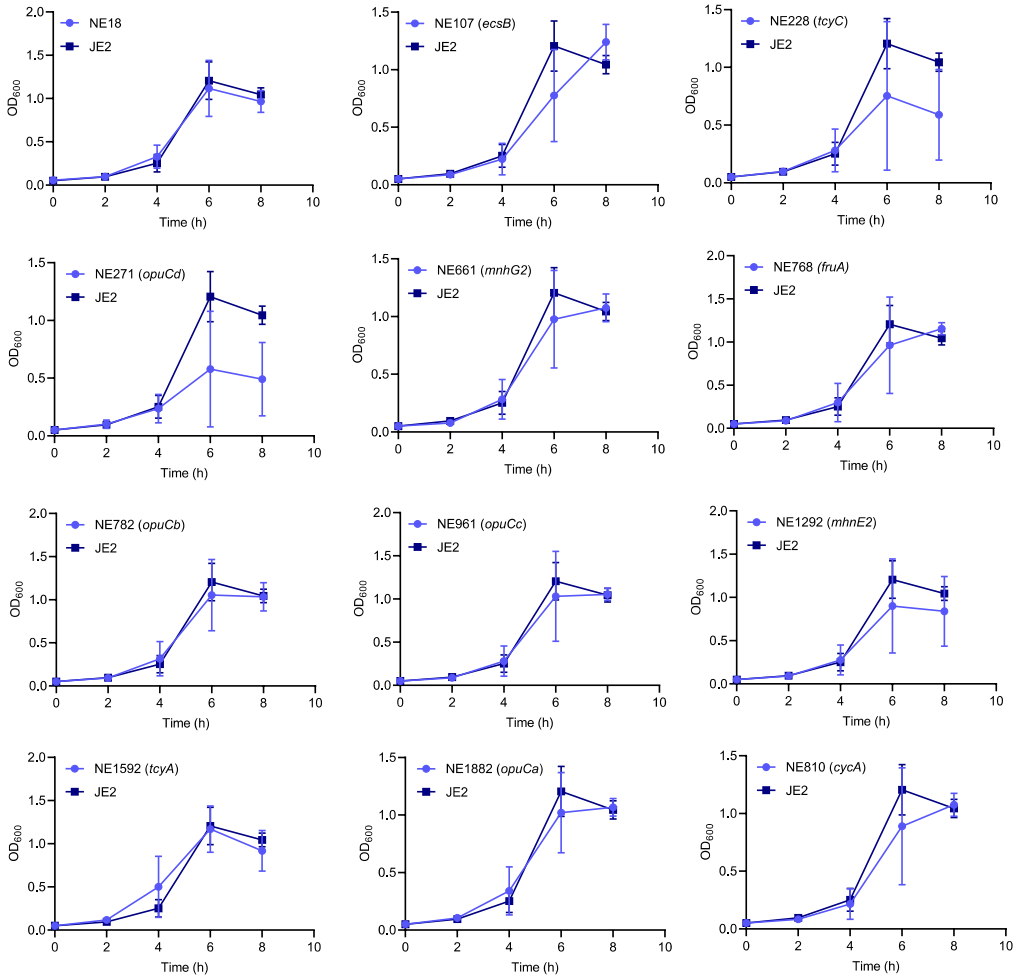

Fig. 4.7. Growth of putative amino acid transporter mutants was not impaired in CDM supplemented with 1 µg/ml oxacillin.

Putative amino acid permease mutants were grown in 5 ml CDM supplemented with 1 µg/ml oxacillin in 50 ml falcon tubes at 37°C with 200 rpm shaking. OD_{600} was recorded at 2 h intervals for 8 h. All data presented are the average of 4 independent experiments and error bars represent standard deviation. The same JE2 growth curve is shown alongside each mutant strain to allow for comparison of mutant versus wild-type.

To address this possibility, the transporter mutants listed in Table 4.2 were transduced into the *cycA* markerless mutant using phage 80α, and a series of double mutants were constructed. Growth of these double mutants was then compared to the wild-type JE2 and each single transporter mutant in CDM supplemented with 1 μg/ml oxacillin (Fig. 4.8). Of the 11 mutants screened, only the *cycA/ecsB* double mutant exhibited increased oxacillin susceptibility in CDM (Fig. 4.8). The *cycA/ecsB* double mutant exhibited slightly impaired growth compared to JE2, NE107 and NE810 in CDM and CDMG lacking oxacillin (Fig. 4.9). To further investigate the possibility that reduced alanine transport in the *cycA*/*ecsB* double mutant may impact oxacillin resistance levels, the susceptibility of the mutant to oxacillin was compared in CDM supplemented with 0, 100, 200 and 400 mg/ml exogenous L-alanine. This experiment revealed an alanine concentration-dependent increase in oxacillin resistance in the *cycA*/*ecsB* double mutant (Fig. 4.10), suggesting that other alternative and perhaps low affinity alanine transporter(s) may substitute for CycA and EcsB under these growth conditions.

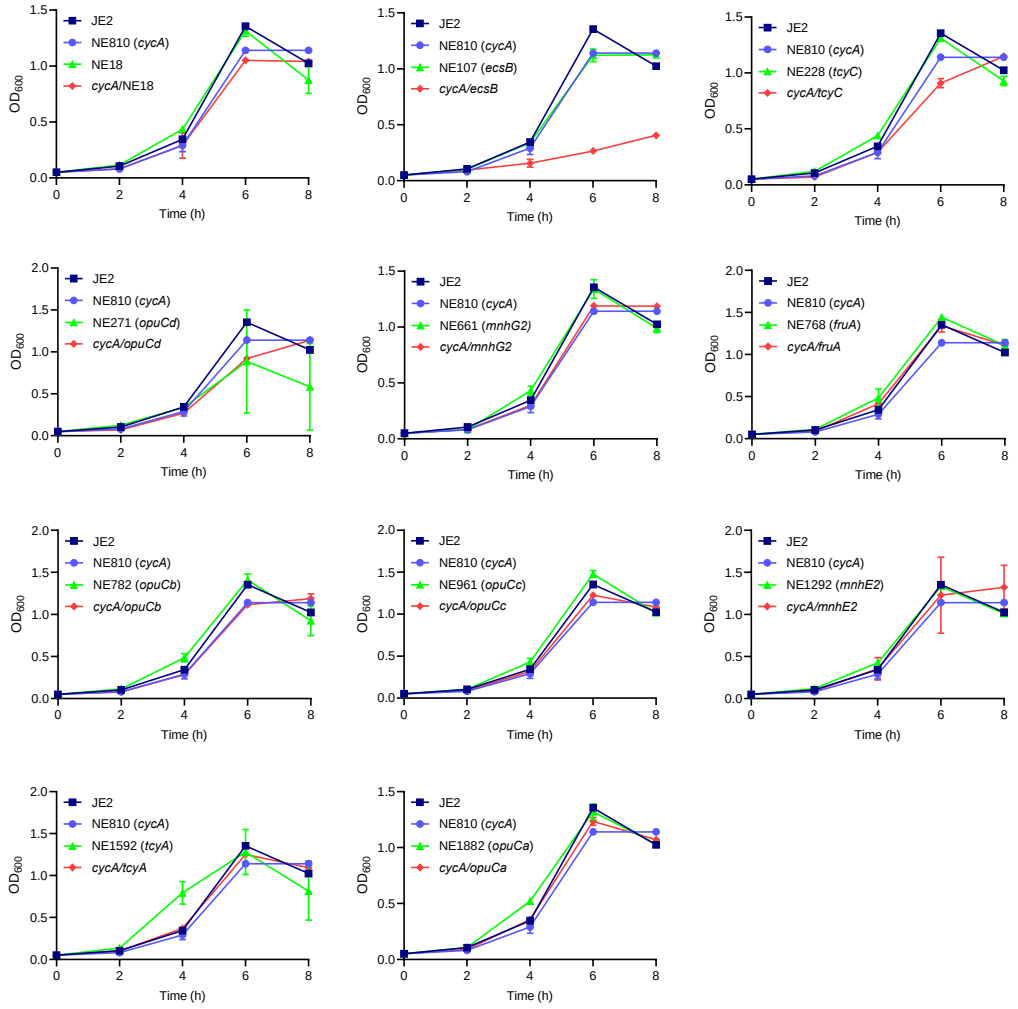

Fig. 4.8. Mutation of *ecsB*, and not other putative amino acid transporter genes, in a *cycA* mutant increases susceptibility to oxacillin during growth in CDM.

Each double mutant was grown in 5 ml CDM supplemented with 1 µg/ml oxacillin in a 50 ml falcon tube at 37°C with 200 rpm shaking. OD_{600} was recorded at 2 h intervals for 8 h. Each graph shows JE2, NE810, the putative amino acid permease mutant , and the double mutant lacking *cycA* and the putative amino acid permease gene. The same data set for JE2 and NE810 is shown on each graph. All data presented are the average of 2 independent experiments and error bars represent standard deviation.

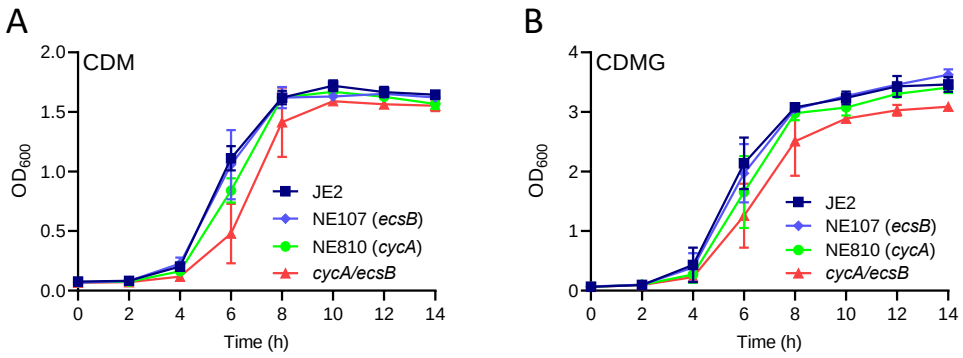

Fig. 4.9. Comparison of JE2, NE107 (*ecsB*) , NE810 (*cycA*) and *cycA/ecsB* growth in (A) CDM and (B) CDMG.

Each strain was grown in 25 ml CDM or CDMG in a 250 ml flask at 37°C with 200 rpm shaking. OD_{600} was recorded at 2 h intervals for 14 h. All data presented are the average of 4 independent experiments and error bars represent standard deviation.

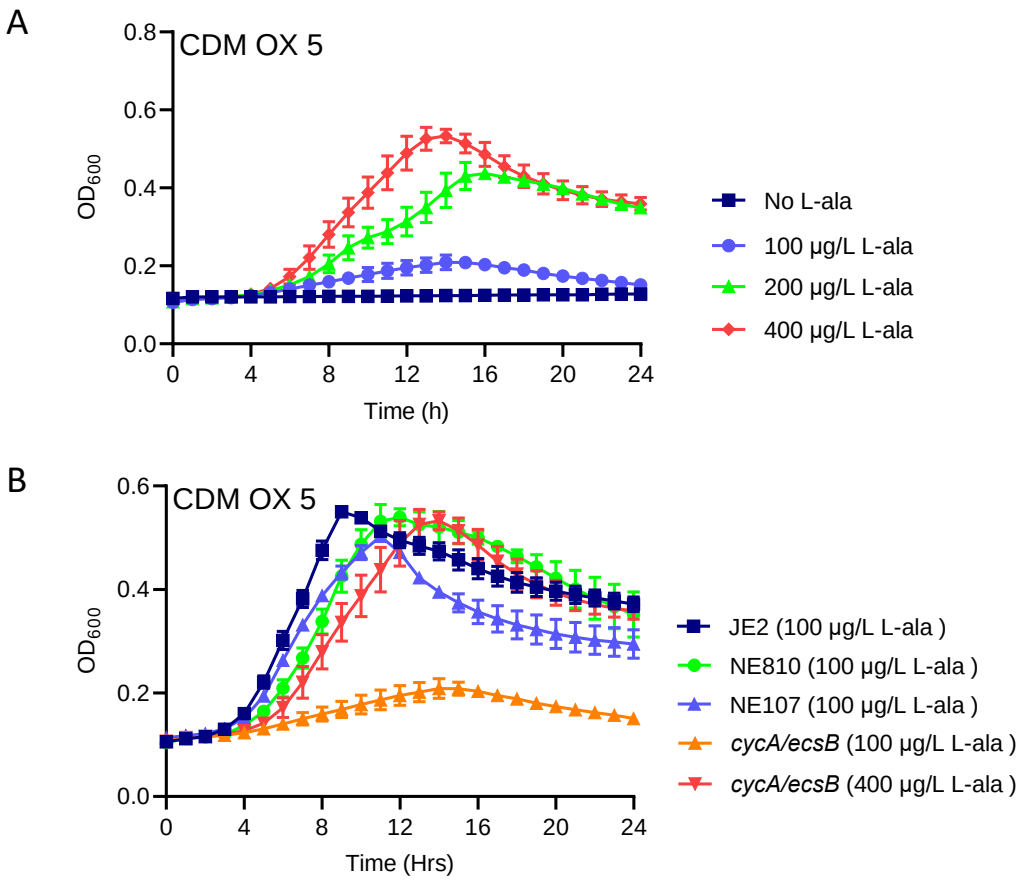

Fig. 4.10. Growth of the *cycA/ecsB* double mutant in oxacillin in CDM is restored by supplementation of the media with excess alanine.

(A) Growth of the *cycA*/*ecsB* double mutant in CDM and 5 µg/ml oxacillin, supplemented with 0, 100, 200 or 400 µg/ml L-alanine. (B) Growth of JE2, NE107, NE810 and *cycA/ecsB* in CDM supplemented with 5 µg/ml oxacillin and L-alanine at the concentrations indicated. Cultures were grown in a Tecan Sunrise incubated microplate reader for 24 h at 37˚C. OD_{600} was recorded at 1 h intervals and growth curves were plotted in Prism software (GraphPad). The data presented are the average of 3 independent biological replicates, and error bars represent standard deviations.

4.3.7 A *cycA/ecsB* double mutant remains capable of alanine transport during growth in CDM.

Next, alanine consumption was measured in a preliminary experiment performed by our collaborator Dr Fareha Razvi in Prof Paul Fey's group at UNMC, Omaha. Alanine consumption by the *cycA/ecsB* double mutant was only marginally reduced in CDM during exponential growth (Fig. 4.11), and after 10 hours JE2, NE107, NE810 and *cycA*/*ecsB* had consumed all of the alanine in the media (Fig. 4.11). Consistent with our previous data [132], mutation of *cycA* was associated with impaired transport of alanine in CDMG, and mutation of *ecsB* had no additional effect (Fig. 4.12). Although the alanine transport data presented in Figure 4.11 is from a single experiment and should be viewed as preliminary, it is difficult to conclude that mutation of *cycA* and *ecsB* increases susceptibility to oxacillin during growth in CDM via impaired alanine consumption. These data further suggest that, an alternative low affinity alanine permease(s) may undertake alanine transport in the absence of *cycA*. Work is ongoing in our laboratory to identify new alanine transporter(s).

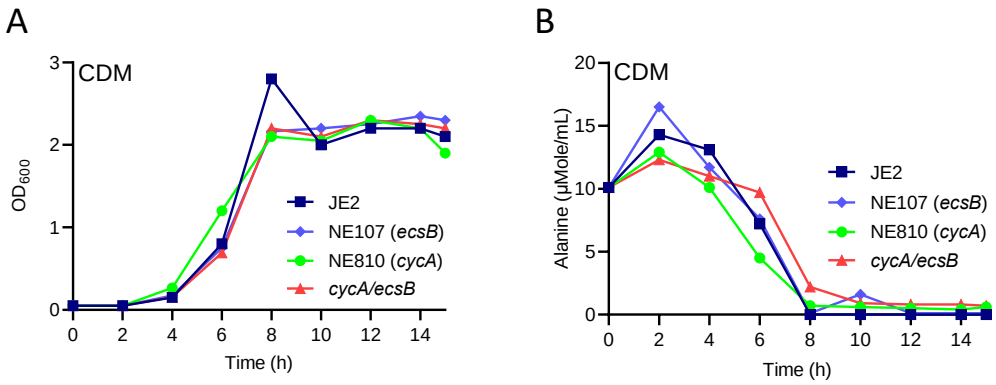

Fig. 4.11. Alanine consumption by the *cycA/ecsB* double mutant is not reduced during growth in CDM.

(A) Growth of JE2, NE107, NE810 and *cycA/ecsB* in CDM. Each strain was grown in 25 ml CDM in a 250 ml flask at 37°C with 200 rpm shaking. OD_{600} was recorded at 0, 4, 6, 8,10, 12, 14 and 15 h. (B) Alanine consumption by JE2, NE107, NE810 and *cycA/ecsB* grown aerobically in CDM. Residual amino acid was measured in spent media after 0, 4, 6, 8,10, 12, 14 and 15 h growth. These experiments were

performed on the same set of cultures and data represents a single biological replicate.

This data was generated by Dr Fareha Ravzi in the laboratory of Prof Paul Fey at the University of Nebraska Medical Centre, Omaha.

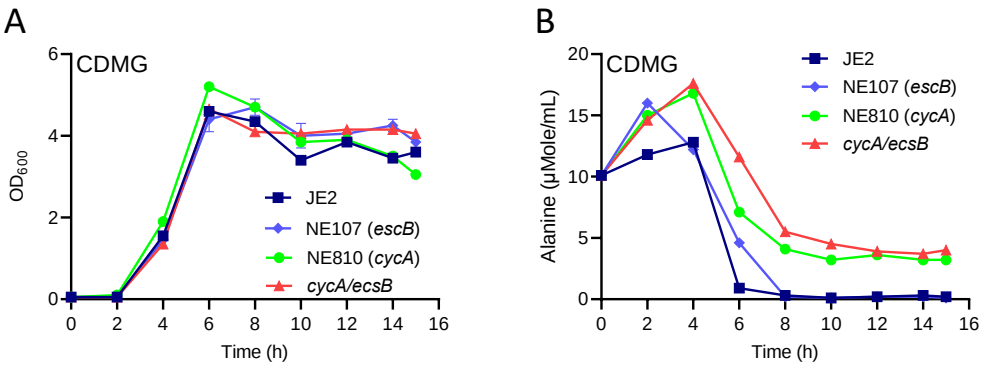

Fig. 4.12. Mutation of *ecsB* does not impact alanine consumption in CDMG.

(A) Growth of JE2, NE107, NE810 and *cycA/ecsB* in CDMG. Each strain was grown in 25 ml CDMG in a 250 ml flask at 37°C with 200 rpm shaking. OD_{600} was recorded at 2 h intervals for 15 h. (B) Alanine consumption by JE2, NE107, NE810 and *cycA/ecsB* grown in 25 ml CDMG in a 250 ml flask at 37°C with 200 rpm shaking. Residual alanine was measured in spent media after 0, 4, 6, 8,10, 12, 14 and 15 h growth. These experiments were performed on the same set of cultures and data represents a single biological replicate.

This data was generated by Dr Fareha Ravzi in the laboratory of Prof Paul Fey at the University of Nebraska Medical Centre, Omaha.

4.4 Discussion

The exploitation of antibiotic re-purposing as part of concerted efforts to address the antimicrobial resistance crisis has been hampered by a lack of mechanistic data to explain demonstrated therapeutic potential and the perception that studies attempting to identify new uses for existing drugs are not hypothesis-driven. In this study, we revealed that CycA was required for full expression of resistance to β-lactam antibiotics and DCS. Loss of function of this putative alanine transporter significantly increased the susceptibility of MRSA to β-lactam antibiotics, an outcome that could be reproduced through exposure to DCS, which targets the Alr and Ddl enzymes in the early steps of cell wall biosynthesis.

The potential of β-lactam/DCS combinations for treatment of MRSA infections follows a recent report that DCS can also potentiate the activity of vancomycin against a laboratory-generated vancomycin highly-resistant *S. aureus* (VRSA) strain *in vitro* and in a silkworm infection model [205]. The excellent safety profile of β-lactam antibiotics makes these drugs particularly attractive as components of combination antimicrobial therapies. When used in the treatment of tuberculosis DCS (trade name Seromycin, The Chao Centre) is typically administered orally in 250 mg tablets twice daily for up to two years. At this dosage, the DCS concentration in blood serum is generally 25-30 μg/ml, which is similar to the concentrations used in our *in vitro* and *in vivo* experiments. The known neurological side effects associated with DCS therapy [206, 207] mean that this antibiotic is unlikely to be considered for the treatment of MRSA infections unless alternative therapeutic approaches have been exhausted. Oxacillin/DCS combination therapy was significantly more effective than DCS or oxacillin alone over a 5-day therapeutic window suggesting that further studies on using DCS to augment β-lactams as a treatment option for recalcitrant staphylococcal infections are merited.

Mutation of *cycA* increases the susceptibility of MRSA to β-lactam antibiotics and results in hyper-susceptibility to DCS, whereas a *cycA* point mutation in *M. bovis* contributes, in part, to increased DCS resistance presumably by interfering with

transport into the cell [203]. In *E. coli*, *cycA* mutations can also result in increased resistance or have no effect on DCS susceptibility depending on the growth media [208-212], suggesting that CycA is primarily important for DCS resistance under conditions when its contribution to amino acid transport is also important. Our data showing that mutation of *cycA* was not associated with increased DCS resistance strongly suggests that CycA has no role in uptake of this antibiotic in *S. aureus*.

Under growth conditions where CycA is required for alanine transport (in nutrient/glucose-replete media), our collaborators Dr Laura Alvarez and Dr Felipe Cava demonstrated that mutation of *cycA* or DCS-exposure have similar effects on the structure of *S. aureus* peptidoglycan [132]. Consistent with previous studies in *S. aureus* [131] and in *M. tuberculosis* [213], their analysis showed a dose-dependent accumulation of muropeptides with a tripeptide stem in MRSA exposed to DCS [132]. The *cycA* mutation was also associated with the increased accumulation of muropeptides with a tripeptide stem [132]. These data indicate that a reduced intracellular alanine pool or inhibition of Alr and Ddl is associated with reduced D-ala-D-ala incorporation into the PG stem peptide. The increased accumulation of tripeptides in turn interferes with normal PBP transpeptidase activity and offers a plausible explanation for increased susceptibility to β-lactam antibiotics. The importance of the terminal stem peptide D-ala-D-ala for β-lactam resistance has previously been reported. Mutation of the *murF*-encoded ligase, which catalyses of the D-ala-D-ala into the stem peptide also increased β-lactam (but not DCS) susceptibility [214, 215]. Similarly growth of a HoR MRSA strain in media supplemented with high concentrations of glycine was accompanied by replacement of the D-ala-D-ala with D-ala-gly and decreased methicillin resistance [157].

Impaired uptake of alanine in CDMG correlated with increased susceptibility to oxacillin and DCS, suggesting that alanine utilisation via CycA is important to make D-alanine available for cell wall biosynthesis and consequently resistance to β-lactams. Consistent with this, NE810 also exhibited increased oxacillin susceptibility in BHI, TSB and MH media. However, no change in alanine transport

or susceptibility to oxacillin and DCS was measured in CDM lacking glucose, which may explain the failure of oxacillin and DCS to more efficiently eradicate NE810 infections in the mouse bacteraemia model. The availability of nutrients such as glucose and amino acids varies in different niches colonised by *S. aureus* during infection ranging from glucose-rich in organs such as the liver [216], to glucose-depleted in established abscesses [217]. In turn this impacts the role of amino acids as carbon sources [94, 218], and potentially the activity of CycA in alanine transport and β-lactam susceptibility. Furthermore, normal alanine transport in the *cycA* mutant grown in CDM indicates that an alternative alanine transport mechanism(s) may be active under these growth conditions.

Our lab has previously identified several putative amino acid transport genes that were regulated by oxacillin. Here, by screening the impact of mutations in these oxacillin-regulated amino acid transport genes on oxacillin susceptibility in CDM, we identified a role for *ecsB*. However, our data revealed that alanine was consumed from CDM by a mutant lacking both *cycA* and *ecsB* suggesting that yet other transporter(s) must also be involved in alanine uptake under these conditions and that the impact of the *ecsB* mutation of β-lactam susceptibility in CDM must be indirect. Consistent with this, mutation of the *ecsB* locus was previously shown to impact the expression of numerous amino acid transport genes, cell wall homeostasis and virulence [64]. Furthermore, the predicted function of EcsAB as a peptide exporter [64, 173], rather than an amino acid permease is also inconsistent with a direct role in alanine uptake. On balance it seems likely that the *ecsB*/*cycA* double mutation indirectly increases susceptibility to β-lactams in CDM via pleiotropic effects that do not appear to involve impaired alanine transport and may be difficult to disentangle. Research is underway in our laboratory to identify the alanine permease(s) that undertake alanine transport in CDM, which may be important in the development of therapeutic strategies targeting alanine transport to increase β-lactam susceptibility in MRSA, while elucidation of the role of glucose in the control of alanine transport should also provide new insights into β-lactam resistance.

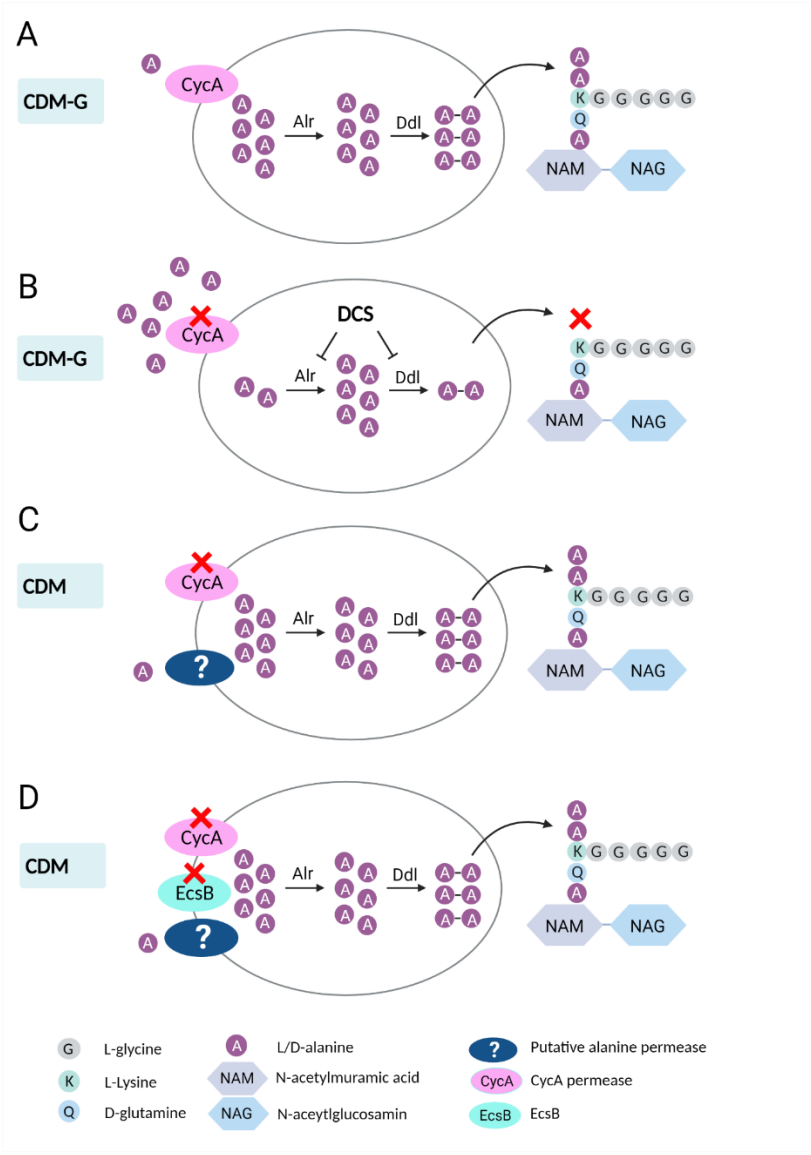

Figure 4.13. Proposed model depicting the effect of *cycA* and *ecsB* mutations, or DCS exposure, on alanine consumption and peptidoglycan biosynthesis, and the impact on β-lactam resistance in MRSA.

(A) When JE2 is grown in CDMG, the CycA permease transports alanine into the cell. Peptidoglycan is not impacted, and the strain is resistant to β-lactam antibiotics. (B) Disruption of *cycA* by transposon insertion impairs both alanine uptake and transfer into the D-Alanine pathway in CDMG, while the alanine analogue antibiotic DCS inhibits the alanine pathway enzymes alanine racemase and D-Alanine ligase. *cycA* inactivation or DCS exposure results in reduced peptidoglycan cross-linking and β-lactam susceptibility. (C) In CDM media , mutation of *cycA* does not result in impaired alanine uptake or β-lactam susceptibility, suggesting that there may be alternative permease(s) transporting alanine into the cell. (D) Mutation of both *cycA* and putative permease gene, *ecsB*, did not lead to impaired alanine uptake in CDM, suggesting that EcsB is not an alanine transporter, and a different unidentified permease is carrying out this function.

4.5 Materials and Methods

4.5.1 Bacterial strains and growth conditions.

Bacterial strains and plasmids used in this study are listed in Table 4.3. *S. aureus* strains were grown in Tryptic Soy Broth (TSB), Tryptic Soy Agar (TSA), chemically defined medium (CDM) and CDM supplemented with 14 mM glucose (CDMG). The default L-alanine concentration in CDM and CDMG was 100 mg/L [94]. Where indicated, cultures were supplemented with erythromycin (Erm) 10 µg/ml, chloramphenicol (Cm) 10 µg/ml, ampicillin (Amp) 50 µg/ml or kanamycin (Km) 75 µg/ml. Overnight cultures were set up by inoculating a single colony from TSA into 5 ml TSB in a 50 ml falcon tube, with selective antibiotic Erm 10 µg/ml. Overnight cultures were incubated at 37°C shaking at 200 rpm for use the following day. When used as inoculum for CDM or CDMG assays, the cells were washed once in PBS to remove residual TSB media.

Minimum inhibitory concentrations (MICs) were determined in accordance with CLSI guidelines using plate and broth dilution assays in MH, or MH 2% NaCl for oxacillin and nafcillin. Oxacillin MICs were also measured using E-tests (Oxoid) on MH agar 2% NaCl. Quality control strains ATCC29213 and ATCC25923 were used for oxacillin and cefoxitin MIC assays, respectively.

Table 4.3. Bacterial strains and plasmids used in this study

Strains/plasmids	Relevant Details
RN4220	Restriction-deficient laboratory *S. aureus*
USA300 FPR3757	Community associated MRSA isolate of the USA300 lineage [92]. SCCmec type IV. CC8.
JE2	USA300 cured of p01 & p03. Parent of Nebraska Transposon Mutant Library (NTML).
NE810	JE2 NTML *cycA* (SAUSA300_1642) mutation. Erm^r.
USA300 *cycA*	USA300 FPR3757 *cycA*. Constructed by transduction of *cycA*::Tn allele from NE810.
NE1868	JE2 NTML *mecA* mutation.
NE1713	JE2 NTML *alr* (SAUSA300_2027) mutation.
COL	MRSA reference strain; SCC*mec* type I; CC8 [219]
ATCC 29213	Methicillin susceptible *S. aureus* strain for antibiotic susceptibility testing.
ATCC 25923	Methicillin susceptible *S. aureus* strain for antibiotic susceptibility testing.
E. coli	*E. coli* HST08
Plasmids	
pLI50	*E. coli-Staphylococcus* shuttle vector. Ap^r (*E. coli*), Cm^r. (*Staphylococcus*)
p*cycA*	pLI50 carrying *cycA* from JE2

4.5.2 Tecan growth experiments.

Tecan growth curves were performed in 96-well hydrophobic polystyrene plates. Overnight TSB cultures were centrifuged, washed once in PBS and adjusted to OD_{600} of 1 with additional PBS. Ten µl of this cell suspension was added to 190 µl of CDM or CDMG media per well, to give a final volume of 200 µl with starting OD_{600} of 0.05. Antibiotics or supplements were added to the media in advance of aliquoting into wells. Plates were incubated at 37°C with shaking on a Tecan Sunrise microplate instrument for 24 h, with OD_{600} recorded at 1 h intervals. At

least 3 independent biological replicates were performed for each experiment, and average data presented.

4.5.3 Flask and falcon tube growth experiments.

Overnight cultures were washed once in PBS and used to inoculate CDM or CDMG to a starting cell density of 0.05 at OD_{600}. For flask assays, 25 ml media was inoculated in a 250 ml flask. For growth assays in falcon tubes, 5 ml media was inoculated into a 50 ml tube. Cultures were incubated at 37°C with shaking at 200 rpm and OD_{600} was recorded at 2 h intervals for at a minimum of 8 h. Four independent biological replicates were performed for flask growth assays while falcon tube growth assays were performed in duplicate. Each strain and growth condition, and average data presented. Growth curves were plotted in Prism software (GraphPad) and error bars represent standard deviations.

4.5.4 Bacterial strains, growth conditions and antimicrobial susceptibility testing.

Bacterial strains (Table 4.3) were grown in Lysogeny broth (LB) (Sigma), brain heart infusion (BHI), Mueller Hinton (MH), nutrient, sheep blood BHI, chemically defined media (CDM) or CDM 14mM glucose (CDMG) [220].

4.5.5 Identification of cefoxitin susceptible MRSA mutant NE810.

Cefoxitin (30 μg) disks (Oxoid) were used to measure susceptibility of NTML mutants. The zone diameters for JE2 was 18 mm NE1868 (*mecA*::Em^r) was >35 mm and NE810 was 22 mm. The *cycA* transposon insertion in NE810 was verified by PCR using the primers NE810_Fwd and NE810_Rev (Table 4.S3). Phage 80α was used to transduce the NE810 *cycA* allele into JE2 and other strains. Genome sequencing was performed by MicrobesNG using the USA300_FPR3757 genome as a reference. To complement NE810, *cycA* was amplified from JE2 on a 1608 bp fragment using primers NE810F1_Fwd and NE810F1_Rev (Table 4.4) and cloned into pLI50 using the Clontech In-fusion kit.

Table 4.4. Oligonucleotides used in this study

Target	Name	Primer Sequence (5' – 3')
cycA	NE810_fwd	ACAGAATAGCCACAAATAGCACC
	NE810_rev	GAACTTAATGTCCCAAGCCCT
ecsB	NE107_fwd	TTTGGTTCAAGCGGACAACA
	NE107_rev	GGTGAAGTCGTTGCATTTGG

4.5.6 Genetic manipulation of *S. aureus*.

The plasmid pTnT, which contains a truncated, markerless transposon was used to construct a markerless *cycA* mutant designated NE810 MM, as described previously [148] Phage 80α was used to transduce the transposon insertion from each of the following NTML mutant strains, NE18, NE107, NE228, NE271, NE661, NE768, NE782, NE961, NE1292, NE1592 and NE1882, into strain NE810 MM, to create double mutants which could then be screened for growth in CDM supplemented with oxacillin. As the double mutant *cycA/ecsB* was selected for further work, its transposon insertions were verified using PCR amplification of target loci using primers listed in Table 4.4.

4.5.7 Amino acid transport studies.

Overnight cultures were grown at 37°C in TSB, washed in PBS and used to inoculate 25 ml of chemically defined medium (CDM) or chemically defined medium supplemented with 14 mM glucose (CDMG) to a starting cell density of 0.05 at OD_{600}. The bacteria were grown aerobically (250 rpm; 10:1 flask to volume ratio, 37°C) and OD_{600} was determined every 2 h for 15 h total. One ml of the bacterial culture was collected every 2 h and pelleted by centrifugation at 14,000x g for 3 min. The spent media was filtered using an Amicon Ultra centrifugal filter (Millipore; 3,000 molecular weight cut-off [MWCO]). Amino acid analysis was performed by the Protein Structure Core Facility, University of Nebraska Medical Center, using a Hitachi L-8800 amino acid analyzer as described previously [94].

4.5.8 Antibiotic synergy analysis using the microdilution checkerboard assay.

Antibiotic synergism was measured using the checkerboard microdilution method in 96-well plates inoculated with 5×10^5 CFU/ml, and growth or no growth was assessed after 24 h at 37°C. The fractional inhibitory concentration index (ΣFIC) was calculated for each drug combination in triplicate experiments with an FIC index of ≤0.5 considered synergistic.

4.5.9 Statistical analysis.

Two-tailed Student's t-Tests and one-way ANOVA with Kruskal-Wallis test followed by Dunn's multiple comparisons test in the GraphPad Prism application (for the mouse infection experiments) were used to determine statistically significant differences in assays performed during this study. A p value <0.05 was deemed significant.

Chapter 5: Discussion

S. aureus represents a formidable risk to health, due to its ubiquitous and commensal nature and its ability to adapt to a number of environments, including healthcare settings, the wider community, and the more recent risk of zoonotic transmission from livestock. Its ability to continually evolve new resistance mechanisms, coupled with the slow pace of antibiotic development in recent years, has led to a rise in infections which would have previously been treatable. While measures such as infection prevention have made an important contribution to preventing the spread of HA-MRSA, there is a critical need for more therapeutic options for those who succumb to infection. By identifying and understanding the factors influencing β-lactam resistance in MRSA, we can use this knowledge to identify treatment strategies.

In screening mutants of the NTML library for altered cefoxitin resistance, we have identified mutations in 3 genes, *cycA*, *sucC* and *lspA*, which lead to changes in β-lactam resistance in the USA300 derived strain JE2. We have demonstrated that mutations in *cycA* and *sucC* lead to a reduction in β-lactam susceptibility. In the case of *cycA*, this rendered the mutant strain clinically susceptible to β-lactam antibiotics while *sucC* mutation led to borderline or intermediate susceptibility. This work highlights these genes and their biosynthetic pathways as potential therapeutic targets. Mutation of the 3rd gene, *lspA*, led to increased β-lactam resistance, and to the best of our knowledge this gene has not previously been implicated in β-lactam resistance. Given that the lipoprotein processing pathway is an attractive drug target, this information serves a note of caution that targeting this pathway could have undesirable or unintended consequences in terms of β-lactam resistance.

5.1 Mutation of *sucC* or *sucD* results in disruption of TCA cycle metabolites, perturbation of the succinylome and altered β-lactam resistance.

The TCA cycle is part of central metabolism, responsible for the generation of metabolic intermediates, reducing potential and energy [89]. The NTML screen of transposon mutants with cefoxitin identified NE569 (*sucC)* and NE1770 (*sucD*), encoding the α and β subunits of succinyl-CoA synthetase respectively. We showed that both mutants led to increased β-lactam susceptibility. This phenotype was not observed in any of the other TCA cycle mutants. We hypothesised that the lack of succinyl-CoA synthetase activity was leading to an accumulation of succinyl-CoA, potentially resulting in altered protein succinylation. This has been reported in a *Saccharomyces cerevisiae* mutant [123]. Succinylation is a widespread post-translational modification in both prokaryotic and eukaryotic cells. It was first described in bacteria in *E. coli* by Zhang *et al.* [106]. Since then the succinylome of several bacterial species has been reported [107, 126, 221] , most recently in *S. epidermidis* [108]. To investigate the aforementioned hypothesis, a double mutant *sucA/sucC* was constructed, the rationale being that if a build-up of succinyl-CoA was mediating the susceptible phenotype, then mutation of *sucA* encoding oxoglutarate dehydrogenase, which catalyses the conversion of α-ketoglutarate into succinyl-CoA might prevent such an accumulation and reverse the phenotype. *sucA/sucC* had wild-type resistance, lending support to the hypothesis. The emergence and identification of suppressor strains with mutations in *sucA* and *sucB* also validated this approach. Subsequent metabolic analysis confirmed that succinyl-CoA was significantly increased in the *sucC* mutant versus JE2. A comprehensive analysis of the succinylome of JE2 and *sucC* revealed that mutation of *sucC* led to perturbation of global succinylome patterns. The major autolysin Atl and PBP2a were among most succinylated proteins in *S. aureus* overall, which in itself does not provide an explanation for their differing phenotypes. Closer examination showed that 12 of the 82 succinyl-lysine residues were significantly more succinylated in the *sucC* mutant NE569 compared to JE2. Autolysis assays showed that autolytic activity was reduced in the *sucC* mutant, and its phenotype was comparable to that of an

autolysin mutant. Perhaps somewhat surprisingly, given that PBP2a was among the most succinylated proteins, the cell wall composition of *sucC* did not differ from JE2, perhaps a reminder that post translational modifications are a complex means of diversifying protein function, and subtle differences may prove more important than absolute quantities.

While the *sucC* mutant exhibits altered β-lactam resistance and reduced autolysis, the specific interactions between the succinylome and these phenotypes remains to be teased out. It is unclear if the autolysis phenotype is mediating increased susceptibility or if the phenotypes are arising independently of one another. Previous work by Boudewijn *et al* showed reduced autolytic activity alongside reduced β-lactam resistance in mutants with transposon insertions in unidentified auxiliary genes, although the parental strain in that instance was homogenously resistant [222].

Recognising the complexity of post translational modifications, future work will include an analysis of the acetylome of JE2 and *sucC*. Our metabolomic analysis revealed significantly reduced levels of acetyl-CoA in the *sucC* mutant, raising the possibility that the acetylome may have been altered, and changes in peptidoglycan acetylation have been implicated in autolysis and antibiotic resistance [136]. Moreover, cross-talk between acetylation and succinylation has been shown to affect enzymatic activity which suggests that perturbation of the succinylome may form part of a larger picture [223].

We have shown that mutation of *sucC* leads to increased susceptibility to β-lactam antibiotics, raising the possibility of succinyl co-A synthetase as a therapeutic target, in sensitising MRSA to these compounds. Additional work to identify the specific pattern of succinylation and possibly acetylation, responsible for this phenotype may produce additional therapeutic targets. At the same time, the discovery of *sucC* suppressor mutations arising in *sucA* and *sucB* that overcame the increased susceptibility is an important reminder that *S. aureus* continues to challenge us, and the clinical implications of such suppressor mutations should be taken into account when targeting this pathway as a therapeutic avenue.

5.2 Roles of *cycA* and *ecsB* in the susceptibility of MRSA to β-lactam antibiotics

The data presented in chapter 4 demonstrates that mutation of the *cycA* gene in MRSA increases susceptibility to the β-lactam antibiotics cefoxitin and oxacillin, and also D-cycloserine (DCS), in CLSI susceptibility testing and in glucose-replete conditions. Alanine uptake studies showed a concomitant impairment of alanine consumption in the *cycA* mutant, while cell wall analysis revealed that mutation of *cycA,* or DCS-exposure, have similar effects on the structure of *S. aureus* peptidoglycan [132]. These phenotypes of increased susceptibility and impaired alanine consumption were notably absent in CDM lacking glucose, prompting us to hypothesise that an alternative permease, or permeases, may be transporting alanine in CDM. Examination of several potential candidates revealed that none of these strains had impaired growth in CDM under oxacillin stress. In USA300_FPR3757 there are at least 292 genes predicted to encode membrane transporters, of which 120 seem to be associated with amino acid, osmolyte or nucleoside transport [224]. In this context it was important to consider that alanine transport in CDM may be undertaken by more than 1 permease, including CycA, and that they might compensate for one another. To address this, the *cycA* mutation was also introduced into these potential permeases. A *cycA/ecsB* mutant showed impaired growth in CDM sub-inhibitory oxacillin, however the amino acid consumption results would seem to indicate that alanine consumption was not impaired in CDM despite the lack of CycA and EcsB activity. Recent work by Schiller *et al* implicated EcsB in peptide export, as opposed to amino acid import [173]. Taken together with our amino acid consumption result, this would suggest that the impaired growth phenotype of *cycA/ecsB* in CDM with oxacillin is not directly linked to alanine transport by EcsB. Nonetheless, the impaired growth of *cycA/ecsB* in these conditions was rescued by supplementation with excess exogenous alanine. It is possible that the *cycA/ecsB* mutant may have impaired growth in CDM with oxacillin due to a separate mechanism, and since CycA and EcsB are not responsible for alanine transport in these conditions, the cells are able to consume and utilise this exogenous alanine to overcome the oxacillin stress and restore wild type growth. It has been demonstrated that excess

exogenous glycine decreases methicillin resistance by completing with alanine, displacing it from the stem peptide, thus impacting peptidoglycan [225]. In this instance it would be something of the opposite scenario whereby excess availability of alanine is allowing the cell to overcoming the stress imposed by oxacillin.

We have shown that impairment of alanine consumption via *cycA* mutation in glucose-replete media can increase sensitivity, while excess alanine in CDM with oxacillin can restore growth of a *cycA/ecsB* mutant. Overall, this demonstrates a role for modulation of β-lactam resistance via alanine. There is growing recognition of the various roles for amino acids in overcoming antimicrobial resistance and our work contributes to this theme [226]. As EcsB appears not to be a main transporter of alanine in CDM, work is ongoing to identify same. By understanding how *S. aureus* resistance and growth can vary according to its nutritional conditions, this will help to identify the conditions in which new treatments are likely to succeed or fail in treating MRSA.

5.3 Mutation of *lspA* or inhibition of LspA with globomycin leads to increased β-lactam resistance.

In contrast to the increased susceptibility conferred by *sucC* and *cycA* mutations, the data in this thesis shows that mutation of the *lspA* gene leads to increased β-lactam resistance. Furthermore, inhibition of LspA activity by the drug globomycin mediates the same effect as genetic mutation in *lspA*. This increased resistance phenotype was demonstrable in clinical strains USA300 and *S. aureus* ATCC43300. At oxacillin and cefotaxime concentrations where these strains were unable to grow, the addition of globomycin led to growth, effectively increasing their MIC to these antibiotics.

Globomycin is a cyclic peptide antibiotic, and its mode of action is to bind and inhibit LspA activity. It has efficacy against Gram-negative bacteria because the inhibition of LspA prevents lipoprotein maturation and inhibits cell wall synthesis

in these cells. In Gram-positive bacteria globomycin does not have the same efficacy since LspA is not essential.

LspA is attractive as a drug target because it has no mammalian equivalent, is essential for Gram-negative bacteria, has an accessible active site, and while not essential in Gram-positive bacteria, it is required for full virulence [179, 227-229]. Although this would suggest that there is more scope for targeting LspA in Gram-negatives, it is plausible that there might be a role for therapeutics in the form of virulence attenuators for Gram-positive organisms such as *S. aureus.* This has led to recent work optimising globomycin analogues as novel antibiotics [181]. While they are mainly proposed for use against Gram-negative organisms, the authors of this study also tested the efficacy of the various analogues against MRSA strain USA300, and found that while the globomycin MIC was >100 μg/ml, some of the analogues demonstrated lower MICs of 25 μg/ml in USA300. If continued improvements led to a globomycin analogue with efficacy against *S. aureus*, it could have therapeutic value, as an antibiotic or a virulence attenuator.

Overall, the development of globomycin analogues with increased efficacy is a positive step for drug development. However, our data indicates that for MRSA infection, the combination of an LspA inhibitor with a β-lactam is contraindicated, as the inhibition of LspA by a globomycin-type drug would inadvertently increase resistance to the β-lactam. There are many situations where a patient might have a chronic, polymicrobial, or recalcitrant infection, and more than 1 antibiotic therapy could be warranted. In this situation, the administration of a globomycin-type drug to target a Gram-negative pathogen, could potentially interfere with concurrent β-lactam treatment, increasing resistance in an MRSA strain in the individual.

The exact mechanism of how LspA inhibition leads to increased resistance is not fully understood. We examined peptidoglycan composition and found no differences between JE2 and the *lspA* mutant to explain the phenotype. The fact that an *lgt* mutant, and a double *lspA/lgt* mutant do not share the same increased resistance as a single *lspA* mutant leads us to hypothesize that an accumulation of

diacylglycerol or mislocalisation of lipoproteins at the membrane may be resulting in increased resistance. Further work is underway to examine this hypothesis and understand the mechanism of how LspA inhibition leads to increased β-lactam resistance.

Overall, the results presented in this thesis identify new genes involved in β-lactam resistance in MRSA. For *cycA* and *sucC*, this adds to the potential therapeutic targets that may overcome β-lactam resistance. In the case of *lspA*, our data shows that mutation of *lspA* increased β-lactam resistance. Although the mechanism is not yet identified, this knowledge should be taken into consideration when evaluating drugs that would target the lipoprotein processing pathway, given the possible interactions between such drugs in combination with β-lactams.

The data in this thesis identifies and adds to our knowledge of factors affecting β-lactam resistance, identifying new therapeutic targets in *cycA* and *sucC*, while also identifying the ways that *S. aureus* continually evolves to match our effects, in the form of *sucC* suppressor mutations and the increased resistance of an *lspA* mutant.

Chapter 6: Bibliography & Appendices

Bibliography

1. Kuehnert, M.J., et al., *Prevalence of Staphylococcus aureus nasal colonization in the United States, 2001-2002.* J Infect Dis, 2006. **193**(2): p. 172-9.
2. Wertheim, H.F., et al., *Risk and outcome of nosocomial Staphylococcus aureus bacteraemia in nasal carriers versus non-carriers.* Lancet, 2004. **364**(9435): p. 703-5.
3. Wertheim, H.F., et al., *The role of nasal carriage in Staphylococcus aureus infections.* Lancet Infect Dis, 2005. **5**(12): p. 751-62.
4. Tong, S.Y., et al., *Staphylococcus aureus infections: epidemiology, pathophysiology, clinical manifestations, and management.* Clin Microbiol Rev, 2015. **28**(3): p. 603-61.
5. Barber, M., *Staphylococcal infection due to penicillin-resistant strains.* Br Med J, 1947. **2**(4534): p. 863-5.
6. Barber, M., *Methicillin-resistant staphylococci.* J Clin Pathol, 1961. **14**: p. 385-93.
7. Appelbaum, P.C., *The emergence of vancomycin-intermediate and vancomycin-resistant Staphylococcus aureus.* Clin Microbiol Infect, 2006. **12 Suppl 1**: p. 16-23.
8. Stryjewski, M.E. and H.F. Chambers, *Skin and soft-tissue infections caused by community-acquired methicillin-resistant Staphylococcus aureus.* Clin Infect Dis, 2008. **46 Suppl 5**: p. S368-77.
9. Pozzi, C., et al., *Methicillin resistance alters the biofilm phenotype and attenuates virulence in Staphylococcus aureus device-associated infections.* PLoS Pathog, 2012. **8**(4): p. e1002626.
10. Rudkin, J.K., et al., *Methicillin resistance reduces the virulence of healthcare-associated methicillin-resistant Staphylococcus aureus by interfering with the agr quorum sensing system.* J Infect Dis, 2012. **205**(5): p. 798-806.
11. Moran, G.J., et al., *Methicillin-resistant S. aureus infections among patients in the emergency department.* N Engl J Med, 2006. **355**(7): p. 666-74.

12. Chambers, H.F. and F.R. Deleo, *Waves of resistance: Staphylococcus aureus in the antibiotic era.* Nat Rev Microbiol, 2009. **7**(9): p. 629-41.
13. Naimi, T.S., et al., *Comparison of community- and health care-associated methicillin-resistant Staphylococcus aureus infection.* JAMA, 2003. **290**(22): p. 2976-84.
14. Blake, K.L., et al., *The nature of Staphylococcus aureus MurA and MurZ and approaches for detection of peptidoglycan biosynthesis inhibitors.* Mol Microbiol, 2009. **72**(2): p. 335-43.
15. Nishida, S., et al., *Identification and characterization of amino acid residues essential for the active site of UDP-N-acetylenolpyruvylglucosamine reductase (MurB) from Staphylococcus aureus.* J Biol Chem, 2006. **281**(3): p. 1714-24.
16. Kim, S.J., J. Chang, and M. Singh, *Peptidoglycan architecture of Gram-positive bacteria by solid-state NMR.* Biochim Biophys Acta, 2015. **1848**(1 Pt B): p. 350-62.
17. Hao, H., et al., *Inhibitors targeting on cell wall biosynthesis pathway of MRSA.* Mol Biosyst, 2012. **8**(11): p. 2828-38.
18. Barreteau, H., et al., *Cytoplasmic steps of peptidoglycan biosynthesis.* FEMS Microbiol Rev, 2008. **32**(2): p. 168-207.
19. Chung, B.C., et al., *Crystal structure of MraY, an essential membrane enzyme for bacterial cell wall synthesis.* Science, 2013. **341**(6149): p. 1012-1016.
20. Bouhss, A., et al., *The biosynthesis of peptidoglycan lipid-linked intermediates.* FEMS Microbiol Rev, 2008. **32**(2): p. 208-33.
21. Schneider, T., et al., *In vitro assembly of a complete, pentaglycine interpeptide bridge containing cell wall precursor (lipid II-Gly5) of Staphylococcus aureus.* Mol Microbiol, 2004. **53**(2): p. 675-85.
22. Georgopapadakou, N.H. and F.Y. Liu, *Penicillin-binding proteins in bacteria.* Antimicrob Agents Chemother, 1980. **18**(1): p. 148-57.
23. Pereira, S.F., et al., *Evidence for a dual role of PBP1 in the cell division and cell separation of Staphylococcus aureus.* Mol Microbiol, 2009. **72**(4): p. 895-904.

24. Reed, P., et al., *Staphylococcus aureus Survives with a Minimal Peptidoglycan Synthesis Machine but Sacrifices Virulence and Antibiotic Resistance.* PLoS Pathog, 2015. **11**(5): p. e1004891.
25. Pinho, M.G., H. de Lencastre, and A. Tomasz, *An acquired and a native penicillin-binding protein cooperate in building the cell wall of drug-resistant staphylococci.* Proc Natl Acad Sci U S A, 2001. **98**(19): p. 10886-91.
26. Pinho, M.G., et al., *Complementation of the essential peptidoglycan transpeptidase function of penicillin-binding protein 2 (PBP2) by the drug resistance protein PBP2A in Staphylococcus aureus.* J Bacteriol, 2001. **183**(22): p. 6525-31.
27. Pinho, M.G., H. de Lencastre, and A. Tomasz, *Cloning, characterization, and inactivation of the gene pbpC, encoding penicillin-binding protein 3 of Staphylococcus aureus.* J Bacteriol, 2000. **182**(4): p. 1074-9.
28. Navratna, V., et al., *Molecular basis for the role of Staphylococcus aureus penicillin binding protein 4 in antimicrobial resistance.* J Bacteriol, 2010. **192**(1): p. 134-44.
29. Memmi, G., et al., *Staphylococcus aureus PBP4 is essential for beta-lactam resistance in community-acquired methicillin-resistant strains.* Antimicrob Agents Chemother, 2008. **52**(11): p. 3955-66.
30. Hackbarth, C.J. and H.F. Chambers, *blaI and blaR1 regulate beta-lactamase and PBP 2a production in methicillin-resistant Staphylococcus aureus.* Antimicrob Agents Chemother, 1993. **37**(5): p. 1144-9.
31. Hartman, B.J. and A. Tomasz, *Low-affinity penicillin-binding protein associated with beta-lactam resistance in Staphylococcus aureus.* J Bacteriol, 1984. **158**(2): p. 513-6.
32. Katayama, Y., T. Ito, and K. Hiramatsu, *A new class of genetic element, staphylococcus cassette chromosome mec, encodes methicillin resistance in Staphylococcus aureus.* Antimicrob Agents Chemother, 2000. **44**(6): p. 1549-55.
33. Berger-Bachi, B. and S. Rohrer, *Factors influencing methicillin resistance in staphylococci.* Arch Microbiol, 2002. **178**(3): p. 165-71.

34. Lewis, R.A. and K.G. Dyke, *MecI represses synthesis from the beta-lactamase operon of Staphylococcus aureus.* J Antimicrob Chemother, 2000. **45**(2): p. 139-44.

35. Hiramatsu, K., et al., *Molecular cloning and nucleotide sequence determination of the regulator region of mecA gene in methicillin-resistant Staphylococcus aureus (MRSA).* FEBS Lett, 1992. **298**(2-3): p. 133-6.

36. Throup, J.P., et al., *The srhSR gene pair from Staphylococcus aureus: genomic and proteomic approaches to the identification and characterization of gene function.* Biochemistry, 2001. **40**(34): p. 10392-401.

37. Arede, P., J. Ministro, and D.C. Oliveira, *Redefining the role of the beta-lactamase locus in methicillin-resistant Staphylococcus aureus: beta-lactamase regulators disrupt the MecI-mediated strong repression on mecA and optimize the phenotypic expression of resistance in strains with constitutive mecA expression.* Antimicrob Agents Chemother, 2013. **57**(7): p. 3037-45.

38. Ryffel, C., F.H. Kayser, and B. Berger-Bachi, *Correlation between regulation of mecA transcription and expression of methicillin resistance in staphylococci.* Antimicrob Agents Chemother, 1992. **36**(1): p. 25-31.

39. Kobayashi, N., K. Taniguchi, and S. Urasawa, *Analysis of diversity of mutations in the mecI gene and mecA promoter/operator region of methicillin-resistant Staphylococcus aureus and Staphylococcus epidermidis.* Antimicrob Agents Chemother, 1998. **42**(3): p. 717-20.

40. Hartman, B.J. and A. Tomasz, *Expression of methicillin resistance in heterogeneous strains of Staphylococcus aureus.* Antimicrob Agents Chemother, 1986. **29**(1): p. 85-92.

41. Sabath, L.D. and S.J. Wallace, *The problems of drug-resistant pathogenic bacteria. Factors influencing methicillin resistance in staphylococci.* Ann N Y Acad Sci, 1971. **182**: p. 258-66.

42. Ryffel, C., et al., *Mechanisms of heteroresistance in methicillin-resistant Staphylococcus aureus.* Antimicrob Agents Chemother, 1994. **38**(4): p. 724-8.

43. Berger-Bachi, B., et al., *FemA, a host-mediated factor essential for methicillin resistance in Staphylococcus aureus: molecular cloning and characterization.* Mol Gen Genet, 1989. **219**(1-2): p. 263-9.

44. Stranden, A.M., et al., *Cell wall monoglycine cross-bridges and methicillin hypersusceptibility in a femAB null mutant of methicillin-resistant Staphylococcus aureus.* J Bacteriol, 1997. **179**(1): p. 9-16.

45. Henze, U., et al., *Influence of femB on methicillin resistance and peptidoglycan metabolism in Staphylococcus aureus.* J Bacteriol, 1993. **175**(6): p. 1612-20.

46. Gustafson, J., et al., *The femC locus of Staphylococcus aureus required for methicillin resistance includes the glutamine synthetase operon.* J Bacteriol, 1994. **176**(5): p. 1460-7.

47. Ornelas-Soares, A., et al., *Reduced methicillin resistance in a new Staphylococcus aureus transposon mutant that incorporates muramyl dipeptides into the cell wall peptidoglycan.* J Biol Chem, 1994. **269**(44): p. 27246-50.

48. Komatsuzawa, H., et al., *Characterization of fmtA, a gene that modulates the expression of methicillin resistance in Staphylococcus aureus.* Antimicrob Agents Chemother, 1999. **43**(9): p. 2121-5.

49. Zhao, Y., et al., *Staphylococcus aureus methicillin-resistance factor fmtA is regulated by the global regulator SarA.* PLoS One, 2012. **7**(8): p. e43998.

50. Komatsuzawa, H., et al., *Cloning and sequencing of the gene, fmtC, which affects oxacillin resistance in methicillin-resistant Staphylococcus aureus.* FEMS Microbiol Lett, 2001. **203**(1): p. 49-54.

51. Peschel, A., et al., *Staphylococcus aureus resistance to human defensins and evasion of neutrophil killing via the novel virulence factor MprF is based on modification of membrane lipids with l-lysine.* J Exp Med, 2001. **193**(9): p. 1067-76.

52. Soldo, B., V. Lazarevic, and D. Karamata, *tagO is involved in the synthesis of all anionic cell-wall polymers in Bacillus subtilis 168.* Microbiology (Reading), 2002. **148**(Pt 7): p. 2079-2087.

53. Campbell, J., et al., *Synthetic lethal compound combinations reveal a fundamental connection between wall teichoic acid and peptidoglycan biosyntheses in Staphylococcus aureus.* ACS Chem Biol, 2011. **6**(1): p. 106-16.

54. Nakao, A., S. Imai, and T. Takano, *Transposon-mediated insertional mutagenesis of the D-alanyl-lipoteichoic acid (dlt) operon raises methicillin resistance in Staphylococcus aureus.* Res Microbiol, 2000. **151**(10): p. 823-9.

55. Mikkelsen, K., et al., *The Novel Membrane-Associated Auxiliary Factors AuxA and AuxB Modulate beta-lactam Resistance in MRSA by stabilizing Lipoteichoic Acids.* Int J Antimicrob Agents, 2021: p. 106283.

56. Gustafson, J.E. and B.J. Wilkinson, *Lower autolytic activity in a homogeneous methicillin-resistant Staphylococcus aureus strain compared to derived heterogeneous-resistant and susceptible strains.* FEMS Microbiol Lett, 1989. **50**(1-2): p. 107-11.

57. de Jonge, B.L., H. de Lencastre, and A. Tomasz, *Suppression of autolysis and cell wall turnover in heterogeneous Tn551 mutants of a methicillin-resistant Staphylococcus aureus strain.* J Bacteriol, 1991. **173**(3): p. 1105-10.

58. Oshida, T., et al., *A Staphylococcus aureus autolysin that has an N-acetylmuramoyl-L-alanine amidase domain and an endo-beta-N-acetylglucosaminidase domain: cloning, sequence analysis, and characterization.* Proc Natl Acad Sci U S A, 1995. **92**(1): p. 285-9.

59. Komatsuzawa, H., et al., *Subcellular localization of the major autolysin, ATL and its processed proteins in Staphylococcus aureus.* Microbiol Immunol, 1997. **41**(6): p. 469-79.

60. Oshida, T. and A. Tomasz, *Isolation and characterization of a Tn551-autolysis mutant of Staphylococcus aureus.* J Bacteriol, 1992. **174**(15): p. 4952-9.

61. Fujimura, T. and K. Murakami, *Increase of methicillin resistance in Staphylococcus aureus caused by deletion of a gene whose product is homologous to lytic enzymes.* J Bacteriol, 1997. **179**(20): p. 6294-301.

62. Krute, C.N., et al., *The disruption of prenylation leads to pleiotropic rearrangements in cellular behavior in Staphylococcus aureus.* Mol Microbiol, 2015. **95**(5): p. 819-32.
63. Eagle, H. and A.D. Musselman, *The rate of bactericidal action of penicillin in vitro as a function of its concentration, and its paradoxically reduced activity at high concentrations against certain organisms.* J Exp Med, 1948. **88**(1): p. 99-131.
64. Jonsson, I.M., et al., *Inactivation of the Ecs ABC transporter of Staphylococcus aureus attenuates virulence by altering composition and function of bacterial wall.* PLoS One, 2010. **5**(12): p. e14209.
65. Jacobs, M., et al., *Bacillus subtilis PrsA is required in vivo as an extracytoplasmic chaperone for secretion of active enzymes synthesized either with or without pro-sequences.* Mol Microbiol, 1993. **8**(5): p. 957-66.
66. Corrigan, R.M., et al., *c-di-AMP is a new second messenger in Staphylococcus aureus with a role in controlling cell size and envelope stress.* PLoS Pathog, 2011. **7**(9): p. e1002217.
67. Oku, Y., et al., *Pleiotropic roles of polyglycerolphosphate synthase of lipoteichoic acid in growth of Staphylococcus aureus cells.* J Bacteriol, 2009. **191**(1): p. 141-51.
68. Dengler, V., et al., *Mutation in the C-di-AMP cyclase dacA affects fitness and resistance of methicillin resistant Staphylococcus aureus.* PLoS One, 2013. **8**(8): p. e73512.
69. Bowman, L., et al., *New Insights into the Cyclic Di-adenosine Monophosphate (c-di-AMP) Degradation Pathway and the Requirement of the Cyclic Dinucleotide for Acid Stress Resistance in Staphylococcus aureus.* J Biol Chem, 2016. **291**(53): p. 26970-26986.
70. Griffiths, J.M. and A.J. O'Neill, *Loss of function of the gdpP protein leads to joint beta-lactam/glycopeptide tolerance in Staphylococcus aureus.* Antimicrob Agents Chemother, 2012. **56**(1): p. 579-81.
71. Mwangi, M.M., et al., *Whole-genome sequencing reveals a link between beta-lactam resistance and synthetases of the alarmone (p)ppGpp in Staphylococcus aureus.* Microb Drug Resist, 2013. **19**(3): p. 153-9.

72. Hantke, K. and V. Braun, *Covalent binding of lipid to protein. Diglyceride and amide-linked fatty acid at the N-terminal end of the murein-lipoprotein of the Escherichia coli outer membrane.* Eur J Biochem, 1973. **34**(2): p. 284-96.

73. Shahmirzadi, S.V., M.T. Nguyen, and F. Gotz, *Evaluation of Staphylococcus aureus Lipoproteins: Role in Nutritional Acquisition and Pathogenicity.* Front Microbiol, 2016. **7**: p. 1404.

74. Dartois, V., T. Djavakhishvili, and J.A. Hoch, *KapB is a lipoprotein required for KinB signal transduction and activation of the phosphorelay to sporulation in Bacillus subtilis.* Mol Microbiol, 1997. **26**(5): p. 1097-108.

75. Bengtsson, J., et al., *Subunit II of Bacillus subtilis cytochrome c oxidase is a lipoprotein.* J Bacteriol, 1999. **181**(2): p. 685-8.

76. Mei, J.M., et al., *Identification of Staphylococcus aureus virulence genes in a murine model of bacteraemia using signature-tagged mutagenesis.* Mol Microbiol, 1997. **26**(2): p. 399-407.

77. Nielsen, J.B. and J.O. Lampen, *Membrane-bound penicillinases in Gram-positive bacteria.* J Biol Chem, 1982. **257**(8): p. 4490-5.

78. Nguyen, M.T., et al., *The nuSaalpha Specific Lipoprotein Like Cluster (lpl) of S. aureus USA300 Contributes to Immune Stimulation and Invasion in Human Cells.* PLoS Pathog, 2015. **11**(6): p. e1004984.

79. Nguyen, M.T., et al., *Lipoproteins in Gram-Positive Bacteria: Abundance, Function, Fitness.* Front Microbiol, 2020. **11**: p. 582582.

80. Kovacs-Simon, A., R.W. Titball, and S.L. Michell, *Lipoproteins of bacterial pathogens.* Infect Immun, 2011. **79**(2): p. 548-61.

81. Nguyen, M.T., et al., *Skin-Specific Unsaturated Fatty Acids Boost the Staphylococcus aureus Innate Immune Response.* Infect Immun, 2015. **84**(1): p. 205-15.

82. Inouye, S., et al., *Amino acid sequence for the peptide extension on the prolipoprotein of the Escherichia coli outer membrane.* Proc Natl Acad Sci U S A, 1977. **74**(3): p. 1004-8.

83. Buddelmeijer, N., *The molecular mechanism of bacterial lipoprotein modification--how, when and why?* FEMS Microbiol Rev, 2015. **39**(2): p. 246-61.

84. Sankaran, K. and H.C. Wu, *Lipid modification of bacterial prolipoprotein. Transfer of diacylglyceryl moiety from phosphatidylglycerol.* J Biol Chem, 1994. **269**(31): p. 19701-6.

85. Ichihara, S., M. Hussain, and S. Mizushima, *Mechanism of export of outer membrane lipoproteins through the cytoplasmic membrane in Escherichia coli. Binding of lipoprotein precursors to the peptidoglycan layer.* J Biol Chem, 1982. **257**(1): p. 495-500.

86. Gardiner, J.H.t., et al., *Lipoprotein N-Acylation in Staphylococcus aureus Is Catalyzed by a Two-Component Acyl Transferase System.* mBio, 2020. **11**(4).

87. Leskela, S., et al., *Lipid modification of prelipoproteins is dispensable for growth but essential for efficient protein secretion in Bacillus subtilis: characterization of the lgt gene.* Mol Microbiol, 1999. **31**(4): p. 1075-85.

88. Stoll, H., et al., *Staphylococcus aureus deficient in lipidation of prelipoproteins is attenuated in growth and immune activation.* Infect Immun, 2005. **73**(4): p. 2411-23.

89. Somerville, G.A. and R.A. Proctor, *At the crossroads of bacterial metabolism and virulence factor synthesis in Staphylococci.* Microbiol Mol Biol Rev, 2009. **73**(2): p. 233-48.

90. Strasters, K.C. and K.C. Winkler, *Carbohydrate Metabolism of Staphylococcus aureus.* J Gen Microbiol, 1963. **33**: p. 213-29.

91. Chambers, H.F., *Methicillin-resistant Staphylococcus aureus. Mechanisms of resistance and implications for treatment.* Postgrad Med, 2001. **109**(2 Suppl): p. 43-50.

92. Diep, B.A., et al., *Complete genome sequence of USA300, an epidemic clone of community-acquired meticillin-resistant Staphylococcus aureus.* Lancet, 2006. **367**(9512): p. 731-9.

93. Dordel, J., et al., *Novel determinants of antibiotic resistance: identification of mutated loci in highly methicillin-resistant subpopulations of methicillin-resistant Staphylococcus aureus.* MBio, 2014. **5**(2): p. e01000.

94. Halsey, C.R., et al., *Amino Acid Catabolism in Staphylococcus aureus and the Function of Carbon Catabolite Repression.* mBio, 2017. **8**(1).

95. Somerville, G.A., et al., *Staphylococcus aureus aconitase inactivation unexpectedly inhibits post-exponential-phase growth and enhances stationary-phase survival.* Infect Immun, 2002. **70**(11): p. 6373-82.

96. Sadykov, M.R., et al., *CcpA coordinates central metabolism and biofilm formation in Staphylococcus epidermidis.* Microbiology, 2011. **157**(Pt 12): p. 3458-68.

97. Zalis, E.A., et al., *Stochastic Variation in Expression of the Tricarboxylic Acid Cycle Produces Persister Cells.* mBio, 2019. **10**(5).

98. Thomas, V.C., et al., *A dysfunctional tricarboxylic acid cycle enhances fitness of Staphylococcus epidermidis during beta-lactam stress.* MBio, 2013. **4**(4).

99. Keaton, M.A., et al., *Exposure of clinical MRSA heterogeneous strains to beta-lactams redirects metabolism to optimize energy production through the TCA cycle.* PLoS One, 2013. **8**(8): p. e71025.

100. Rosato, R.R., et al., *TCA cycle-mediated generation of ROS is a key mediator for HeR-MRSA survival under beta-lactam antibiotic exposure.* PLoS One, 2014. **9**(6): p. e99605.

101. Christensen, D.G., et al., *Post-translational Protein Acetylation: An Elegant Mechanism for Bacteria to Dynamically Regulate Metabolic Functions.* Front Microbiol, 2019. **10**: p. 1604.

102. Stram, A.R. and R.M. Payne, *Post-translational modifications in mitochondria: protein signaling in the powerhouse.* Cell Mol Life Sci, 2016. **73**(21): p. 4063-73.

103. Gao, J., et al., *The involvement of post-translational modifications in cardiovascular pathologies: Focus on SUMOylation, neddylation, succinylation, and prenylation.* J Mol Cell Cardiol, 2020. **138**: p. 49-58.

104. Azevedo, C. and A. Saiardi, *Why always lysine? The ongoing tale of one of the most modified amino acids.* Adv Biol Regul, 2016. **60**: p. 144-150.

105. Pawson, T. and J.D. Scott, *Protein phosphorylation in signaling--50 years and counting.* Trends Biochem Sci, 2005. **30**(6): p. 286-90.

106. Zhang, Z., et al., *Identification of lysine succinylation as a new post-translational modification.* Nat Chem Biol, 2011. **7**(1): p. 58-63.

107. Gaviard, C., et al., *Lysine Succinylation and Acetylation in Pseudomonas aeruginosa.* J Proteome Res, 2018. **17**(7): p. 2449-2459.

108. Zhao, Y., et al., *Comprehensive Succinylome Profiling Reveals the Pivotal Role of Lysine Succinylation in Energy Metabolism and Quorum Sensing of Staphylococcus epidermidis.* Frontiers in Microbiology, 2021. **11**(3556).

109. Ronau, J.A., J.F. Beckmann, and M. Hochstrasser, *Substrate specificity of the ubiquitin and Ubl proteases.* Cell Res, 2016. **26**(4): p. 441-56.

110. Unnikrishnan, A., et al., *The role of DNA methylation in epigenetics of aging.* Pharmacol Ther, 2019. **195**: p. 172-185.

111. Barnes, C.E., D.M. English, and S.M. Cowley, *Acetylation & Co: an expanding repertoire of histone acylations regulates chromatin and transcription.* Essays Biochem, 2019. **63**(1): p. 97-107.

112. Rowland, E.A., C.K. Snowden, and I.M. Cristea, *Protein lipoylation: an evolutionarily conserved metabolic regulator of health and disease.* Curr Opin Chem Biol, 2018. **42**: p. 76-85.

113. Fey, P.D., et al., *A genetic resource for rapid and comprehensive phenotype screening of nonessential Staphylococcus aureus genes.* MBio, 2013. **4**(1): p. e00537-12.

114. Robinson, D.A. and M.C. Enright, *Evolutionary models of the emergence of methicillin-resistant Staphylococcus aureus.* Antimicrob Agents Chemother, 2003. **47**(12): p. 3926-34.

115. O'Neill, E., et al., *Association between methicillin susceptibility and biofilm regulation in Staphylococcus aureus isolates from device-related infections.* J Clin Microbiol, 2007. **45**(5): p. 1379-88.

116. Aedo, S. and A. Tomasz, *Role of the Stringent Stress Response in the Antibiotic Resistance Phenotype of Methicillin-Resistant Staphylococcus aureus.* Antimicrob Agents Chemother, 2016. **60**(4): p. 2311-7.

117. Mittenhuber, G., *Comparative genomics and evolution of genes encoding bacterial (p)ppGpp synthetases/hydrolases (the Rel, RelA and SpoT proteins).* J Mol Microbiol Biotechnol, 2001. **3**(4): p. 585-600.

118. Mechold, U., et al., *Intramolecular regulation of the opposing (p)ppGpp catalytic activities of Rel(Seq), the Rel/Spo enzyme from Streptococcus equisimilis.* J Bacteriol, 2002. **184**(11): p. 2878-88.

119. Geiger, T., et al., *Role of the (p)ppGpp synthase RSH, a RelA/SpoT homolog, in stringent response and virulence of Staphylococcus aureus.* Infect Immun, 2010. **78**(5): p. 1873-83.

120. Geiger, T., et al., *Two small (p)ppGpp synthases in Staphylococcus aureus mediate tolerance against cell envelope stress conditions.* J Bacteriol, 2014. **196**(4): p. 894-902.

121. Bhawini, A., et al., *RelQ Mediates the Expression of beta-Lactam Resistance in Methicillin-Resistant Staphylococcus aureus.* Front Microbiol, 2019. **10**: p. 339.

122. Waters, E.M., et al., *Redeploying beta-lactam antibiotics as a novel antivirulence strategy for the treatment of methicillin-resistant Staphylococcus aureus infections.* J Infect Dis, 2017. **215**(1): p. 80-87.

123. Weinert, B.T., et al., *Lysine succinylation is a frequently occurring modification in prokaryotes and eukaryotes and extensively overlaps with acetylation.* Cell Rep, 2013. **4**(4): p. 842-51.

124. Zeng, J., et al., *Comprehensive profiling of protein lysine acetylation and its overlap with lysine succinylation in the Porphyromonas gingivalis fimbriated strain ATCC 33277.* Mol Oral Microbiol, 2020. **35**(6): p. 240-250.

125. Pan, J., et al., *Global Analysis of Protein Lysine Succinylation Profiles and Their Overlap with Lysine Acetylation in the Marine Bacterium Vibrio parahemolyticus.* J Proteome Res, 2015. **14**(10): p. 4309-18.

126. Xie, L., et al., *First succinyl-proteome profiling of extensively drug-resistant Mycobacterium tuberculosis revealed involvement of succinylation in cellular physiology.* J Proteome Res, 2015. **14**(1): p. 107-19.

127. Smestad, J., et al., *Chromatin Succinylation Correlates with Active Gene Expression and Is Perturbed by Defective TCA Cycle Metabolism.* iScience, 2018. **2**: p. 63-75.

128. Beausoleil, S.A., et al., *A probability-based approach for high-throughput protein phosphorylation analysis and site localization.* Nat Biotechnol, 2006. **24**(10): p. 1285-92.

129. Chalkley, R.J. and K.R. Clauser, *Modification site localization scoring: strategies and performance.* Mol Cell Proteomics, 2012. **11**(5): p. 3-14.

130. Vickery, C.R., et al., *Reconstitution of Staphylococcus aureus Lipoteichoic Acid Synthase Activity Identifies Congo Red as a Selective Inhibitor.* J Am Chem Soc, 2018. **140**(3): p. 876-879.

131. Sieradzki, K. and A. Tomasz, *Suppression of beta-lactam antibiotic resistance in a methicillin-resistant Staphylococcus aureus through synergic action of early cell wall inhibitors and some other antibiotics.* J Antimicrob Chemother, 1997. **39 Suppl A**: p. 47-51.

132. Gallagher, L.A., et al., *Impaired Alanine Transport or Exposure to d-Cycloserine Increases the Susceptibility of MRSA to beta-lactam Antibiotics.* J Infect Dis, 2020. **221**(6): p. 1000-1016.

133. Liu, Q., et al., *The ATP-Dependent Protease ClpP Inhibits Biofilm Formation by Regulating Agr and Cell Wall Hydrolase Sle1 in Staphylococcus aureus.* Front Cell Infect Microbiol, 2017. **7**: p. 181.

134. Thalso-Madsen, I., et al., *The Sle1 Cell Wall Amidase Is Essential for beta-Lactam Resistance in Community-Acquired Methicillin-Resistant Staphylococcus aureus USA300.* Antimicrob Agents Chemother, 2019. **64**(1).

135. Kind, S., J. Becker, and C. Wittmann, *Increased lysine production by flux coupling of the tricarboxylic acid cycle and the lysine biosynthetic pathway--metabolic engineering of the availability of succinyl-CoA in Corynebacterium glutamicum.* Metab Eng, 2013. **15**: p. 184-95.

136. Sychantha, D., et al., *Mechanistic Pathways for Peptidoglycan O-Acetylation and De-O-Acetylation.* Front Microbiol, 2018. **9**: p. 2332.

137. Sen, S., et al., *Growth-Environment Dependent Modulation of Staphylococcus aureus Branched-Chain to Straight-Chain Fatty Acid Ratio and Incorporation of Unsaturated Fatty Acids.* PLoS One, 2016. **11**(10): p. e0165300.

138. Marshall, J.H. and G.J. Wilmoth, *Pigments of Staphylococcus aureus, a series of triterpenoid carotenoids.* J Bacteriol, 1981. **147**(3): p. 900-13.

139. Garcia-Fernandez, E., et al., *Membrane Microdomain Disassembly Inhibits MRSA Antibiotic Resistance.* Cell, 2017. **171**(6): p. 1354-1367 e20.

140. Fisher, J.F. and S. Mobashery, *beta-Lactams against the Fortress of the Gram-Positive Staphylococcus aureus Bacterium.* Chem Rev, 2021. **121**(6): p. 3412-3463.

141. McCarthy, H.E., *Ctrl-atl-delete: Re-thinking the mechanisms of biofilm formation by staphylococci.* *https://aran.library.nuigalway.ie/bitstream/handle/10379/5003/HannahEMcCarthy.pdf*, in *Microbiology*. 2015, National University of Ireland: Galway, Ireland. p. https://aran.library.nuigalway.ie/bitstream/handle/10379/5003/HannahEMcCarthy.pdf?sequence=1&isAllowed=y.

142. Baba, T. and O. Schneewind, *Targeting of muralytic enzymes to the cell division site of Gram-positive bacteria: repeat domains direct autolysin to the equatorial surface ring of Staphylococcus aureus.* EMBO J, 1998. **17**(16): p. 4639-46.

143. Boquist, L. and I. Ericsson, *Inhibition by streptozotocin of the activity of succinyl-CoA synthetase in vitro and in vivo.* FEBS Lett, 1986. **196**(2): p. 341-3.

144. CLSI, *Performance Standards for Antimicrobial Disk Susceptibility Tests; approved standard—12th ed. M02-A13.* 2018: Wayne, PA.

145. CLSI, *Methods for Dilution Antimicrobial Susceptibility Tests for Bacteria That Grow Aerobically. 11th ed. CLSI standard M07.* 2018: Wayne, PA.

146. CLSI, *Performance Standards for Antimicrobial Susceptibility Testing. 30th ed. CLSI supplement M100.* 2020: Wayne, PA.

147. Fingleton, C., et al., *Mutation of lipoprotein processing pathway gene lspA or inhibition of LspA activity by globomycin increases MRSA resistance to β-lactam antibiotics.* bioRxiv, 2021: p. 2021.02.03.429649.

148. Bose, J.L., P.D. Fey, and K.W. Bayles, *Genetic tools to enhance the study of gene function and regulation in Staphylococcus aureus.* Appl Environ Microbiol, 2013. **79**(7): p. 2218-24.

149. Tomasz, A., S. Nachman, and H. Leaf, *Stable classes of phenotypic expression in methicillin-resistant clinical isolates of staphylococci.* Antimicrob Agents Chemother, 1991. **35**(1): p. 124-9.

150. Liebeke, M., et al., *Metabolome analysis of gram-positive bacteria such as Staphylococcus aureus by GC-MS and LC-MS.* Methods Mol Biol, 2012. **815**: p. 377-98.

151. Zecha, J., et al., *TMT Labeling for the Masses: A Robust and Cost-efficient, In-solution Labeling Approach.* Mol Cell Proteomics, 2019. **18**(7): p. 1468-1478.

152. Vasaikar, S., et al., *Proteogenomic Analysis of Human Colon Cancer Reveals New Therapeutic Opportunities.* Cell, 2019. **177**(4): p. 1035-1049 e19.

153. Kim, S. and P.A. Pevzner, *MS-GF+ makes progress towards a universal database search tool for proteomics.* Nat Commun, 2014. **5**: p. 5277.

154. Monroe, M.E., et al., *MASIC: a software program for fast quantitation and flexible visualization of chromatographic profiles from detected LC-MS(/MS) features.* Comput Biol Chem, 2008. **32**(3): p. 215-7.

155. Huang da, W., B.T. Sherman, and R.A. Lempicki, *Systematic and integrative analysis of large gene lists using DAVID bioinformatics resources.* Nat Protoc, 2009. **4**(1): p. 44-57.

156. Alvarez, L., et al., *Ultra-Sensitive, High-Resolution Liquid Chromatography Methods for the High-Throughput Quantitative Analysis of Bacterial Cell Wall Chemistry and Structure.* Methods Mol Biol, 2016. **1440**: p. 11-27.

157. de Jonge, B.L., et al., *Peptidoglycan composition of a highly methicillin-resistant Staphylococcus aureus strain. The role of penicillin binding protein 2A.* J Biol Chem, 1992. **267**(16): p. 11248-54.

158. De Jonge, B.L., D. Gage, and N. Xu, *The carboxyl terminus of peptidoglycan stem peptides is a determinant for methicillin resistance in Staphylococcus aureus.* Antimicrob Agents Chemother, 2002. **46**(10): p. 3151-5.

159. Kuhner, D., et al., *From cells to muropeptide structures in 24 h: peptidoglycan mapping by UPLC-MS.* Sci Rep, 2014. **4**: p. 7494.

160. Boneca, I.G., et al., *Structural characterization of an abnormally cross-linked muropeptide dimer that is accumulated in the peptidoglycan of methicillin- and cefotaxime-resistant mutants of Staphylococcus aureus.* J Biol Chem, 1997. **272**(46): p. 29053-9.

161. Gründling, A., *Cell Wall Assembly and Physiology*, in *Staphylococcus: Genetics and Physiology*, G.A. Somerville, Editor. 2016, Caister Academic Press: UK. p. 133-170.

162. Panchal, V.V., et al., *Evolving MRSA: High-level beta-lactam resistance in Staphylococcus aureus is associated with RNA Polymerase alterations and fine tuning of gene expression.* PLoS Pathog, 2020. **16**(7): p. e1008672.

163. Baek, K.T., et al., *beta-Lactam resistance in methicillin-resistant Staphylococcus aureus USA300 is increased by inactivation of the ClpXP protease.* Antimicrob Agents Chemother, 2014. **58**(8): p. 4593-603.

164. Jensen, C., et al., *The ClpX chaperone controls autolytic splitting of Staphylococcus aureus daughter cells, but is bypassed by beta-lactam antibiotics or inhibitors of WTA biosynthesis.* PLoS Pathog, 2019. **15**(9): p. e1008044.

165. Schmollinger, M., et al., *ParSeq: searching motifs with structural and biochemical properties.* Bioinformatics, 2004. **20**(9): p. 1459-61.

166. Hayashi, S. and H.C. Wu, *Lipoproteins in bacteria.* J Bioenerg Biomembr, 1990. **22**(3): p. 451-71.

167. Braun, V. and H.C. Wu, *Lipoproteins, structure, function, biosynthesis and model for protein export*, in *New Comprehensive Biochemistry*, J.-M. Ghuysen and R. Hakenbeck, Editors. 1994, Elsevier. p. 319-341.

168. Sankaran, K., S.D. Gupta, and H.C. Wu, *Modification of bacterial lipoproteins.* Methods Enzymol, 1995. **250**: p. 683-97.

169. Tschumi, A., et al., *Identification of apolipoprotein N-acyltransferase (Lnt) in mycobacteria.* J Biol Chem, 2009. **284**(40): p. 27146-56.

170. Asanuma, M., et al., *Structural evidence of alpha-aminoacylated lipoproteins of Staphylococcus aureus.* FEBS J, 2011. **278**(5): p. 716-28.

171. An, F.Y., M.C. Sulavik, and D.B. Clewell, *Identification and characterization of a determinant (eep) on the Enterococcus faecalis chromosome that is involved in production of the peptide sex pheromone cAD1.* J Bacteriol, 1999. **181**(19): p. 5915-21.

172. Varahan, S., et al., *An ABC transporter is required for secretion of peptide sex pheromones in Enterococcus faecalis.* mBio, 2014. **5**(5): p. e01726-14.

173. Schilcher, K., et al., *Processing, Export, and Identification of Novel Linear Peptides from Staphylococcus aureus.* mBio, 2020. **11**(2).

174. Gan, K., et al., *Isolation and characterization of a temperature-sensitive mutant of Salmonella typhimurium defective in prolipoprotein modification.* J Biol Chem, 1993. **268**(22): p. 16544-50.

175. Gohring, N., et al., *New role of the disulfide stress effector YjbH in beta-lactam susceptibility of Staphylococcus aureus.* Antimicrob Agents Chemother, 2011. **55**(12): p. 5452-8.

176. Chan, Y.G., et al., *SagB Glucosaminidase Is a Determinant of Staphylococcus aureus Glycan Chain Length, Antibiotic Susceptibility, and Protein Secretion.* J Bacteriol, 2016. **198**(7): p. 1123-36.

177. Inukai, M., et al., *Mechanism of action of globomycin.* J Antibiot (Tokyo), 1978. **31**(11): p. 1203-5.

178. Inukai, M., et al., *Globomycin, a new peptide antibiotic with spheroplast-forming activity. II. Isolation and physico-chemical and biological characterization.* J Antibiot (Tokyo), 1978. **31**(5): p. 421-5.

179. Vogeley, L., et al., *Structural basis of lipoprotein signal peptidase II action and inhibition by the antibiotic globomycin.* Science, 2016. **351**(6275): p. 876-80.

180. Yakushi, T., et al., *Lethality of the covalent linkage between mislocalized major outer membrane lipoprotein and the peptidoglycan of Escherichia coli.* J Bacteriol, 1997. **179**(9): p. 2857-62.

181. Garland, K., et al., *Optimization of globomycin analogs as novel gram-negative antibiotics.* Bioorg Med Chem Lett, 2020. **30**(20): p. 127419.

182. Parvez, M.A., et al., *No relationship exists between PBP 2a amounts expressed in different MRSA strains obtained clinically and their beta-lactam MIC values.* J Med Invest, 2008. **55**(3-4): p. 246-53.

183. Brown, S., et al., *Methicillin resistance in Staphylococcus aureus requires glycosylated wall teichoic acids.* Proc Natl Acad Sci U S A, 2012. **109**(46): p. 18909-14.

184. Lee, S.H., et al., *Antagonism of chemical genetic interaction networks resensitize MRSA to beta-lactam antibiotics.* Chem Biol, 2011. **18**(11): p. 1379-89.

185. Gardete, S., et al., *Role of VraSR in antibiotic resistance and antibiotic-induced stress response in Staphylococcus aureus.* Antimicrob Agents Chemother, 2006. **50**(10): p. 3424-34.

186. Jousselin, A., et al., *The posttranslocational chaperone lipoprotein PrsA is involved in both glycopeptide and oxacillin resistance in Staphylococcus aureus.* Antimicrob Agents Chemother, 2012. **56**(7): p. 3629-40.

187. Jousselin, A., et al., *The Staphylococcus aureus Chaperone PrsA Is a New Auxiliary Factor of Oxacillin Resistance Affecting Penicillin-Binding Protein 2A.* Antimicrob Agents Chemother, 2015. **60**(3): p. 1656-66.

188. Roch, M., et al., *Thermosensitive PBP2a requires extracellular folding factors PrsA and HtrA1 for Staphylococcus aureus MRSA beta-lactam resistance.* Commun Biol, 2019. **2**: p. 417.

189. Baumgartner, M., et al., *Inactivation of Lgt allows systematic characterization of lipoproteins from Listeria monocytogenes.* J Bacteriol, 2007. **189**(2): p. 313-24.

190. Henneke, P., et al., *Lipoproteins are critical TLR2 activating toxins in group B streptococcal sepsis.* J Immunol, 2008. **180**(9): p. 6149-58.

191. Karinou, E., et al., *Inactivation of the Monofunctional Peptidoglycan Glycosyltransferase SgtB Allows Staphylococcus aureus To Survive in the Absence of Lipoteichoic Acid.* J Bacteriol, 2019. **201**(1).

192. Horsburgh, M.J., et al., *sigmaB modulates virulence determinant expression and stress resistance: characterization of a functional rsbU strain derived from Staphylococcus aureus 8325-4.* J Bacteriol, 2002. **184**(19): p. 5457-67.

193. Kreiswirth, B.N., et al., *The toxic shock syndrome exotoxin structural gene is not detectably transmitted by a prophage.* Nature, 1983. **305**(5936): p. 709-12.

194. Lee, C.Y., S.L. Buranen, and Z.H. Ye, *Construction of single-copy integration vectors for Staphylococcus aureus.* Gene, 1991. **103**(1): p. 101-5.

195. Clatworthy, A.E., E. Pierson, and D.T. Hung, *Targeting virulence: a new paradigm for antimicrobial therapy.* Nat Chem Biol, 2007. **3**(9): p. 541-8.

196. Davis, J.S., et al., *Combination of Vancomycin and beta-Lactam Therapy for Methicillin-Resistant Staphylococcus aureus Bacteremia: A Pilot Multicenter Randomized Controlled Trial.* Clin Infect Dis, 2016. **62**(2): p. 173-80.

197. Tong, S.Y., et al., *CAMERA2 - combination antibiotic therapy for methicillin-resistant Staphylococcus aureus infection: study protocol for a randomised controlled trial.* Trials, 2016. **17**(1): p. 170.

198. Chambers, H.F., *Methicillin resistance in staphylococci: molecular and biochemical basis and clinical implications.* Clin Microbiol Rev, 1997. **10**(4): p. 781-91.

199. Chambers, H.F. and C.J. Hackbarth, *Effect of NaCl and nafcillin on penicillin-binding protein 2a and heterogeneous expression of methicillin resistance in Staphylococcus aureus.* Antimicrob Agents Chemother, 1987. **31**(12): p. 1982-8.

200. Sabath, L.D. and S.J. Wallace, *The problems of drug-resistant pathogenic bacteria. Factors influencing methicillin resistance in staphylococci.* Ann N Y Acad Sci, 1971. **182**: p. 258-66.

201. Mlynek, K.D., et al., *Effects of Low-Dose Amoxicillin on Staphylococcus aureus USA300 Biofilms.* Antimicrob Agents Chemother, 2016. **60**(5): p. 2639-51.

202. Desjardins, C.A., et al., *Genomic and functional analyses of Mycobacterium tuberculosis strains implicate ald in D-cycloserine resistance.* Nat Genet, 2016. **48**(5): p. 544-51.

203. Chen, J.M., et al., *A point mutation in cycA partially contributes to the D-cycloserine resistance trait of Mycobacterium bovis BCG vaccine strains.* PLoS One, 2012. **7**(8): p. e43467.

204. Soper, T.S. and J.M. Manning, *Synergy in the antimicrobial action of penicillin and beta-chloro-D-alanine in vitro.* Antimicrob Agents Chemother, 1976. **9**(2): p. 347-9.

205. Tabuchi, F., et al., *D-cycloserine increases the effectiveness of vancomycin against vancomycin-highly resistant Staphylococcus aureus.* J Antibiot (Tokyo), 2017. **70**(8): p. 907-910.

206. Fujihira, T., et al., *Selective increase in the extracellular D-serine contents by D-cycloserine in the rat medial frontal cortex.* Neurochem Int, 2007. **51**(2-4): p. 233-6.

207. Batson, S., et al., *Inhibition of D-Ala:D-Ala ligase through a phosphorylated form of the antibiotic D-cycloserine.* Nat Commun, 2017. **8**(1): p. 1939.

208. Baisa, G., N.J. Stabo, and R.A. Welch, *Characterization of Escherichia coli D-cycloserine transport and resistant mutants.* J Bacteriol, 2013. **195**(7): p. 1389-99.

209. Curtiss, R., 3rd, et al., *Kinetic and genetic analyses of D-cycloserine inhibition and resistance in Escherichia coli.* J Bacteriol, 1965. **90**(5): p. 1238-50.

210. Russell, R.R., *Mapping of a D-cycloserine resistance locus in escherichia coli K-12.* J Bacteriol, 1972. **111**(2): p. 622-4.

211. Wargel, R.J., C.A. Hadur, and F.C. Neuhaus, *Mechanism of D-cycloserine action: transport mutants for D-alanine, D-cycloserine, and glycine.* J Bacteriol, 1971. **105**(3): p. 1028-35.

212. Feher, T., et al., *Characterization of cycA mutants of Escherichia coli. An assay for measuring in vivo mutation rates.* Mutat Res, 2006. **595**(1-2): p. 184-90.

213. Prosser, G.A., et al., *Glutamate Racemase Is the Primary Target of beta-Chloro-d-Alanine in Mycobacterium tuberculosis.* Antimicrob Agents Chemother, 2016. **60**(10): p. 6091-9.

214. Sobral, R.G., et al., *Normally functioning murF is essential for the optimal expression of methicillin resistance in Staphylococcus aureus.* Microb Drug Resist, 2003. **9**(3): p. 231-41.

215. Sobral, R.G., et al., *Role of murF in cell wall biosynthesis: isolation and characterization of a murF conditional mutant of Staphylococcus aureus.* J Bacteriol, 2006. **188**(7): p. 2543-53.

216. Li, C., et al., *CcpA mediates proline auxotrophy and is required for Staphylococcus aureus pathogenesis.* J Bacteriol, 2010. **192**(15): p. 3883-92.

217. Thurlow, L.R., G.S. Joshi, and A.R. Richardson, *Peroxisome Proliferator-Activated Receptor gamma Is Essential for the Resolution of Staphylococcus aureus Skin Infections.* Cell Host Microbe, 2018. **24**(2): p. 261-270 e4.

218. Lehman, M.K., et al., *Protease-Mediated Growth of Staphylococcus aureus on Host Proteins Is opp3 Dependent.* MBio, 2019. **10**(2).

219. Gill, S.R., et al., *Insights on evolution of virulence and resistance from the complete genome analysis of an early methicillin-resistant Staphylococcus aureus strain and a biofilm-producing methicillin-resistant Staphylococcus epidermidis strain.* J Bacteriol, 2005. **187**(7): p. 2426-38.

220. Hussain, M., J.G. Hastings, and P.J. White, *A chemically defined medium for slime production by coagulase-negative staphylococci.* J Med Microbiol, 1991. **34**(3): p. 143-7.

221. Kosono, S., et al., *Changes in the Acetylome and Succinylome of Bacillus subtilis in Response to Carbon Source.* PLoS One, 2015. **10**(6): p. e0131169.

222. de Jonge, B.L., et al., *Peptidoglycan composition in heterogeneous Tn551 mutants of a methicillin-resistant Staphylococcus aureus strain.* J Biol Chem, 1992. **267**(16): p. 11255-9.
223. Sun, L., et al., *Comprehensive analysis of the lysine acetylome in Aeromonas hydrophila reveals cross-talk between lysine acetylation and succinylation in LuxS.* Emerg Microbes Infect, 2019. **8**(1): p. 1229-1239.
224. Zeden, M.S., et al., *Exploring amino acid and peptide transporters as therapeutic targets to attenuate virulence and antibiotic resistance in Staphylococcus aureus.* PLoS Pathog, 2021. **17**(1): p. e1009093.
225. de Jonge, B.L., et al., *Effect of exogenous glycine on peptidoglycan composition and resistance in a methicillin-resistant Staphylococcus aureus strain.* Antimicrob Agents Chemother, 1996. **40**(6): p. 1498-503.
226. Idrees, M., et al., *Multimodal Role of Amino Acids in Microbial Control and Drug Development.* Antibiotics (Basel), 2020. **9**(6).
227. Paetzel, M., et al., *Signal peptidases.* Chem Rev, 2002. **102**(12): p. 4549-80.
228. Venema, R., et al., *Active lipoprotein precursors in the Gram-positive eubacterium Lactococcus lactis.* J Biol Chem, 2003. **278**(17): p. 14739-46.
229. Olatunji, S., et al., *Structures of lipoprotein signal peptidase II from Staphylococcus aureus complexed with antibiotics globomycin and myxovirescin.* Nat Commun, 2020. **11**(1): p. 140.

6.2 Appendix

Table 6.1. Proteins that have increased succinylation at 1 or more lysine residues in NE569 (*sucC*) versus JE2.

Uniprot Name	Gene Name	Protein Description	Number of lysine residues with increased succinylation in NE569 (*sucC*) versus JE2
Q2FG38	*accA*	Acetyl-coenzyme A carboxylase carboxyl transferase subunit alpha	1
Q2FG27	*ackA*	Acetate kinase	1
A0A0H2XKH5	*acnA*	Aconitate hydratase	1
Q2FHK6	*acpP*	Acyl carrier protein	1
A0A0H2XH08	*agrA*	Accessory gene regulator protein A	1
Q2FJN4	*ahpC*	Alkyl hydroperoxide reductase C	3
Q2FF55	*alr*	Alanine racemase	1
A0A0H2XDZ4	*ampA*	Cytosol aminopeptidase	1
Q2FG92	*apt*	Adenine phosphoribosyltransferase	1
Q2FGY6	*asnS*	Asparagine--tRNA ligase	1
Q2FEV0	*asp23*	Alkaline shock protein 23	2
A0A0H2XIJ3	*atl*	Autolysin	12
Q2FF22	*atpA*	ATP synthase subunit alpha	1
A0A0H2XG87	*birA*	Bifunctional ligase/repressor BirA	1
A0A0H2XGE8	*budA*	Alpha-acetolactate decarboxylase	1
A0A0H2XGX4	*cap5F*	Capsular polysaccharide biosynthesis protein Cap5F	1
A0A0H2XGE9	*cidC*	Pyruvate oxidase	1
A0A0H2XG16	*clfA*	Clumping factor A	5
A0A0H2XFR7	*clpB*	Chaperone protein ClpB	1
Q2FDV8	*clpL*	ATP-dependent Clp protease ATP-binding subunit ClpL	2
Q2FHI3	*codY*	GTP-sensing transcriptional pleiotropic repressor CodY	1
Q2FH36	*cspA*	Cold shock protein CspA	3
Q2FH47	*cvfB*	Conserved virulence factor B	1
Q2FF43	*ddl*	D-alanine--D-alanine ligase	2
Q2FGW7	*der*	GTPase Der	2
Q2FGE3	*dnaK*	Chaperone protein DnaK	1
A0A0H2XHU3	*dnaN*	Beta sliding clamp	1
Q2FGJ3	*efp*	Elongation factor P	2
Q2FIK4	*emp*	Extracellular matrix protein-binding protein emp	1
Q2FIL7	*eno*	Enolase	2

Uniprot Name	Gene Name	Protein Description	Number of lysine residues with increased succinylation in NE569 (*sucC*) versus JE2
Q2FGF6	*era*	GTPase Era	9
A0A0H2XFP1	*esaA*	Type VII secretion system accessory factor EsaA	1
Q2FG20	*ezrA*	Septation ring formation regulator EzrA	1
A0A0H2XJF4	*fabF*	3-oxoacyl-[acyl-carrier-protein] synthase 2	3
A0A0H2XHZ5	*fba*	Fructose bisphosphate aldolase	4
Q2FEM9	*femX*	Lipid II:glycine glycyltransferase	4
Q2FG06	*fhs*	Formate--tetrahydrofolate ligase	1
Q2FI15	*folD*	Bifunctional protein FolD	1
Q2FHH9	*frr*	Ribosome-recycling factor	2
A0A0H2XDY2	*fruA*	Fructose specific permease	1
A0A0H2XGW5	*ftsH*	ATP-dependent zinc metalloprotease FtsH	1
Q2FJ93	*fusA*	Elongation factor G	4
A0A0H2XHX6	*gap*	Glyceraldehyde-3-phosphate dehydrogenase	2
Q2FFJ5	*gatA*	Glutamyl-tRNA(Gln) amidotransferase subunit A	4
Q2FFJ6	*gatB*	Aspartyl/glutamyl-tRNA(Asn/Gln) amidotransferase subunit B	2
Q2FGI5	*gcvT*	Aminomethyltransferase	2
Q2FEX1	*glmM*	Phosphoglucosamine mutase	1
A0A0H2XHM8	*glnA*	Glutamine synthetase	1
Q2FHD8	*glpD*	Aerobic glycerol-3-phosphate dehydrogenase	1
A0A0H2XGL1	*gltA*	Citrate synthase	1
Q2FJB2	*gltX*	Glutamate--tRNA ligase	2
Q2FF15	*glyA*	Serine hydroxymethyltransferase	1
Q2FGW8	*gpsA*	Glycerol-3-phosphate dehydrogenase [NAD(P)+]	2
Q2FGZ4	*gpsB*	Cell cycle protein GpsB	2
Q2FF95	*groL*	60 kDa chaperonin	1
Q2FF94	*groS*	10 kDa chaperonin	1
Q2FGE2	*grpE*	Protein GrpE	1
A0A0H2XK83	*gtfA*	UDP-N-acetylglucosamine--peptide N-acetylglucosaminyltransferase GtfA subunit	1
Q2FJM6	*guaB*	Inosine-5'-monophosphate dehydrogenase	2
Q2FKQ1	*gyrB*	DNA gyrase subunit B	1
Q2FJ89	*hchA*	Protein/nucleic acid deglycase HchA	1
A0A0H2XGS5	*hemH*	Ferrochelatase	1
Q2FIN3	*hprK*	HPr kinase/phosphorylase	1
A0A0H2XIK8	*hsdS*	Type I restriction-modification enzyme, S subunit	1
A0A0H2XF50	*hup*	DNA-binding protein HU	5
Q2FHP4	*ileS*	Isoleucine--tRNA ligase	1

Uniprot Name	Gene Name	Protein Description	Number of lysine residues with increased succinylation in NE569 (*sucC*) versus JE2
Q2FHG9	*infB*	Translation initiation factor IF-2	2
Q2FG56	*infC*	Translation initiation factor IF-3	1
Q2FDT8	*isaA*	Probable transglycosylase IsaA	1
Q2FH99	*katA*	Catalase	1
Q2FFY0	*leuS*	Leucine--tRNA ligase	1
A0A0H2XIP4	*lipL*	Octanoyl-[GcvH]:protein N-octanoyltransferase	1
A0A0H2XIQ2	*lpdA*	Dihydrolipoyl dehydrogenase	9
Q2FJC3	*lysS*	Lysine--tRNA ligase	1
A0A0H2XG88	*map*	Methionine aminopeptidase	2
A0A0H2XHY4	*mecA*	Penicillin-binding protein 2	1
A0A0H2XID2	*metS*	Methionine--tRNA ligase	5
Q2FDE9	*mnmG*	tRNA uridine 5-carboxymethylaminomethyl modification enzyme MnmG	1
A0A0H2XIY9	*moaB*	Molybdenum cofactor biosynthesis protein B	1
A0A0H2XHG3	*mqo*	Probable malate:quinone oxidoreductase	1
A0A0H2XG99	*mreC*	Cell shape-determining protein MreC	1
A0A0H2XGP3	*murA*	UDP-N-acetylglucosamine 1-carboxyvinyltransferase	1
Q2FH20	*murG*	UDP-N-acetylglucosamine--N-acetylmuramyl-(pentapeptide) pyrophosphoryl-undecaprenol N-acetylglucosamine transferase	1
Q2FHE2	*mutL*	DNA mismatch repair protein MutL	1
A0A0H2XEX6	*nusA*	Transcription termination/antitermination protein NusA	1
Q2FG83	*obg*	GTPase Obg	1
Q2FH25	*odhA*	2-oxoglutarate dehydrogenase E1 component	1
Q2FH26	*odhB*	Dihydrolipoyllysine-residue succinyltransferase component of 2-oxoglutarate dehydrogenase complex	1
A0A0H2XI32	*pbp2*	Penicillin binding protein 2	2
A0A0H2XJ39	*pbp3*	Penicillin-binding protein 3	1
A0A0H2XJZ5	*pbpA*	Penicillin-binding protein 1	1
A0A0H2XHD5	*pdhA*	Pyruvate dehydrogenase E1 component subunit alpha	2
A0A0H2XIW1	*pepF*	Oligoendopeptidase F	1
A0A0H2XI24	*pepS*	Aminopeptidase PepS	1
A0A0H2XGD7	*pfkA*	ATP-dependent 6-phosphofructokinase	1
Q2FIB3	*pgi*	Glucose-6-phosphate isomerase	1
Q2FIM0	*pgk*	Phosphoglycerate kinase	2
Q2FHU3	*pheS*	Phenylalanine--tRNA ligase alpha subunit	1

Uniprot Name	Gene Name	Protein Description	Number of lysine residues with increased succinylation in NE569 (*sucC*) versus JE2
A0A0H2XI11	*phoH*	Phosphate starvation-induced protein, PhoH family	1
A0A0H2XGG5	*pknB*	Protein kinase	1
Q2FHG4	*pnp*	Polyribonucleotide nucleotidyltransferase	1
A0A0H2XGR4	*polA*	DNA polymerase I	1
Q2FI57	*prfC*	Peptide chain release factor 3	1
A0A0H2XGB3	*proC*	Pyrroline-5-carboxylate reductase	1
P0C804	*psmA3*	Phenol-soluble modulin alpha 3 peptide	2
Q2FJD9	*pth*	Peptidyl-tRNA hydrolase	1
Q2FK73	*ptsG*	PTS system glucose-specific EIICBA component	1
A0A0H2XFS4	*purD*	Phosphoribosylamine--glycine ligase	2
Q2FG40	*pyk*	Pyruvate kinase	4
Q2FI17	*qoxA*	Probable quinol oxidase subunit 2	1
A0A0H2XFW9	*recA*	Protein RecA	1
A0A0H2XHA4	*ribD*	Riboflavin biosynthesis protein RibD	1
Q2FHJ4	*rnhB*	Ribonuclease HII	1
Q2FHZ1	*rnj1*	Ribonuclease J 1	1
Q2FHG3	*rnj2*	Ribonuclease J 2	1
Q2FJA2	*rplA*	50S ribosomal protein L1	3
Q2FEP2	*rplB*	50S ribosomal protein L2	1
Q2FEN9	*rplC*	50S ribosomal protein L3	2
Q2FEQ1	*rplE*	50S ribosomal protein L5	1
Q2FEQ4	*rplF*	50S ribosomal protein L6	2
Q2FJA0	*rplL*	50S ribosomal protein L7/L12	2
Q2FEQ8	*rplO*	50S ribosomal protein L15	2
Q2FG58	*rplT*	50S ribosomal protein L20	1
Q2FG80	*rplU*	50S ribosomal protein L21	1
Q2FEQ0	*rplX*	50S ribosomal protein L24	1
Q2FJE0	*rplY*	50S ribosomal protein L25	1
Q2FG82	*rpmA*	50S ribosomal protein L27	1
Q2FHL4	*rpmB*	50S ribosomal protein L28	1
Q2FHV3	*rpmF*	50S ribosomal protein L32	1
Q2FH98	*rpmG1*	50S ribosomal protein L33 1	1
Q2FER2	*rpmJ*	50S ribosomal protein L36	2
Q2FJ98	*rpoB*	DNA-directed RNA polymerase subunit beta	1
Q2FJ97	*rpoC*	DNA-directed RNA polymerase subunit beta'	3
A0A0H2XKA5	*rpoD*	RNA polymerase sigma factor SigA	2
Q2FF00	*rpoE*	Probable DNA-directed RNA polymerase subunit delta	1

Uniprot Name	Gene Name	Protein Description	Number of lysine residues with increased succinylation in NE569 (*sucC*) versus JE2
Q2FHM8	*rpoZ*	DNA-directed RNA polymerase subunit omega	3
Q2FHI2	*rpsB*	30S ribosomal protein S2	2
Q2FEP5	*rpsC*	30S ribosomal protein S3	4
Q2FG18	*rpsD*	30S ribosomal protein S4	1
Q2FEQ6	*rpsE*	30S ribosomal protein S5	3
Q2FJP8	*rpsF*	30S ribosomal protein S6	1
Q2FJ94	*rpsG*	30S ribosomal protein S7	1
Q2FES2	*rpsI*	30S ribosomal protein S9	1
Q2FER4	*rpsK*	30S ribosomal protein S11	2
Q2FJ95	*rpsL*	30S ribosomal protein S12	1
Q2FER3	*rpsM*	30S ribosomal protein S13	1
Q2FH97	*rpsN*	30S ribosomal protein S14	1
Q2FEP8	*rpsQ*	30S ribosomal protein S17	3
Q2FGD8	*rpsT*	30S ribosomal protein S20	2
Q2FEQ2	*rpsZ*	30S ribosomal protein S14 type Z	1
A0A0H2XH68	*rsbU*	Sigma-B regulation protein	1
A0A0H2XFH1	*rsfS*	Ribosomal silencing factor RsfS	1
Q2FJE9	*rsmA*	Ribosomal RNA small subunit methyltransferase A	1
Q2FDF0	*rsmG*	Ribosomal RNA small subunit methyltransferase G	1
Q2FHQ8	*rsmH*	Ribosomal RNA small subunit methyltransferase H	1
A0A0H2XKH6	SAUSA300_0067	Universal stress protein family	1
A0A0H2XHZ1	SAUSA300_0070	Putative lysophospholipase	1
A0A0H2XKM1	SAUSA300_0094	Uncharacterized protein	2
A0A0H2XJH7	SAUSA300_0113	Immunoglobulin G binding protein A	1
A0A0H2XFU2	SAUSA300_0198	Uncharacterized protein	1
A0A0H2XDN2	SAUSA300_0212	Oxidoreductase, Gfo/Idh/MocA family	1
A0A0H2XKA0	SAUSA300_0248	Putative teichoic acid biosynthesis protein F	1
A0A0H2XIC9	SAUSA300_0251	Putative teichoic acid biosynthesis protein	1
A0A0H2XF10	SAUSA300_0252	Glycosyl transferase, group 2 family protein	4
A0A0H2XI72	SAUSA300_0320	Triacylglycerol lipase	2
A0A0H2XH82	SAUSA300_0372	Putative lipoprotein	1
A0A0H2XIC4	SAUSA300_0383	Uncharacterized protein	1
Q2FJG3	SAUSA300_0453	Nucleoid-associated protein SAUSA300_0453	1
A0A0H2XI16	SAUSA300_0468	Hydrolase, TatD family	1
A0A0H2XIW6	SAUSA300_0484	S4 RNA-binding domain-containing protein	1

Uniprot Name	Gene Name	Protein Description	Number of lysine residues with increased succinylation in NE569 (*sucC*) versus JE2
A0A0H2XEG5	SAUSA300_0486	Polyribonucleotide nucleotidyltransferase	1
A0A0H2XF92	SAUSA300_0518	Uncharacterized protein	1
A0A0H2XI40	SAUSA300_0526	Methyltransferase small domain	1
A0A0H2XJW8	SAUSA300_0535	Putative pyridoxal phosphate-dependent acyltransferase	1
Q2FJ87	SAUSA300_0538	Uncharacterized epimerase/dehydratase SAUSA300_0538	1
A0A0H2XEE1	SAUSA300_0544	Hydrolase, haloacid dehalogenase-like family	1
Q2FJ70	SAUSA300_0555	3-hexulose-6-phosphate synthase	1
A0A0H2XJQ4	SAUSA300_0643	Acetyltransferase, GNAT family	1
A0A0H2XDE4	SAUSA300_0672	Transcriptional regulator, MarR family	1
A0A0H2XH29	SAUSA300_0683	Transcriptional regulator, DeoR family	1
A0A0H2XH45	SAUSA300_0693	Putative lipoprotein	1
A0A0H2XI26	SAUSA300_0717	Ribonucleoside-diphosphate reductase, beta subunit	1
Q2FIJ2	SAUSA300_0786	Organic hydroperoxide resistance protein-like	1
A0A0H2XFZ3	SAUSA300_0788	Nitroreductase family protein	1
A0A0H2XGY2	SAUSA300_0814	Uncharacterized protein	2
Q2FIF6	SAUSA300_0822	UPF0051 protein SAUSA300_0822	1
Q2FID4	SAUSA300_0844	NADH dehydrogenase-like protein SAUSA300_0844	1
A0A0H2XGD6	SAUSA300_0847	4HBT domain-containing protein	1
A0A0H2XGI5	SAUSA300_0859	NADH-dependent flavin oxidoreductase	1
Q2FIA7	SAUSA300_0871	Uncharacterized protein SAUSA300_0871	1
A0A0H2XIJ1	SAUSA300_0912	Enoyl-[acyl-carrier-protein] reductase [NADPH]	1
Q2FI62	SAUSA300_0916	Putative phosphoesterase SAUSA300_0916	1
Q2FI55	SAUSA300_0923	Serine protease HtrA-like	2
A0A0H2XFE7	SAUSA300_0939	Glycosyl transferase, group 1 family protein	1
A0A0H2XJA7	SAUSA300_0945	Isochorismate synthase family protein	1
A0A0H2XEX3	SAUSA300_0982	Uncharacterized protein	1
A0A0H2XJG3	SAUSA300_0995	Dihydrolipoamide acetyltransferase component of pyruvate dehydrogenase complex	5
Q2FHX4	SAUSA300_1006	UPF0637 protein SAUSA300_1006	1
A0A0H2XHI3	SAUSA300_1007	Inositol monophosphatase family protein	1
A0A0H2XFL4	SAUSA300_1020	Glycerophosphoryl diester phosphodiesterase family protein	1
A0A0H2XHV3	SAUSA300_1040	Cell division protein ZapA	1
A0A0H2XK06	SAUSA300_1042	DNA-dependent DNA polymerase family X	1

Uniprot Name	Gene Name	Protein Description	Number of lysine residues with increased succinylation in NE569 (*sucC*) versus JE2
Q2FHL2	SAUSA300_1119	Uncharacterized protein SAUSA300_1119	1
A0A0H2XK72	SAUSA300_1136	Ribosome biogenesis GTPase A	1
A0A0H2XH28	SAUSA300_1160	DUF448 domain-containing protein	1
A0A0H2XIG7	SAUSA300_1181	Uncharacterized protein	2
A0A0H2XHA9	SAUSA300_1182	Pyruvate ferredoxin oxidoreductase, alpha subunit	1
A0A0H2XFW0	SAUSA300_1183	Pyruvate ferredoxin oxidoreductase, beta subunit	1
A0A0H2XEC3	SAUSA300_1197	Glutathione peroxidase	3
A0A0H2XEI1	SAUSA300_1236	Uncharacterized protein	1
A0A0H2XGG6	SAUSA300_1285	ABC transporter, ATP-binding protein	2
A0A0H2XFM1	SAUSA300_1344	Putative DNA replication protein DnaD	1
A0A0H2XI83	SAUSA300_1351	Uncharacterized protein	1
A0A0H2XE76	SAUSA300_1458	Glyoxalase family protein	1
A0A0H2XG76	SAUSA300_1464	Dihydrolipoamide acetyltransferase component of pyruvate dehydrogenase complex	2
A0A0H2XIH4	SAUSA300_1474	Uncharacterized protein	1
A0A0H2XHH5	SAUSA300_1478	Putative lipoprotein	1
A0A0H2XGB2	SAUSA300_1495	Rhodanese domain-containing protein	1
Q2FGG0	SAUSA300_1523	Putative pyruvate, phosphate dikinase regulatory protein	1
A0A0H2XE66	SAUSA300_1534	NfeD domain-containing protein	1
A0A0H2XFA5	SAUSA300_1556	Putative GTP-binding protein	1
Q2FGB1	SAUSA300_1572	UPF0473 protein SAUSA300_1572	1
A0A0H2XKI8	SAUSA300_1579	Aminotransferase, class V	1
A0A0H2XJ48	SAUSA300_1583	Uncharacterized protein	1
A0A0H2XKG5	SAUSA300_1590	GTP pyrophosphokinase	1
A0A0H2XGI9	SAUSA300_1624	MutT/nudix family protein	1
A0A0H2XFW2	SAUSA300_1652	Usp domain-containing protein	2
A0A0H2XH06	SAUSA300_1658	N6_Mtase domain-containing protein	1
A0A0H2XGV4	SAUSA300_1674	Putative serine protease HtrA	1
A0A0H2XJG9	SAUSA300_1684	Uncharacterized protein	1
Q2FFZ9	SAUSA300_1685	UPF0478 protein SAUSA300_1685	2
A0A0H2XJ82	SAUSA300_1691	Glutamyl-aminopeptidase	1
A0A0H2XJI3	SAUSA300_1706	Elp3 domain-containing protein	1
A0A0H2XET4	SAUSA300_1725	Transaldolase	1

Uniprot Name	Gene Name	Protein Description	Number of lysine residues with increased succinylation in NE569 (*sucC*) versus JE2
A0A0H2XHD3	SAUSA300_1729	NERD domain-containing protein	1
Q2FFQ0	SAUSA300_1795	UPF0342 protein SAUSA300_1795	3
A0A0H2XKH0	SAUSA300_1797	HTH cro/C1-type domain-containing protein	1
A0A0H2XH52	SAUSA300_1804	Uncharacterized protein	1
A0A0H2XHS7	SAUSA300_1844	Bacterioferritin comigratory protein	1
A0A0H2XHR8	SAUSA300_1856	DJ-1_PfpI domain-containing protein	1
A0A0H2XG95	SAUSA300_1884	CamS sex pheromone cAM373	1
Q2FFH4	SAUSA300_1902	Uncharacterized protein SAUSA300_1902	1
A0A0H2XEY2	SAUSA300_1909	Uncharacterized protein	3
A0A0H2XFR8	SAUSA300_1970	Putative exonuclease	1
Q2FF06	SAUSA300_2076	Putative aldehyde dehydrogenase	2
A0A0H2XH96	SAUSA300_2085	Uncharacterized protein	1
A0A0H2XHA0	SAUSA300_2094	EVE domain-containing protein	1
Q2FEW1	SAUSA300_2130	Probable uridylyltransferase SAUSA300_2130	1
Q2FEV9	SAUSA300_2132	UPF0457 protein SAUSA300_2132	1
A0A0H2XIL0	SAUSA300_2164	MAP domain-containing protein	1
A0A0H2XGP0	SAUSA300_2209	N-acetyltransferase domain-containing protein	1
A0A0H2XFG0	SAUSA300_2235	Iron compound ABC transporter, iron compound-binding protein	1
A0A0H2XGA1	SAUSA300_2251	Dehydrogenase family protein	2
Q2FEI5	SAUSA300_2258	Putative formate dehydrogenase SAUSA300_2258	1
A0A0H2XI51	SAUSA300_2261	HTH deoR-type domain-containing protein	1
A0A0H2XGW1	SAUSA300_2265	Putative amino acid permease	1
A0A0H2XIZ7	SAUSA300_2272	Uncharacterized protein	1
A0A0H2XIB6	SAUSA300_2288	ABC transporter, ATP-binding protein	1
A0A0H2XI37	SAUSA300_2296	Esterase-like protein	1
A0A0H2XGV3	SAUSA300_2316	Acetyltransferase, GNAT family	1
A0A0H2XJH3	SAUSA300_2327	Putative_PNPOx domain-containing protein	2
A0A0H2XJ64	SAUSA300_2328	Uncharacterized protein	1
A0A0H2XGT6	SAUSA300_2418	Alkyl hydroperoxide reductase AhpD	4
A0A0H2XE56	SAUSA300_2447	Uncharacterized protein	2
A0A0H2XJY0	SAUSA300_2464	Hydrolase, haloacid dehalogenase-like family	1
A0A0H2XH59	SAUSA300_2482	Peptidase C51 domain-containing protein	1

Uniprot Name	Gene Name	Protein Description	Number of lysine residues with increased succinylation in NE569 (*sucC*) versus JE2
A0A0H2XJ90	SAUSA300_2496	D-isomer specific 2-hydroxyacid dehydrogenase family protein	1
Q2FDS6	SAUSA300_2518	Uncharacterized hydrolase SAUSA300_2518	1
A0A0H2XHR6	SAUSA300_2542	Putative AMP-binding enzyme	3
A0A0H2XJW3	*scrB*	Sucrose-6-phosphate hydrolase	2
A0A0H2XHU1	*sdhA*	Succinate dehydrogenase, flavoprotein subunit	1
A0A0H2XHE6	*sdhB*	Succinate dehydrogenase, iron-sulfur protein	1
A0A0H2XF56	*secF*	Multifunctional fusion protein	1
Q2FGH0	*sodA*	Superoxide dismutase [Mn/Fe] 1	1
A0A0H2XGJ0	*speG*	Spermidine N(1)-acetyltransferase	1
Q2FJE4	*spoVG*	Putative septation protein SpoVG	2
A0A0H2XEA7	*spsB*	Signal peptidase I	1
A0A0H2XI68	*srrA*	Staphylococcal respiratory response protein, SrrA	2
A0A0H2XEL7	*ssaA*	Secretory antigen SsaA	1
A0A0H2XGI6	*ssb*	Single-stranded DNA-binding protein	1
A0A0H2XG15	*sufC*	FeS assembly ATPase SufC	3
A0A0H2XGY0	*sufD*	FeS assembly protein SufD	2
A0A0H2XFK6	*tagA*	N-acetylglucosaminyldiphosphoundecaprenol N-acetyl-beta-D-mannosaminyltransferase	1
A0A0H2XDW4	*tcaR*	Transcriptional regulator TcaR	1
Q2FG61	*tig*	Trigger factor	4
A0A0H2XIH6	*tkt*	Transketolase	1
Q2FEN5	*topB*	DNA topoisomerase 3	1
A0A0H2XHL5	*tpx*	Thiol peroxidase	1
Q2FFR1	*traP*	Signal transduction protein TRAP	3
Q2FHI7	*trmFO*	Methylenetetrahydrofolate--tRNA-(uracil-5-)-methyltransferase TrmFO	1
Q2FHI1	*tsf*	Elongation factor Ts	7
Q2FJ92	*tuf*	Elongation factor Tu	2
A0A0H2XFL9	*typA*	GTP-binding protein	2
Q2FG72	*valS*	Valine--tRNA ligase	1
Q2FJM8	*xpt*	Xanthine phosphoribosyltransferase	1
A0A0H2XEQ2	*zwf*	Glucose-6-phosphate 1-dehydrogenase	1

Table 6.2 Proteins that have increased succinylation at 1 or more lysine residues in JE2 versus NE569 (*sucC*).

Uniprot Name	Gene Name	Protein description	Number of lysine residues with increased succinylation in JE2 versus NE569 (*sucC*)
Q2FG27	*ackA*	Acetate kinase	1
A0A0H2XKH5	*acnA*	Aconitate hydratase	1
Q2FG97	*aspS*	Aspartate--tRNA ligase	2
Q2FF24	*atpD*	ATP synthase subunit beta	1
A0A0H2XH11	*betB*	Glycine betaine aldehyde dehydrogenase	1
A0A0H2XH43	*ccpA*	Catabolite control protein A	1
Q2FG62	*clpX*	ATP-dependent Clp protease ATP-binding subunit ClpX	1
Q2FHI3	*codY*	GTP-sensing transcriptional pleiotropic repressor CodY	1
Q2FF45	*cshA*	DEAD-box ATP-dependent RNA helicase CshA	3
Q2FH09	*cvfC*	Conserved virulence factor C	1
Q2FJB0	*cysS*	Cysteine--tRNA ligase	1
Q2FGW7	*der*	GTPase Der	1
Q2FIE3	*dltA*	D-alanine--D-alanyl carrier protein ligase	2
A0A0H2XH34	*dltD*	Protein DltD	3
Q2FGE3	*dnaK*	Chaperone protein DnaK	1
Q2FIL7	*eno*	Enolase	1
A0A0H2XFP1	*esaA*	Type VII secretion system accessory factor EsaA	1
A0A0H2XJL0	*est*	Carboxylesterase	1
Q2FG20	*ezrA*	Septation ring formation regulator EzrA	1
A0A0H2XHZ5	*fba*	Fructose bisphosphate aldolase	1
Q2FDQ4	*fda*	Fructose-bisphosphate aldolase class 1	1
A0A0H2XHG6	*femB*	Methicillin resistance protein FemB	1
Q2FG06	*fhs*	Formate--tetrahydrofolate ligase	1
A0A0H2XFP5	*fmt*	Fmt protein	1
Q2FFK2	*ftnA*	Bacterial non-heme ferritin	1
Q2FJ93	*fusA*	Elongation factor G	1
A0A0H2XHX6	*gap*	Glyceraldehyde-3-phosphate dehydrogenase	2
Q2FFJ6	*gatB*	Aspartyl/glutamyl-tRNA(Asn/Gln) amidotransferase subunit B	1
Q2FGF8	*glyQS*	Glycine--tRNA ligase	1
Q2FHM9	*gmk*	Guanylate kinase	1
Q2FE81	*gpmA*	2,3-bisphosphoglycerate-dependent phosphoglycerate mutase	1
Q2FGB6	*greA*	Transcription elongation factor GreA	1
Q2FJM5	*guaA*	GMP synthase [glutamine-hydrolyzing]	1
A0A0H2XHC2	*gudB*	Glutamate dehydrogenase	1
Q2FKQ0	*gyrA*	DNA gyrase subunit A	1

Uniprot Name	Gene Name	Protein description	Number of lysine residues with increased succinylation in JE2 versus NE569 (*sucC*)
Q2FJ89	*hchA*	Protein/nucleic acid deglycase HchA	1
Q2FIN3	*hprK*	HPr kinase/phosphorylase	1
A0A0H2XF50	*hup*	DNA-binding protein HU	1
Q2FHP4	*ileS*	Isoleucine--tRNA ligase	1
Q2FH99	*katA*	Catalase	1
Q2FFJ1	*ligA*	DNA ligase	1
Q2FI34	*menD*	2-succinyl-5-enolpyruvyl-6-hydroxy-3-cyclohexene-1-carboxylate synthase	1
A0A0H2XID2	*metS*	Methionine--tRNA ligase	1
A0A0H2XGY9	*modA*	Molybdenum ABC transporter, molybdenum-binding protein ModA	1
A0A0H2XHG3	*mqo*	Probable malate:quinone oxidoreductase	4
A0A0H2XFT6	*murA*	UDP-N-acetylglucosamine 1-carboxyvinyltransferase	1
Q2FFZ8	*murC*	UDP-N-acetylmuramate--L-alanine ligase	1
A0A0H2XHB9	*nixA*	Nickel/cobalt efflux system	1
Q2FH26	*odhB*	Dihydrolipoyllysine-residue succinyltransferase component of 2-oxoglutarate dehydrogenase complex	1
A0A0H2XIJ5	*oppA*	Oligopeptide ABC transporter, substrate-binding protein	1
A0A0H2XFT3	*parE*	DNA topoisomerase 4 subunit B	1
A0A0H2XGA9	*pbuX*	Xanthine permease	1
A0A0H2XI24	*pepS*	Aminopeptidase PepS	1
Q2FIP8	*pepT*	Peptidase T	1
A0A0H2XGD7	*pfkA*	ATP-dependent 6-phosphofructokinase	3
Q2FIB3	*pgi*	Glucose-6-phosphate isomerase	1
A0A0H2XHB4	*prs*	Ribose-phosphate pyrophosphokinase	1
Q2FFQ5	*prsA*	Foldase protein PrsA	2
P0C7Y0	*psmA1*	Phenol-soluble modulin alpha 1 peptide	2
P0C817	*psmA4*	Phenol-soluble modulin alpha 4 peptide	3
A0A0H2XHL4	*pta*	Phosphate acetyltransferase	2
A0A0H2XFY4	*purF*	Amidophosphoribosyltransferase	1
Q2FI05	*purH*	Bifunctional purine biosynthesis protein PurH	1
Q2FI07	*purM*	Phosphoribosylformylglycinamidine cyclo-ligase	2
A0A0H2XHX4	*purR*	Pur operon repressor	2
Q2FG40	*pyk*	Pyruvate kinase	1
Q2FHI0	*pyrH*	Uridylate kinase	1
Q2FHZ1	*rnj1*	Ribonuclease J 1	2
Q2FHG3	*rnj2*	Ribonuclease J 2	1
A0A0H2XIK4	*rocD*	Ornithine aminotransferase	1
Q2FEP0	*rplD*	50S ribosomal protein L4	1
Q2FJA0	*rplL*	50S ribosomal protein L7/L12	1

Uniprot Name	Gene Name	Protein description	Number of lysine residues with increased succinylation in JE2 versus NE569 (*sucC*)
Q2FER6	*rplQ*	50S ribosomal protein L17	1
Q2FG58	*rplT*	50S ribosomal protein L20	1
Q2FG80	*rplU*	50S ribosomal protein L21	2
Q2FEP4	*rplV*	50S ribosomal protein L22	2
Q2FEP1	*rplW*	50S ribosomal protein L23	1
Q2FG82	*rpmA*	50S ribosomal protein L27	1
Q2FHL4	*rpmB*	50S ribosomal protein L28	1
Q2FF08	*rpmE2*	50S ribosomal protein L31 type B	1
Q2FG57	*rpmI*	50S ribosomal protein L35	1
Q2FJ98	*rpoB*	DNA-directed RNA polymerase subunit beta	1
Q2FJ97	*rpoC*	DNA-directed RNA polymerase subunit beta'	4
A0A0H2XE01	*rpoF*	RNA polymerase sigma factor	1
Q2FHI2	*rpsB*	30S ribosomal protein S2	1
Q2FJP8	*rpsF*	30S ribosomal protein S6	1
Q2FEQ3	*rpsH*	30S ribosomal protein S8	2
Q2FJ95	*rpsL*	30S ribosomal protein S12	2
Q2FJP6	*rpsR*	30S ribosomal protein S18	1
A0A0H2XG98	*rsbV*	Anti-sigma factor antagonist	1
Q2FIT5	*saeS*	Histidine protein kinase SaeS	1
A0A0H2XJH7	SAUSA300_0113	Immunoglobulin G binding protein A	2
A0A0H2XJL5	SAUSA300_0173	Uncharacterized protein	1
A0A0H2XIC9	SAUSA300_0251	Putative teichoic acid biosynthesis protein	2
A0A0H2XF10	SAUSA300_0252	Glycosyl transferase, group 2 family protein	1
A0A0H2XDX3	SAUSA300_0274	Uncharacterized protein	1
A0A0H2XFX2	SAUSA300_0277	Putative staphyloxanthin biosynthesis protein	1
A0A0H2XFL7	SAUSA300_0308	ABC transporter, permease protein	1
A0A0H2XI16	SAUSA300_0468	Hydrolase, TatD family	1
A0A0H2XI40	SAUSA300_0526	Methyltransferase small domain	1
A0A0H2XHX5	SAUSA300_0541	Deoxynucleoside kinase family protein	1
Q2FJ56	SAUSA300_0569	Putative heme-dependent peroxidase SAUSA300_0569	1
A0A0H2XDE4	SAUSA300_0672	Transcriptional regulator, MarR family	1
A0A0H2XES4	SAUSA300_0716	Ribonucleoside-diphosphate reductase	1
A0A0H2XI26	SAUSA300_0717	Ribonucleoside-diphosphate reductase, beta subunit	2
A0A0H2XHU8	SAUSA300_0725	Uncharacterized protein	1
Q2FIM4	SAUSA300_0753	Epimerase family protein SAUSA300_0753	1

Uniprot Name	Gene Name	Protein description	Number of lysine residues with increased succinylation in JE2 versus NE569 (*sucC*)
A0A0H2XK09	SAUSA300_0841	Pyr_redox_2 domain-containing protein	1
Q2FID4	SAUSA300_0844	NADH dehydrogenase-like protein SAUSA300_0844	1
A0A0H2XEX3	SAUSA300_0982	Uncharacterized protein	1
A0A0H2XHV3	SAUSA300_1040	Cell division protein ZapA	1
A0A0H2XH00	SAUSA300_1052	Fibrinogen-binding protein	1
A0A0H2XGG8	SAUSA300_1068	Antibacterial protein	2
A0A0H2XGD0	SAUSA300_1100	3-dmu-9_3-mt domain-containing protein	1
A0A0H2XI96	SAUSA300_1101	Putative fibronectin/fibrinogen binding protein	1
A0A0H2XHI7	SAUSA300_1107	TM2 domain-containing protein	2
Q2FHL2	SAUSA300_1119	Uncharacterized protein SAUSA300_1119	1
A0A0H2XG09	SAUSA300_1170	Transcriptional regulator, GntR family	1
A0A0H2XH03	SAUSA300_1303	Uncharacterized protein	2
A0A0H2XGQ5	SAUSA300_1332	Putative 5'-3' exonuclease	1
Q2FGL9	SAUSA300_1463	UPF0403 protein SAUSA300_1463	1
A0A0H2XFA5	SAUSA300_1556	Putative GTP-binding protein	1
A0A0H2XKG5	SAUSA300_1590	GTP pyrophosphokinase	1
A0A0H2XH06	SAUSA300_1658	N6_Mtase domain-containing protein	1
A0A0H2XI92	SAUSA300_1673	1-acyl-sn-glycerol-3-phosphate acyltransferases	1
A0A0H2XGV4	SAUSA300_1674	Putative serine protease HtrA	1
A0A0H2XGK8	SAUSA300_1740	DUF4352 domain-containing protein	1
A0A0H2XJW7	SAUSA300_1788	Uncharacterized protein	1
A0A0H2XHA7	SAUSA300_1809	Putative membrane protein	1
A0A0H2XI52	SAUSA300_1863	Uncharacterized protein	4
A0A0H2XEN6	SAUSA300_1864	Putative membrane protein	1
A0A0H2XG38	SAUSA300_1904	Uncharacterized protein	2
A0A0H2XHG8	SAUSA300_1910	Putative membrane protein	1
A0A0H2XH16	SAUSA300_1988	Delta-hemolysin	1
A0A0H2XFU0	SAUSA300_2021	S1 RNA binding domain protein	1
A0A0H2XIK5	SAUSA300_2080	DUF2529 domain-containing protein	1
A0A0H2XGU4	SAUSA300_2125	Iron-sulfur cluster carrier protein	1
A0A0H2XEB0	SAUSA300_2136	Iron compound ABC transporter, iron compound-binding protein	1
A0A0H2XI39	SAUSA300_2144	Uncharacterized protein	1

Uniprot Name	Gene Name	Protein description	Number of lysine residues with increased succinylation in JE2 versus NE569 (*sucC*)
A0A0H2XIR0	SAUSA300_2147	Alcohol dehydrogenase, zinc-containing	2
A0A0H2XER4	SAUSA300_2213	AcrB/AcrD/AcrF family protein	1
A0A0H2XFG0	SAUSA300_2235	Iron compound ABC transporter, iron compound-binding protein	1
Q2FEI5	SAUSA300_2258	Putative formate dehydrogenase SAUSA300_2258	2
A0A0H2XGG3	SAUSA300_2267	Hydrolase, haloacid dehalogenase-like family	1
A0A0H2XI61	SAUSA300_2287	Putative membrane protein	1
A0A0H2XKJ6	SAUSA300_2289	Uncharacterized protein	1
A0A0H2XGW2	SAUSA300_2326	Transcription regulatory protein	1
A0A0H2XJH3	SAUSA300_2327	Putative_PNPOx domain-containing protein	1
A0A0H2XFK1	SAUSA300_2350	Uncharacterized protein	1
A0A0H2XK42	SAUSA300_2359	Amino acid ABC transporter, amino acid-binding protein	1
A0A0H2XK17	SAUSA300_2431	Putative helicase	2
A0A0H2XH33	SAUSA300_2529	3-dmu-9_3-mt domain-containing protein	1
Q2FDN2	SAUSA300_2562	Uncharacterized protein SAUSA300_2562	3
Q2FE79	*sbi*	Immunoglobulin-binding protein Sbi	3
A0A0H2XEW3	*serA*	D-3-phosphoglycerate dehydrogenase	1
Q2FJH7	*sle1*	N-acetylmuramoyl-L-alanine amidase sle1	1
A0A0H2XEL7	*ssaA*	Secretory antigen SsaA	1
Q2FHJ3	*sucC*	Succinate--CoA ligase [ADP-forming] subunit beta	1
Q2FJ01	*tagH*	Teichoic acids export ATP-binding protein TagH	2
Q2FHI8	*topA*	DNA topoisomerase 1	1
Q2FHT6	*trxA*	Thioredoxin	1
A0A0H2XHQ2	*trxB*	Thioredoxin reductase	2
Q2FHI1	*tsf*	Elongation factor Ts	1
Q2FJ92	*tuf*	Elongation factor Tu	1
Q2FF16	*upp*	Uracil phosphoribosyltransferase	1
A0A0H2XGP1	*yajC*	Preprotein translocase, YajC subunit	1
A0A0H2XG28	*ychF*	Ribosome-binding ATPase YchF	1
A0A0H2XEQ2	*zwf*	Glucose-6-phosphate 1-dehydrogenase	2

Table 6.3: Proteins and specific peptide sequence with greater than 2-fold differences in lysine succinylation between JE2 and NE569 (*sucC*).

Uniprot Name	Protein Description	Gene name	Peptide sequence (K# represents succinylated lysine)	log(SucC_Stat/JE2_Stat)
Q2FGL9	UPF0403 protein SAUSA300_1463	SAUSA300_1463	R.LVTVFAGQDK#EATQR.A	-2.05
A0A0H2XH34	Protein DltD	dltD	K.LK#PFLPILISG.A	-2.02
Q2FF15	Serine hydroxymethyltransferase	glyA	K.TYQQQVVK#.N	2.05
Q2FDT8	Probable transglycosylase IsaA	isaA	A.AEVNVDQAHLVDLAHNHQDQLNAAPIK#.D	2.19
A0A0H2XHV3	Cell division protein ZapA	SAUSA300_1040	K.QQIHK#LQQR.E	2.19
Q2FFZ9	UPF0478 protein SAUSA300_1685	SAUSA300_1685	R.RGSANYK#ANNVATDANHSYTSR.V	2.21
A0A0H2XF10	Glycosyl transferase, group 2 family protein	SAUSA300_0252	R.ISVLSDKAYYYATK#R.E	2.21
A0A0H2XIY9	Molybdenum cofactor biosynthesis protein B	moaB	K.LIFSIPGSTGAVK#.L	2.25
A0A0H2XIJ3	Autolysin	atl	K.AGQNTLYK#MR.W	2.28
A0A0H2XJH3	Putative_PNPOx domain-containing protein	SAUSA300_2327	K.VGVLSTAYNNK#PNSR.Y	2.29
Q2FGW7	GTPase Der	der	R.VAGYAHEQGK#.A	2.34
A0A0H2XJQ4	Acetyltransferase, GNAT family	SAUSA300_0643	K.K#LYQHR.G	2.36
Q2FEP5	30S ribosomal protein S3	rpsC	R.RVQK#QAITR.A	2.39
A0A0H2XGI5	NADH-dependent flavin oxidoreductase	SAUSA300_0859	K.SFGQK#QEHSAR.E	2.43
A0A0H2XIJ3	Autolysin	atl	K.TSLPK#YKPQVNSSINDYIR.K	2.45

Uniprot Name	Protein Description	Gene name	Peptide sequence (K# represents succinylated lysine)	log(SucC_Stat/JE2_Stat)
A0A0H2XJG3	Dihydrolipoamide acetyltransferase component of pyruvate dehydrogenase complex	SAUSA300_0995	R.QIDGATGQNAM*NHIK#R.L	2.52
Q2FJA0	50S ribosomal protein L7/L12	rplL	K.IKVVK#AVK.E	2.60
A0A0H2XI51	HTH deoR-type domain-containing protein	SAUSA300_2261	K.YCNVSK#R.T	2.64
Q2FFR1	Signal transduction protein TRAP	traP	R.LLRPAK#GTTYK.I	2.67
A0A0H2XFW9	Protein RecA	recA	R.RAEQLK#QGQEIVGNR.T	2.86
A0A0H2XH06	N6_Mtase domain-containing protein	SAUSA300_1658	R.LFHTLDEK#.A	2.86